Physical Studies on Subunit Interactions in Oligomeric Enzymes.

by

K. R. Leonard.

A Thesis submitted for the degree of Doctor of Philosophy.

Magdalen College,
Oxford.

January, 1970

ACKNOWLEDGEMENTS.

I would like to express my thanks to the Medical Research Council for supporting me financially during the course of this work and to Professor Sir Hans Krebs and Professor Rodney Porter for allowing me to use the facilities of the Department of Biochemistry.

I am also much indebted to Miss Pat Henson for her assistance with some of the more tedious parts of writing the thesis.

Finally, my deepest gratitude must go to my supervisor, Dr Ian Walker, for his unfailing help and encouragement during the time that I have been working in his laboratory.

ABSTRACT

This thesis is concerned with the physical structure and the protein-protein interactions in the two oligomeric proteins, Phosphofructokinase (PFK) and Aldolase. PFK is known to play an important part in the regulation of glycolysis and the activity of the enzyme is modified by a variety of low molecular weight metabolites including ATP, AMP, F-6-P, FDP, and citrate. Physical studies on PFK were, therefore, made with particular reference to the conformational changes which might accompany the regulation of activity.

The studies on Aldolase are less extensive and represent a continuation of earlier work (K.R.Leonard, Part II thesis, 1966). In contrast to PFK, aldolase is not a regulatory protein. It is,however, composed of subunits and therefore serves as a useful comparison for PFK. Aldolase is also related to PFK in that they are both enzymes of Glycolysis, having adjacent places in the pathway, so that the product of the PFK reaction, FDP, is also the substrate of the Aldolase reaction.

Aldolase was purchased from a commercial source and was found to be quite suitable for physical studies. The commercially available PFK, however, was not suitable for physical studies for a number of reasons, including

the presence of a large amount of inactive protein which was visible in the sedimentation patterns and a strong tendency to precipitate when dialysing against buffer to remove ammonium sulphate. The PFK used was therefore prepared in this laboratory by an adaptation of a published method.

The sedimentation velocity experiments using schlieren optics to measure protein concentration confirmed that PFK undergoes reversible self-association above 0.5mg/ml. This aspect of the protein-protein interactions of PFK was investigated in some detail. Evidence for a reversible association was manifested by the appearance of the sedimentation pattern of the pure protein (three peaks with s_{app} of approx. 13 S , 18 S and 22-30 S). Further evidence was the behavior of the fastest peak which increased in s_{app} from 22 S at 0.5mg/ml to 30 S at 10mg/ml in direct contrast to the normal decrease in s_{app} with increasing concentration for a non-interacting species.

This association of PFK was found to be prevented by mild alkaline pH, high ionic strength, low concentrations of SDS (detergent) and low concentrations of PCMB (thiol reagent). Addition of any of these reagents to PFK solutions resulted in a change of the sedimentation pattern to a single boundary with s_{app} = 12 S (approx)

This corresponds to the slowest sedimenting species in the pattern for native PFK at high concentration and is probably the unassociated 'Monomer' of the equilibrium. Measurement of s_{app} for PFK at the concentration level of the enzyme assay (approx. 1µg/ml) gave a value of about 11 S for the active species, which indicated that PFK is present as the 'monomer' at this low concentration.

The 12 S material, which was obtained by direct pH adjustment to pH 10.5, slowly broke down to give protein sedimenting at lower speed. The presence of 0.5mM FDP, however, had a marked stabilising effect, and protein dialysed into pH 10.5 buffer containing FDP sedimented as a sharp symmetrical boundary with $s^{o}_{20,w}$ of 11.9±0.4. Similar concentrations of F-6-P, ATP and AMP had no stabilising effect on the 12 S protein. The diffusion coefficient of the FDP-stabilised material was measured by the spreading boundary method and a value of D^{o}_{20} equal to $3.2 \pm 0.3 \times 10^{-7}$ obtained. This combined with the sedimentation coefficient gave a value of $3.4 \pm 0.3 \times 10^{5}$ for the molecular weight. This agreed with the value of $3.45 \pm 0.1 \times 10^{5}$ obtained from sedimentation equilibrium.

Equilibrium centrifugation studies of a series of concentrations of PFK over the range 0.5 - 10mg/ml

enabled curves of weight-average and Z-average molecular weights against concentration for the polymerisation to be constructed. These were found to be sigmoid in shape, and the Z-average tended to a value of $3-4 \times 10^5$ at low concentration (where the 12S species only will be present) and to a plateau of about 5.5 x (monomer mol.wt) at about 7mg/ml, followed by a slight reduction in molecular weight caused by non-ideality at higher protein concentration.

These curves were compared with calculated theoretical curves for a number of model polymerising systems, and it was deduced, from the shape of the curves, that the association was to a closed polymer rather than to an indefinite, open polymerisation. A calculated curve which was a reasonable fit to the experimental points was obtained by assuming that the degree of polymerisation ,n, was six, that there was a negligible concentration of intermediate polymers present at equilibrium and that BM_W (the non-ideality term) had a value close to the theoretical value for a globular protein. A tentative closed-shell structure was proposed for the hexamer.

Assuming that n = 6, the equilibrium constant for the association per mole of hexamer was estimated to be 6×10^{25} $Ltr^5 / Mole^5$ and hence the value of ΔG° per mole of hexamer was -35 Kcal. at $20^\circ C$. Data for M_Z was also

obtained at 2°C and this, combined with the results at 20°C gave values of ΔH° = 36 Kcal and ΔS° = 240 e.u. per mole of hexamer, for the association. These results show that the principle contributing factor to the free energy of the interaction is the gain in entropy which results from the release of bound water as the monomers associate. This would implicate either hydrophobic or electrostatic interactions as chief contributors to the protein-protein binding. The effect of high salt concentration, which prevents the association, unequivocally supports the importance of electrostatic interactions in the polymerisation.

PFK at pH 12 in the presence of SDS had a molecular weight of about 8.8×10^4, estimated by sedimentation equilibrium, which is about one fourth of the molecular weight obtained for the 12 S protein. The molecular weight in 6M GuHCl, 0.1M 2-mercaptoethanol was $7.6 \pm 0.5 \times 10^4$ by sedimentation equilibrium and about 8×10^4 calculated from the value of the sedimentation coefficient. Allowing for experimental error, in particular in the value of the partial specific volume, these results agree with the figure obtained at high pH in the presence of SDS. Thus, the 12 S protein is made up of four subunits, each consisting of a single polypeptide chain.

In order to test whether the association of PFK had any effect on the enzymic activity it was necessary to carry out the assay at the 1mg/ml enzyme level. The F-6-P activity of PFK is too high to be measured by normal spectrophotometric methods at this concentration. However, PFK will also catalyse the phosphorylation of G-1-P at a much lower rate and this activity can be assayed at the higher concentration. It was found, that there was no change in the G-1-P specific activity over the concentration range 0.2 - 2.0 mg/ml where the enzyme is known to associate. In order to test whether dissociation of PFK might occur at low concentration in the presence of inhibitors (reversible dissociation to an inactive form could form the basis of a regulatory mechanism), the sedimentation coefficient was measured under the conditions of normal activity and total inhibition by ATP. At approx. 1 µg/ml of protein, the sedimentation coefficient was found to be 11.3±1.2 S in the presence of 6mM ATP (known to cause almost complete inactivation) and 10.6±0.9 in the presence of 1mM FDP. It would appear, therefore, that dissociation is not a mechanism of the ATP inactivation. These results indicate that association or dissociation of PFK are not primary factors in the regulation of PFK activity.

Circular Dichroism (CD) and Optical Rotatory Dispersion (ORD) studies were carried out on PFK and Aldolase under various conditions. Both proteins showed near-UV bands, but whereas Aldolase also showed a measurable Cotton effect at 290nm in the ORD curve, PFK exhibited no detectable near-UV Cotton effect. The far-UV ORD and CD curves for native Aldolase and PFK were rather similar in size and shape.

The CD curves were converted into the corresponding ORD curves by application of the Kronig-Kramers transform using an Algol computer program to resolve the CD bands and a second program to carry out the transform. There was good agreement between the calculated and experimental ORD curves in the far-UV, which suggests that there is little contribution to the measurable far-UV ORD bands from optically active chromophores other than those that are observable in the far-UV CD curve. In the near-UV, the calculated curve for aldolase showed a sharp peak in the 290nm region, produced by the overlap of two near-UV CD bands of opposite sign, which satisfactorily explained the near-UV Cotton effect. The calculated curve for PFK in the near-UV showed a much smaller Cotton effect which explains why no anomaly was detectable in the experimental ORD curve.

CD studies were made on the aromatic model compounds, L-tryptophan, N-acetyl-L-tryptophan ethyl ester, L-tyrosine and N-acetyl-L-tyrosine ethyl ester and bands between 300nm and 190nm were obtained. The latter compound was also studied at high pH to assess the effect of ionisation of the phenolic group on the CD spectrum. The values for the molar ellipticities for the model compounds were at least an order of magnitude lower than the values which would be expected from the size of the near-UV bands of the proteins. It was therefore concluded that the near-UV optical activity of these chromophores must be enhanced by their presence in the tertiary structure of the protein.

The effect of pH on the dichroic bands of the two enzymes was correlated with the conformational changes which take place at pH 10 - pH 11 for aldolase and PFK and at pH 4 for aldolase.(PFK is insoluble below pH 6 and could not therefore be studied). It was found that the near-UV bands of aldolase dissappeared completely when the enzyme denatured at pH 4 - pH 3.5 supporting the observation that the near-UV optical activity is enhanced by the three-dimensional structure of the native protein. At high pH, the near-UV band system of native aldolase was replaced by a single positive band with maximum ellipticity at about 255nm. This band was correlated with

the red-shift of the tyrosine band at 225nm as the pH is increased. The tail of this red-shifted band is superimposed on the negative dichroic band from the peptide chromophore, producing a positive 'band' at 255nm.

PFK at high pH also showed this 255nm band, but in addition there was a small positive band centred on 290nm which was attributed to optically active tryptophan residues. As we have seen, the presence of near-UV optical activity implies some degree of tertiary structure, so that PFK even as high as pH 12 seems to behaving as a folded protein structure.

In the far-UV smaller changes in the 200nm -250nm negative peptide bands with increased pH were observed for PFK than for aldolase, which again suggests that the former enzyme is less denatured at high pH. An attempt was made to fit the far-UV bands with different percentages of the three types of regular secondary structure (α-helix, β-structure and random coil). It was unsuccessful for native aldolase and PFK and for PFK at pH 12, but a reasonable fit to the data was obtained for acid or alkali denatured aldolase.

Hydrogen ion binding data was obtained for PFK in 0.05M Na_2SO_4 which agreed reasonably well with the total of ionisable groups found in the amino acid analysis.

Unlike aldolase (see below) it was possible to account for all the histidine residues by inspection of the titration curve. Spectrophotometric titrations were carried out in the presence and absence of 1mM FDP. It was found that FDP caused a shift of the titration curve to higher pH which was related to a change in pK from about 10.25 to about 11.5 for about two tyrosine residues per 100,000g of protein.

The earlier work on aldolase suggested that a number of the histidine residues might be titrating anomalously or be buried in the native protein, possibly associated with the inter-subunit interactions of the oligomer. The histidine titration region was therefore measured more carefully by estimating the ΔH_{app} for ionisation of the various groups from the temperature difference titration. The results indicated that few if any of the histidine residues are buried, but that a number may titrate with an abnormally low pK and be involved in the enzyme activity of the protein.

A temperature difference titration was also carried out over the acid pH range at which aldolase undergoes a co-operative dissociation and denaturation as shown by a step in the forward titration curve. The effect of temperature was to shift the step to lower

pH with lower temperature(i.e. there is a stabilisation of the protein interactions on reducing the temperature). This result indicates that there must be a negative enthalpy change in going from the dissociated, denatured subunits to the native oligomer, which could implicate hydrogen bonding as a factor in the protein interactions.

INDEX

Page

Chapter 6. (continued)

ABBREVIATIONS

These were explained in the text whenever possible. The abbreviations used for some of the reagents are listed below.

Tris: Tri (hydroxymethyl) methylamine.

EDTA: Ethylenediamine tetra-acetic acid.

GuHCl: Guanidine hydrochloride.

SDS : Sodium dodecyl sulphate.

PCMB: p-choromercuribenzoate (Na salt).

ATP: Adenosine triphosphate

ADP: " diphosphate

AMP: " monophosphate.

FDP: D-fructose-1,6-diphosphate

F-6-P: D-fructose-6-phosphate

G-1-P: glucose-1-phosphate.

PFK: Phosphofructokinase.

P_i: Inorganic Phosphate. (PO_4^{3-}).

NADH : Nicotinamide-adenine dinucleotide (reduced form)

Chapter 1. Introduction.

(i) Glycolysis.

The system of glycolysis, the first metabolic sequence to be described completely, was elucidated by the pioneering work of Harden, Meyerhof, Embden, Warburg, Cori and others. The sequence of reactions, their intermediates and the enzymes involved are shown in Fig. 1.1 .

Glycolysis is made use of in skeletal muscle to generate ATP by the anaerobic conversion of glucose to lactate and in heart muscle to generate ATP by the complete aerobic combustion of glucose. In both cases, the ATP is required to supply the energy for muscle contraction. The glycolytic pathway is also important in microbial fermentation of glucose to ethanol, lactate, glycerol and other compounds, providing the energy needed for the growth of the organism.

The two enzymes studied in this work, both from skeletal muscle, are Aldolase (Fructose-1,6-diphosphate, D-glyceraldehyde-3-phosphate lyase, E.C. 4.1.2.13) and Phosphofructokinase (ATP, D-fructose-6-phosphate 1-phosphotransferase, E.C. 2.7.1.11). These enzymes catalyse adjacent reactions in the glycolytic pathway, so that the product of the phosphofructokinase reaction becomes

1.

Fig. 1.1. Glycolytic Pathway (Taken from Mahler & Cordes, 1966)

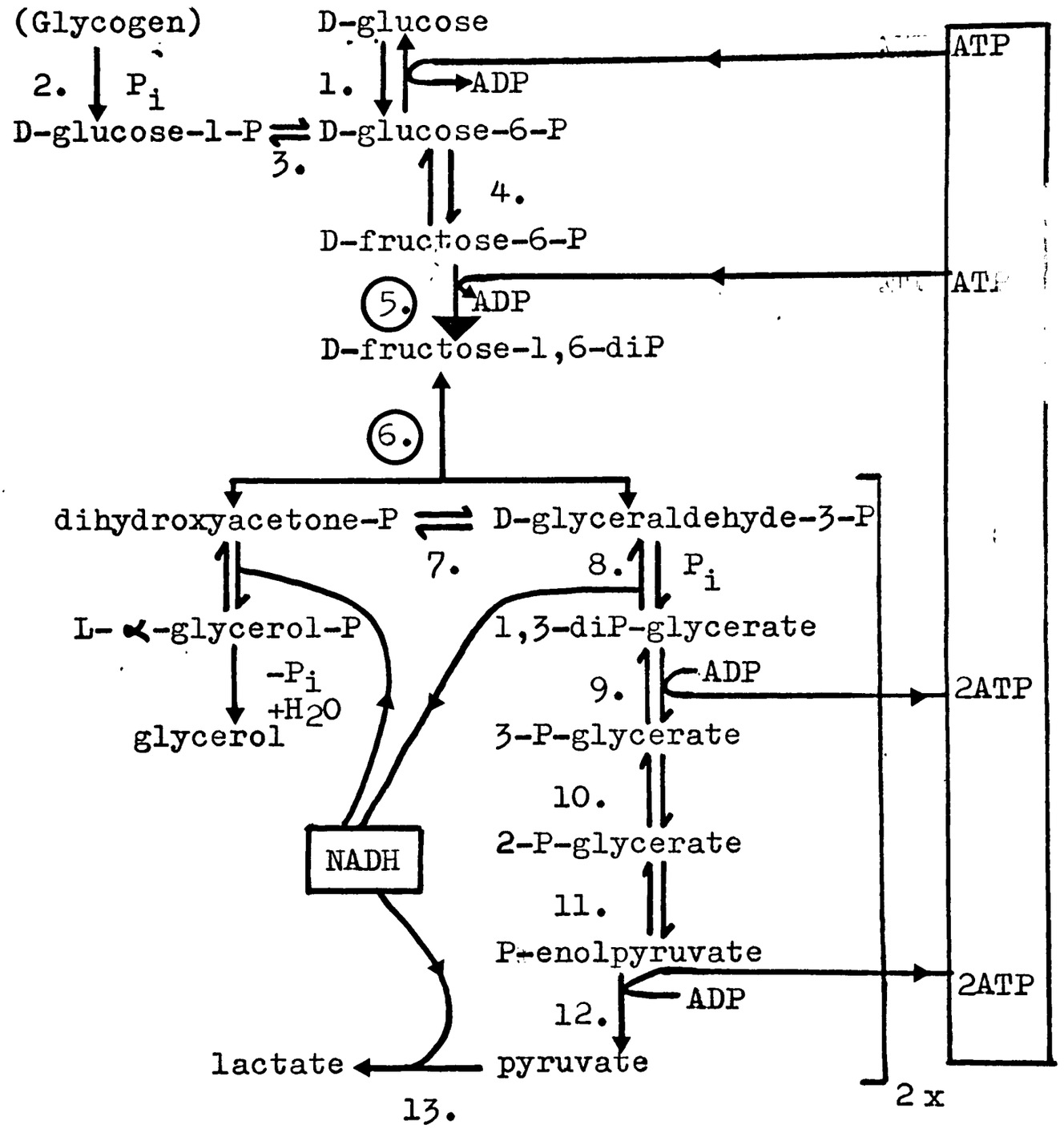

Enzymes.

1. Hexokinase
2. Phosphorylase
3. Phosphoglucomutase
4. Phosphoglucoisomerase
5. Phosphofructokinase
6. Aldolase
7. Triosephosphateisomerase
8. Triose-P dehydrogenase
9. P-glycerate kinase
10. P-glyceromutase
11. Enolase
12. Pyruvate kinase
13. Lactate dehydrogenase.

the substrate of the aldolase reaction.

Both enzymes are oligomers, i.e. they are composed of protein subunits. Aldolase is now generally agreed to be a tetramer of four subunits, each of molecular weight about 40,000 (Kawahara and Tanford, 1966[2]). This has been shown by electron microscopy to be a tetrahedral structure (Penhoet et al, 1967[3]). The same workers showed that aldolase exists as different isoenzymes in different tissues such as brain and muscle and can show heterogeneity of the subunit composition. Phosphofructokinase has been reported to have a molecular weight of 360,000 for the active form which can be dissociated into protomers (identical subunits) of molecular weight 93,000 which can be further degraded to polypeptide chains of molecular weight 25,000 (Paetkau et al, 1968)[4]. Electron microscope studies (Parmeggiani et al, 1966[5]) suggest that the active unit is a flat molecule with the subunits arranged in a square-planar fashion.

(ii) <u>The importance of Phosphofructokinase (PFK) in the control of glycolysis.</u>

In cells which are capable of degrading glucose in both the presence and the absence of oxygen (e.g. muscle or yeast cells), the glucose disappears more rapidly

under anaerobic conditions than under aerobic conditions. This inhibition of glycolysis by oxygen was first observed by Pasteur and is known as the "Pasteur Effect". It was later confirmed by Meyerhof and Warburg. It is now generally believed that this effect results from a change in the activity of PFK which is a key enzyme in the control of glycolysis.

In vitro studies on PFK from muscle[6], heart[7], yeast[8] and Escherichia Coli[9] as well as other sources have shown that the enzyme is strongly inhibited by ATP and activated by a number of metabolites including F-6-P (substrate), FDP (product), AMP, ADP and phosphate ion. The enzyme shows non-Michaelis Menton kinetics, giving sigmoid shaped curves of initial rate v. F-6-P concentration in the presence of inhibiting levels of ATP.

These controls ensure that when there is a high ATP level in the cell (e.g. when lactate and pyruvate are oxidised to CO_2 by the Krebs cycle) glycolysis will be shut down. Under anaerobic conditions, when glycolysis is required for the production of ATP, the level of ATP will be low and the levels of ADP (or AMP) and phosphate will be high, so that the activity of PFK is stimulated and the rate of glycolysis increases. Heart PFK has also been shown to be inhibited by citrate (Garland et al,

1963)[10] which suggests that there may also be feedback control of glycolysis from the Krebs cycle. pH may also be important in changing the response of PFK to the various inhibitors and activators (Danforth, 1965;[11] Freyer et al, 1968).[12]

A number of theories have been proposed to explain the behavior of regulatory enzymes, of which PFK is a good example; these are outlined in section (iv) below.

Although aldolase has been reported to be inhibited by high concentrations of triose-phosphate (product) (Richards and Rutter, 1961),[13] in vivo studies indicate that it does not play any part in the regulation of glycolysis.

(iii) The Association of PFK at high concentration.

Another difference between PFK and aldolase is the reversible aggregation shown by the former enzyme at high concentration. Sedimentation patterns of pure PFK show several peaks, indicating that some form of self-association is taking place. This sedimentation behavior is not exhibited by aldolase, which moves in the ultracentrifuge as a single symmetrical boundary. The association of PFK molecules could have a biological function as the effective enzyme concentration in muscle tissue may be as high as 1mg/ml (Lowry, 1965)[14] at which concentrat-

ion there is appreciable association of the pure protein.

(iv) Models for the mode of action of regulatory enzymes.

(a) Allosteric Control.

Monod, Changeux and Jacob (1963)[15] pointed out that many biological pathways are regulated by the concentration of metabolites which modify the activity of certain rate-limiting enzymes by interaction with so-called "allosteric sites" which are different from the active site. Monod, Wyman and Changeux (1965)[16] extended this idea and produced a theory to account for the sigmoid oxygen saturation curve of haemoglobin and for the similarly shaped kinetic curves for regulatory enzymes. They proposed that all regulatory proteins are oligomers composed of identical subunits (protomers) which may themselves be composed of smaller subunits. Because the protomers are identical they must be equivalent in the oligomer, and their individual conformations are constrained by their association with the other protomers so that the overall symmetry of the molecule is maintained. This symmetry requirement allows the protein only a restricted number of conformations which must be in equilibrium with each other.

In a regulatory protein there are two important conformations; the'R-state' which has a high affinity for the substrate (or oxygen in the case of haemoglobin) and

the 'T-state' which has a low affinity for substrate. An increase in substrate concentration will shift the R - T equilibrium in favour of the R-state causing a co-operative increase in the amount of substrate bound which manifests itself as an increase in the rate of the enzyme catalysed reaction. This is known as a 'homotropic effect'. Alternatively, a substance unrelated to substrate may be bound at a second type of site (the allosteric site), resulting in either activation or inhibition. This is known as a 'heterotropic effect'. A heterotropic effector which has a greater affinity for the T-state will shift the equilibrium in its favour and so reduce the amount of substrate bound. One which has a greater affinity for the R-state will cause co-operative activation.

The allosteric model has the advantage of simplicity and should enable the maximum number of predictions to be made from a minimum knowledge of the parameters of the system. This model has been used to explain the kinetic behavior of PFK from E. Coli[17] and from skeletal muscle[18]

(b) The 'Induced Fit' theory.

Koshland (1958)[19] suggested that the binding of substrate to an enzyme involves an induced alteration of the shape of the active site. Koshland et al, (1966)[20] extended this theory to explain the oxygen binding data for haemoglobin

and postulated that it is a general mechanism for enzyme regulation. They suggest that a ligand may induce a conformational change in a given subunit, which then causes progressive changes in the conformations of neighbouring subunits. This change in conformation is linked to the activity of other binding sites on the other subunits If there is strong inter-subunit coupling, binding of substrate at one site will induce a large change in the neighbouring site(s) and there will be a strongly co-operative increase in activity. If there is weak inter-subunit coupling, there will be poor co-operativity.

The Koshland model, therefore, requires the presence of subunit structure but does not demand overall conservation of symmetry as in the Allosteric model. The Induced-fit model has been applied to the kinetic data for PFK by Atkinson et al, (1965)[21] .

(c) Control by association or dissociation of the enzyme.

In their 1965 paper, Monod et al[16] consider the possibility of dissociation accompanying the R - T transition and give as an example the well known dimerisation of Phosphorylase b which occurs on phosphorylation of a serine residue.

Nichol et al, (1967)[22] have interpreted sigmoid binding curves in terms of a monomer-polymer model. In the case where polymerisation sites and the ligand binding sites

are coincident (i.e. there is competition between ligand binding and polymerisation for the available sites), they showed that sigmoid binding curves would result. The degree of sigmoid shape increases with the extent of polymerisation.

If association or dissociation accompanies the regulatory activity of the enzyme, the regulatory effectors should influence the degree of polymerisation as well as the activity. In the case of heart PFK, evidence has been given to suggest that inactivation by ATP involves a change in sedimentation coefficient from 14.5 S to 7 S. (Mansour and Ahlfors, 1968)[23]. Dissociation was reported to be prevented by FDP which is an activator of the enzyme.

(d) The Alternative Pathway Mechanism.

The theories of enzyme regulation examined so far have required some form of association between enzyme subunits and the presence of more than one Ligand binding site per molecule of enzyme. "Allosteric" behavior may, however, be possible in the case of only one active site if two substrates are involved in the enzyme-catalysed reaction. In this case, two pathways to the products can be envisaged as shown below.

$$S_1 + E \rightleftharpoons ES_1 + S_2 \rightleftharpoons ES_1S_2 \longrightarrow \text{Products}$$

or

$$S_2 + E \rightleftharpoons ES_2 + S_1 \rightleftharpoons ES_1S_2 \longrightarrow \text{Products}$$

Dalziel (1958)[24] has shown that the effects of substrate activation or inhibition are possible, depending on the relationship between the kinetic parameters of the alternative paths. This idea has been extended to the particular case of PFK by Ferdinand (1966).[25] He showed that the theoretical curves for substrate activation and inhibition predicted by this model are very similar to the experimental curves for the activity of PFK v. concentration of ATP and F-6-P. This model cannot, however, account completely for the regulatory behavior of PFK since other effectors such as citrate and AMP exist, and must presumably interact with PFK at a second site.

(v) Protein-protein Interactions.

The general factors which are involved in protein-protein quaternary interactions are those which have been reviewed by Kauzmann (1959)[26] in relation to protein tertiary structure. Protein structure at any level above that of primary structure relies upon a balance between disruptive forces and stabilising forces. The principle driving force behind the dissociation or denaturation of a protein oligomer is the gain in entropy which results from the greater randomness of the dissociated or denatured state. The principle stabilising factors which oppose breakdown of the protein structure are summarised below.

(a) Covalent Bonds.

The only covalent protein-protein linkage whose existence is well established is the cystine disulphide bond, but side-chain ester or imide linkages may occur.

(b) Non-covalent Interactions.

Hydrogen-bonds: These may be interpeptide, like those which have been shown to contribute to the stability of the α-helix and the β-pleated-sheet structure. Other types of H-bond may also occur including tyrosine-carboxylate or thiol-carboxylate linkages. Hydrogen bonds are characterised by a negative ΔH of formation of up to -5 Kcal per mole.

Hydrophobic Interactions: A large proportion of the amino-acid side chains found in proteins, including those of valine, leucine, alanine, phenylalanine, and tryptophan are non-polar and have a low affinity for water. Protein chains therefore tend to associate so that these residues occur in non-polar pockets out of contact with water.

These hydrophobic interactions have been shown to have a positive ΔH term, so that an entropy increase must result from the removal of the non-polar group from the aqueous environment if the overall Free-energy change is to be negative. When in contact with water, these non-polar groups exert an ordering influence on the water

molecules which surround them. The formation of a hydrophobic interaction results in the release of this ordered water and a consequent gain in entropy.

Coulombic interactions - Salt Linkages: A small number of ionised side chains may be involved in interactions between groups of opposite charge. The principle contributor to the Free-energy of such an interaction is again the increase in entropy which results from the breakdown of the hydration sphere of the charged group as it interacts with another group to form an ion-pair.

Van der Waals Forces: These may also play a part in interactions between protein molecules. London dispersive attraction will occur between atoms which are in close contact in the inter-protein binding site. They tend to favour the interaction of like side chains - aromatic with aromatic and aliphatic with aliphatic.

(vi) The Investigation of Protein-protein Interactions.

Much useful information can be obtained from the study of the thermodynamic parameters of the interaction and from the effects of dissociating reagents. If,for example, hydrophobic interactions were important in maintaining the protein quaternary structure,dissociation should be favoured by a high concentration of urea. Ionic interactions, on the other hand, should be weakened by an

increase in the ionic strength of the solution, since dissolved electrolyte will produce a stabilising Debye-Huckel atmosphere around the charged side chains. If disulphide bonds were involved in the protein-protein interactions, reducing agents or mercurials might be expected to favour dissociation.

Like all other aspects of protein structure, the most detailed information about protein-protein interactions will be provided by X-ray Crystallography. So far, two three-dimensional structures of protein oligomers have been determined, which show the different types of non-covalent interactions described in section (v) above . These are the oxyhaemoglobin tetramer (Perutz et al, 1968)[27,28] and the insulin dimer (Adams et al, 1969)[29]. Insulin is not strictly a true oligomer but shows a marked tendency to dimerise in solution, so that the close contact between two molecules found in the crystal structure probably results from this interaction.

In the case of oxyhaemoglobin, the contacts between the α and β chains appeared to be mainly between non-polar side chains (suggesting hydrophobic and and Van der Waals interactions) with a small number of probable H-bonds. The $\alpha\alpha$ and $\beta\beta$ inter-subunit regions were not so clearly defined, but it was suggested that there may be salt-likages between the terminal residues.

The results for insulin show that there are many close non-polar contacts in the binding region, which occurs between the B-chains. There was also a five residue section in each B-chain which appeared to be hydrogen-bonded as a pleated sheet to the corresponding region of the opposite chain.

(vii) The biological significance of protein-protein interactions in enzymes.

The presence of subunit structure and the existence of strong coupling between enzyme subunits may, as we have seen, be important in the mechanism of regulation of some enzymes. All the known examples of regulatory enzymes have been shown to be oligomeric.

Protein-protein interactions may also be important in the grouping together of related enzymes into functionally significant assemblages. The efficiency of metabolic pathways and their ease of control would be greatly improved if the enzymes involved were assembled into a soluble multienzyme complex or are bound to a membrane or structural unit. Although there is no direct evidence that the glycolytic enzymes are grouped in this way, there is some quite good indirect evidence for an organised glycolytic system.

Arnold and Pette (1968)[30] have shown that aldolase,

PFK and other glycolytic enzymes will bind to muscle proteins, in particular to F-actin molecules, at low ionic strength. Aldolase and glyceraldehyde-3-phosphate dehydrogenase have been shown to produce mixed crystals which may indicate some form of interaction between the two enzymes (Baranowski and Niederland, 1949)[31]. Pogell et al (1968)[32] have reported an in vitro association between PFK and FDPase. The latter enzyme is not a member of the glycolytic system, but catalyses the reverse reaction to that of PFK during gluconeogenesis. There is also evidence that a group of five glycolytic enzymes occur in equimolar proportions in different tissues (Pette, 1965;[33] Mier and Cotton, 1966)[34] suggesting that they may form an organised unit.

(viii) The scope of this thesis.

The physical studies carried out on PFK were mainly concerned with the reversible association which takes place at high concentration and with the effect of pH and disruptive reagents on the structure of the enzymically active oligomer. It was hoped to gain some insight into the forces responsible for these different levels of protein-protein interaction and to determine their biological significance, if any exists. Optical rotatory dispersion, circular dichroism and titration studies were also made to investigate any conformational changes which

might accompany the associative and dissociative changes. It was also hoped that some information might be obtained about the influence of allosteric effectors such as ATP, F-6-P and FDP on the protein-protein interactions involved in the reversible association of PFK and between subunits of the enzymically active oligomer.

The work done on the second enzyme, Aldolase, was an extension of hydrodynamic and other physical studies which were submitted earlier for a Chemistry Part II thesis. The new work was mainly restricted to ORD and CD measurements and temperature titrations which were carried out to obtain information about the dissociation of the aldolase oligomer at high and low pH , which had been established during the earlier study.

The properties of PFK and Aldolase were studied to a certain extent in parallel, since they are both examples of oligomeric enzymes, but differ in that the former is a regulatory enzyme and the latter is non-regulatory.

Chapter 2. Materials and General Methods

(Including the preparation of PFK)

(i) Reagents.

Unless otherwise stated, all reagents used were 'Analar' or 'Biochemical' grade (British Drug Houses). Ammonium sulphate with a specially low heavy metal content (BDH) was used in the enzyme preparation. Sodium dodecyl sulphate was obtained from Sigma Chemicals and N-acetyl-L-tryptophan ethyl ester from Mann Research Laboratories. 2-mercapto ethanol, dithiothreitol, p-mercuribenzoate and tris base were obtained from Koch-Light Ltd.

The coenzymes and substrates NADH, ATP, sodium pyruvate, F6P and FDP were obtained from Boehringer and Soehne. F6P, FDP and FDP (80 % pure) were also obtained from Wessex Biochemicals Ltd.

(ii) Enzymes.

The enzymes aldolase, triosephosphate isomerase, glyceraldehyde-3-phosphate dehydrogenase, pyruvate kinase and lactate dehydrogenase were purchased from Boehringer and Soehne. Rabbit Muscle Phosphofructokinase from the same source was found to be unsuitable for physical studies for several reasons. The enzyme tended to precipitate when dialysed into phosphate buffer to remove ammonium sulphate. It had a relatively low

specific activity (less than 60 units/mg) compared with 160 units/mg reported by Parmeggiani et al (1966)[5], and the sedimentation pattern (Fig. 2.1) was also unlike those of Ling et al (1965)[35] and Parmeggiani et al.[5] The slowest sedimenting component was isolated and found to be enzymically inactive.

It was therefore necessary to prepare the enzyme, which was done by the method described below. The sedimentation pattern of this material (Fig. 2.2) was very similar to those previously reported. The enzyme had a much smaller tendency to precipitate, and the activity was close to the reported value.

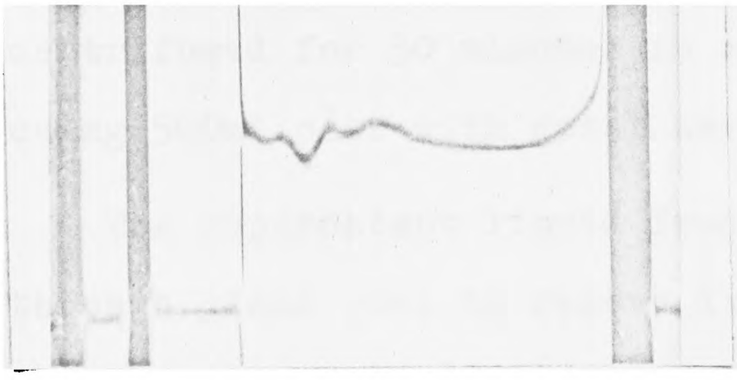

Fig. 2.1.
Sedimentation pattern of PFK purchased from Boehringer

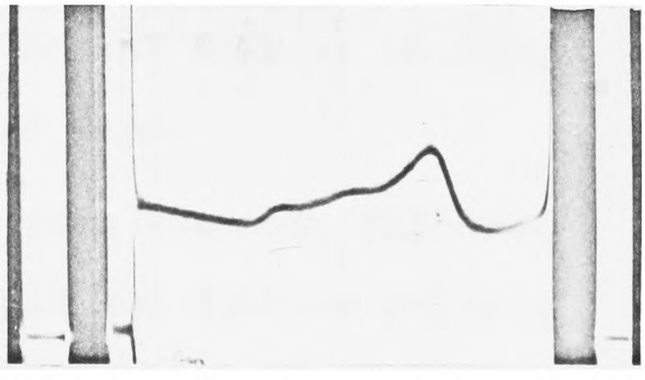

Fig. 2.2.
Sedimentation pattern of PFK prepared in this laboratory.

(iii)
Preparation of Phosphofructokinase.

PFK was prepared as follows, the method being based on that of Parmeggiani et al (1966)[5].

The rabbit was killed by intravenous injection of sodium phenobarbitol, decapitated and bled from the neck. After removal of the skin, the muscle from the hind legs and back was removed and chilled in ice for about 15 minutes. This and all the subsequent operations were carried out in a cold room at 4°C.

The chilled muscle was minced in an electric mincer and 200 gram lots homogenised in a Townson and Mercer top-drive macerator for 30 seconds with 200ml of 4mM EDTA, 30mM NaF (pH 7). This was followed by a further homogenisation for 45 sec. with an additional 400ml. of the extraction medium. The homogenised material was then centrifuged for 30 minutes in a Sorval RC2B at 14,000g using 500ml pots with metal screw tops.

The supernatant liquid from this step was filtered through glass wool to remove lipid and fibrous material and the clear liquid adjusted to pH5 with 1N acetic acid. Below pH 6 a heavy precipitate was formed, and, after allowing the solution to stand at pH 5 for about 15 min., the precipitate was collected by centrifugation at 14,000 g for 30min.

The protein pellets were washed out of the centrifuge

pots with 100mM sodium glycerophosphate, 4mM EDTA, 30mM NaF (pH 8), using about the same volume as the pellets. A further amount of 50mM glycerophosphate, 2mM EDTA, 15mM NaF (pH 7) was added to a final volume of about 240ml per Kg of muscle used. The protein precipitate was then dispersed using a 50ml teflon-in-glass homogeniser to break up the insoluble material. This was followed by a 90 minute centrifugation at 30,000 rpm in a Spinco Model L centrifuge (No. 30 rotor). The supernatant liquid was recentrifuged for a further 240 min. in a No. 40 rotor at 40,000 rpm.

After discarding the supernatant, 0.5ml of 50mM glycerophosphate, 2mM EDTA, 15mM NaF (pH 7) was added to each tube and the tubes left at 4°C for 8 hours. Any pelleted material which had not dissolved after this time was broken up with a glass rod and the contents of the tubes transferred to a 50ml conical flask. Each tube was washed with a further 0.5ml of buffer and the washings added to the flask. The contents of the flask were stirred at room temperature for about an hour to disperse aggregated material.

The cloudy liquid was heated in a water bath set at 70°C , the temperature of the enzyme preparation being kept between 55°C and 60°C for 5 minutes. The heat aggregated protein material was then centrifuged off using a No. 30 rotor at 15,000 rpm for 15 minutes and the supernatant solution collected, A volume of ammonium

sulphate solution (saturated at 4°C) equal to two thirds of the volume of the supernatant was added and the light precipitate which formed was removed by centrifugation at 15,000rpm for 15 minutes. A further amount of ammonium sulphate solution is added to a final volume (ammonium sulphate plus heat treatment supernatant) equal to twice the volume of the supernatant. The heavy precipitate is collected by centrifugation at 15,000 rpm for 15 minutes. The pellets are resuspended and homogenised in about 4 to 5 ml of 50% saturated ammonium sulphate/50% glycerophosphate buffer, pH 8 with a teflon-in-glass homogeniser. This suspension of PFK was stored at 4°C, and used, after dialysis to remove ammonium sulphate, in the studies described in this work.

In order to make optimum use of centrifuge time, about 1.33Kg of muscle is required, which can be obtained from two medium sized rabbits, total body weight about 5Kg. This material, after homogenisation and extraction, fills 10 Sorvall pots. After adjustment to pH 5 , the volume of solution is accomodated in 8 pots, making a total of 3 Sorvall runs. The suspended precipitates are taken up in 240ml of buffer per Kg of muscle which requires the use of one No. 30 rotor and two No. 40 rotors.

An attempt was also made to prepare PFK by the isopropanol precipitation method of Kemp and Forrest (1968)[36]. Although this method gave enzyme of quite high activity, the sedimentation pattern showed large amounts of slow

sedimenting material similar to that present in the enzyme purchased from Boehringer.

Table 2.1 - Activity of PFK during the preparation.

Fraction	Total activity/1.2Kg muscle	
	This work	Parmeggiani et al
First extract	76,000 units	120,000 units
Acid ppt.	34,000 "	58,000 "
30,000rpm snt.	31,000 "	47,000 "
40,000rpm ppt.	28,000 "	38,000 "
Heat treatment supernatant.	13,000 "	34,000 "
$(NH_4)_2SO_4$ ppt.	11,000 "	26,000 "

The yield of enzyme was always lower than that reported by Parmeggiani et al (1966)[5], although the specific activity of the second ammonium sulphate fraction was the same (150-160 units/mg). On average, about 40 to 50 mg of PFK per Kg of muscle were obtained. The results of a typical preparation are shown in Table 2.1 above. There is a lower initial activity, possibly caused by the longer time required to homogenise the muscle in small batches. There also appeared to be a greater loss of activity at the heat treatment stage.

Enzyme preparations were kept at 4°C as the ammonium sulphate suspension (50% sat. $(NH_4)_2SO_4$, 50mM glycerophosphate 2mM EDTA, 15mM NaF (pH 8).) and were normally used within two months of preparation. Loss of activity was less than 10% during this time. The enzyme crystallised as hexagonal

microcrystals on slowly increasing the concentration of ammonium sulphate in the presences of 2 mM ATP.

As mentioned previously, the sedimentation pattern of the enzyme prepared by the method described above was very similar to those described by other workers. The amino acid analysis and spectrum (see below) also agreed quite well with those reported in the literature.

(iv) Amino Acid Analysis of PFK.

The analyses were carried out using a Locarte Mini Amino Acid Analyser by the method of Spackman, Stein and Moore (1958).[37] The protein was hydrolysed by heating in sealed glass tubes at 120°C with 50% Aristar hydrochloric acid. Duplicate samples were measured, and hydrolyses were carried out for 24 and 72 hours to correct for the loss of acid-labile amino acids. This was done by extrapolation to zero time of hydrolysis assuming first order kinetics for the degredation of the amino acids. The results are shown in Table 2.2 which also includes the analyses which have been published by Paetkau et al[4] (1968) and Parmeggiani et al (1966).[5]

The agreement between the three analyses is good for most of the residues, although there are some differences. The proline figure obtained in this work supports that of Paetkau et al, whereas the values for aspartic acid and alanine are closer to those obtained by Parmeggiani et al. The values for isoleucine and leucine obtained in this

work were lower than the values reported; there did not seem to be any obvious explanation for this.

Table 2.2 - Amino Acid Analyses of Rabbit Muscle PFK.

Residue	Moles per 100,000g protein recovered [1]		
	This Work	Paetkau [4]	Parmeggiani [5]
Aspartic Acid	83.8±1	88.0	81.2
Threonine [2]	64.9±5	57.0	63.8
Serine [2]	50.7±5	46.5	42.0
Glutamic Acid	82.9±1	85.8	83.9
Proline	39.8±2	37.2	28.6
Glycine	98.0±1	93.9	94.7
Alanine	82.5±1	68.4	77.8
½ Cystine [2]	17.4±5	19.0	18.2
Valine	72.7±1	70.0	68.5
Methionine [2]	19.1±4	23.6	25.8
Isoleucine	44.9±1	52.1	52.6
Leucine	62.9±1	73.8	77.4
Tyrosine	17.5±1	19.1	18.6
Phenylalanine	31.1±1	32.4	34.0
Tryptophan [3]	12.5±1	13.2	13.81
Histidine	22.1±1	21.6	22.3
Lysine	49.5±2	48.6	47.4
Arginine	61.0±1	60.8	61.7
Amide [4]	50±10	-	68·8

1. Not including the ammonia peak.
2. Extrapolated to zero time of hydrolysis.
3. Determined spectroscopically by the method of Goodwin and Morton (1946).[38]
4. Estimated from the ammenia released during hydrolysis.

The analyses were carried out by Mr. Colin Castle of the Dept. of Biochemistry.

The number of amide groups was estimated from the amount of ammonia released during hydrolysis, corrected for the ammonia produced by the decomposition of labile amino acids. It can, therefore, be only an approximate value. The value reported by Parmaggiani et al was obtained by alkaline hydrolysis. No value for amide was reported by Paetkau et al.

Two anomalous peaks were observed in the chromatograms. A very small peak between methionine and isoleucine was probably allo-isoleucine, but the other peak, which was about equal in size to the methionine peak and eluted just in front of aspartic acid, was not identified.

(v)
Near U.V. Spectrum of PFK.

The spectrum between 240nm and 320nm was measured with a Unicam SP800 spectrophotometer and is shown in Fig.2.3. The shape of the spectrum, with a shoulder at 290nm, a peak at 279nm and a trough at 249nm, agrees with the spectrum described by Parmeggiani et al. They obtained a 279/249nm ratio of 2.3 compared with the value of 2.25 ±0.1 from this work.

(vi)
Protein Concentrations.

These were based on $E^{1\%}_{280} = 9.1$ for aldolase (Szabolcsi and Biszku, 1961)[39] and $E^{1\%}_{279} = 10.2$ for PFK (Parmeggiani et al, 1966)[5] Scattering corrections were made, when necessary, by extrapolation of a log-log plot of the optical density above 320nm to shorter wavelengths.(Doty and Steiner, 1950).[40]

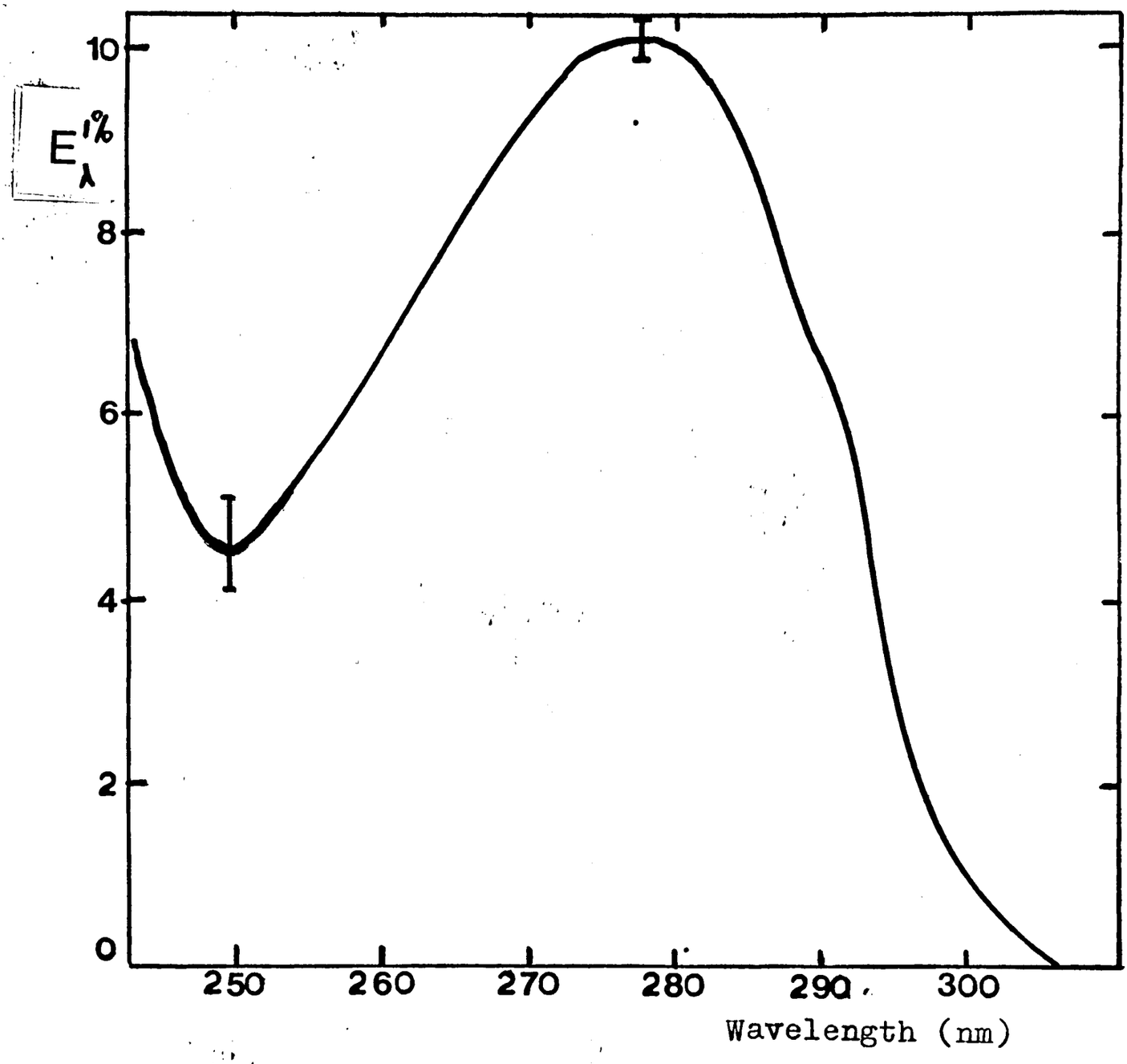

Fig. 2.3. Near-UV spectrum of PFK in 0.1M tris-phosphate 10mM 2-mercaptoethanol, pH 8. (Corrected for scattering).

Chapter 3. Methods of Enzyme Assay and Results.

(A) PFK.

As extensive work has been done in other laboratories on the kinetics of PFK, the measurement of PFK activity in this work was confined to the characterisation of the enzyme preparation, to the establishment of conditions for inhibition and activation and to the investigation of whether the activity is related to the association or dissociation of the enzyme.

(i) Methods of Assay.

Two methods were used for the measurement of enzyme activity. Routine assays were carried out using a method based on that of Parmeggiani *et al* (1966)[5]. The PFK reaction is coupled via aldolase and triosephosphate isomerase to the glycerol-1-phosphate dehydrogenase reduction of dihydroxyacetone phosphate, as shown below.

$$\text{F-6-P} + \text{ATP} \xrightarrow[Mg^{++}]{\text{PFK}} \text{FDP} + \text{ADP}$$

$$\text{FDP} \xrightleftharpoons{\text{ALD}} \text{G-3-P} + \text{DHAP}$$

$$\text{G-3-P} \xrightleftharpoons{\text{TIM}} \text{DHAP}$$

$$2\text{DHAP} + 2\text{NADH} + 2\text{H}^{+} \xrightarrow{\text{G-1-PDH}} 2\text{G-1-P} + 2\text{NAD}^{+}$$

The following solutions were made up: -

Solution A — 400µg/ml aldolase, 100µg/ml G-1-PDH, 40µg/ml TIM } { $(NH_4)_2SO_4$ suspension diluted with H_2O

Solution B
0.05M glycyl-glycine buffer, pH 8.2
2mM EDTA
0.01% Bovine Serum Albumin
0.5mM ATP
25mM 2-Mercaptoethanol

Solution C
0.1M glycyl-glycine, pH 8.2
1mM EDTA
0.02% BSA
18mM Magnesium Acetate.
2.5mM ATP
3mM F-6-P (disodium salt)
0.9mM NADH , 50mM 2-Mercaptoethanol.

The appropriate amount of PFK solution was diluted with solution B, and 0.25ml of this solution added to 0.25ml of A and 0.25ml of C in a 1ml, 1cm pathlength cuvette. The activity is calculated from the change in optical density at 340nm, taking a value of ΔO.D. = 2.07 for the oxidation of 1 µmole of NADH.

The second method of assay, which was used to measure the glucose-1-phosphate activity of PFK, and the activating effects of F-6-P and FDP follows the reaction

scheme: -

$$(G\text{-}1\text{-}P)\ F\text{-}6\text{-}P + ATP \xrightarrow[Mg^{++}]{PFK} (GDP)\ FDP + ADP$$

$$ADP + PEP \xrightarrow{PK} ATP + Pyruvate$$

$$Pyruvate + NADH + H^{+} \xrightarrow{LDH} L\text{-}Lactate + NAD^{+}$$

The following assay solutions were used: -

<u>Solution A</u> 20µg/ml Pyruvate Kinase, 50µg/ml Lactate Dehydrogenase } { $(NH_4)SO_4$ susp dil. with H_2O

<u>Solution B</u> 0.05M glycyl-glycine, pH 8.2

or 0.05M imidazole, pH 7.0

2mM EDTA

0.01 % BSA

0.5mM ATP

25mM 2-Mercaptoethanol

<u>Solution C</u> 0.1M glycyl-glycine, pH 8.2

or 0.1M imidazole, pH 7.0

1mM EDTA

0.02% BSA

3mM G-1-P or F-6-P

18mM Mg^{++}

3mM phosphoenol pyruvate

0.9mM NADH

50mM 2-Mercaptoethanol

As before, the PFK was diluted with B and added to a 1ml cuvette containing A + C. In both assays, the oxidation

of NADH was measured at 25°C with a Beckman DB spectrophotometer, using a reference cuvette containing the assay mixture minus the enzyme.

(ii) Inhibition and Activation of PFK.

The non-Michaelis Menton kinetic behavior of PFK has been well established by other workers.[6,7,8,9] The preparations of enzyme used in this work also showed non-hyperbolic activity v. substrate concentration curves. There was marked inhibition by ATP at concentrations greater than 1mM as shown in Fig. 3.1. Enzyme which had been partially inhibited by ATP gave a sigmoid curve of activity with increasing F-6-P concentration (Fig. 3.2). In each case, aldolase was present in the assay mixture to remove the FDP produced. FDP was found to reverse completely the inhibitory effect of ATP, the concentration required being less than 0.1mM at pH 7. These results are essentially the same as those obtained by Passoneau and Lowry (1962).[6]

(iii) The effect of association at high enzyme concentration

PFK is known to undergo self-association at concentrations greater than 0.5mg/ml (see Chapter 4) and it is possible that this could alter the enzyme activity. The F-6-P activity is too high at this concentration to be measured by normal spectrophotometric methods. Stopped-flow techniques cannot be used because of the lag effects which would occur in the coupled enzyme system used to assay PFK.

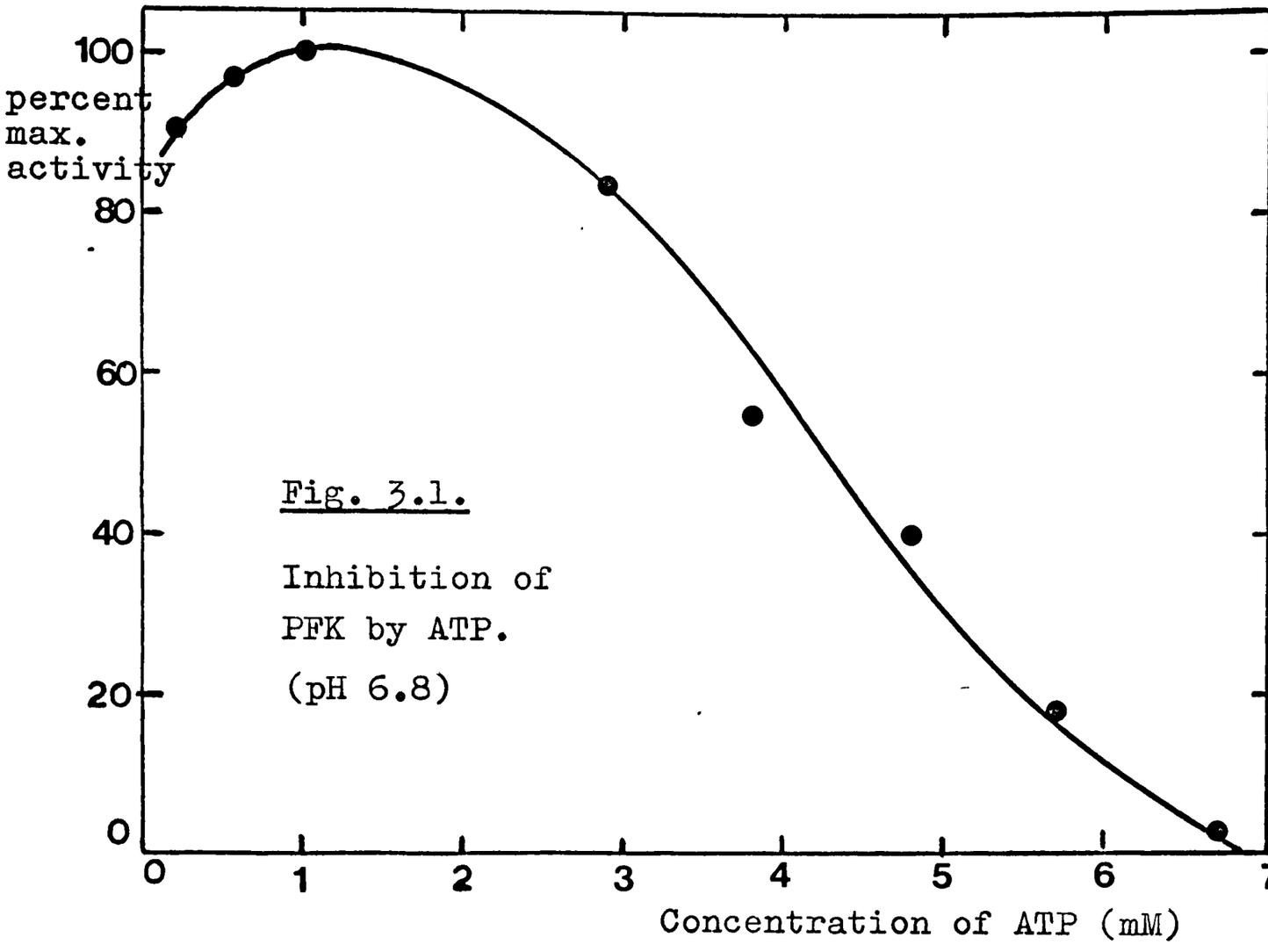

Fig. 3.1.

Inhibition of PFK by ATP. (pH 6.8)

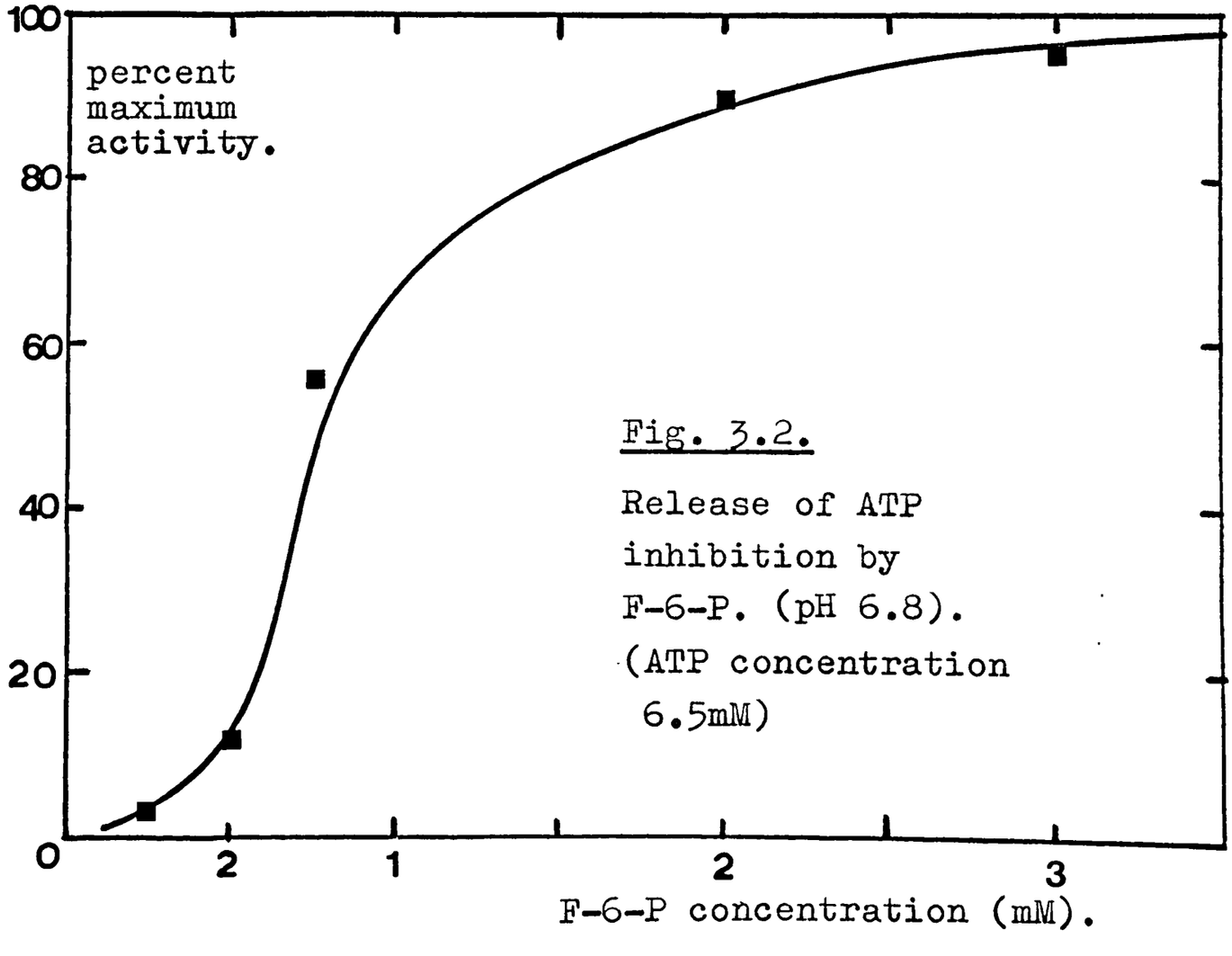

Fig. 3.2.

Release of ATP inhibition by F-6-P. (pH 6.8). (ATP concentration 6.5mM)

It has, however, been observed that PFK will also catalyse the phosphorylation of glucose-1-phosphate at a much lower rate than that for F-6-P. (Eyre and Pette,1967)[41] Furthermore, the G-1-P activity is modified by the same inhibitors and activators as the F-6-P activity, and the two substrates compete for the same active site. The G-1-P activity is sufficiently low to enable measurements to be made at the high enzyme concentration. It was found (Fig. 3.3) that there was a linear relationship between the activity and protein concentration over the range 0.2 - 2.0 mg/ml where there is a significant change in the state of aggregation of the enzyme. This result shows that the G-1-P activity and probably the F-6-P activity of PFK is not affected by the self-association of the enzyme.

(iv) Replacement of Magnesium by Manganese.

The activity of PFK is dependent on the presence of magnesium ions, which are complexed by the substrate ATP. It was found that the substitution of manganese for magnesium resulted in almost no change in the F-6-P activity. Although this observation was not pursued, it opens up the possibility of the use of Nuclear Magnetic Resonance techniques to investigate the active site and mechanism of the enzyme.

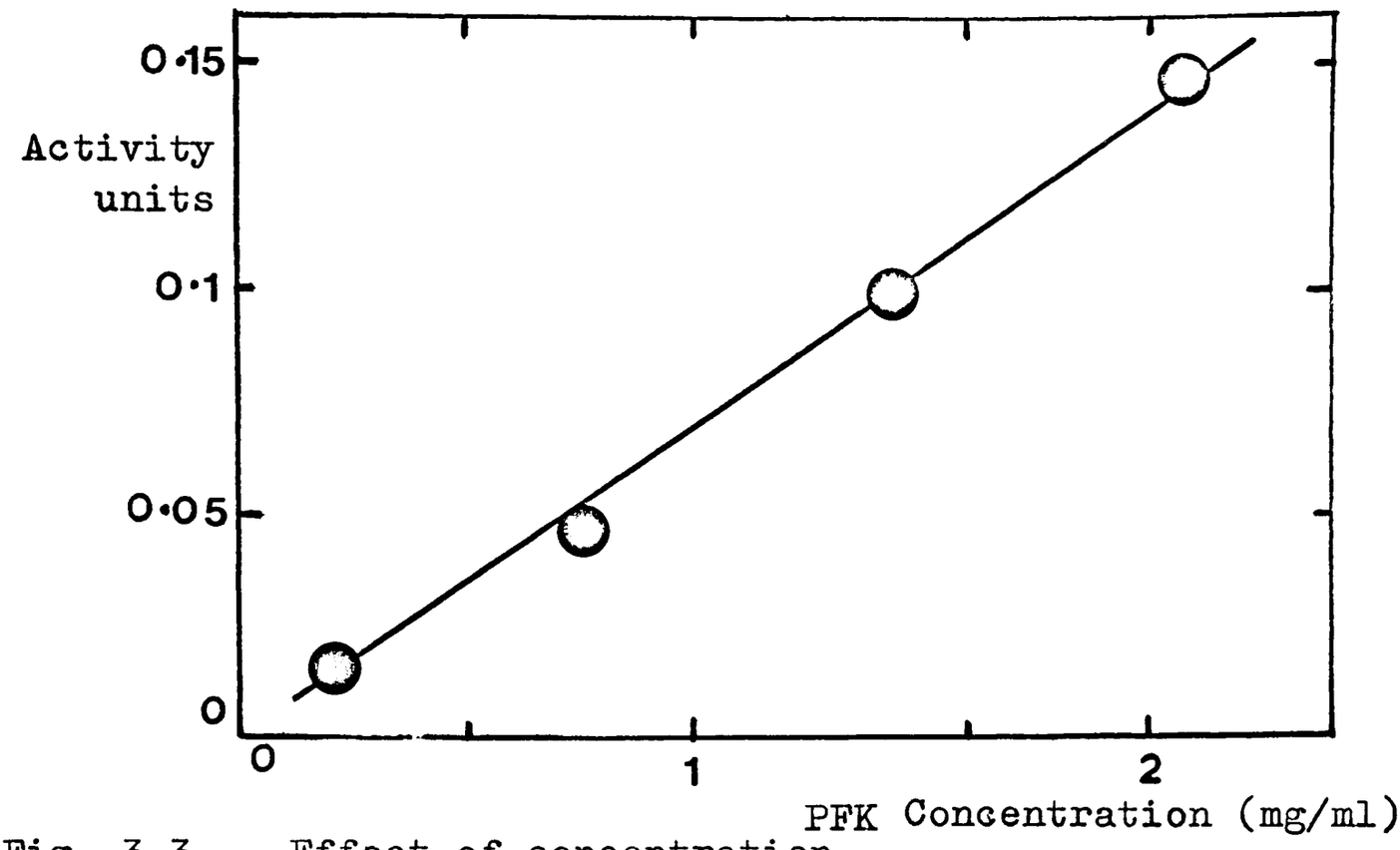

Fig. 3.3. Effect of concentration on G-1-P activity of PFK.

(B) Aldolase.

Aldolase was assayed by the method of Jagannathan et al (1956).[42] The dihydroxy-acetone phosphate formed on cleavage of FDP is reacted with hydrazine and the rate of hydrazone formation, which is proportional to the enzyme activity, is measured by the increase in optical density at 240nm. 1 ml of the diluted enzyme was added to 1 ml of hydrazine sulphate (7μM/ml) and 1 ml of FDP solution (12μM/ml) in 0.1M Tris buffer, pH 7, contained in a 3ml cuvette. Measurements were made at 25°c using a Beckman DB spectrophotometer with a reference cuvette containing the same reagents.

Chapter 4. Hydrodynamic Studies.

1. Theoretical Introduction.

(i) The Sedimentation Coefficient.

The sedimentation coefficient of a particle in a centrifugal field is defined as the velocity per unit field strength,

$$s = \frac{\frac{dr}{dt}}{\omega^2 r}$$

Where s is the sedimentation coefficient, r is the distance of the particle from the axis of rotation, ω is the angular velocity and t is time (seconds).

The integral of this equation is,

$$s = \frac{1}{\omega^2} \frac{\ln r}{t} + \text{a constant.}$$

Using this equation, the sedimentation coefficient is derived from the slope of ln r against t. For convenience, s is normally measured in Svedberg units (S) where

$$1\,S = 1 \times 10^{-13} \text{ sec.}$$

The sedimentation coefficient is normally converted to standard conditions for water at 20°C.

$$s_{20,w} = s_{app} \frac{\eta_t}{\eta_{20,w}} \frac{(1 - \bar{v}\rho_{20,w})}{(1 - \bar{v}\rho_t)}$$

Where η_t and $\eta_{20,w}$ are the viscosities of solvent at t°C and water at 20°C respectively, $\bar{v}$ is the partial specific volume of the sedimenting species and ρ_t, $\rho_{20,w}$ the

densities of the solvent at t°C and water at 20°C resp. The sedimentation coefficient can also be extrapolated to infinite dilution using values of $s_{20,w}$ at a number of concentrations, giving $s^{o}_{20,w}$. This eliminates the effect of concentration on the sedimentation coefficient, since the value of $s_{20,w}$ normally decreases as the sedimenting species becomes more concentrated.

(ii) The Frictional Ratio.

By equating the centrifugal force with the frictional resistance for a particle moving at uniform velocity, the following equation is obtained,

$$\omega^2 rm(1 - \bar{v}\rho) = f \frac{dr}{dt}$$

Where m is the particulate molecular weight, $\bar{v}$ its partial specific volume and f is a constant.

Since, $s = \frac{1}{\omega^2 r} \frac{dr}{dt}$ and $M = Nm$, (N = Avogadro's Number)

the above equation becomes,

$$f = \frac{M(1 - v\rho)}{Ns}$$

The 'frictional factor', f, is related to the shape of the sedimenting particle, and increases with increasing asymmetry.

For rigid, unsolvated spheres, f has a minimum value, f_o, which is given by Stokes Law :

$$f_o = 6\pi\eta r$$

For a molecule of partial specific volume $\bar{v}$,

$$r = \left(\frac{3M\bar{v}}{4\pi N}\right)^{1/3}$$

therefore,

$$f_o = 6\pi\eta\left(\frac{3Mv}{4\pi N}\right)^{1/3}$$

If s, M, and $\bar{v}$ are known for the molecule, the ratio $\frac{f}{f_o}$ can be calculated. This is known as the 'frictional ratio'. If the value of $\frac{f}{f_o}$ determined experimentally is equal to unity, the molecule must be spherical. If the frictional ratio is greater than 1, it may be asymmetric or hydrated, or both. Assuming that there is no hydration, a maximum value for the asymmetry in terms of the axial ratio can be can be calculated from the equations of Perrin[43] by considering the particle to approximate in shape to an oblate or prolate ellipsoid.

Conversely, if the molecule is assumed to be spherical, the maximum hydration can be calculated from

$$\frac{f}{f_o} = \left(1 + \frac{w}{\bar{v}}\right)^{1/3}$$

Where w is grams of water per gram of sedimenting particle.

(iii) Determination of molecular weights from sedimentation and diffusion data.

By application of Fick's Law of diffusion it can be shown that the frictional factor is also related to the Diffusion coefficient at infinite dilution, D^o, by the equation,

$$f = \frac{RT}{D^o N}$$

If this is combined with the [redacted] equation at infinite dilution, the following equation is obtained:

$$M = \frac{s^o}{D^o} \frac{[redacted] RT}{(1 - \bar{v}\rho)}$$

Thus, the molecular weight can be calculated from the ratio of s^o to D^o .

Diffusion coefficients were measured in the centrifuge by the spreading boundary method. Using schlieren optics, a synthetic boundary was formed between solvent and solution. As the boundary spread by the diffusion of solute into the solvent, the height, h, and the area, A, of the schlieren peak was measured at known time intervals, t . If the centrifuge is run at a low speed so that centrifugal transport is negligible, the diffusion coefficient is given by,

$$D = \frac{1}{4\pi t}\left(\frac{A}{h}\right)^2$$

and can be determined from a plot of $\left(\frac{A}{h}\right)^2$ against t . The diffusion coefficient obtained in this way was extrapolated to infinite dilution to obtain D^o .

(iv) Viscosity.

As shown by Einstein[44] for spherical particles and Simha[45] for ellipsoids, the viscosity, η' , of a particulate suspension is given by,

$$\eta' = \eta (1 + \nu\phi)$$

Where η is the solvent viscosity and ϕ the volume fraction

of solute particles. ν is a constant which equals ~2.5 for spherical particles and is greater than 2.5 for ellipsoidal or asymmetric particles. ν like $\frac{f}{f_o}$ is related to the axial ratio of the ellipsoid. This equation is only valid for infinitely dilute solutions and for Newtonian viscosity where there is random orientation of the solute particles.

Viscosity data can be expressed in terms of the specific viscosity, $\eta_{sp} = \frac{\eta' - \eta}{\eta}$

Therefore, $\eta_{sp} = \nu\phi$,

and is proportional, at infinite dilution, to the concentration of suspended particles. Thus, the limiting value of η_{sp}/C (the reduced viscosity) is independent of C (the concentration) as C tends to zero. This is known as the intrinsic viscosity, $[\eta]$.

$$[\eta] = \lim_{C \to 0} \frac{\eta_{sp}}{C}$$

For a rigid, solvated macromolecule, $[\eta]$ is independent of the molecular weight but is related to ν the shape parameter.

2. Experimental Details.

(i) Sedimentation Velocity Experiments.

These and the sedimentation equilibrium studies described in Chapter 5 were carried out with a Beckman Spinco Model E analytical ultracentrifuge.

(a) Studies at high concentration.

At protein concentrations higher than 0.5mg/ml the schlieren optical system was used to measure the rate of movement of sedimenting boundaries.

A 2^{o} sector Kel-F 12mm centrepiece was used for most of the sedimentation experiments. This had the advantage of conserving material, since it required half the volume of solution necessary for the standard 4^{o} centrepiece, and was less subject to attack by alkali. For experiments where a solvent baseline was required (e.g. determination of concentration from the area of schlieren peaks) an aluminium-filled Epon double sector centrpiece was used.

Photographic plates were measured with a Projectorscope micro comparator using a 10 x magnification objective. The areas of schlieren peaks were measured by tracing an enlarged (approx 20 x) image on to graph paper. A planimeter was used to find the area of the tracing, which, after correction for enlargement gave the area of the schlieren pattern.

(b) Studies at low concentration.

Sedimentation coefficients at concentrations too low to be measured by the normal direct optical methods were estimated by the method of Goldwasser (1966)[146], using a moving partition separation cell.

The speed and time of sedimentation are chosen so that the sedimenting boundary moves part of the way between the meniscus and the partition rest position. Thus, there is a difference in the concentration of the sedimenting species in the upper part of the cell after sedimentation compared with that before sedimentation.

$$\text{If } Q = \frac{\text{concentration after sedimentation}}{\text{concentration before sedimentation}}$$

then, for a homogeneous material, neglecting diffusion, it can be shown[46] that,

$$s = \frac{-2.303}{2\omega^2 t} \log_{10}\left\{\left(\frac{r_m}{r_p}\right)^2 + Q\left[1 - \left(\frac{r_m}{r_p}\right)^2\right]\right\}$$

The concentration ratio, Q, can be determined by any method, including the activity in the case of an enzyme.

Graphs of ω^2 against t are plotted for acceleration and deceleration and $\omega^2 t$ estimated from the areas under the two curves is added to $\omega^2 t$ for the time that the centrifuge is running at constant speed. The meniscus position, r_m, and the partition position, r_p, are estimated from photographs taken at full-speed and 1000 rpm respectively

(ii) Viscosity Measurements

These were made in an Ostwald-type capillary viscometer (Fig. 4.1). The capillary was 26 cm long and 0.38 mm in diameter, giving a flow time for water of about 150 sec. The whole viscometer was immersed in a water bath maintained at 25±0.2°C. 2 ml of solution were pipetted into the wide limb of the U-tube and gentle suction with a filter-pump used to draw the liquid through the capillary into the top reservoir. The time taken for the solution to pass through the capillary under the force of gravity was measured with a stop watch. Measurements were made for the solvent at the beginning and end of a series of solution readings.

It was found that cleaning of the viscometer with a solution of NaOH in ethanol between measurements was essential to prevent erratic results caused by uneven wetting and surface tension effects.

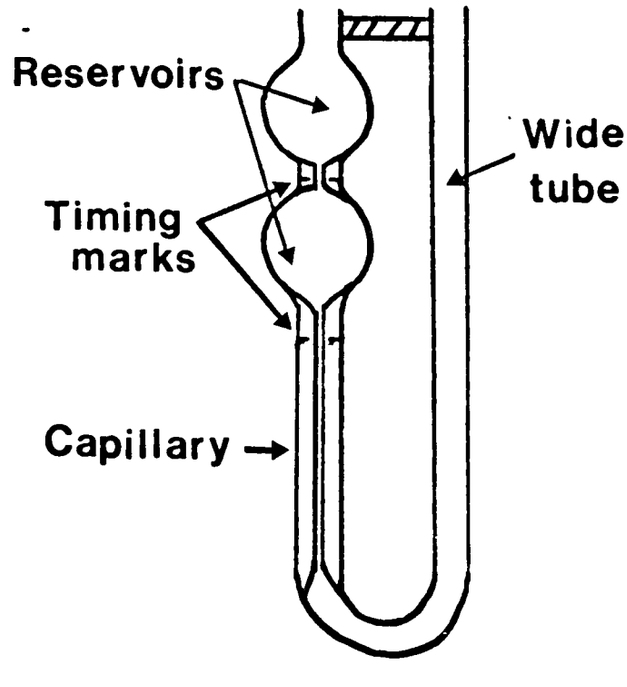

Fig. 4.1.

Ostwald Viscometer
(Not to scale)

3. Results.

(i) Sedimentation velocity experiments.

(a) Native PFK at pH 8.

The sedimentation pattern of PFK in 0.1 M Tris-phosphate buffer, pH 8, containing 10mM 2-mercaptoethanol and 0.5 mM FDP is shown in Fig. 4.2. This pattern of three overlapping peaks, of which the fastest moving is the most well defined, was characteristic of all preparations of the enzyme. Fig. 4.2 also shows how the proportion of the fastest component increased with increasing concentration. The appearence of the sedimentation pattern and the sedimentation coefficients of the individual peaks did not change significantly in the presence of 1 mM ATP, FDP or F-6-P. FDP was, however, added routinely to the buffer as it was found to prevent precipitation of the enzyme during dialysis against the buffer to remove ammonium sulphate.

The sedimentation coefficients for a number of PFK preparations are shown in Table 4.1 . The scatter of the values for the sedimentation coefficients of the two slowest components results mainly from the difficulty of measuring small rounded peaks which are not well separated from each other. The variation in s_{app} for the fast component, which can be measured quite accurately, results from the difference in concentration of each preparation.

(s_{NOP} = sedimentation coeff. uncorrected for concentration dependence.)

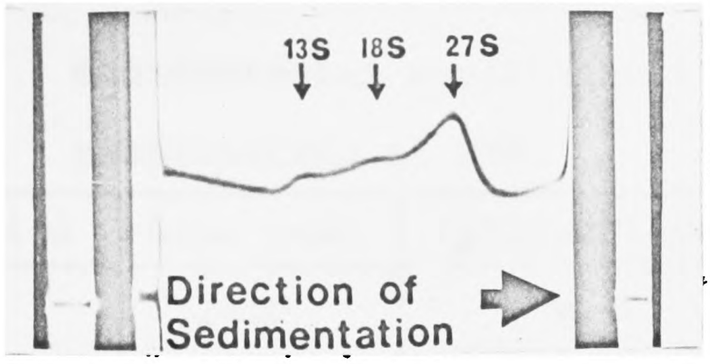

(a) 3mg/ml (approx) Schlieren angle 55°, speed 56100 rpm, photo taken 20 min. after reaching max. speed

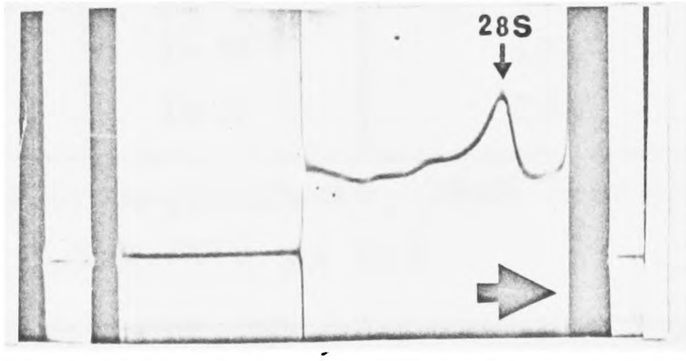

(b) 5mg/ml approx. Schl. angle 65°, speed 56100 rpm, photo taken 16 min. after reaching max. speed.

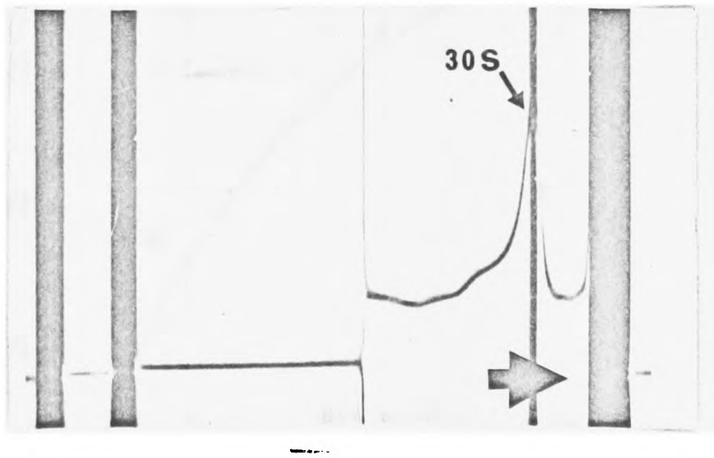

(c) 10mg/ml approx, Schl. angle 70°, speed 52640 rpm, photo taken 16 min. after reaching maximum speed.

Fig. 4.2. Sedimentation patterns for native PFK in 0.1 M tris-phosphate buffer, pH 8 ; 10mM 2-mercaptoethanol, 0.5mM FDP. Temperature 20°C.

Table 4.1 Sedimentation coefficients for a number of preparations of PFK.

Preparation	Slow peak	Intermediate peak	Fast peak
HM 4	14 S	20 S	31 S
HM 5	13 S	18 S	25 S
HM 6	12 S	17 S	27 S
HM 7	13 S	18 S	28 S
HM 9	13 S	18 S	28 S
HM 10	11 S	19 S	32 S
HM 11	14 S	18 S	29 S
HM 13	14 S	18 S	28 S

(All in 0.1M tris-phosphate, 10mM 2-mercaptoethanol, 0.5mM FDP, pH 8.)

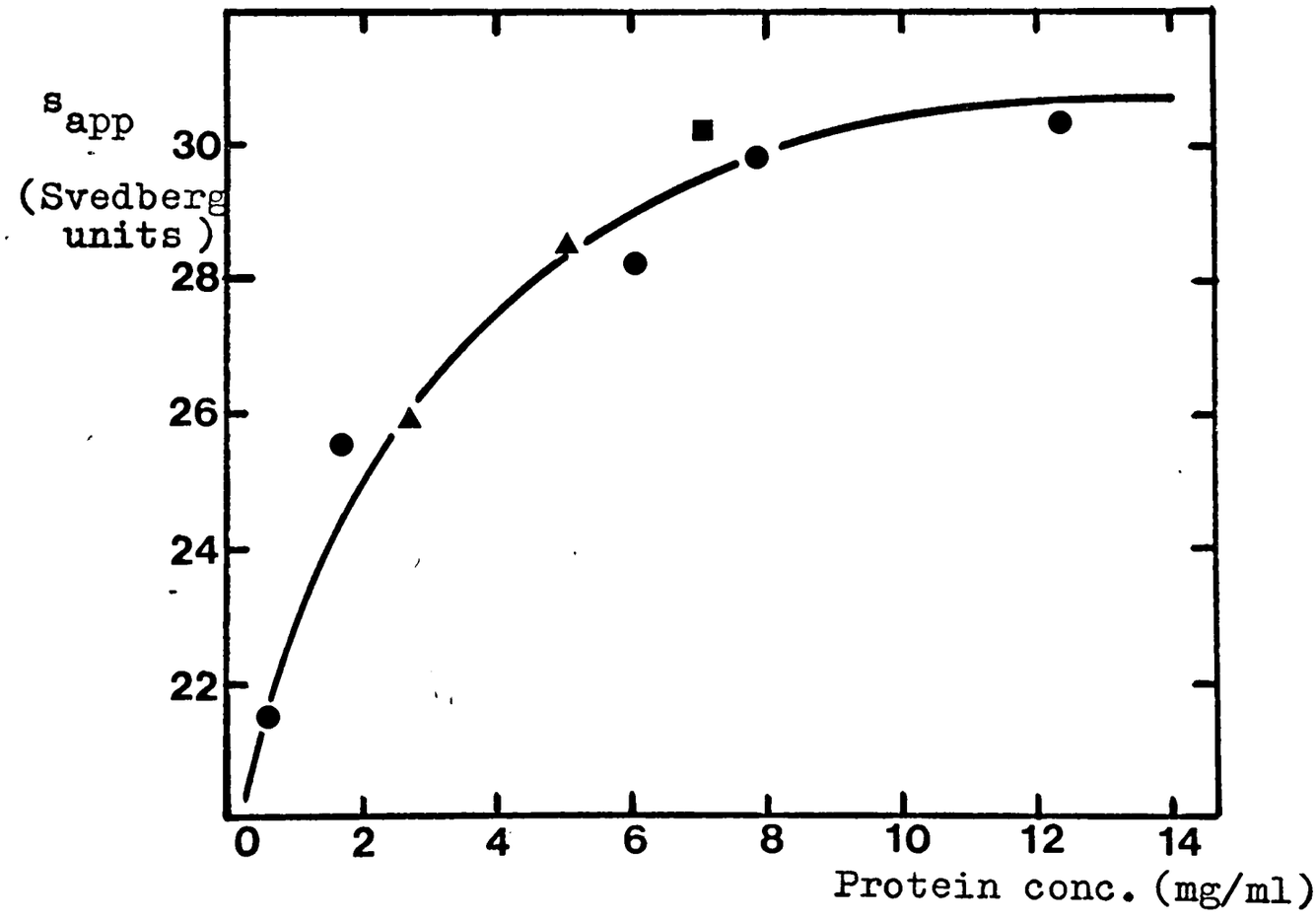

Fig. 4.3 Variation of s_{app} with protein concentration for the fast peak of the PFK sedimentation pattern. The symbols are for three preparations of the enzyme.

If s_{app} is plotted against concentration a curve is obtained (Fig. 4.3) which rises from 21 S at 0.5 mg/ml to about 30 S at 8 mg/ml above which there is little change. The sedimentation pattern and the behavior of s_{app} for the fast peak are both characteristic of a reversibly associating protein system.

(b) The effect of pH on the self-association of PFK.

As we have seen, the sedimentation pattern at pH 8 is dominated by the fast sedimenting, 30 S, material at high concentration. On increasing the pH, the pattern changes in favour of the slowest component, which has s_{app} equal to about 11 - 12 S. Above pH 11, there is a further reduction in sedimentation coefficient to about 4.5 Svedberg units. These changes are shown in Fig. 4.4.

The above changes were observed within one hour of direct adjustment of the pH by addition of NaOH solution. If, however, the pH is varied by dialysis rather than by direct adjustment, similar changes take place but at lower pH, so that at pH 10.5 there is a mixture of 11 S and slower moving material.

FDP was found to be highly effective in stabilising the slowest component of the native PFK sedimentation pattern. Dialysis of PFK into 0.1 M carbonate-bicarbonate buffer, pH 10.5 containing 10 mM 2-mercaptoethanol and

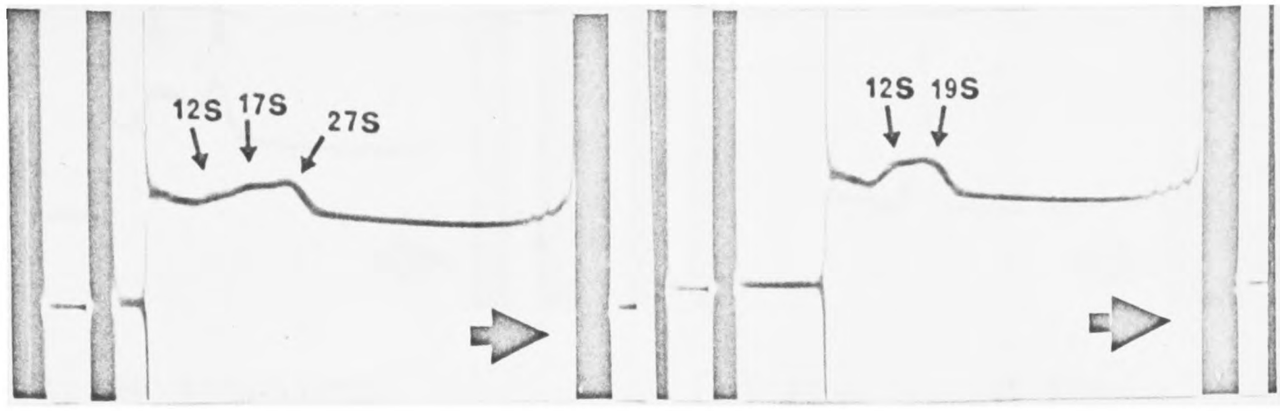

(a) pH 7.8 (b) pH 9

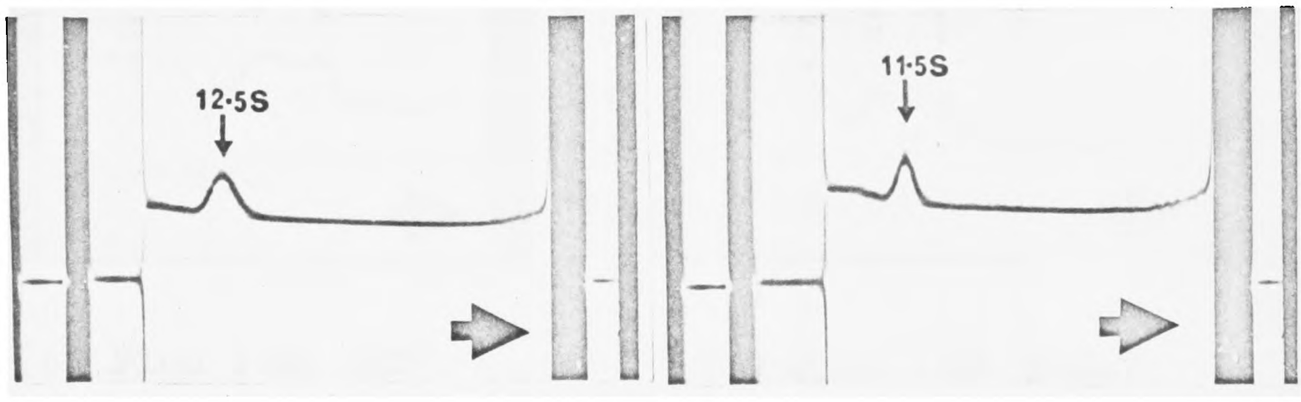

(c) pH 9.8 (d) pH 10.5

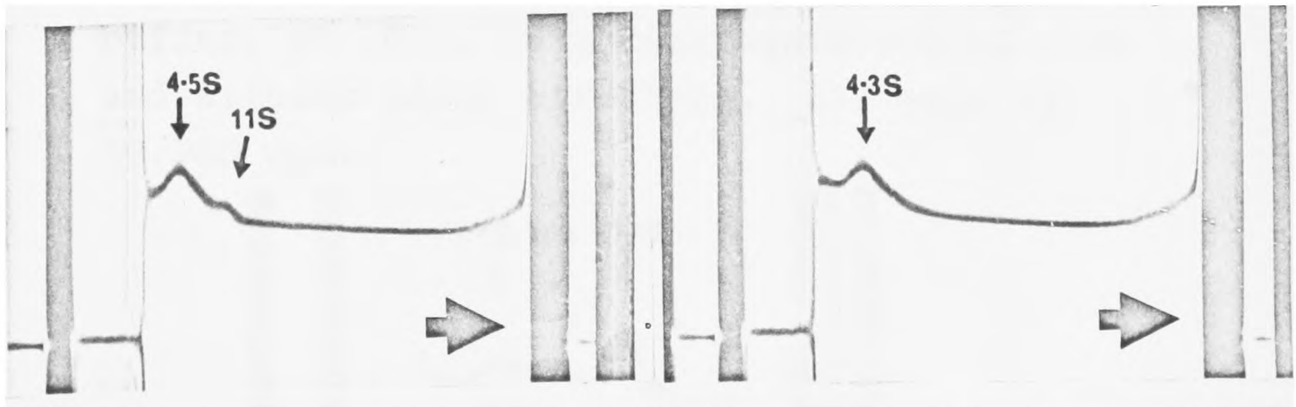

(e) pH 11 (f) pH 11.5

Fig. 4.4 Changes in the sedimentation pattern with increasing pH. (a), (b) and (c) were at 52640 rpm, (d), (e) and (f) at 59780 rpm

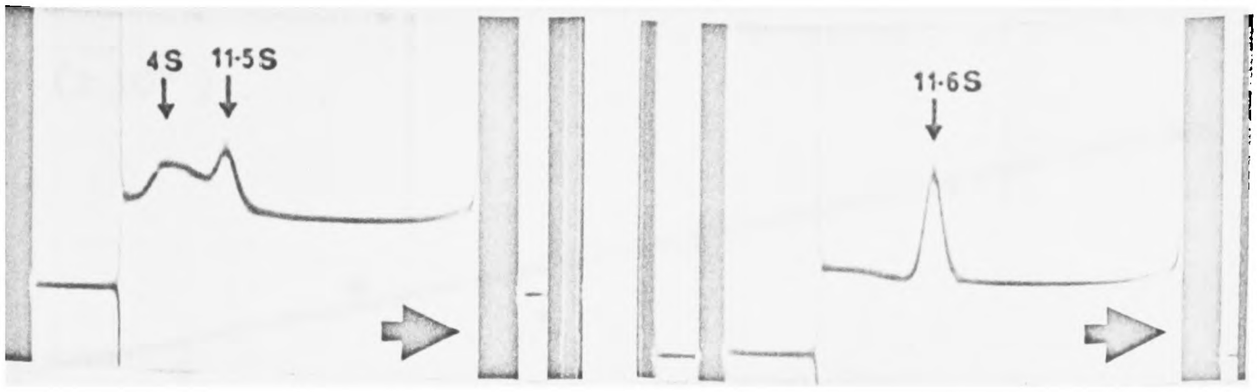

(a) No additions (b) Plus 0.5mM FDP

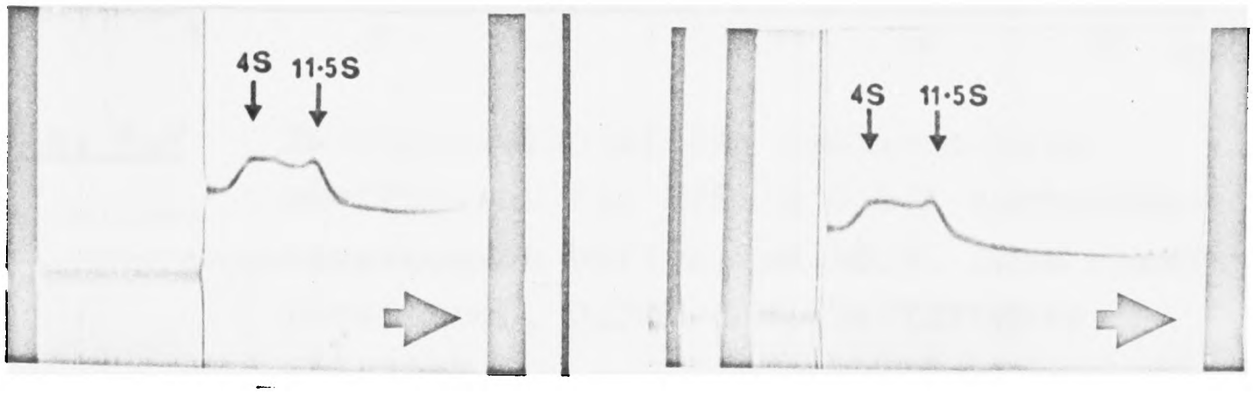

(c) Plus 1 mM ATP (d) Plus 1 mM F-6-P

Fig. 4.5 Sedimentation patterns of PFK which had been dialysed into 0.1 M carbonate-bicarbonate buffer, pH 10.5, 10mM 2-mercaptoethanol with and without added effectors. All were at 59,780 rpm.

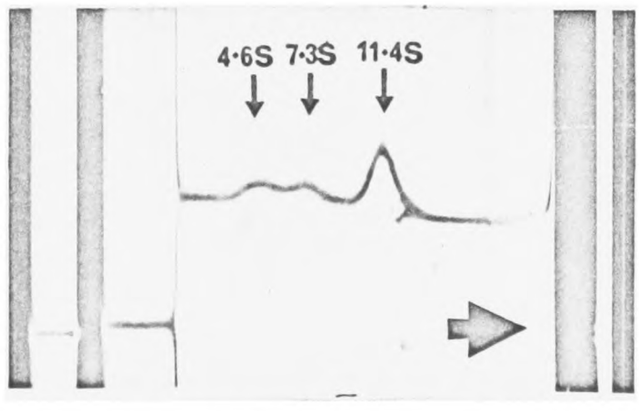

Fig. 4.6 Sedimentation pattern of PFK which had been dialysed into 0.1 M glycine-NaOH buffer, pH 11.1 plus 10mM 2-mercaptoethanol, 0.5mM FDP. Speed 59,780 rpm. Photo taken 30 min. after reaching full speed.

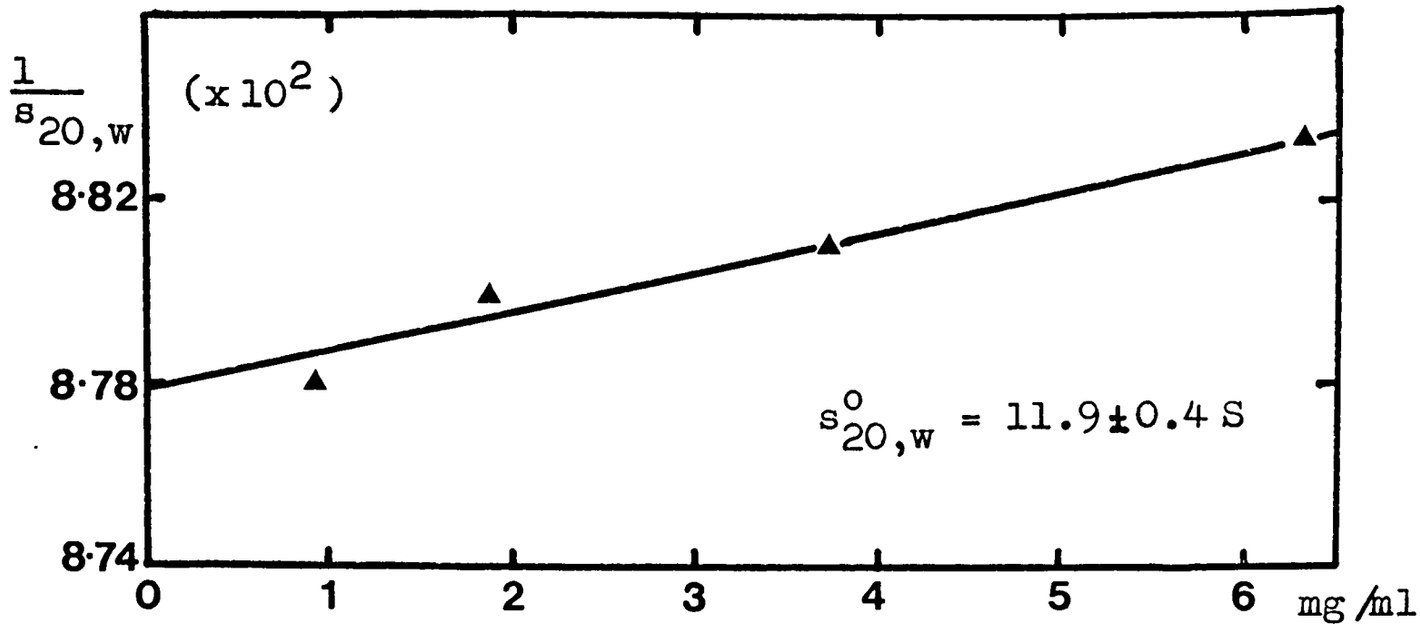

Fig. 4.7 Extrapolation of the sedimentation coefficient for PFK in 0.1 M carbonate-bicarbonate buffer, pH 10.5, 10mM 2-mercaptoethanol, 0.5mM FDP, to infinite dilution.

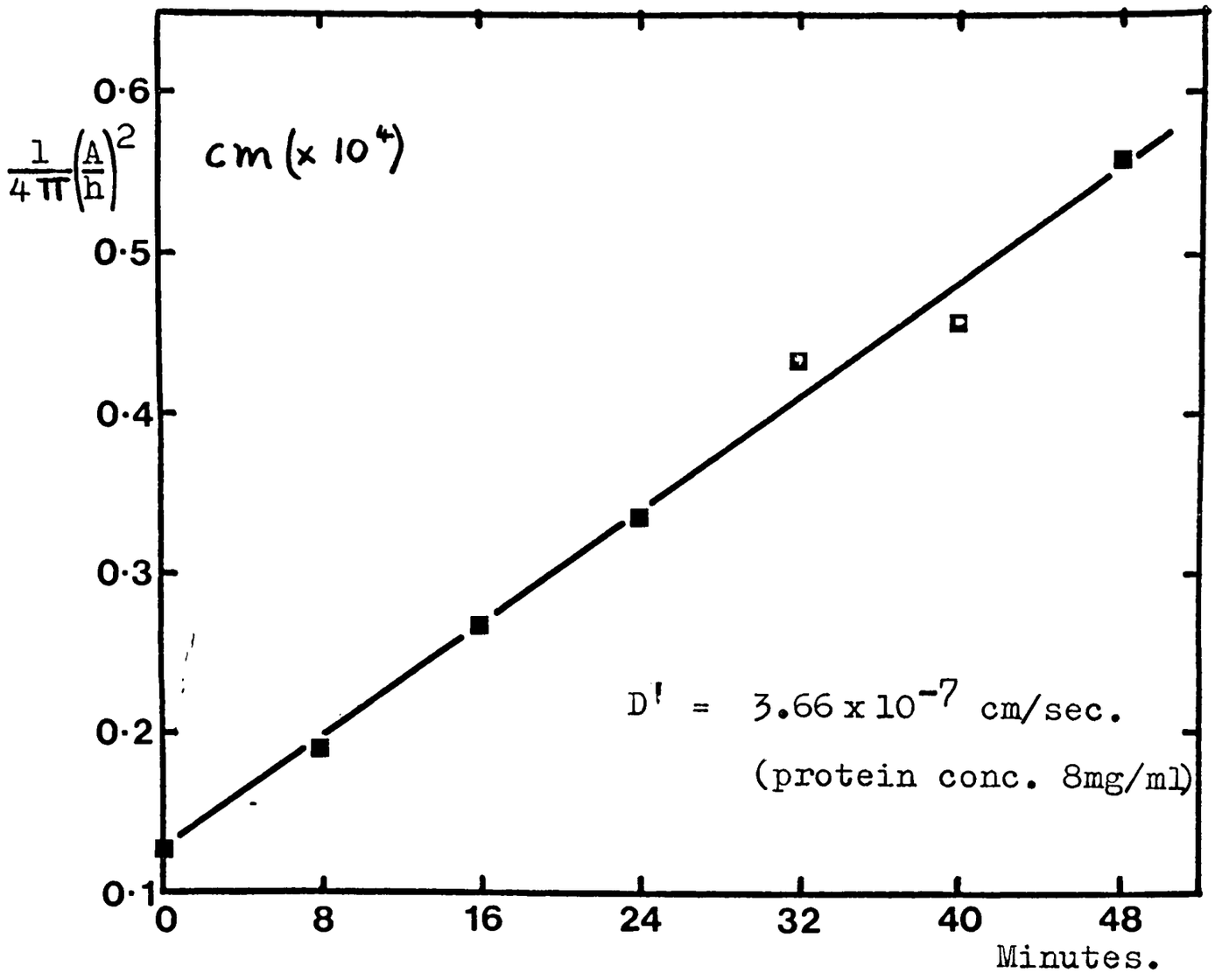

Fig. 4.8 Spreading boundary analysis for one concentration.

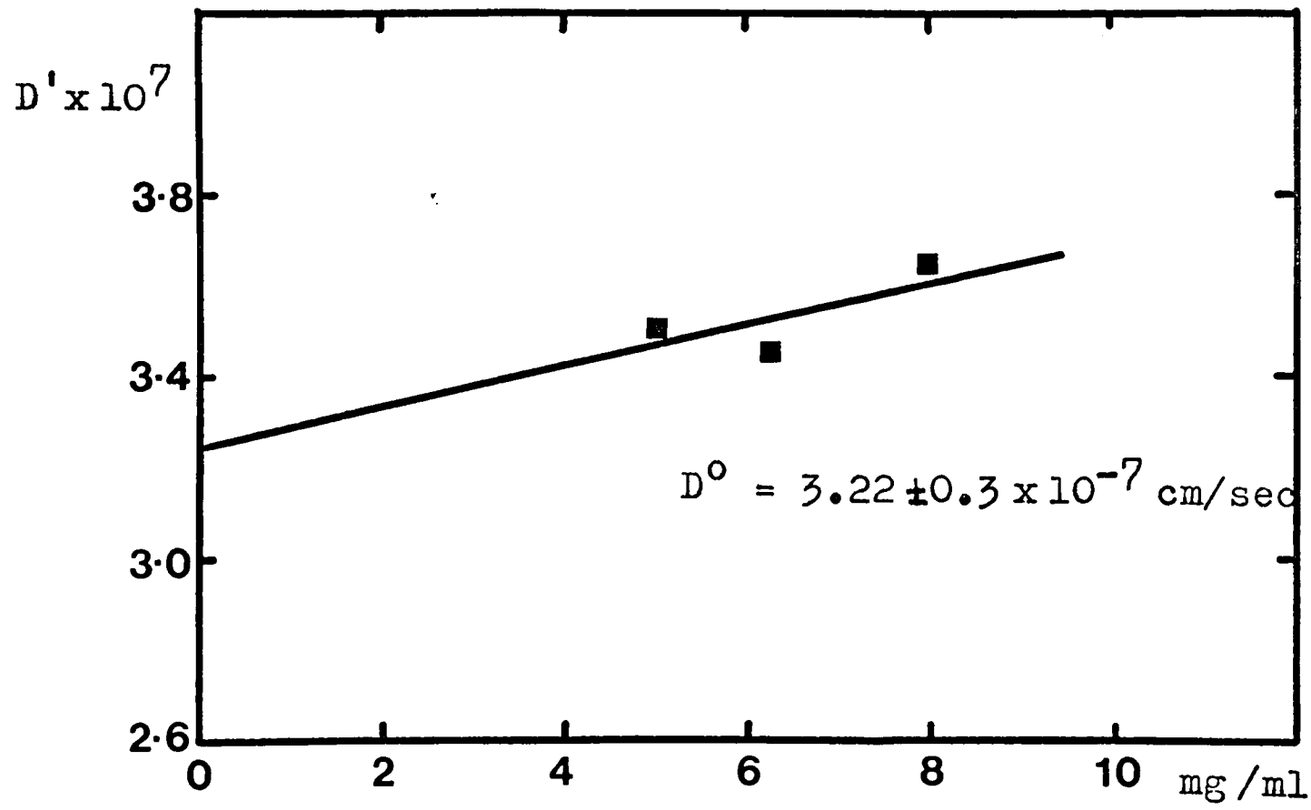

Fig. 4.9 Extrapolation of D' for the 12 S protein to infinite dilution.

0.5 mM FDP gave a single, sharp, symmetrical boundary. In the absence of FDP or in the presence of 1mM ATP or F-6-P there is a large amount of slower, presumably broken down, material present.(Fig. 4.5). At higher pH the FDP-stabilised material showed three distinct schlieren boundaries.(Fig. 4.6)

The sedimentation coefficient extrapolated to infinite dilution for the FDP stabilised protein at pH 10.5 (Fig. 4.7) was $s^{o}_{20,w}$ = 11.9±0.4 . The apparent diffusion coefficient for the stabilised '12 S' protein was also determined at three concentrations (Figs. 4.8 and 4.9). The value of $D^{o}_{20,}$ corrected for concentration dependence was $3.2 \pm 0.3 \times 10^{-7}$ cm sec^{-1}. This combined with the value of $s^{o}_{20,w}$ gives a molecular weight of $3.4 \pm 0.3 \times 10^{5}$ for the 12 S material.

(c) <u>The effect of high ionic strength.</u>

Dialysis of PFK into solutions of high salt concentration resulted in a disappearance of the triple boundary pattern characteristic of the native enzyme at pH 8. In 1 M sodium chloride, there was a single asymmetric boundary with $s_{20,w}$ = 13.4 Svedberg units. In 2 M NaCl, the boundary was symmetrical with $s_{20,w}$ equal to 11.9 S . On dialysis of the 2 M NaCl sample back into 0.1M buffer, the 'native' PFK pattern reappears. The appearance of PFK in 2M sodium chloride is shown in Fig. 4.10.

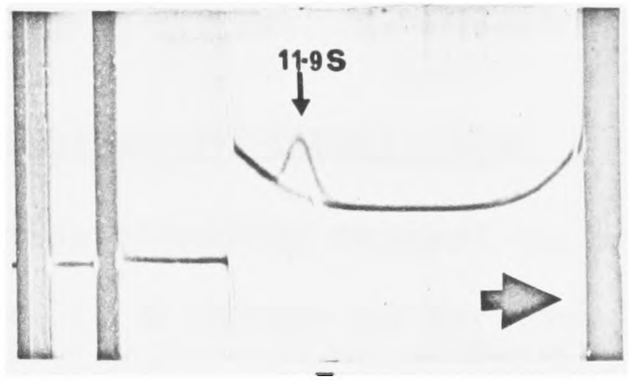

Fig. 4.10 The sedimentation pattern of PFK in 2 M sodium chloride, pH 8.
Speed 59,780 rpm.

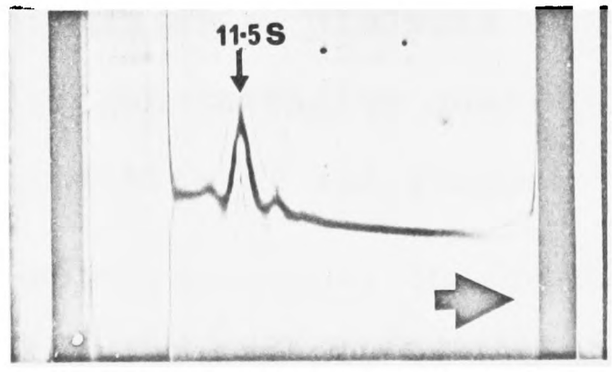

Fig. 4.11 The sedimentation pattern of PFK in 0.1M tris-phosphate buffer, pH 8, 10mM 2-mercaptoethanol, 0.5 mM FDP plus 0.03% wt/vol SDS .
Speed 59780 rpm

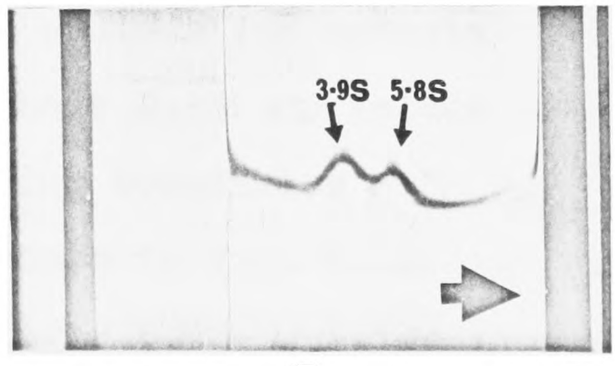

Fig. 4.12 The sedimentation pattern of PFK in 0.1M tris-phosphate buffer, pH 8, 10mM 2-mercaptoethanol, 0.5mM FDP plus 0.4% wt/vol SDS.
Speed 59,780 rpm.

(d) The effect of p-chloromercuribenzoate(PCMB).

Addition of this thiol blocking reagent to PFK solutions at pH 8 resulted in a change in the sedimentation pattern to a single peak with $s_{20,w}$ = 12.5. The change took place quite sharply at PCMB concentrations between 0.1 and 0.2 mM corresponding to an excess of between 5 and 10 moles of PCMB per 100,000g PFK. On allowing the PCMB treated material to stand, or on dialysis of PFK against PCMB solutions, a slight turbidity developed followed by complete precipitation of the enzyme.

Addition of excess 2-mercaptoethanol to the PCMB-treated enzyme results in the reformation of the native sedimentation pattern.

(e) The effect of sodium dodecyl sulphate (SDS).

At low concentrations of the detergent, the sedimentation pattern showed mainly a sharp 12 S peak, with small amounts of discrete faster sedimenting material (Fig. 4.11). At SDS concentrations of about 0.2% wt/ volume the enzyme sedimented as two slow moving boundaries with s_{app} equal to about 4 S and 6 S, as shown in Fig. 4.12. At higher concentrations of SDS a single 3.0 S species is present.

(f) Sedimentation coefficient at low concentration.

This was measured by the method outlined in section 2 (i)(b) above. The experiments were carried out in 0.1 M imidazole buffer, pH 7 using solutions containing approx. 1 μg/ml of PFK. The concentration of protein in the upper half of the partition cell after sedimentation was estimated from the enzyme activity relative to a duplicate sample which was placed in a second centrifuge cell for the duration of the sedimentation experiment.

The following results were obtained: -

PFK + 6mM ATP, $s_{app} = 11.3 \pm 1.2$

PFK + 1mM FDP, $s_{app} = 10.6 \pm 0.9$

PFK + No ATP or FDP, $s_{app} = 10.5$ (one determination only)

It would appear, therefore, that the sedimentation coefficient of PFK at the enzymic level is close to the value for the slowest component of the sedimentation pattern at high concentration. Furthermore, there did not appear to be any change in sedimentation coefficient in the presence of a concentration of ATP which causes complete inhibition of the enzyme (see Chapter 3).

To check the method, the sedimentation coefficient of aldolase was also measured at 50 μg/ml using both the enzyme activity and the UV absorption at 190nm.to measure the protein concentration. The former method gave s_{app}

equal to 6±1.1 S and the latter 6.5±0.8 S compared with the value of 7.5 S measured by schlieren optics at high concentration.

(g) Sedimentation in 6M Guanidine hydrochloride, 0.1 M 2-mercaptoethanol.

This solvent has been shown by Tanford et al (1967)[47] to destroy completely the tertiary and secondary structure of proteins so that they behave as random coils. The reducing agent, 2-mercaptoethanol, is added to break any inter or intra-polypeptide disulphide bonds and to prevent their formation in the denatured protein. From results for several proteins of differing molecular weight, the following relationship between s^{o}_{25} and the chain length, n, was obtained,

$$\frac{s^{o}_{25}}{(1 - \bar{v}^{*}\rho)} = 0.286\, n^{0.473}$$

Where $\bar{v}^{*}$ is the partial specific volume of the protein in 6 M GuHCl, taken as 0.01 less than the psv in water.

Protein solutions were dialysed for 3 days against 3 changes of GuHCl to ensure complete equilibration. The sedimentation coefficient was measured at 25°C and 52640 rpm on a synthetic boundary formed in a double sector cell. Figure 4.13 shows results obtained for PFK and aldolase. The value of s^{o}_{25} for aldolase was 0.768±0.022 Svedberg units

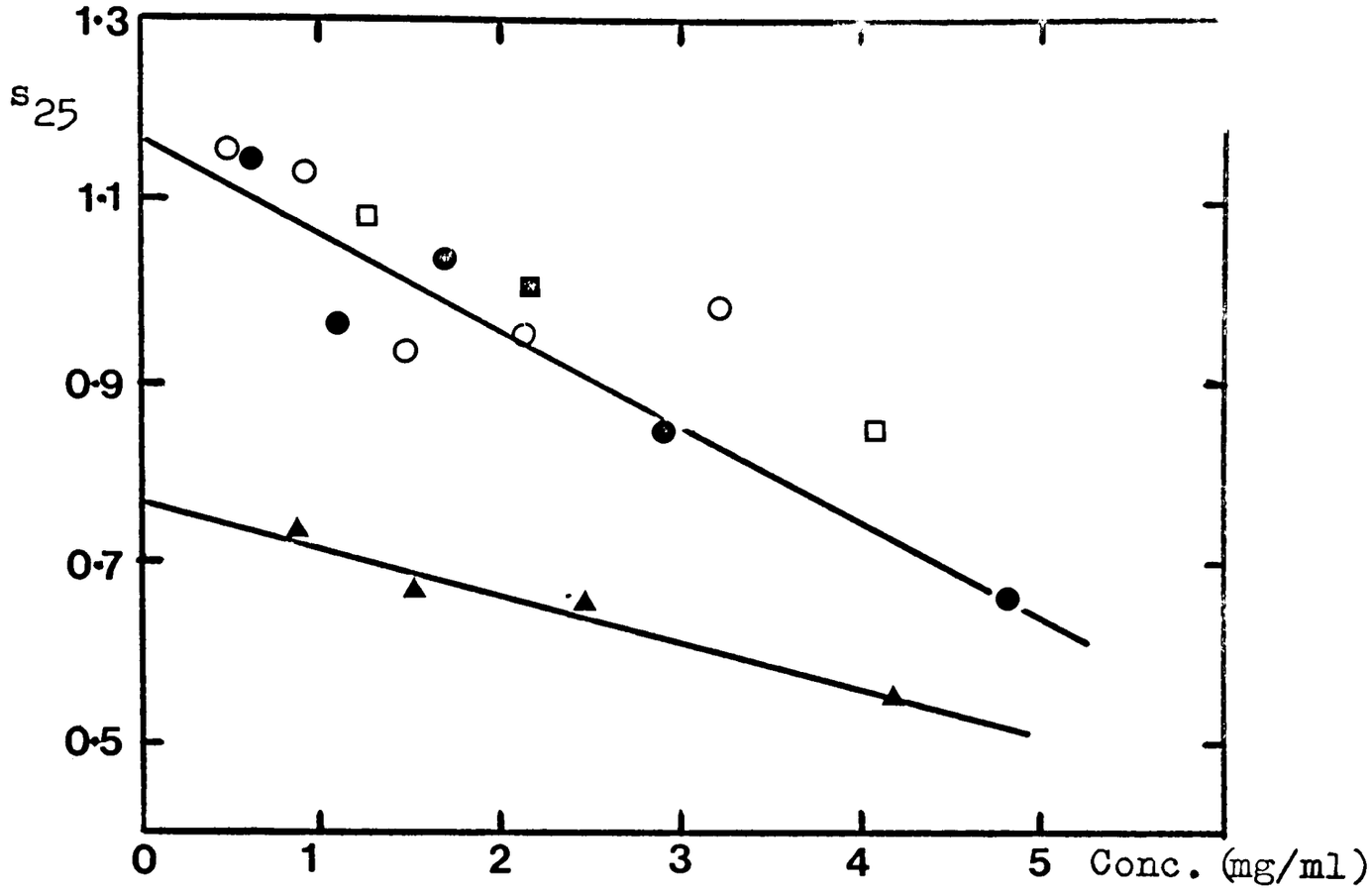

Fig. 4.13. Extrapolation of the sedimentation coefficients at 25°C for aldolase and PFK in 6 M GuHCl, 0.1 M 2-mercaptoethanol (or dithiothreitol) to infinite dilution.

Symbols:-

▲ Aldolase.

● and ○ PFK , 0.1M 2-mercaptoethanol, pH 7

□ PFK, 0.1M 2-mercaptoethanol, pH 3.

■ PFK, 0.1M dithiothreitol, pH 7.

compared with 0.725 reported by Tanford,[47] corresponding to a molecular weight of $3.9 \pm 0.25 \times 10^4$. The value for PFK was 1.17±0.05 S corresponding to a molecular weight of about 90,000 (Taking 115 to be the mean residue molecular weight).

These results were obtained for the GuHCl solution adjusted to pH 7 which is the optimum pH for reduction of disulphide bonds (Tanford et al, 1967).[47] Measurements were also made at pH 3 with 2-mercaptoethanol and at pH 7 with dithiothreitol as the reducing reagent. Although complete extrapolations were not done under these conditions, the values of s_{app} fell on, or close to, the lines for extrapolation of the data at pH 7.

(ii) Viscosity Results.

The results for aldolase and PFK are shown in Fig. 4.14. The intrinsic viscosity for aldolase was about 4±1 ml/gram, a value which is typical for compact globular proteins, and which agrees with the value of 4ml/gm obtained by Stellwagen and Schachman (1962).[48] Although the results for PFK show greater scatter, especially at the lower concentrations, it can be seen that the intrinsic viscosity is much higher (about 11±2.5 ml/gm) and that the specific viscosity varies with concentration in an anomalous manner. The curve falls off to a minimum at about 5 mg/ml and then

begins to rise again. The concentration range over which the viscosity falls off is also the range over which changes in the sedimentation coefficient took place (section (i)(a) above).

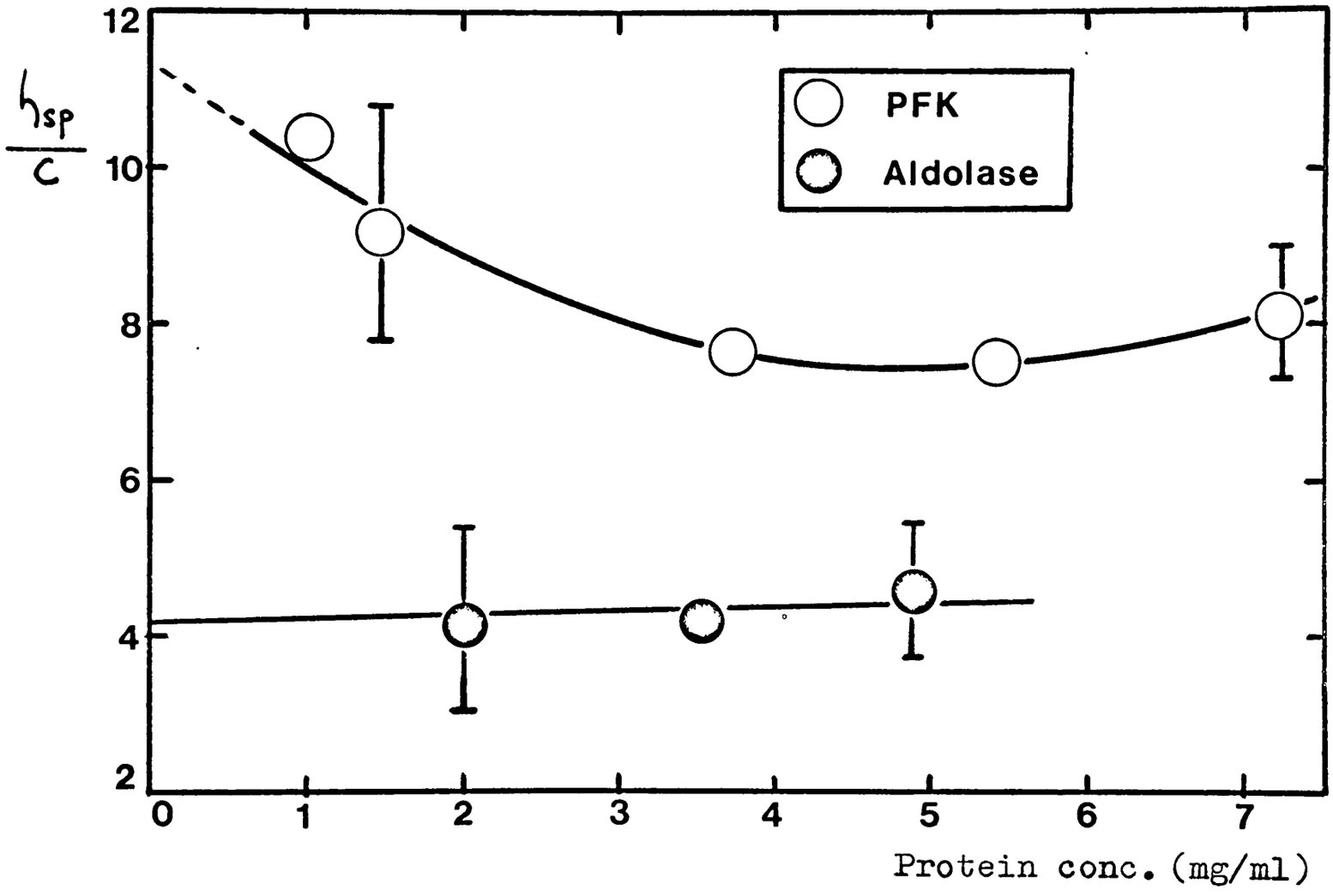

Fig. 4.14. Viscosity results for Aldolase and PFK. Aldolase was measured in 0.1 M NaCl, and PFK in 0.1 M tris-phosphate, 0.5mM FDP, pH 8.

4. Discussion of Hydrodynamic Results.

(i) Sedimentation velocity results.

(a) Native PFK at pH 8 (high protein concentration).

The sedimentation pattern of native PFK and the decrease in sedimentation coefficient of the fast peak with decreasing concentration are characteristic of a reversibly interacting protein system (Schachman, 1959;[46] Kegeles et al, 1964).[49]

Although the pattern indicates that self-association of the protein is taking place, and will give qualitative information about the effect of pH or other reagents on the equilibrium, it is only possible in the simplest of cases to obtain quantitative information about monomer-polymer equilibria from transport experiments. Various attempts have been made to calculate theoretical distribution patterns for associating systems.

Gilbert (1959)[50] has shown that in the simplest case of monomer $\rightleftharpoons$ n-mer with no intermediate species present, a single boundary would be observed in the case of monomer $\rightleftharpoons$ dimer, and a bimodal boundary in the case of monomer $\rightleftharpoons$ n-mer, where $n > 2$. If kinetic effects become important (i.e. the half time of the association or dissociation is of the same order of magnitude as the time of the sedimentation experiment) the pattern may

become even more complicated. In this case, Belford et al (1962)[51] predict one, two or three schlieren boundaries for a dimerisation reaction under different kinetic conditions. Similar results have been obtained by Bethune and Kegeles (1961)[52] who applied counter-current distribution theory to the problem.

It is therefore dangerous to interpret a sedimentation pattern of this type in terms of the observable schlieren boundaries without other evidence for the number of species present and the nature of the association. For this reason, the suggestion of Ling et al (1965)[35] that the sedimentation pattern of PFK represents a monomer-dimer-tetramer association, based on molecular weights estimated from the sedimentation coefficients, is not valid without other evidence to support it.

(b) The 12 S protein.

The apparently homogeneous material with $s^{o}_{20,w}$ = 11.9 S at pH 10.5 in the presence of FDP, and the native enzyme at low concentration (s_{app} = 10.5 S approx) probably correspond to the slowest component of the native sedimentation pattern at high concentration (s_{app} = 11 - 14 S). This is supported by the change in the sedimentation pattern with increasing pH which must represent a shift in the equilibrium position of the association in favour of

the 12 S 'monomer'.

The frictional ratio calculated from the sedimentation and diffusion coefficients of the 12 S protein is $\left(\frac{f}{f_o}\right)_{max}$ (neglecting hydration) = 1.44. This value indicates that the molecule is either highly asymmetric or has a high degree of solvation. Electron micrographs of PFK (Parmeggiani et al, 1966[5]; this work) show flat, almost rectangular molecules whose approximate dimensions are 100 A x 100 A x 50 A, corresponding to a molecular weight of $3-4 \times 10^5$. This is consistent with the frictional ratio of the 12 S protein as a molecule of this shape would be expected to behave as an asymmetric hydrodynamic particle. For comparison, Pyruvate carboxylase has been shown by electron microscopy to be a square-planar tetramer with four subunits, each of molecular weight 1.6×10^5 (Valentine et al, 1966)[129] This protein has a frictional ratio, neglecting hydration, of 1.59.

The frictional ratio for aldolase, taking $s^o_{20,w}$ = 7.8S, $M = 1.6 \times 10^5$ and $\bar{v} = 0.75$ is 1.24. Electron micrographs of aldolase (Rutter et al, 1967)[3] show it to have four subunits arranged as a tetrahedron. The molecule thus approximates more closely to a spherical hydrodynamic particle, giving a lower value for the frictional ratio.

(c) The effect of dissociating reagents.

The association of PFK at high concentration can be prevented by relatively mild dissociating conditions such as weakly alkaline pH, low concentrations of detergent and high ionic strength. Breakdown of the 12 S protein requires stronger denaturing conditions. The protein-protein interactions involved in the polymerisation of the 12 S protein must, therefore, be considerably weaker than those involved in the stabilisation of its quaternary and tertiary structure. The latter interactions are stabilised by FDP, but this and other effectors do not have any measureable influence on the association. This is in complete contrast to Glutamate dehydrogenase (GDH) which shows a decrease in the polymerisation,which occurs at high protein concentration, on binding the allosteric effector NADH (Eisenberg and Tomkins, 1968;[53] Frieden,1966[54])

The effect of high ionic strength,which prevents the association of the 12 S protein, points clearly to the participation of charge interactions (i.e. salt-linkages) in the interprotein binding. The effect of very low concentrations of detergent, which also inhibit polymerisation, may indicate some degree of hydrophobic interinteraction, since the detergent would be expected to interact with hydrophobic regions. However, it could also be explained in terms of electrostatic binding of the

anionic detergent molecule to the protein which would inhibit polymerisation.

The disaggregating effect of PCMB suggests at first sight that labile disulphide bonds may also be involved in the polymerisation process. The polymerisations of cytochrome b_2 (Armstrong et al, 1960)[55] and urease[56] (Creeth and Nichol ,1960) have been attributed to disulphide formation. In the latter case, addition of sulphite ion, which cleaves disulphide bonds and reacts with free SH groups, completely prevented the association. This reagent(0.05 M Na_2SO_3) was added to PFK and had no effect on the sedimentation pattern. The method of Chan (1968)[57] which utilises sulphite in the presence of O_2 with catalytic amounts of cysteine to sulphonate SH residues also gave negative results. The effect of PCMB may therefore be simply steric, preventing the close contact of two polymerisation sites.

The effect of SDS at pH 8 is interesting as it appears to act selectively at different levels of the protein structure. Thus, at low concentrations (less than 0.1%) it prevents the association of the 12 S protein. At intermediate concentrations (0.1% - 0.5%), two discrete sedimenting species are present with $s_{app} \simeq 4$ S and 6 S . A Z-average molecular weight (Chapter 5) of 1.4×10^5 was obtained for PFK in 0.4% SDS which is consistent with a mixture of two components, $M = 9 \times 10^4$ and 1.8×10^5 approx.,

which would be about 1/4 and 1/2 of the molecular weight of the 12 S protein. The 6 S material in SDS and the 6 - 7 S intermediate peak observed in the sedimentation pattern at pH 11.5 in the presence of FDP (Fig. 4.6) are probably the same as the 7 S dimer ($M = 1.92 \times 10^5$) obtained in 0.8 M urea, 0.8mM FDP, pH 5.8 by Paetkau and Lardy (1967).[58]

At higher concentrations of SDS (greater than 0.5%) the 6 S peak disappears and there is a reduction in s_{app} for the slower component to about 3 S . This high concentration of detergent appears to have almost completely denatured the protein so that the sedimentation coefficient approaches the value of $s^o_{20,w} = 2.74$ obtained in 6 M GuHCl, 0.1 M 2-mercaptoethanol.

The results of the sedimentation studies in 6 M GuHCl, 0.1 M 2-mercaptoethanol are discussed with the results of the equilibrium studies in Chapter 5.

(ii) Viscosity results.

The high value of the intrinsic viscosity for PFK (11 ± 2.5 ml/gm) suggests a molecule with a high degree of asymmetry which is consistent with the high value of $\left(\frac{f}{f_o}\right)_{max}$ obtained for the 12 S protein.from the sedimentation studies. The anomalous decrease in viscosity over the range of concentration at which PFK undergoes self-association may reflect a decrease in asymmetry as the protein associates.

It is interesting to compare the viscosity of PFK with that obtained for GDH by Sund (1963).[59] GDH, which is thought to form a long rod-like polymer at high concentration (Eisenberg and Tomkins, 1968),[53] has a reduced viscosity at 8mg/ml of 24.5 ml/gm and a molecular weight(M_w) of 1.6×10^6. PFK at the same concentration has a reduced viscosity of about 8 ml/gm and a weight-average molecular weight of again about 1.6×10^6 (see Chapter 5). Thus, for the same molecular weight, PFK has a much lower viscosity suggesting that it is much less asymmetric than GDH at this concentration.

Chapter 5. Sedimentation Equilibrium Studies on PFK.

1. Theoretical Introduction.

(i) Monodisperse Solutions.

An expression for the concentration distribution of a macromolecular solution at sedimentation equilibrium was first derived by Svedberg and Pedersen (1940)[60] who considered centrifugal transport to be balanced by centripetal diffusion. The theory was placed on a firmer basis by Goldberg (1953)[61] who carried out a thermodynamic analysis of the equilibrium process. He considered the potential energy of the solute macromolecules to be composed of two parts, the chemical potential which is a function of concentration and the centrifugal potential which is a function of the distance of the macromolecule from the axis of rotation of the centrifuge. Since the total potential is constant, for any species ,i,

$$d\mu_i - M_i\omega^2 r\, dr = 0$$

This leads to the following equation for the concentration distribution of i ,

$$M_i = \frac{RT}{(1 - \bar{v}\rho)\omega^2} \cdot \frac{1}{C_i} \cdot \frac{1}{r} \cdot \frac{dC_i}{dr}$$

Where: M is the molecular weight,
R is the gas constant, T the absolute temperature
$\bar{v}$ is the partial specific volume of the macromolecule, ρ the solvent density, ω the angular velocity, C the concentration and r the radial dist

This equation is strictly valid only in the case of a two component system, e.g. a homogeneous macromolecule in aqueous solution. In practice, equilibrium experiments are carried out in the presence of a third low molecular weight component, the buffer or electrolyte added to supress charge effects (see section (v) below). In this case, Casassa and Eisenberg (1964)[62] have shown that the above equation is valid if the macromolecular solution is dialysed to equilibrium against the buffer or electrolyte and a refractometric method, with the dialysis medium as the solvent reference, used to measure the concentration of the macromolecule.

A plot of $\frac{1}{r}\frac{dC}{dr}$ against C for a monodisperse solution of the macromolecule will give a straight line from the slope of which M can be calculated.

(ii) Polydisperse Solutions.

In the case of a solution where the molecular weight is inhomogeneous, such as a mixture of different macromolecules or a single macromolecule which undergoes self association with increasing concentration, a plot of $\frac{1}{r}\frac{dC}{dr}$ against C will not be linear since the effective molecular weight changes throughout the cell. Information about the molecular weight distributions can, however, be obtained.

If we consider the point r in the cell, then for each component, which may either be a discrete macromolecule or a component of a concentration dependent association, we can write,

$$\frac{1}{r}\left(\frac{dC_1}{dr}\right)_r = K(M_1C_1)_r$$

$$\frac{1}{r}\left(\frac{dC_2}{dr}\right)_r = K(M_2C_2)_r$$

$$\frac{1}{r}\left(\frac{dC_3}{dr}\right)_r = K(M_3C_3)_r$$

etc. to M_n

Where $K = \dfrac{(1 - \bar{v}\rho)\omega^2}{R\,T}$

" M_1 is the molecular weight of component 1

" $\left(\dfrac{dC_1}{dr}\right)_r$ is the concentration gradient of component 1 at the point r.

etc.

Therefore, at the point r in the cell, summing the contributions from each species,

$$\frac{1}{r}\left(\frac{dC}{dr}\right)_r = K(M_1C_1 + M_2C_2 + M_3C_3 + \ldots\ldots\ldots)_r$$

but, the weight-average molecular weight, M_w , is given by

$$M_w = \frac{M_1C_1 + M_2C_2 + M_3C_3 + \ldots\ldots\ldots}{C_1 + C_2 + C_3 + \ldots\ldots\ldots}$$

Therefore, $\dfrac{1}{r}\left(\dfrac{dC}{dr}\right)_r = K(M_wC)_r$

Where C is now the total concentration of the different species at the point r.

Thus, M_w at the point r is given by : -

$$\frac{1}{KC_r} \cdot \frac{1}{r}\left(\frac{dC}{dr}\right)_r$$

The slope of the curve at the point r is given by

$$\left(\frac{d}{dC}\left(\frac{1}{r}\frac{dC}{dr}\right)\right)_r$$

In terms of the individual components this is equal to

$$\frac{1}{r}\left(\frac{d}{dC}\cdot\frac{dC_1}{dr} + \frac{d}{dC}\cdot\frac{dC_2}{dr} + \frac{d}{dC}\cdot\frac{dC_3}{dr} + \cdots\cdots\right)_r$$

but, $$\left(\frac{d}{dC}\right) = \left(\frac{d}{dC_n}\right)_r x \left(\frac{dC_n}{dr}\right)_r x \left(\frac{dr}{dC}\right)_r$$

Therefore, $$\left(\frac{d}{dC}\cdot\frac{dC_n}{dr}\right)_r = \left(\frac{dr}{dC}\right)_r x\ Kr\left(M_nC_n\right)_r x \left(\frac{d}{dC_n}\cdot\frac{dC_n}{dr}\right)_r$$

but, $$\left(\frac{d}{dC_n}\cdot\frac{dC_n}{dr}\right)_r = K\,r\,M_{nr}$$

Therefore, $$\left(\frac{d}{dC}\cdot\frac{1}{r}\frac{dC}{dr}\right)_r = \frac{1}{r}\left(\frac{dr}{dC}\right)_r K^2r^2\left(M_1^2C_1 + M_2^2C_2 + M_3^2C_3\cdots\right)_r$$

but, $$\left(\frac{dr}{dC}\right)_r = 1/r\,K\left(M_1C_1 + M_2C_2 + M_3C_3 + \cdots\cdots\right)_r$$

so that, $$\left(\frac{d}{dC}\cdot\frac{1}{r}\frac{dC}{dr}\right)_r = K\left(\frac{M_1^2C_1 + M_2^2C_2 + M_3^2C_3 + \cdots}{M_1C_1 + M_2C_2 + M_3C_3 + \cdots}\right)_r$$

$$= K M_{z(r)}$$

Thus, the Z-average molecular weight at the point r is given by the slope of $\frac{1}{r}\cdot\frac{dC}{dr}$ v. concentration at that point.

Data for the variation of concentration with r will thus enable both M_w and M_z to be calculated at any point in the cell. If the absolute value of C is not known, a plot of $\frac{1}{r}\frac{dC}{dr}$ against ΔC measured from some convenient reference point (e.g. the meniscus of the solution) will still enable M_z to be calculated from the gradient of the curve. This latter method of plotting the data was first suggested by Van Holde and Baldwin (1958).[63]

In the case of a monodisperse solution, the Van Holde-Baldwin plot will be a straight line, and the molecular weight of the macromolecule can be calculated from the slope. For a mixture of macromolecules of different molecular weights, Van Holde and Baldwin[63] showed that the slope of a line joining the points on the curve at $r_{meniscus}$ and $r_{cell\ base}$ gives the Z-average molecular weight of the starting mixture.

Other methods of treating equilibrium sedimentation data are possible, for example, the integrated form of the general equation,

$$M = \frac{2RT}{(1 - \bar{v}\rho)\omega^2} \frac{d \ln C}{dr^2}$$

or the Lamm method, $$M = \frac{2RT}{(1 - \bar{v}\rho)\omega^2} \frac{1}{r^2} \ln\left(\frac{1}{r} \cdot \frac{dC}{dr}\right)$$

but these were not used in the following studies.

(iii) Non-Ideality.

Deviations from ideality can be allowed for by including the activity coefficient in the general equation for a two-component system.

$$M = \frac{RT}{(1 - \bar{v}\rho)\omega^2} \cdot \frac{1}{C} \cdot \frac{1}{r}\frac{dC}{dr}\left(1 + C\left(\frac{\partial \ln y}{\partial C}\right)_{TP}\right)$$

or by a virial expansion,

$$M = \frac{RT}{(1 - \bar{v}\rho)\omega^2} \cdot \frac{1}{C} \cdot \frac{1}{r}\frac{dC}{dr}\left(1 + 2BMC + 3\bar{C}MC^2 + ..\right)$$

Where y is the activity coefficient,
and B, $\bar{C}$ etc. are virial coefficients

If we ignore virial coefficients higher than the second, we can write,

$$M_{app} = \frac{M}{(1 + 2BMC)}$$

and, for a polydisperse system, it can be shown that,

$$M_{w(app)} = \frac{M_w}{(1 + 2BM_wC)} \quad ; \quad M_{z(app)} = \frac{M_z}{(1 + 2BM_wC)^2}$$

For globular proteins, close to their isoelectric point or at high ionic strength, the second virial coefficient represents chiefly the volume of the macromolecule from which solvent is excluded. In this case, the term BM is a constant and has been found, for a number of proteins, to agree closely with the theoretical value of about 3 cgs units. (Tanford, 1961)[64]

(iv) Solute Effects.

Very high concentrations of dissolved solute, such as 6 M guanidine hydrochloride which is used to dissociate protein oligomers, might be expected to cause inaccurate values of the measured molecular weights by binding to the macromolecules. A high degree of solute binding could also change the partial specific volume of the protein.

In the case of GuHCl, however, Ullmann et al, (1968)[65] have shown that for six proteins of well established molecular weight only a small correction is necessary for the effect of solute. This can be expressed for 6 M Gu HCl as,

$$M = 0.968 \lim_{C \to 0} M_{app} \frac{(1 - \bar{v}^* \rho)}{(1 - \bar{v} \rho)}$$

where $\bar{v}^*$ is the partial specific volume of the protein in 6 M Gu HCl.

Tanford et al (1967)[47], on the basis of measurements made on γ-globulin and myosin, suggest that $\bar{v}^*$ should be taken as 0.01 lower than the value of the partial specific volume measured in dilute solution.

The effect of bound SDS on the molecular weight is less well known. A value of 44,000 for the molecular weight of Aldolase in 1% SDS at pH 6 has been obtained in an earlier study (K.R. Leonard, Part II Thesis, 1966).[66] This is about 10% higher than the generally accepted value for the subunit molecular weight.

(v) Charge Effects.

The distribution of a charged macromolecule at sedimentation equilibrium in a solution of low ionic strength will not be the same as that of an uncharged molecule. In the case of the charged macromolecule, the charge gradient set up by the differential distribution of low molecular weight counter-ions and high molecular weight macro-ions will tend to oppose the redistribution of the latter in the centrifugal field.

Lamm (1944)[67] and Johnson et al (1954)[68] have shown that, in the absence of a third electrolyte component, the molecular weight of the macro-ion will be reduced by a factor $\frac{1}{(1+\bar{Z})}$, where $\bar{Z}$ is the charge on the macro-ion. If an excess of supporting electrolyte is present, the charge effect is reduced and may become negligible if the pH is close to the isoelectric point.

The true molecular weight in this case is given by,

$$M = M_{app} + 0.5\,\bar{Z}\,M_e\,(1 + \bar{v}_e\rho)(1 - \bar{v}\rho)$$

Where M_e is the mol. weight, $\bar{v}_e$ the partial specific volume, of the dissolved electrolyte. (Tanford, 1961)[69]

Taking $\bar{v}_e$ to be 0.3 (approx.) and M_e to be about 60 for NaCl or KCl, the correction factor becomes about $90\,\bar{Z}$.

2. Experimental Details.

(i) Optical Systems Used.

The Rayleigh interference optical system was used for protein concentrations lower than about 6mg/ml. Above this concentration, the fringe density was too high to measure accurately, and Schlieren optics were used. The centrifuge was fitted with a 'Push-pull' light source slit, with the fixed jaws set 0.001 inches apart. The chamber slit mounting was adjustable and the intermediate (0.75mm) width interference slits were used. The cylindrical lens mount was adjustable and was set at the optimum position for schlieren or interference.

Longer exposure times had to be used with the interference optical system than with the schlieren system. Using Kodak II-G or Ilford R-30 photographic plates, the minimum exposure was about 90 seconds and the optimum exposure around 200 sec. The shutter cam was modified to give an exposure time of 90 sec. and a 1 - 24 hour interval timer (Crouzet Ltd.) was fitted to enable photographs to be taken at intervals greater than the normal maximum of 64 minutes. Photographs were taken at 4 hour intervals during equilibrium experiments to assess whether equilibrium had been reached.

The ultracentrifuge was also non-standard in that

a door was fitted at the rear of the camera in line with the optical axis. This facilitated alignment of the optical system and was also used to set the narrow image mask (see section (iii) below). The Beckman ruled camera grating was fitted when taking interference photographs as it gave a convenient reference from which the fringe height could be measured. About 10 - 15 fringes were measurable across a typical interference pattern.

(ii) Cells Used.

Standard double sector cells with sapphire windows were used for all equilibrium experiments. Liquid columns were 1mm or less in height, using the standard double sector synthetic boundary centrepiece or the special boundary forming centrepiece (see below). Yphantis 6 or 8 channel centrepieces were also used for some experiments.

The stepped gradient forming centrepiece (Fig. 5.1) was fabricated from a double-sector synthetic boundary centrepiece according to the pattern given by Griffith(1967)[70]. This produces a concentration gradient at the commencement of the equlibrium experiment which approximates to the final gradient, thus considerably reducing the time required to attain equilibrium. The three small reservoirs and the solution side of the centrepiece are filled with 0.025ml of increasingly concentrated solution (the lowest concentration in the reservoir closest to the axis of rotation).

The concentrations which are used depend on the molecular weight of the sample and the speed of rotation of the centrifuge. The rotor is accelerated slowly and the contents of the reservoirs run into the main solution sector and form the concentration gradient.

Solvent which had been dialysed against the solution was used as the reference in the other sector of the cell. When possible, a blank experiment was carried out by refilling the solution half of the cell with solvent before dismantling it. This was rerun under the same conditions of speed, temperature etc. as the equilibrium experiment and photographs taken to check for distortion of the interference fringes caused by window strain or other optical aberrations. In practice, it was found that this distortion was very small for low speed equilibrium experiments if sapphire windows were used.

A small amount of FC 43 fluorocarbon oil was added to each sector of the cell to give a clearer boundary at the base of the cell.

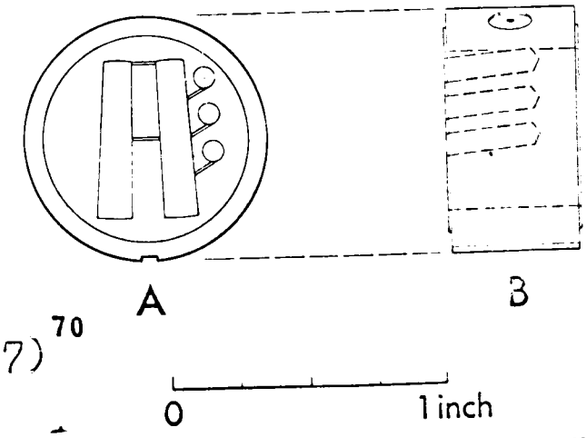

Fig. 5.1. Step gradient forming centrepiece. (Taken from Griffith, 1967)[70]

(A) Front view of modified synthetic boundary cell. (B) Side view of same cell showing angle at which the filling holes were drilled.

(iii) Measurement of true concentration.

Interference optics give a fringe pattern which measures the relative concentration across the cell. The absolute concentration at the meniscus, to which the concentration at all other points in the cell can be related, was measured by the 'fringe-shift' method.

Using a capillary (double-sector) synthetic boundary cell or the step-gradient forming cell in which the innermost reservoir is filled with solvent, the initial condition that $C_{meniscus}$ = zero is obtained. As the protein solution diffuses back towards the meniscus, the movement of the fringes is followed by taking a series of photographs of the meniscus region of the cell using the Beckman narrow camera mask and the short distance plate movement. This is shown in Fig. 5.2 and a typical plot of the fringe movement in Fig. 5.3. Thus, the protein concentration at the meniscus at equilibrium is given in terms of fringes by the total fringe shift. This can be related to the concentration in mg/ml by a separate synthetic boundary experiment.

At high concentrations of protein, when schlieren optics were used, the meniscus concentration was estimated by integration of the schlieren pattern over the whole cell. The meniscus concentration can then be calculated from the known starting concentration of protein.

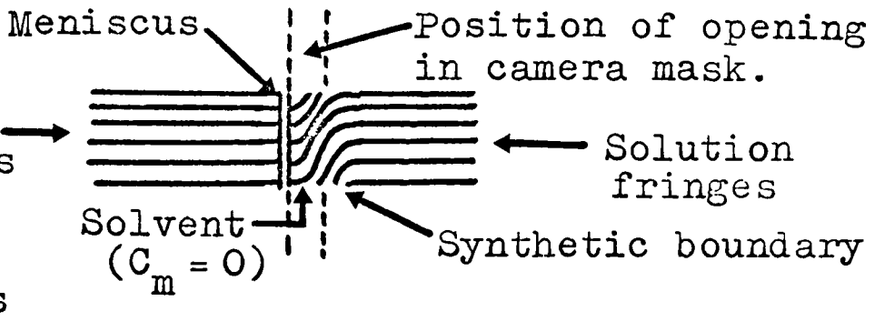

Fig. 5.2 'Fringe shift' method of measuring meniscus concentration.

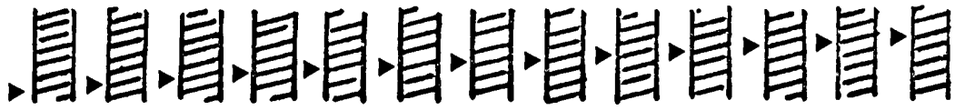

Schematic representation of the appearance of the photographic plate showing shift of fringes as the solution diffuses back towards the meniscus. Photographs are taken at 8 minute intervals initially and the time interval increased as the solution concentration at the meniscus equilibrates.

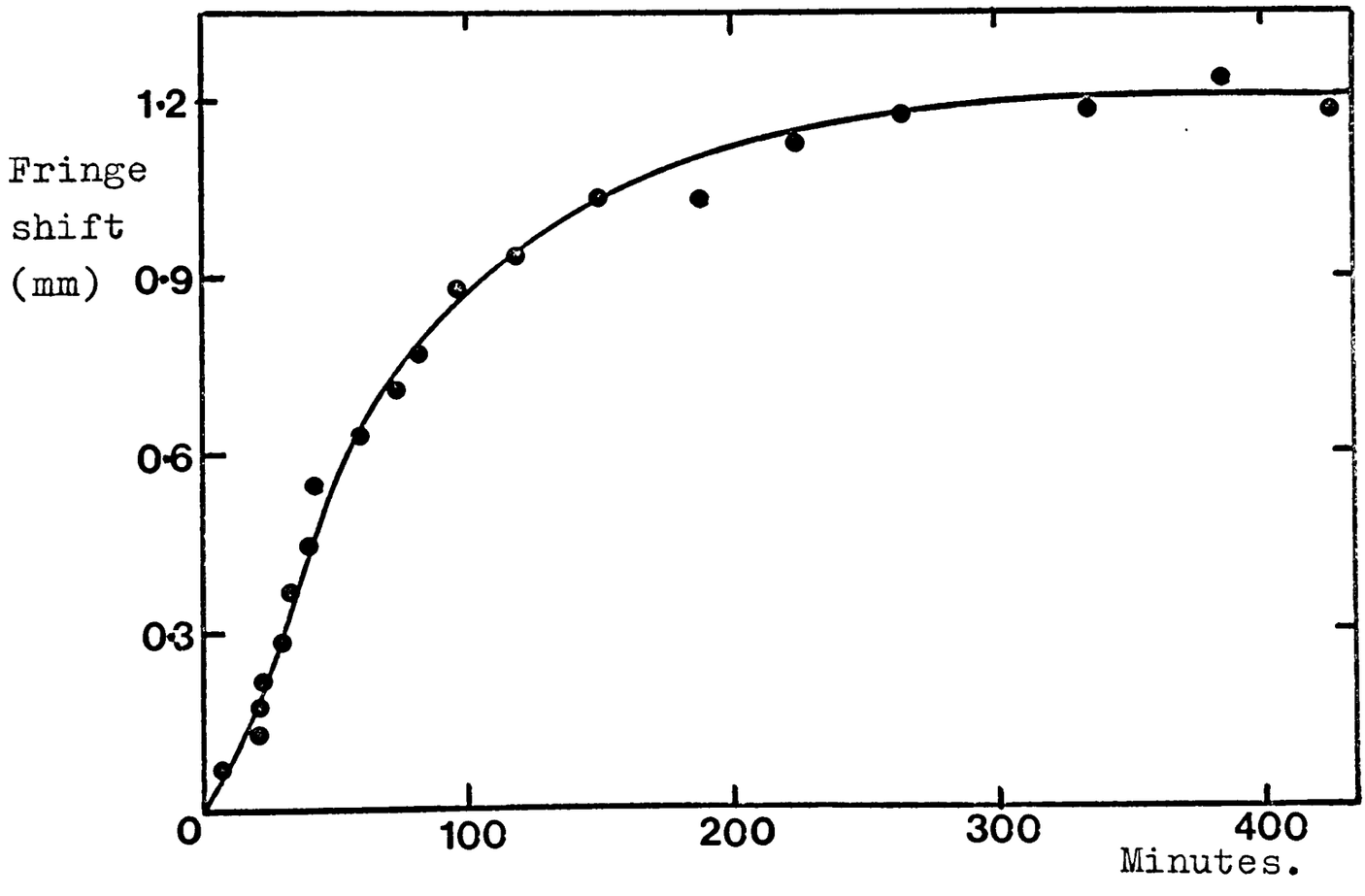

Fig. 5.3. Typical plot of fringe movement with time.

(iv) Calculation of Molecular Weights.

Molecular weights were calculated from curves of $\frac{1}{r}\frac{dC}{dr}$ against C or ΔC as described in Section 1(ii) above. The interference optical system measures the variation of concentration, C, with radial distance, r. Values of $\frac{dC}{dr}$ were computed from this data by numerical differentiation . The Schlieren optical system gives the variation of the derivative, $\frac{dC}{dr}$, with the radial distance. The differential was converted into concentration units by numerical integration. Both these operations were carried out by programs written for an Olivetti Programma 101 desk computer.

Numerical differentiation was also used to obtain M_z from the slope of the Van Holde-Baldwin curve when this was non-linear.

3. Results.

(i) The Effect of Concentration on the Molecular Wt. of PFK.

The molecular weight of native PFK was measured in 0.1M Tris-phosphate buffer, 0.5mM FDP, 10mM 2-mercaptoethanol pH 8 . In this solvent there was no significant precipitation of the protein during the time (circa 24 - 48 hrs) required to reach equilibrium.

The centrifuge was run at speeds between 1957 rpm for the highest protein concentration and 8227rpm for the lowest. Use of the heavy titanium AN-E rotor was found to eliminate precession which tends to occur at these low speeds.

Plots of M_w and M_z (calculated from the experimental data for the variation of C with r by the methods given in section 1(ii) above) against concentration at 20°C are shown in Figs. 5.4 and 5.5. Incomplete data for 2°C is also shown in Fig. 5.5 . At 20°C the M_z plot rises rapidly from about 3 - 4 $\times 10^5$ at low concentration to a plateau value of about 19 $\times 10^5$ at 7mg/ml above which concentration the Z-average molecular weight decreases slightly. The M_w curve increases more slowly over the same concentration range to about 17 $\times 10^5$.

The data for 2° C shows the same trend in molecular weight, but the curve is shifted downwards, indicating

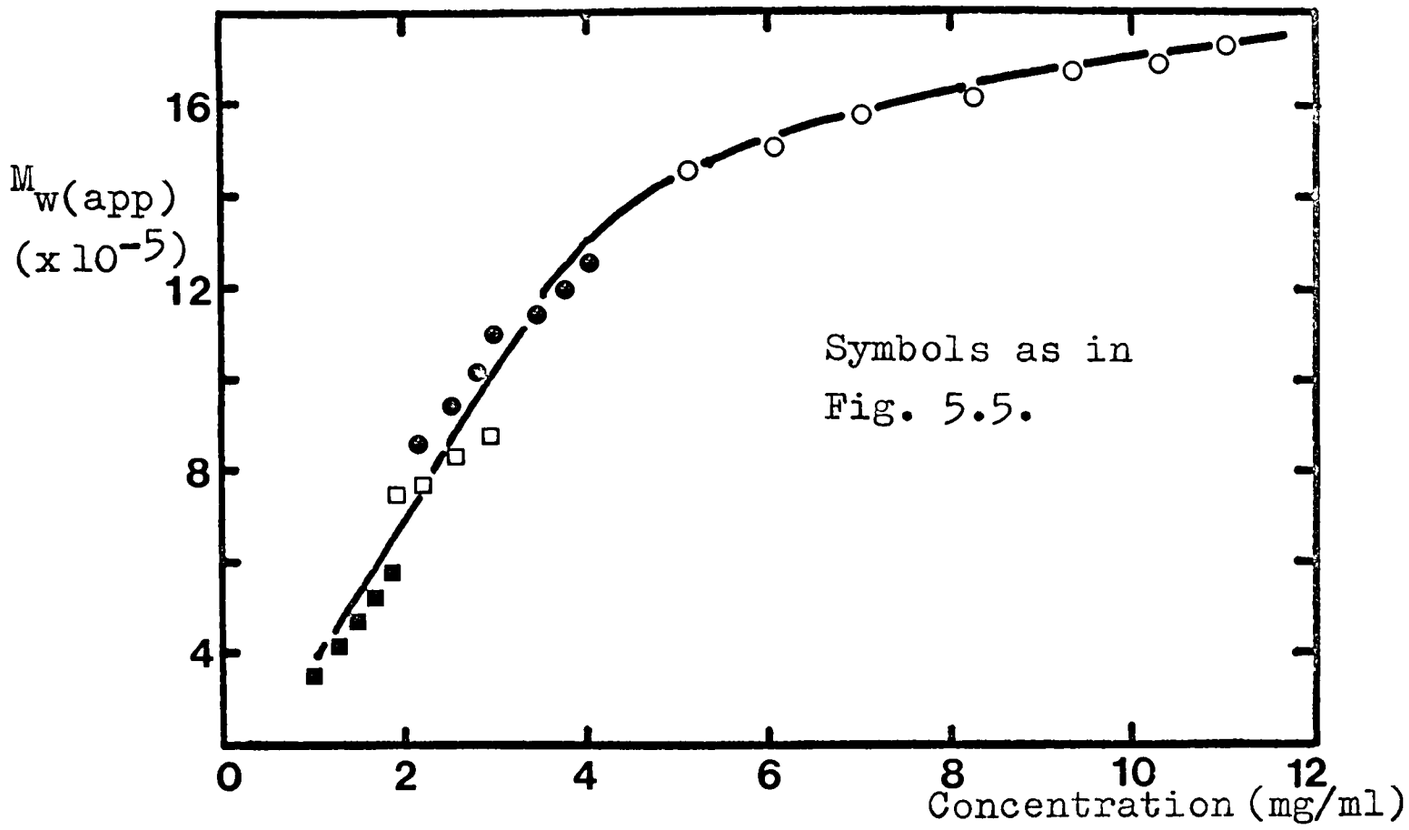

Fig. 5.4. Variation of $M_{w(app)}$ with C for PFK at pH 8 and 20°C.

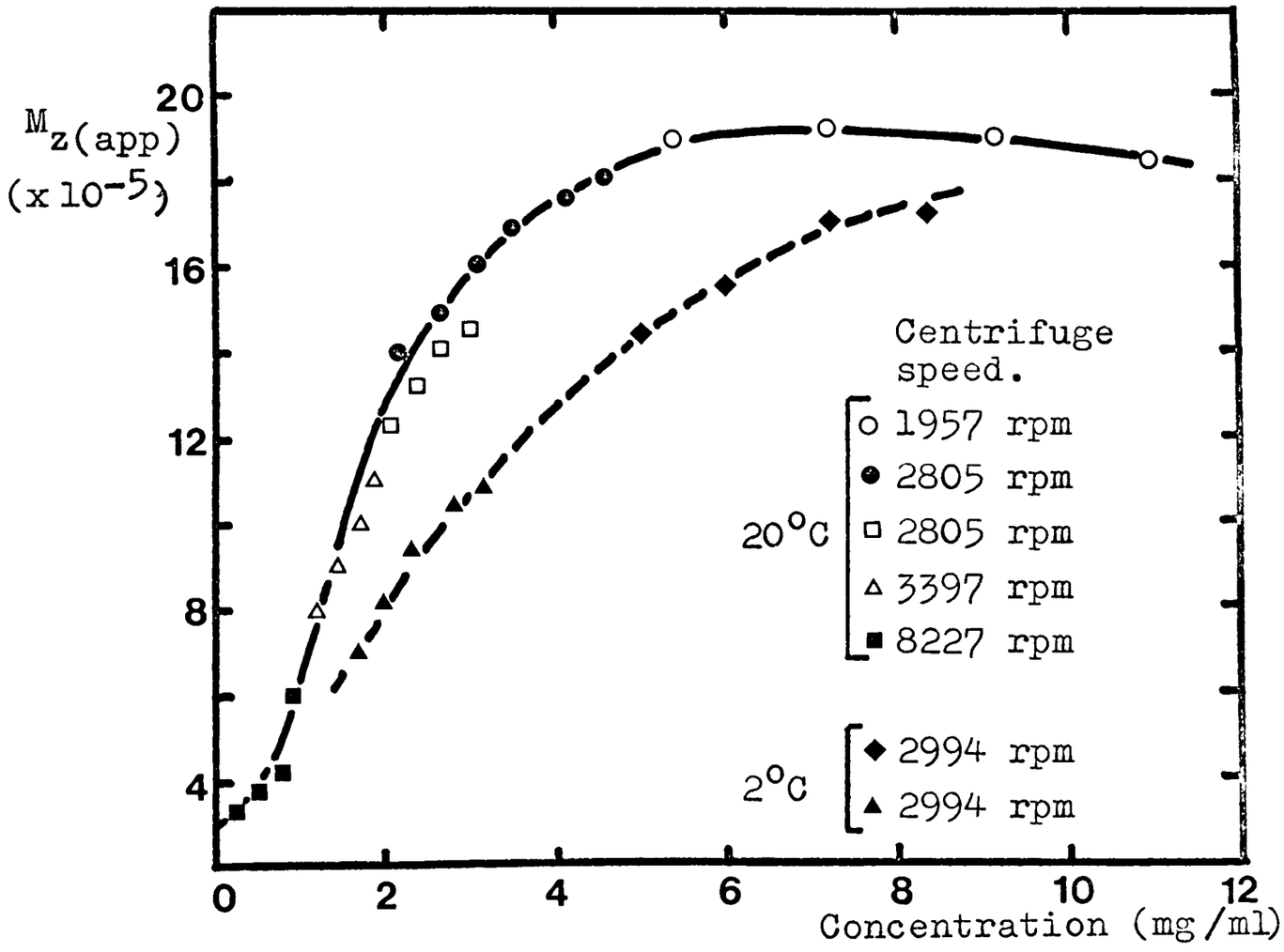

Fig. 5.5. Variation of $M_{z(app)}$ with C for PFK at pH 8, 20 °C and 2°C.

that the degree of association is less at the lower temperature.

The partial specific volume of the protein was taken to be 0.728 (the value reported by Lardy, 1967[58]) and was assumed to be independent of the degree of polymerisation of the protein or the variation in temperature.

(ii) <u>The Molecular Weight of the 12S Protein.</u>

The Van Holde-Baldwin plot for PFK in 0.1M carbonate-bicarbonate buffer, 0.5mM FDP, 10mM 2-mercaptoethanol pH 10.5 is shown in Fig. 5.6 . It is linear for measurements taken over 90% of the liquid column and an average of six determinations of the molecular weight gave $3.3 \pm 0.12 \times 10^5$ taking $\bar{v}$ to be 0.728 . This value agrees with the figure of 3.3×10^5 obtained by combining s^o and D^o (Chapter 4). The plot of $\frac{1}{r}\frac{dC}{dr}$ against ΔC is quite linear, indicating that the material is homogeneous, which is also apparent from the sedimentation pattern.

The effect of charge on the protein may be significant at this pH. The titration curve for PFK (Chapter 7) gives a value of about 50 per 100,000g for $\bar{Z}$ at pH 10.5. If we use the correction factor of $90\bar{Z}$ (section 1(v) above) the molecular weight is increased to $3.45 \pm 0.1 \times 10^5$. This is close to the value of 3.6×10^5 estimated by Paetkau <u>et al</u>,[4] (1968) .

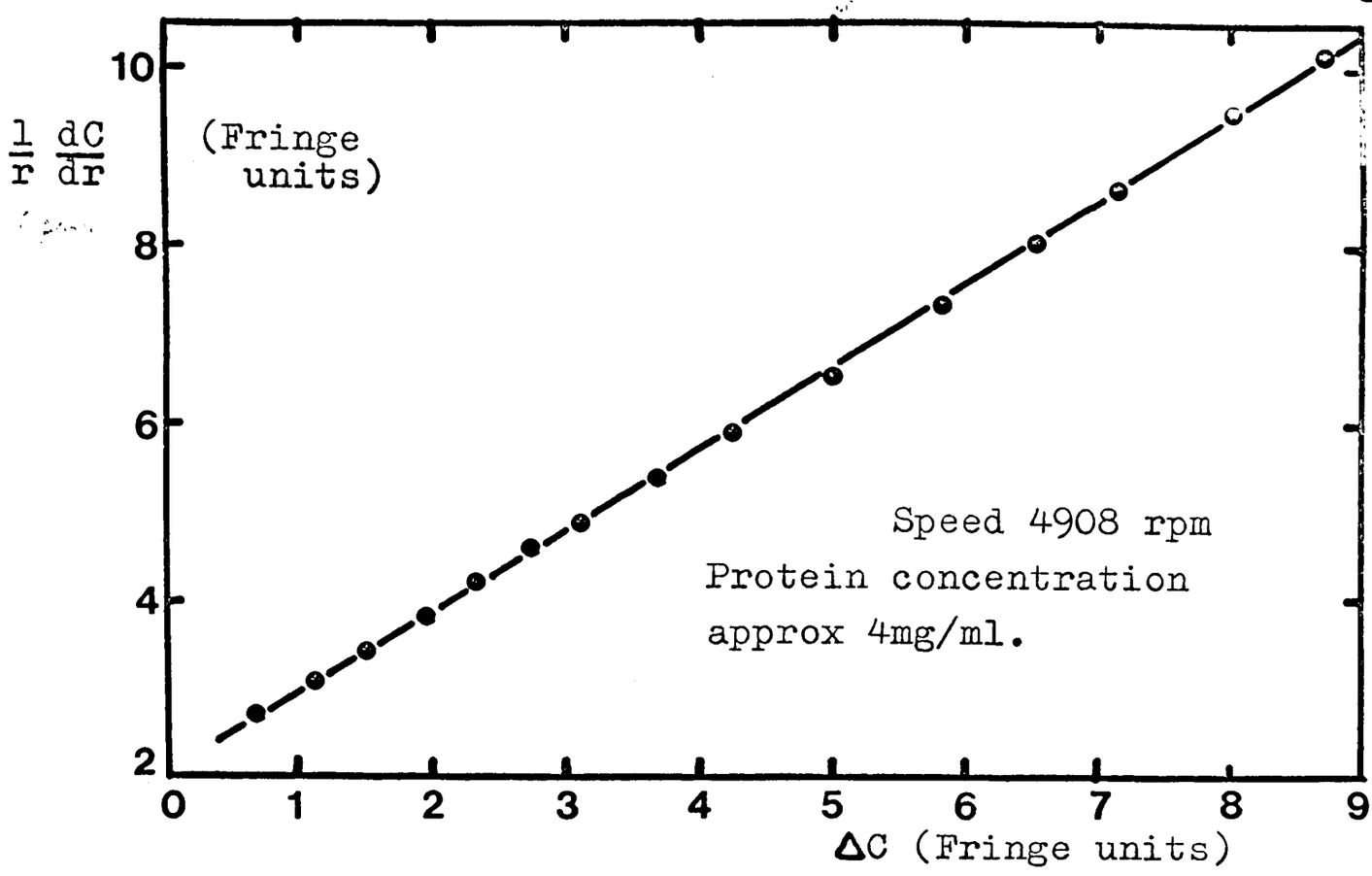

Fig. 5.6. Van Holde-Baldwin analysis of equilibrium interference data for PFK, pH 10.5 + 0.5mM FDP (12 S protein).

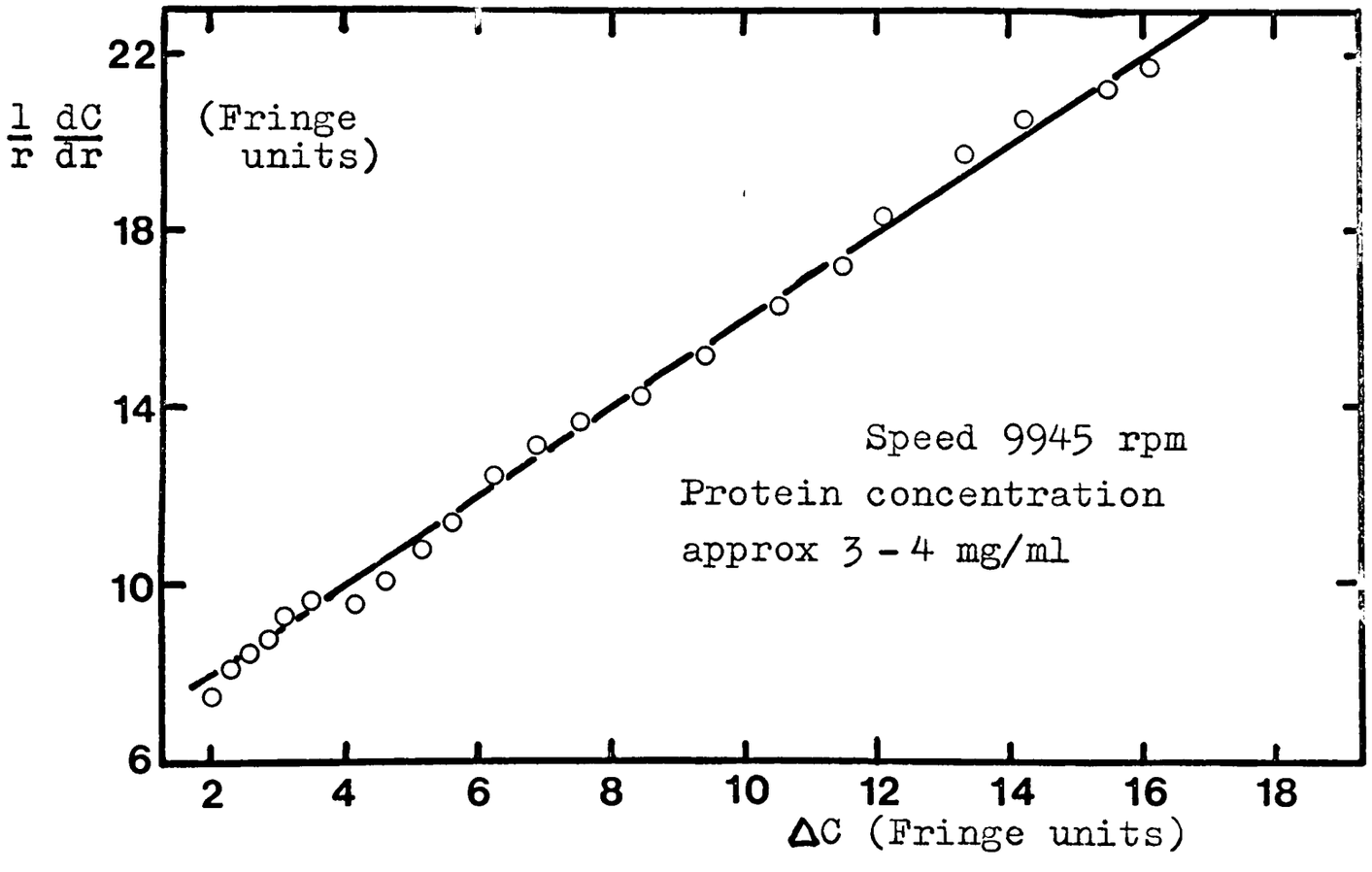

Fig. 5.7. Van Holde-Baldwin analysis of data for PFK pH 12, 4mM SDS.

(iii) The Molecular Weight of the Dissociated Enzyme.

PFK at pH 12 in the presence of 4mM SDS (0.1%) had a molecular weight of $8 \pm 0.1 \times 10^4$. The Van Holde-Baldwin analysis gave a straight line indicating homogeneity of the material (Fig. 5.7). $\bar{Z}$ at pH 12 is about 110, so that the maximum effect of charge would be to increase the molecular weight to about 8.8×10^4. The effect of SDS binding is probably small at this pH as the detergent and the protein will both be negatively charged.

The molecular weight of PFK in 6 M GuHCl, 0.1 M 2-mer captoethanol was also measured by sedimentation equilibrium. The plot of $\frac{1}{r}\frac{dC}{dr}$ v. ΔC was quite straight (Fig. 5.8) and gave a value of $7.6 \pm 0.5 \times 10^4$ taking $\bar{v}$ to be 0.718. This figure agrees reasonably well with the molecular wt. measured at pH 12, in the presence of SDS, and also with the value calculated from the sedimentation coefficient in 6 M GuHCl (Chapter 4).

PFK at pH 11.6 in the absence of SDS gives a curved Van Holde-Baldwin plot with M_z for the overall mixture equal to 2.2×10^5 (Fig. 5.9). The sedimentation pattern under these conditions shows a skewed peak with most of the material sedimenting at about 4.5 S. If the Z-average molecular weight resulted from a mixture of two components of molecular weights 3.5×10^5 and 9×10^4 the ratio of

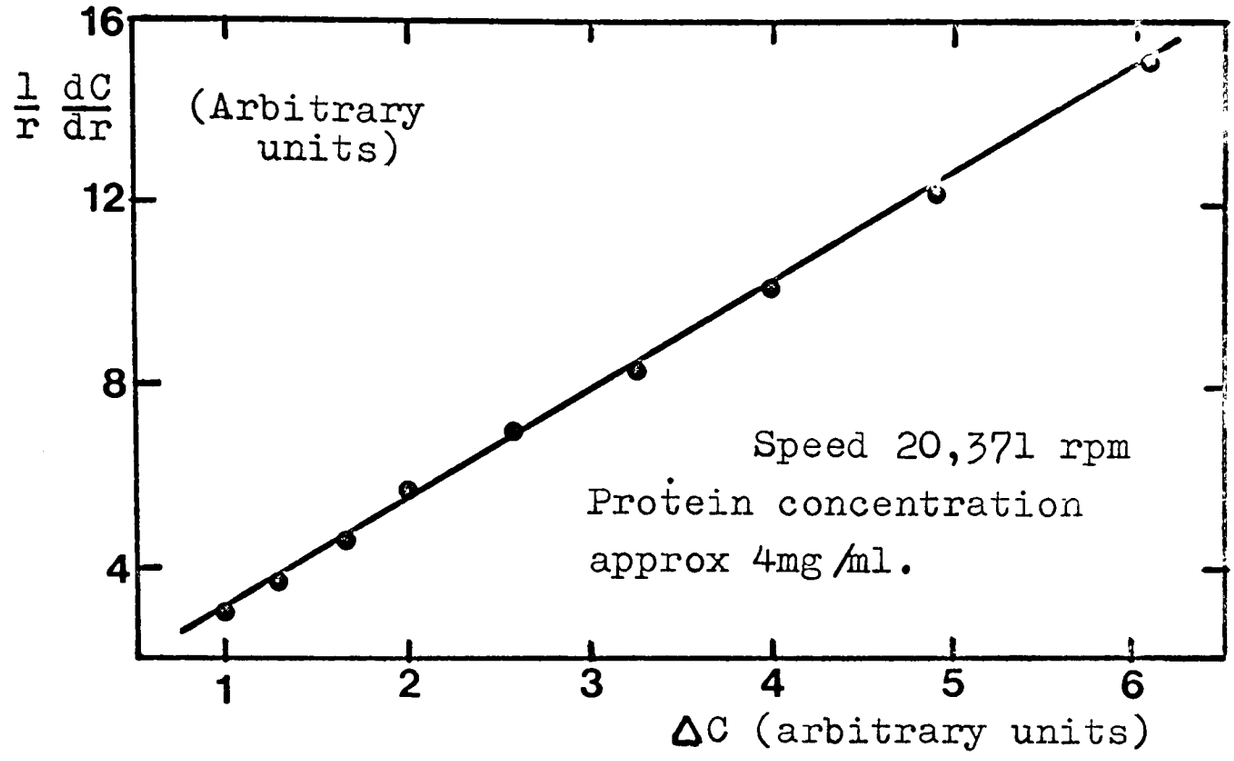

Fig. 5.8. Van Holde-Baldwin analysis of schlieren data for PFK in 6M GuHCl, 0.1M 2-mercaptoethanol.

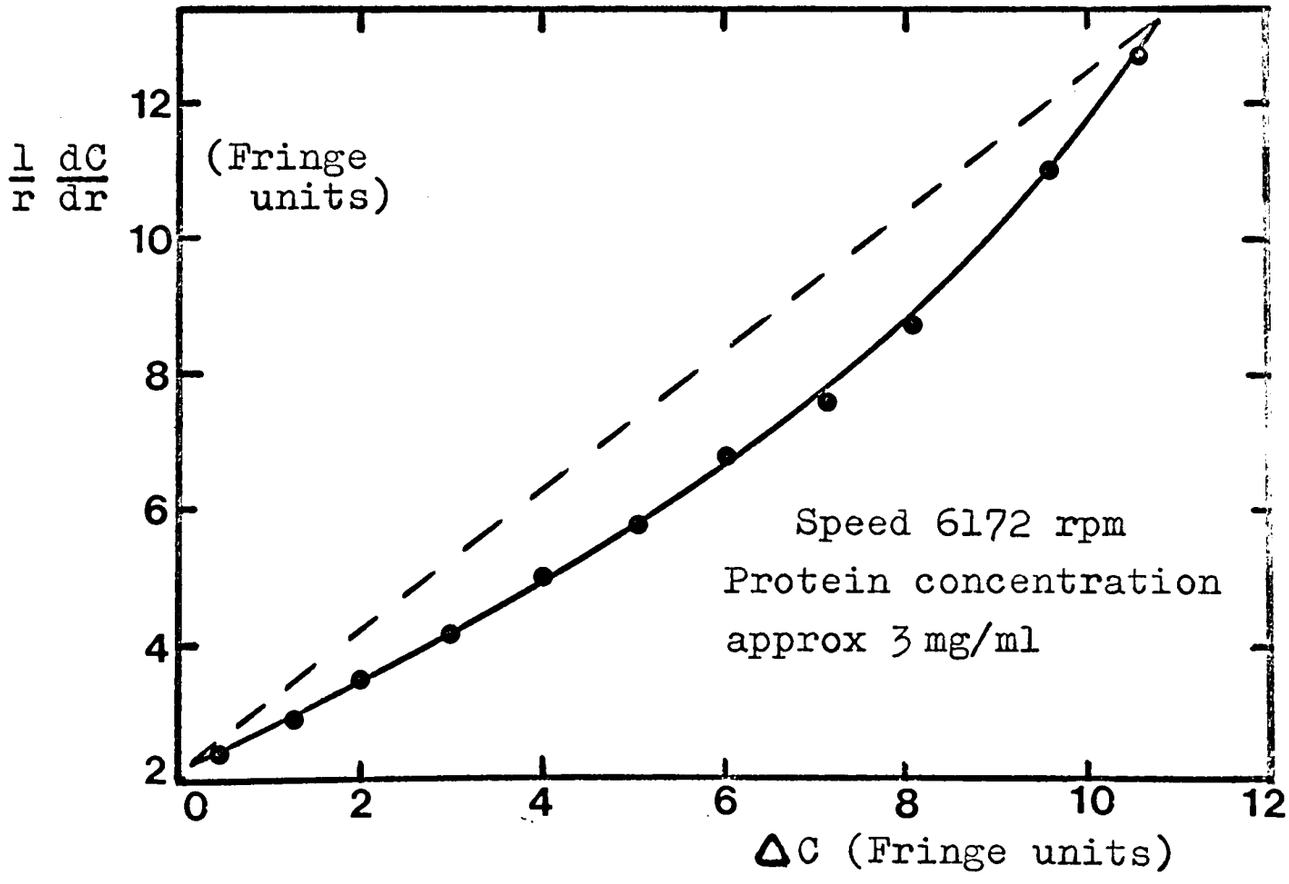

Fig. 5.9. Van Holde-Baldwin analysis of data for PFK in 0.1 M glycine-NaOH, 10mM 2-mercaptoethanol, 0.5mM FDP, pH 11.6.

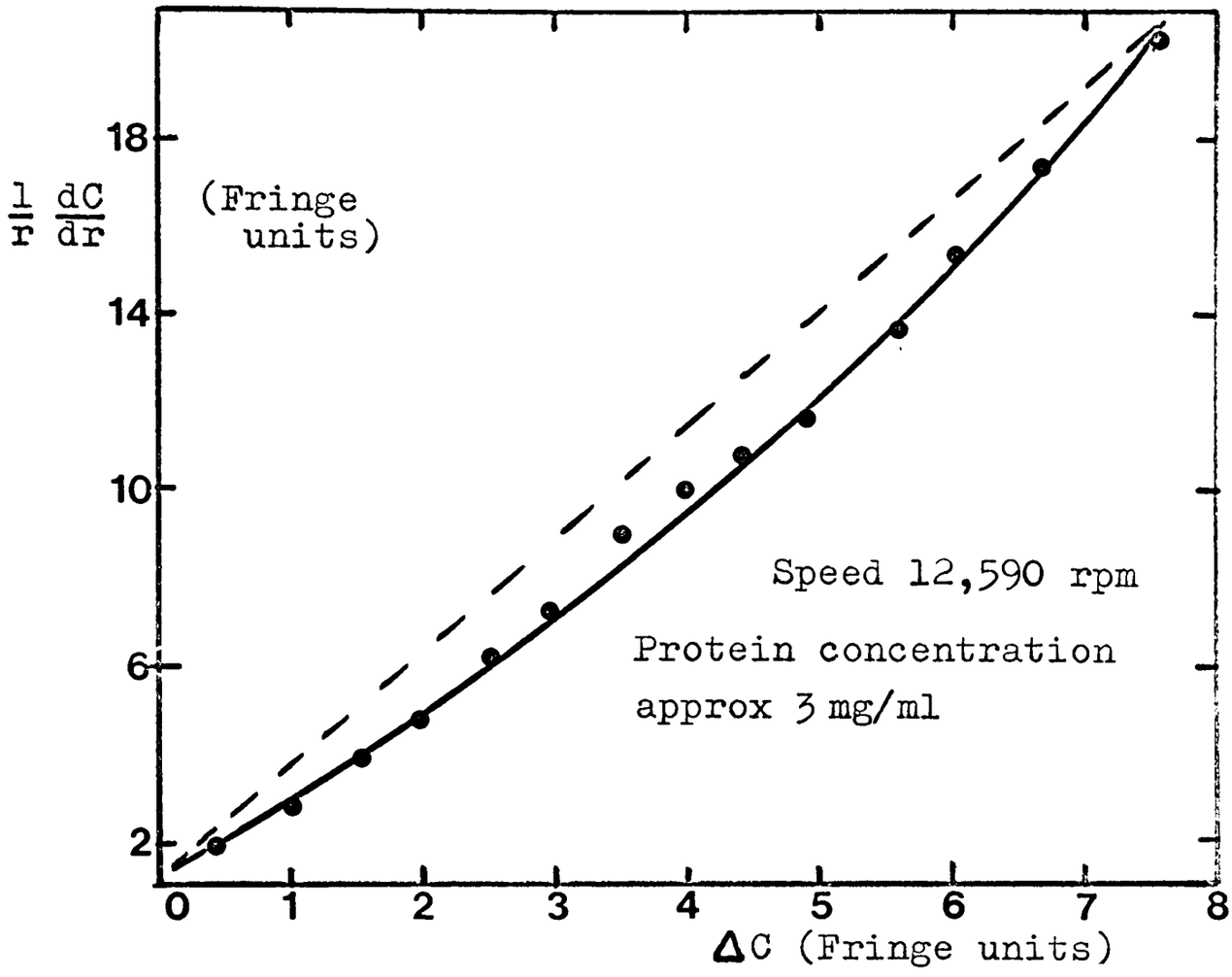

Fig. 5.9(a). Van Holde-Baldwin analysis of interference data for PFK in 0.1 M tris-phosphate, 10mM 2-mercaptoethanol, 0.5mM FDP, 0.4% w/v SDS.

The sedimentation pattern of this material (Chapter 4, section 3(i)(e) and Fig. 4.12) shows two components with s_{app} of approx 4 S and 6 S with a concentration ratio (estimated from the areas under the schlieren peaks) of about 2:1). The Z average molecular weight of the mixture, obtained from the slope of the line joining the ends of the curved Van Holde-Baldwin plot, is 1.4×10^5. This value is consistent with a mixture of 90,000 and 180,000 species in the approximate ratio of 2:1. (These molecular weights were chosen because they are fractional values of the molecular weight of the 12 S protein)

light to heavy material would be about 5:1 which is consistent with the appearance of the sedimentation pattern. See also Fig. 5.9(a).

4. Discussion.

(i) The concentration dependent association.

The effect of pH and mild dissociating reagents on the sedimentation pattern of PFK suggests that the 12 S protein is the 'monomer' of the concentration dependent polymerisation. This is supported by the fact that the curves of $M_{w(app)}$ and $M_{z(app)}$ against C tend to a value of 300,000 to 400,000 at low concentration. If, therefore, we take the molecular weight of the monomer (M_1) to be 3.5×10^5, the data can be more conveniently represented as curves for $\frac{M_w}{M_1}$ and $\frac{M_z}{M_1}$ against C (Figs. 5.10 and 5.11)

Two types of association are possible for a polymerising protein system:

(a) Closed systems: -

Monomer $\rightleftharpoons$ Intermediate polymers $\rightleftharpoons$ n-mer.

(b) Open Systems: -

Monomer $\rightleftharpoons$ Indefinite high polymer(s).

In practice, (b) will have some finite limit where the rate of random breakage of the polymer is equalled by the rate of polymerisation.

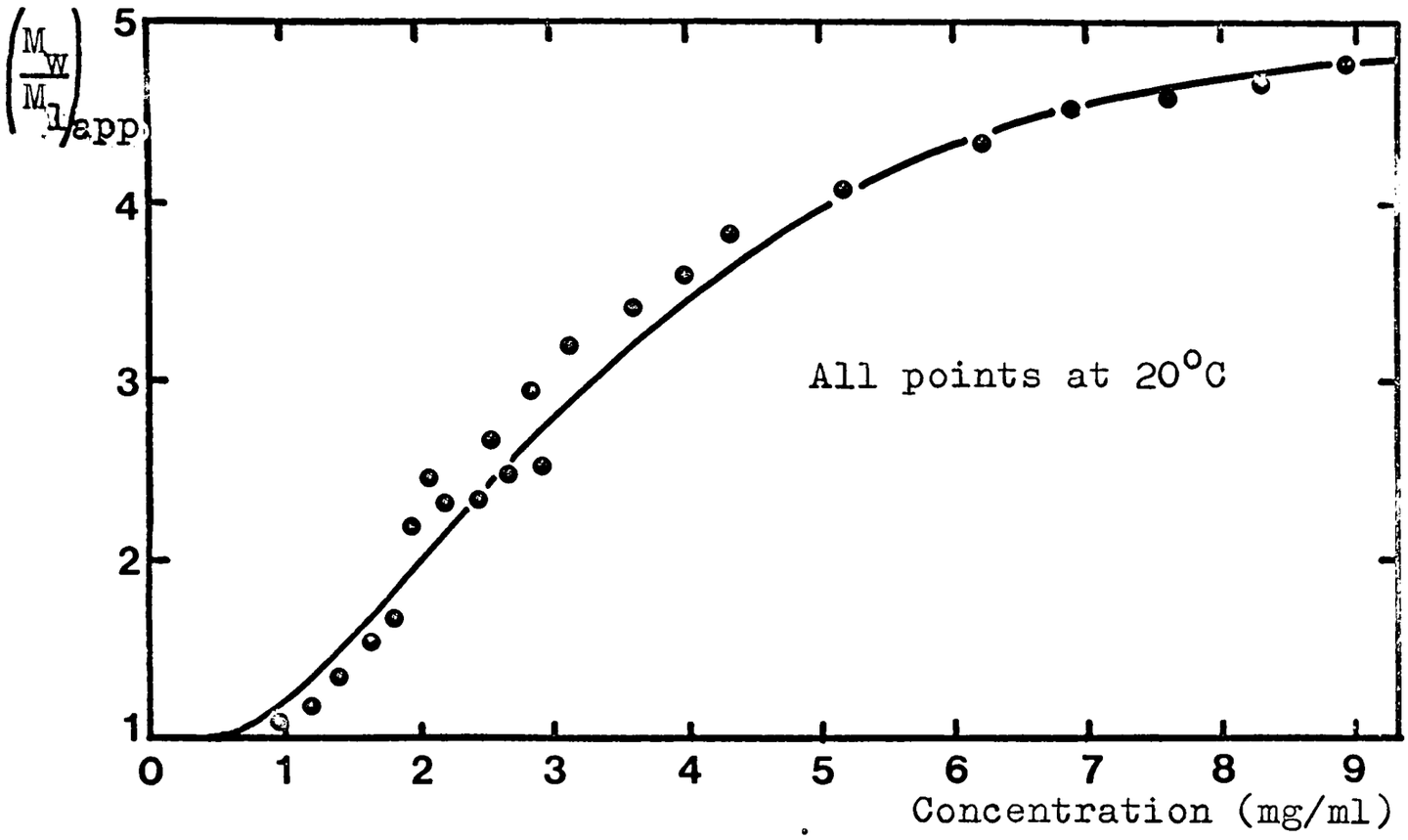

Fig. 5.10. Normalised curve of M_w against C

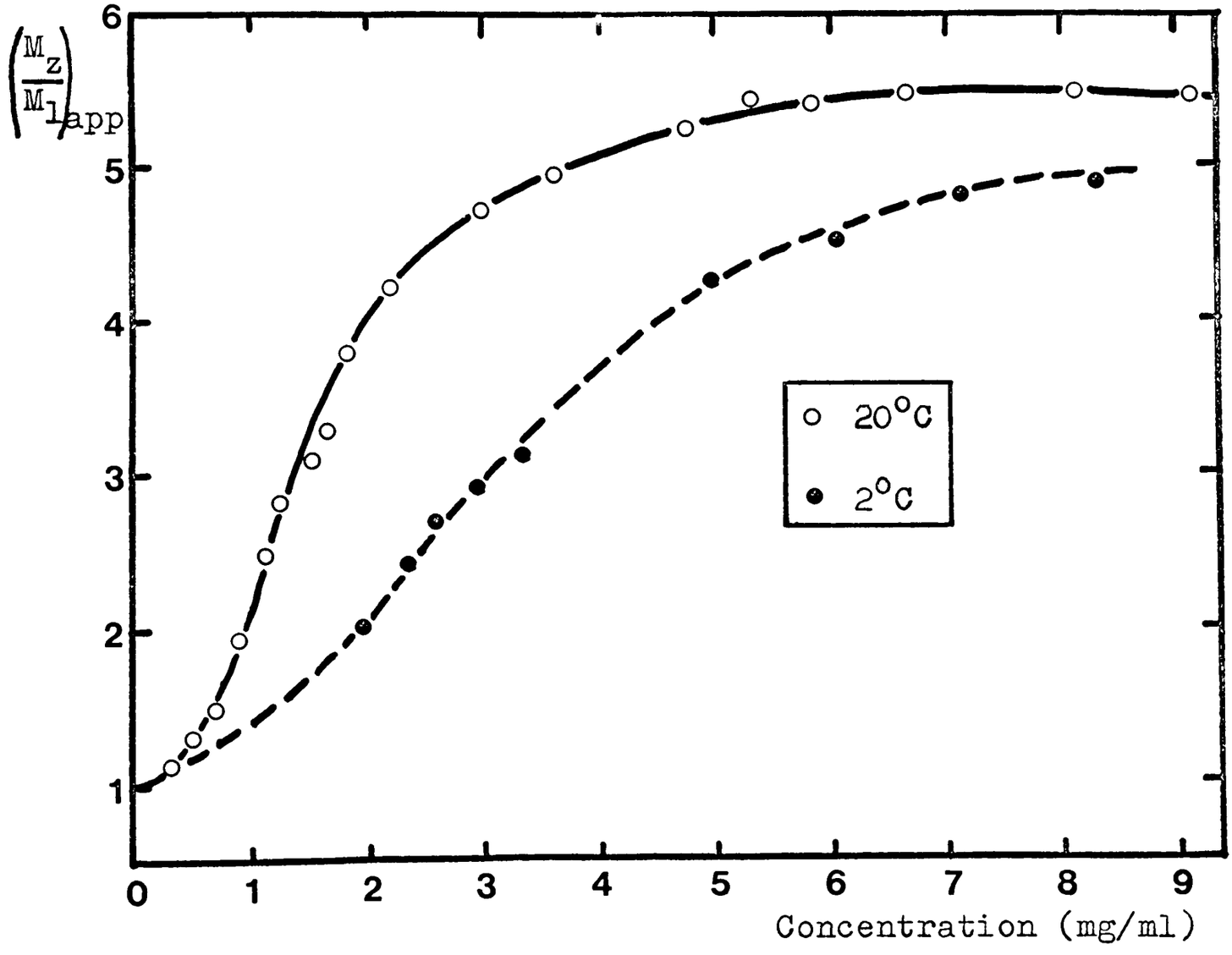

Fig. 5.11. Normalised curves of M_z against C.

(a) Theoretical curves for closed systems.

For a closed polymerisation, M_w and C can be defined as functions of M_1 and C_1 (the mol. wt. and concentration of the monomer) as follows.

$$M_w = \frac{1}{C} (M_1C_1 + M_2C_2 + M_3C_3 + \ldots\ldots M_nC_n)$$

Where 1,2,3 etc. to n are polymers.

also, $C_n = K_nC_1^n$ and $M_2 = 2M_1$, $M_3 = 3M_1$ etc.

Therefore, $M_w = \frac{1}{C} (M_1C_1 + 2K_2C_1^2M_1 + \ldots\ldots nK_nC_1^nM_1)$.

Where K_1, K_2, K_3 ..... K_n are the equilibrium constants for the steps in the polymerisation.

Thus, $$\frac{M_w}{M_1} = \frac{1}{C} (C_1 + 2K_2C_1^2 + 3K_3C_1^3 + \ldots nK_nC_1^n)$$

and, $$C = C_1 + C_2 + C_3 + \ldots\ldots C_n$$

$$= C_1 + K_2C_1^2 + K_3C_1^3 + \ldots\ldots K_nC_1^n$$

Similarly, it can be shown that

$$\frac{M_z}{M_1} = \frac{C_1 + 4K_2C_1^2 + 9K_3C_1^3 + \ldots n^2K_nC_1^n}{C_1 + 2K_2C_1^2 + 3K_3C_1^3 + \ldots\ldots nK_nC_1^n}$$

Using these equations for trial values of C_1 , it is possible to calculate theoretical curves for the variation of $\frac{M_w}{M_1}$ and $\frac{M_z}{M_1}$ with C for different values of

K_n and n. This was done for a number of systems with $n \leqslant 8$

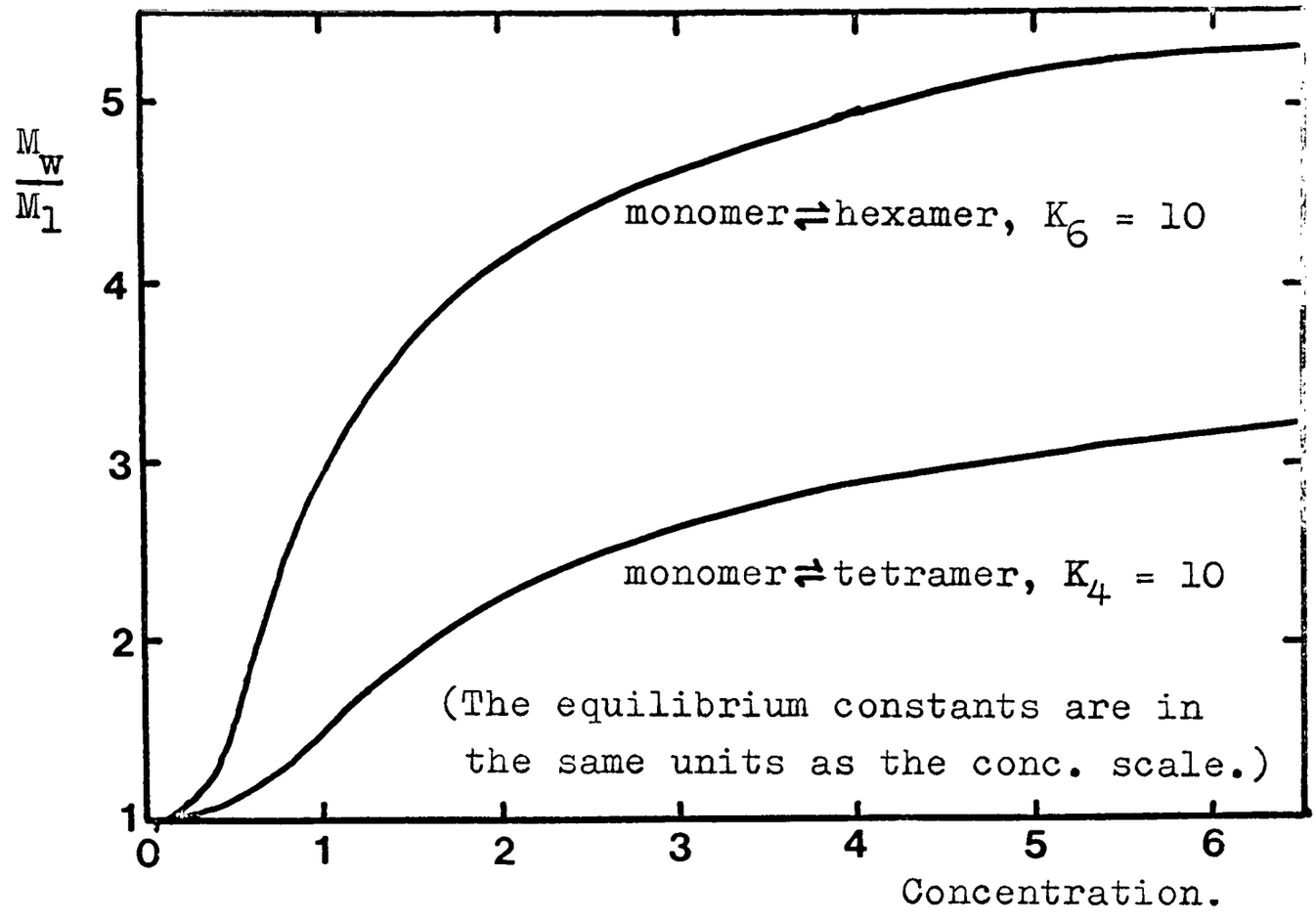

Fig. 5.12. Theoretical curves for monomer-hexamer, tetramer

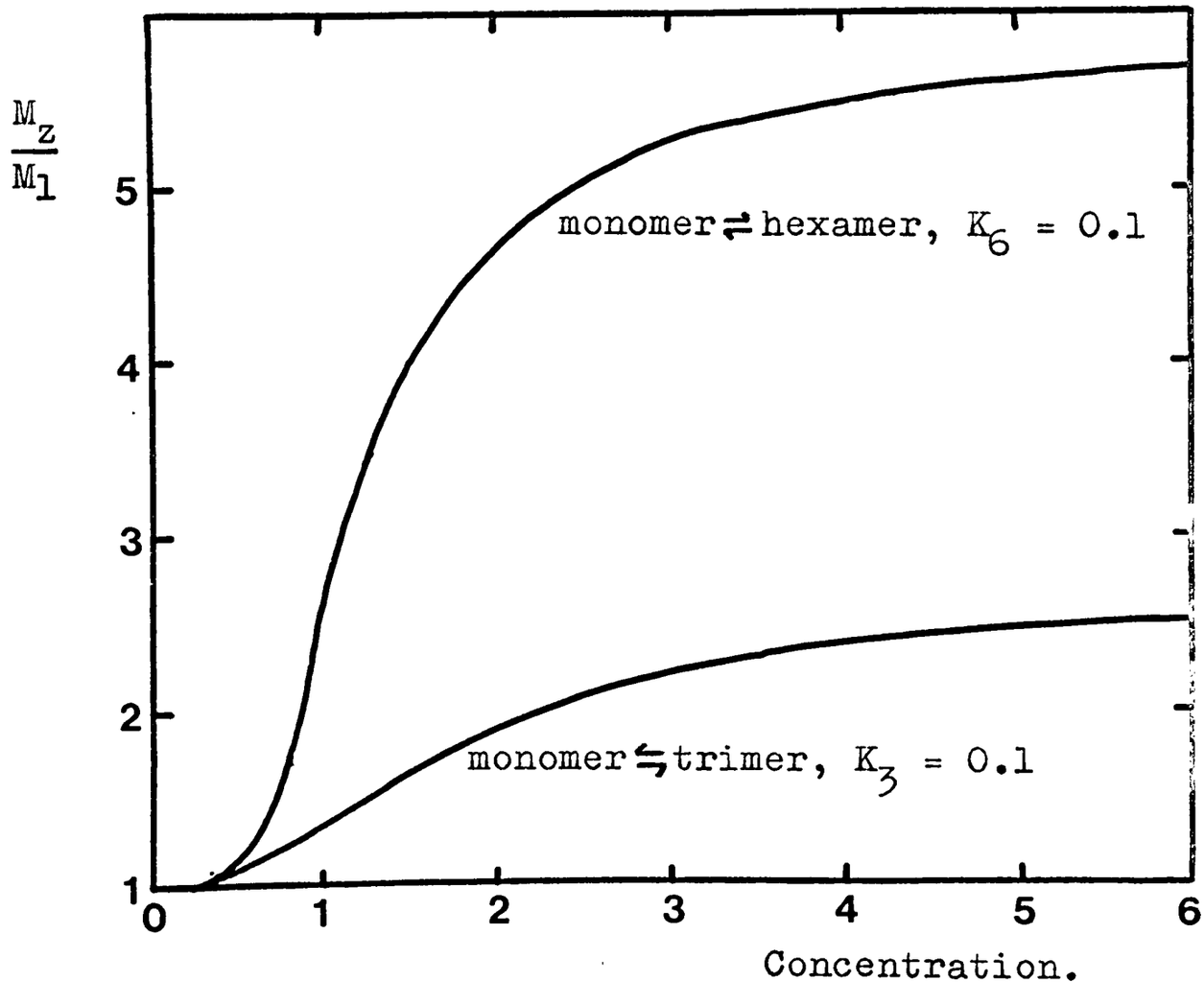

Fig. 5.13. Theoretical curves for M_z/M_1 in the case of monomer⇌hexamer and monomer⇌trimer systems.

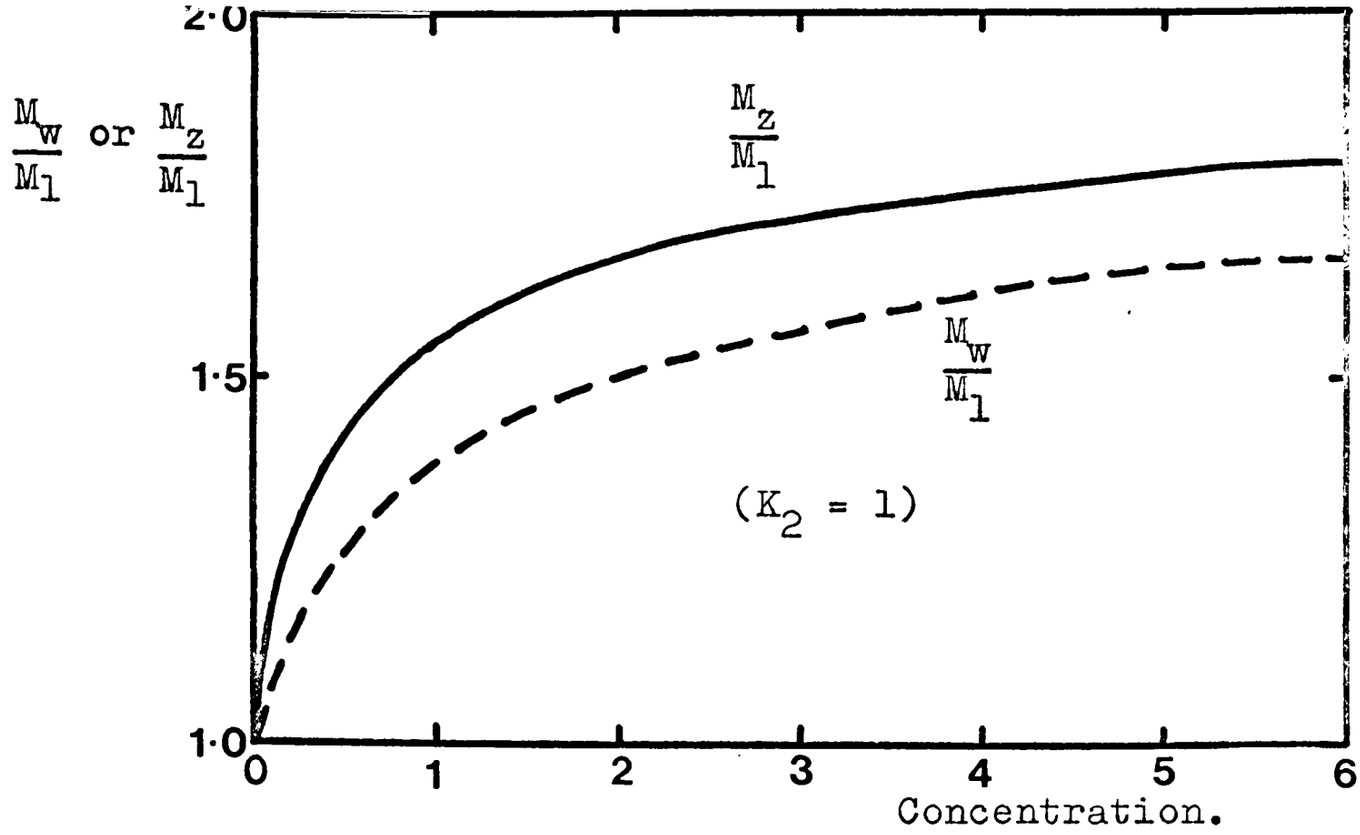

Fig. 5.14. Theoretical curves for monomer⇌dimer equilibrium.

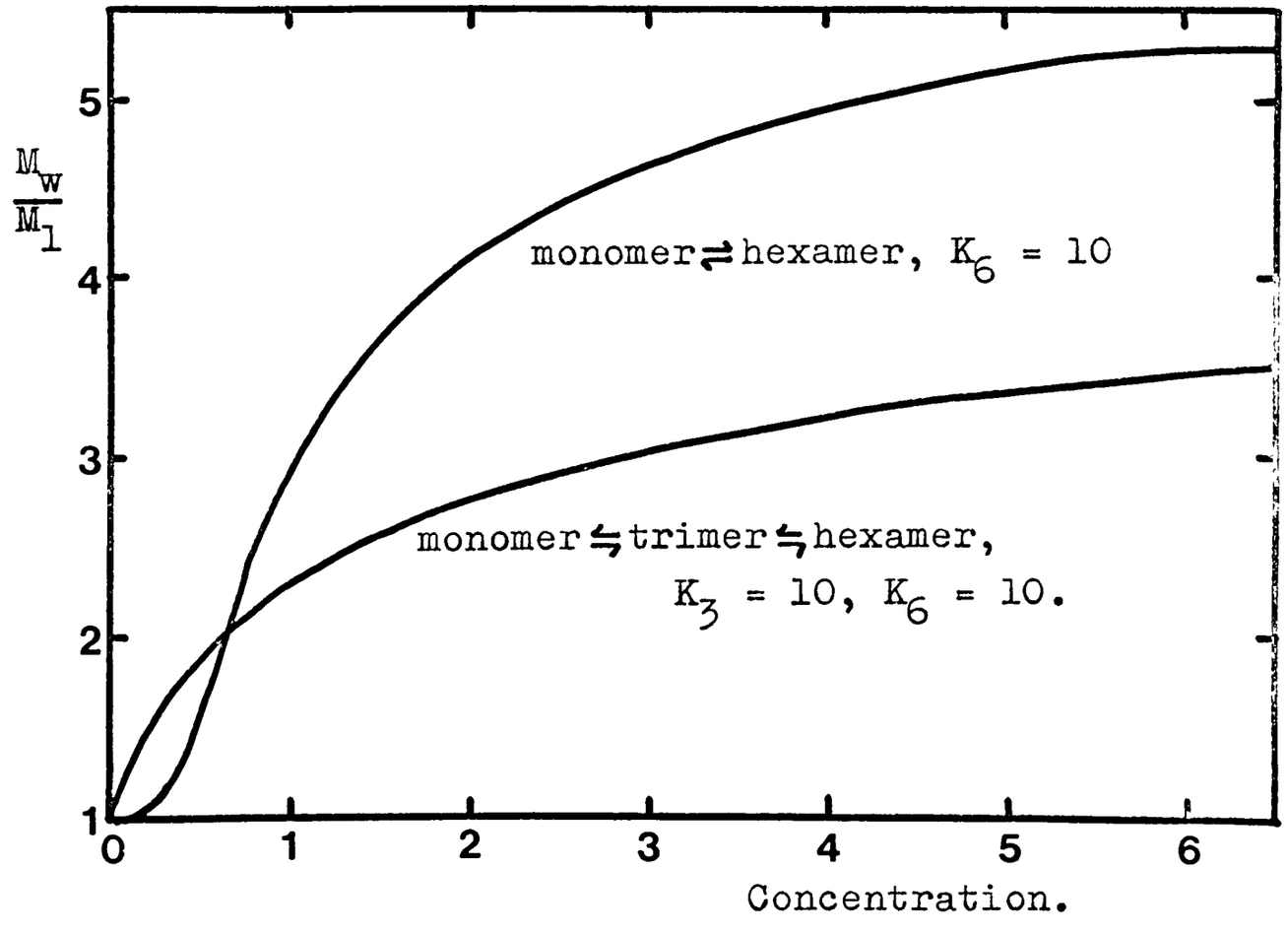

Fig. 5.15. Theoretical curves for monomer⇋hexamer and monomer⇌trimer⇌hexamer equilibria.

and examples of the curves which were obtained are shown in Figs. 5.12 to 5.15. The calculations were made with an Olivetti Programma 101 desk computer.

The following generalisations can be made. Firstly, in the simple case of monomer in equilibrium with a single polymeric species with no intermediates, the curves of M_w / M_1 and M_z / M_1 against C are sigmoid in shape for n greater than 2 and paraboloid in shape for n = 2. Secondly, if the relative concentration of intermediate polymers is low this generalisation still applies, but if the values of $K_{intermediates}$ are chosen so that there are large amounts of the intermediate polymers present at equilibrium, the curves become less sigmoid and more paraboloid as shown in Fig. 5.15.

(b) Theoretical curves for open systems.

In the case of an open polymerisation, the analysis can be simplified by assuming that the equilibrium constants on a molar basis for the individual polymerisation steps are equal. This assumption is not unreasonable as a regular association of identical protein units is likely to be linear or helical, with the same interaction taking place at each step in the polymerisation.

For an open association of this type, we can derive in terms of C_1 as before, $C = C_1 + 2kC_1^2 + 3k^2C_1^3 + \ldots$

$$\frac{M_w}{M_1} = \frac{1 + 4kC_1 + 9k^2C_1^2 + 16k^3C_1^3 + \ldots\ldots\ldots}{1 + 2kC_1 + 3k^2C_1^2 + 4k^3C_1^3 + \ldots\ldots\ldots}$$

and, $$\frac{M_z}{M_1} = \frac{1 + 8kC_1 + 27k^2C_1^2 + 64k^3C_1^3 + \ldots\ldots}{1 + 4kC_1 + 9k^2C_1^2 + 16k^3C_1^3 + \ldots\ldots}$$

Where k is the molar equlibrium constant for the polymerisation process.

If $kC_1 < 1$, the infinite series are convergent and become

$$\frac{M_w}{M_1} = \frac{1 + kC_1}{1 - kC_1}$$

$$\frac{M_z}{M_1} = \frac{1 + 4kC_1 + k^2C_1^2}{(1 - kC_1)^2}$$

$$C = \frac{C_1}{(1 - kC_1)^2}$$

Using these equations, curves were calculated for the variation of M_w/M_1 and M_z/M_1 with C assuming values of k. These are shown in Fig. 5.16 . If the polymerisation is open the curves are paraboloid in shape.

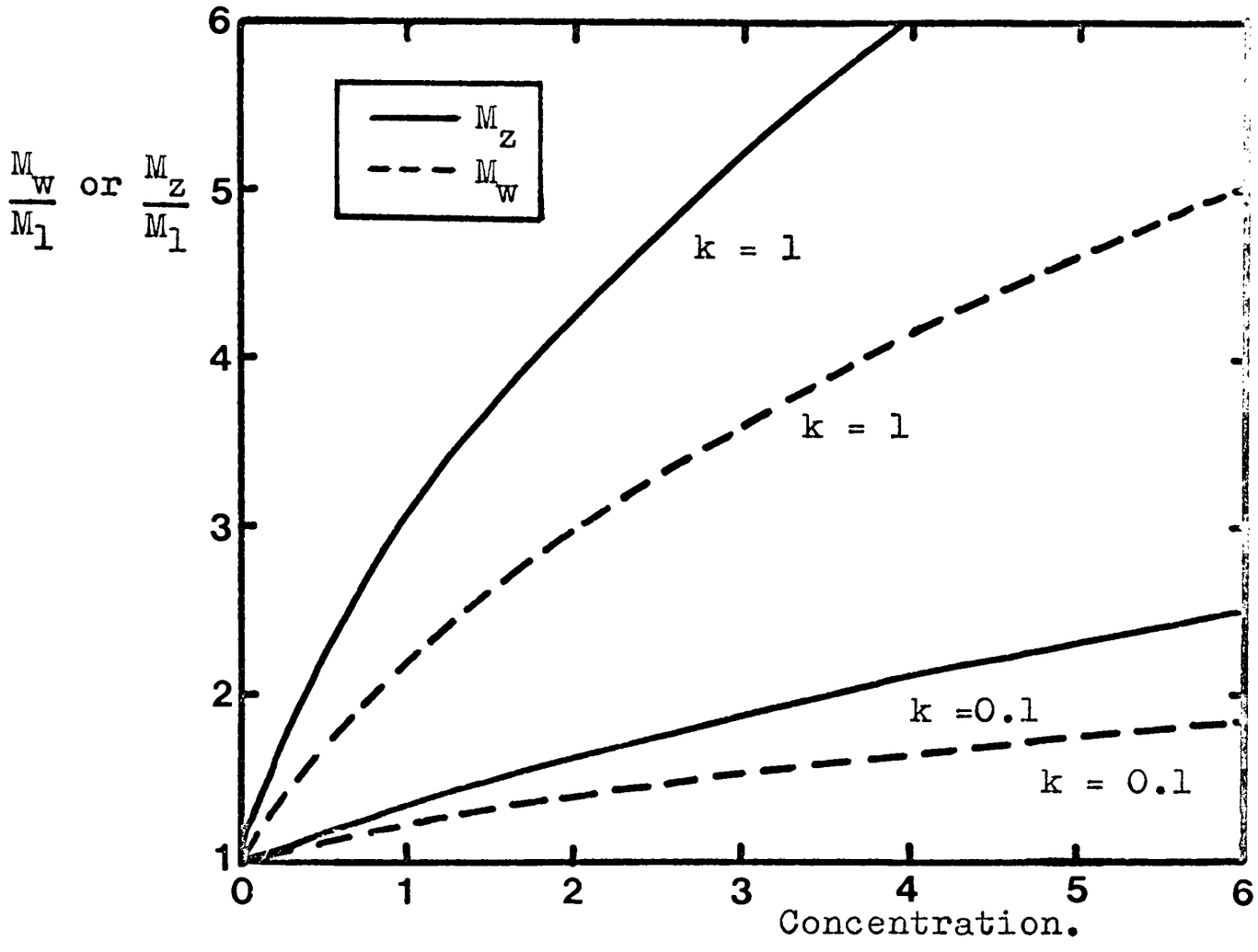

Fig. 5.16. Theoretical curves for open systems.

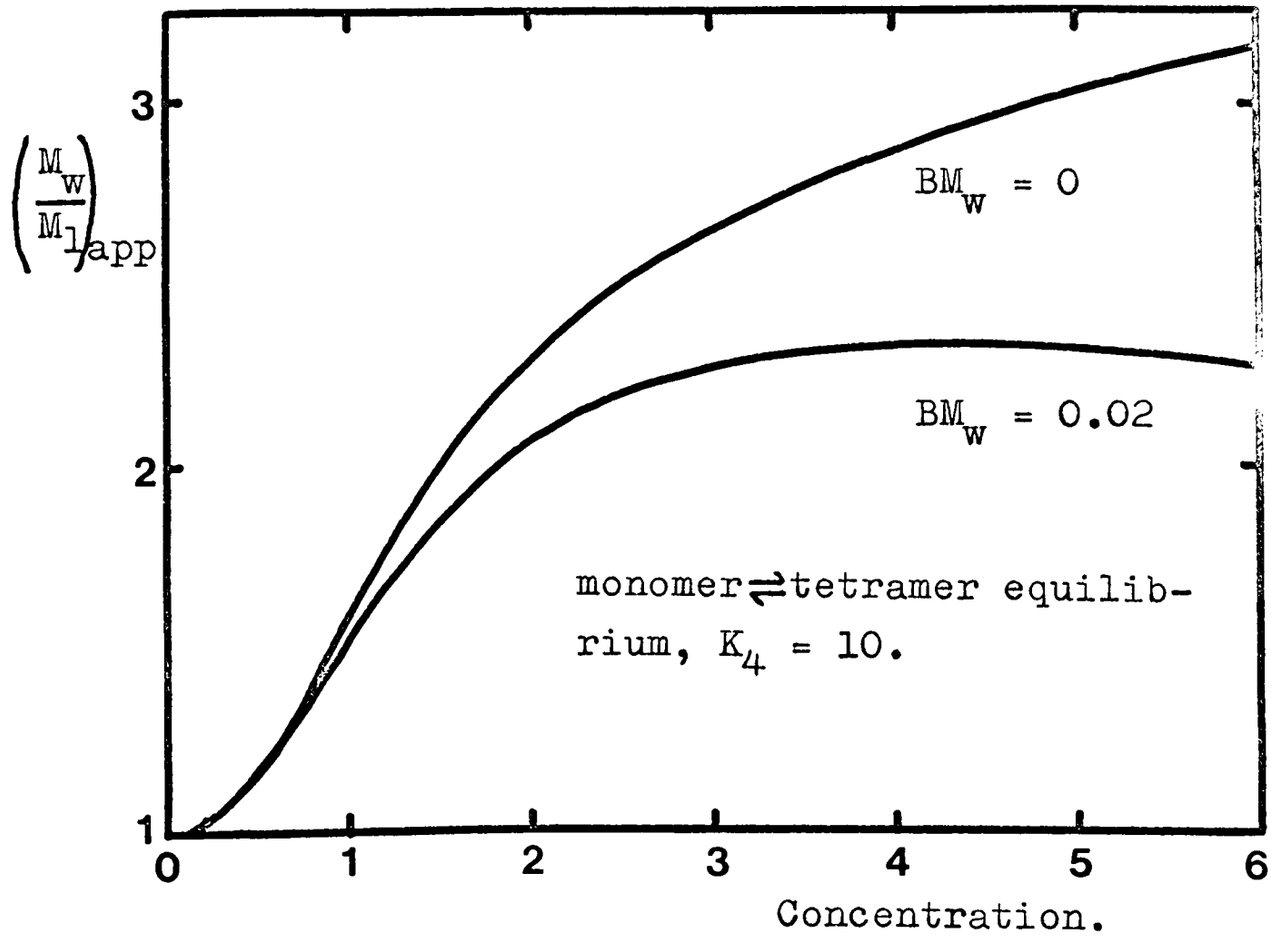

Fig. 5.17. The effect of a positive first virial coefficient on the shape of the theoretical curve for n = 4.

Non-ideality

The effect of the second virial coefficient on the shape of the calculated curves was also determined by making use of the following equations,

$$\left(\frac{M_w}{M_1}\right)_{app} = \left(\frac{M_w}{M_1}\right) \frac{1}{(1 + 2BM_wC)}$$

and,

$$\left(\frac{M_z}{M_1}\right)_{app} = \left(\frac{M_z}{M_1}\right) \frac{1}{(1 + 2BM_wC)^2}$$

The effect of taking a positive second virial coefficient is shown in Fig. 5.17. Unless unrealistically large values of BM_w are chosen, the general shape of the curves remains the same at low concentration, but goes through a maximum and then falls off at higher concentration.

The experimental curves obtained for PFK can now be examined in the light of these theoretical curves. The pronounced sigmoid shape of the curves of $M_{w(app)}/M_1$ and $M_{z(app)}/M_1$ against concentration (Figs. 5.10 and 5.11) suggests that PFK is associating in a closed fashion and that the concentration of any intermediate species is low relative to the concentrations of monomer and n-mer. In contrast, Glutamate Dehydrogenase, which is thought to undergo some form of linear open polymerisation at high concentration, gives a paraboloid curve of M_w against C very similar to the theoretical curves shown in Fig. 5.16. (Eisenberg and Tompkins, 1968)[53].

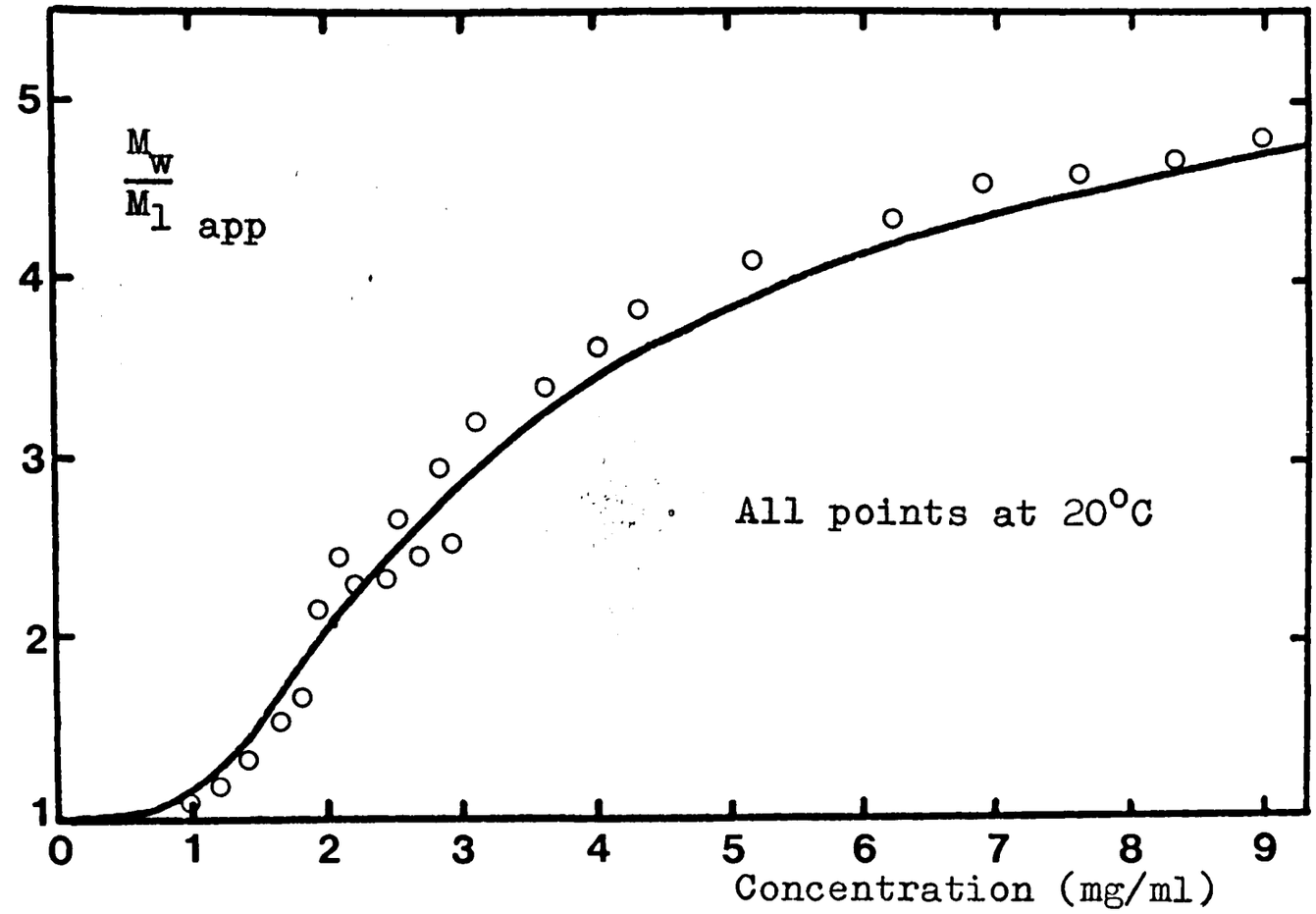

Fig. 5.18. Curve fitted to experimental data, assuming $n = 6$, $K_6 = 0.1$ (mg units) and $BM_w = 0.006$.

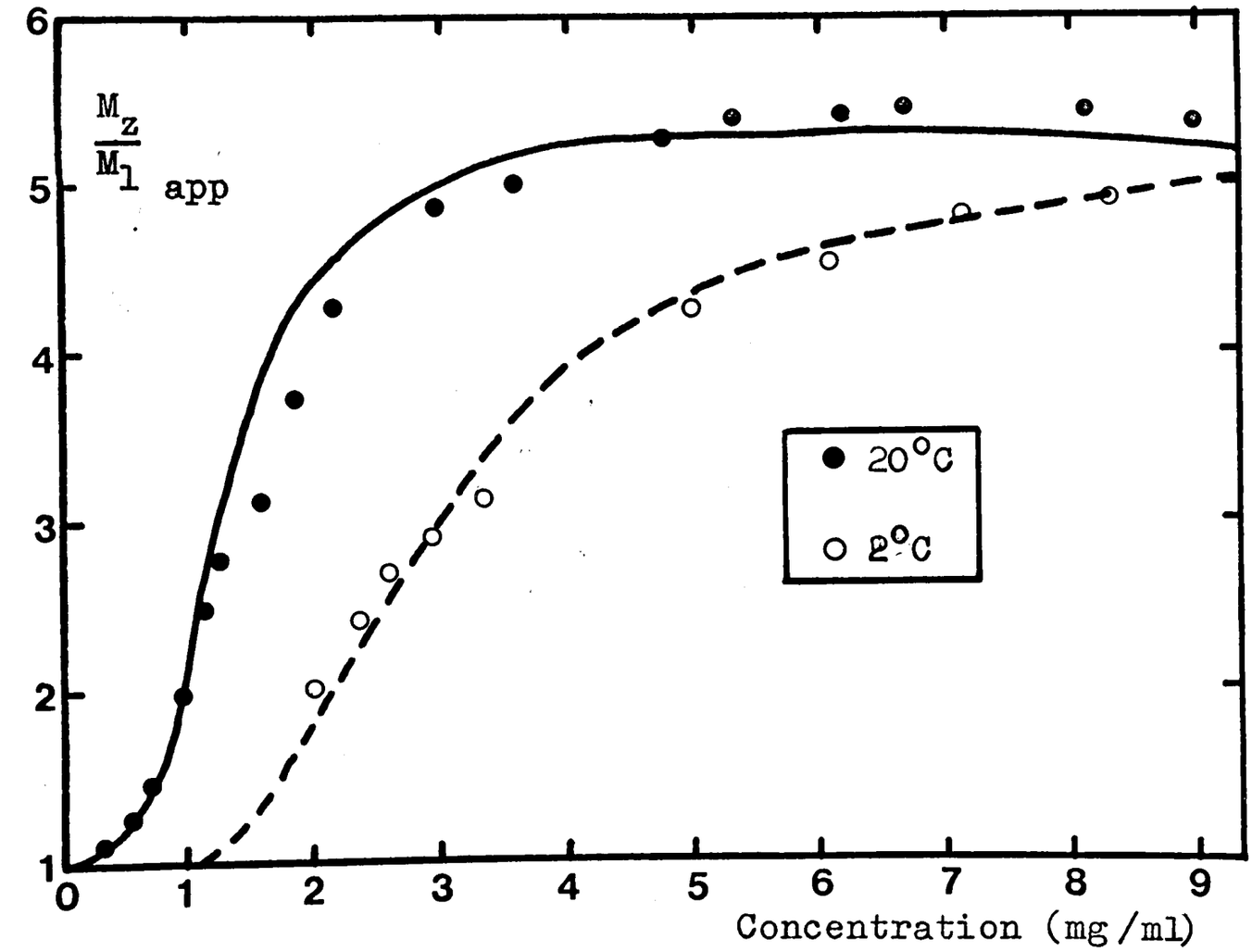

Fig. 5.19. Data fitted assuming $K_6 = 0.1$ at 20°C and 0.001 at 2°C.

If the concentration of any intermediate polymers is assumed to be low (which is suggested by the shape of the PFK curves) and n is taken to be 6, K_6 to be 0.1 mg units and BM_w to be 0.006, curves can be calculated which fit the data for 20°C quite closely (Figs. 5.18 and 5.19). An approximate fit over the rising part of the experimental curve can also be obtained for higher values of n, but this requires the assumption of greater values of the virial term, BM_w, which causes large negative deviations at higher concentrations.

The data for 2°C, although incomplete, can be fitted by a curve which assumes the same values of n and BM_w but uses a smaller value of K_6 (0.001 mg units). This difference in the equilibrium constants leads to a value of 36 Kcal per mole of hexamer for the ΔH of association.

The equilibrium constant for the association at 20°C in molar units is approx 6×10^{25} Ltr^5 / Mole^5.

Therefore, $\Delta G_o = -RT \ln K$

$= -35$ Kcal / Mole

Thus, since $\Delta G_o = \Delta H_o - T\Delta S_o$,

the entropy change for the association is 240 e.u.

(iii) The dissociated enzyme.

The results for the molecular weight of PFK in 0.1% SDS, pH 12 agree with those obtained by Paetkau and Lardy (1968)[4] . The figure of 8.8×10^4 is about one quarter of the molecular weight of the 12S protein, indicating that the latter is probably made up of four of the smaller units. Binding data also indicate a molecular weight of about 90,000 per F-6-P binding site (Kemp and Krebs, 1967).[70]

The sedimentation equilibrium and sedimentation velocity experiments in 6 M Guanidine hydrochloride, 0.1 M 2-mercaptoethanol give a molecular weight of about 8×10^4 for PFK under these conditions. This, allowing for experimental error is the same as that in 0.1% SDS, pH 12 indicating that there has been no further dissociation of the protein. The agreement between the equilibrium and hydrodynamic methods shows that the protein must be behaving as a random coil in this solvent, and the presence of the mercaptoethanol should have eliminated any disulphide bonds. The conclusion must therefore be drawn that PFK contains polypeptide chains of molecular weight equal to about 90,000 Daltons.

These results do not agree with those of Paetkau and Lardy,[4] who found that PFK dissociated into smaller units of molecular weight equal to 51,000 and 25,000 in high concentrations of Gu HCl with dithiothreitol added to break

disulphide bonds. A figure of 90,000 for the basic polypeptide unit of PFK is not, however, unreasonable since *E. Coli* β - galactosidase has been reported to be made up of four polypeptide chains of molecular weight 130,000 (Ullmann *et al*, 1968)[71].

The molecular weight of the 4.5 S protein at pH 11.6, although this material is not completely homogeneous, is probably also 90,000 rather than a higher multiple of this figure. These values of the sedimentation coefficient and molecular weight taken together indicate that the protein under these conditions is still behaving as a compact hydrodynamic unit. For comparison, the value of $s^{o}_{20,w}$ for a completely denatured (random coil) polypeptide chain of this molecular weight would be about 2.7 Svedbergs.

Chapter 6. Optical Rotatory Dispersion and Circular Dichroism.

1. Introduction.

(i) Optical Rotatory Dispersion (ORD).

A beam of light has associated with it time and distance dependent electric and magnetic field vectors which are mutually perpendicular. A plane-polarised ray of light is one in which all the component vectors except those in a single plane have been removed. To an observer looking along the direction of propagation of the light, a monochromatic plane-polarised ray would appear as in Fig.(6.1). (For simplicity, only the electric field vector is shown, but the magnetic field vector will behave in a similar manner).

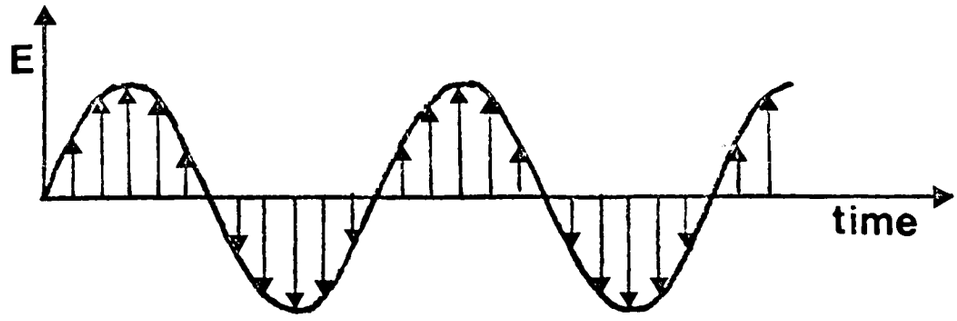

Fig. 6.1.

Monochromatic, plane-polarised light ray.

A circularly-polarised light beam is one in which the field vector appears to rotate at uniform angular velocity about the direction of propagation. (Fig.6.2).

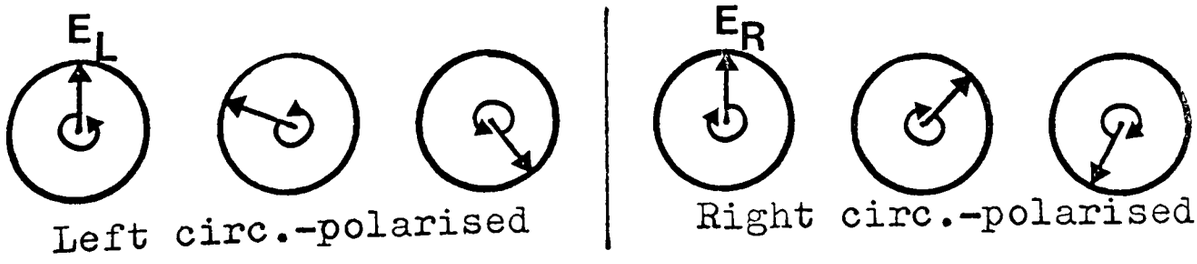

Fig. 6.2. Vectorial representation of circularly-polarised light (Looking along the t axis)

Plane-polarised light can be resolved into equal left and right circularly polarised components as shown below.

Fig. 6.3.

Plane-polarised light resolved into opposite circ. components

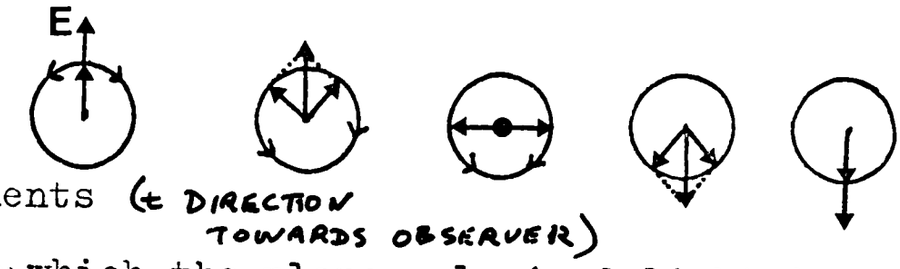

If the medium through which the plane-polarised light is passing has a difference in refractive index for the two components, the speed of rotation of the two vectors will be different. The nett effect is a rotation of the plane of polarisation as the light passes through the medium given by:-

$$\alpha = \frac{\pi d}{\lambda}\left(n_L - n_R\right)$$

Where α is the angle through which the plane of polarisation is rotated.
d is the thickness of the material.
λ is the wavelength of the incident light.
n_L and n_R are the refractive indices for left and right circularly-polarised light resp.

This effect is known as Circular Birefringence, and the change in α with λ is the Optical Rotatory Dispersion.

In spectral regions which are distant from any absorption bands, the variation of α produces a so-called plain dispersion curve. In the vicinity of an absorptive electron transition, the rotation changes in sign, giving rise to a Cotton effect. These are shown in Fig. 6.4 .

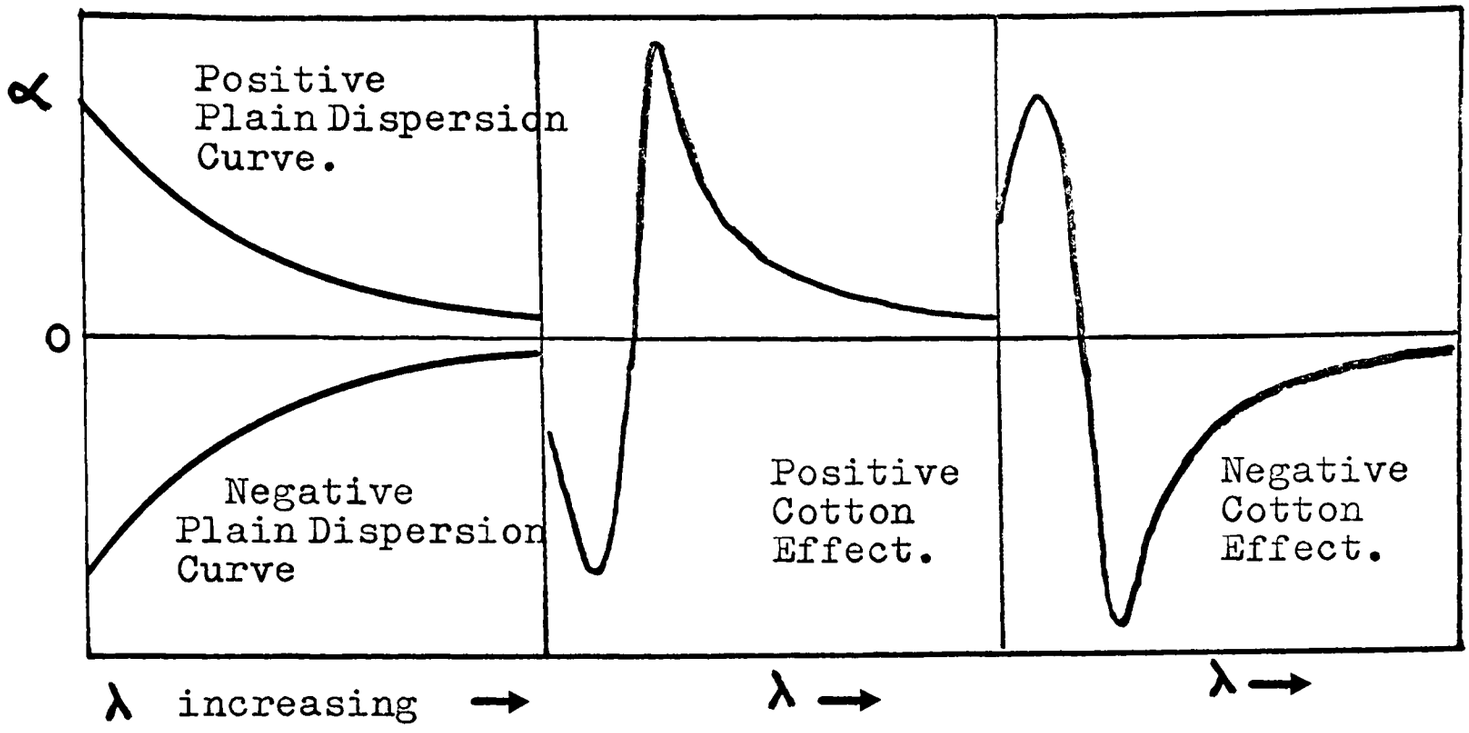

Fig. 6.4. Types of Rotatory Dispersion Curves.

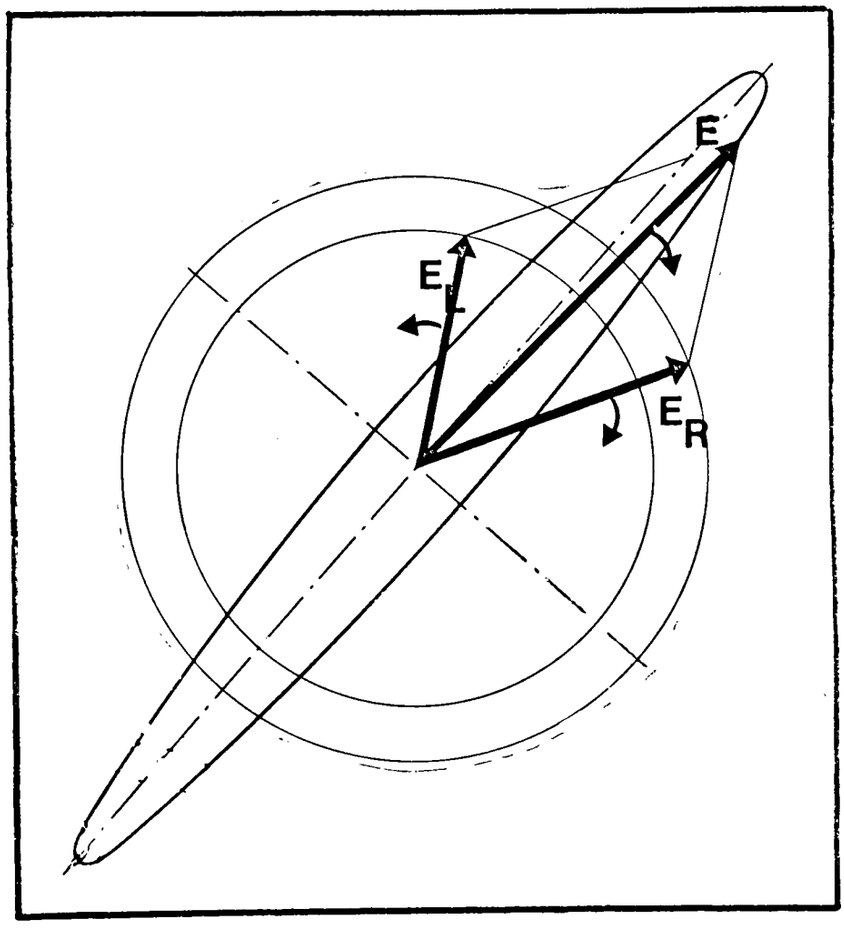

Fig. 6.5. Vectorial Representation of Elliptically Polarised Light.

(ii) Circular Dichroism (CD).

In addition to the difference in refractive index, an optically active substance will have unequal absorption for the two circularly-polarised components. The resultant vector then traces out an ellipse, and the light beam is said to be elliptically polarised (Fig. 6.5). This phenomenon is known as Circular Dichroism.

The major axis of the ellipse is at an angle α to the plane of the incident polarised light which depends on $(n_L - n_R)$ as before. Since the total absorption is always much greater than the difference in absorption coefficients $(A_L - A_R)$ the ellipse is very elongate and in this case, it can be shown(to a good approximation) that the ellipticity per unit length (the angle whose tangent is the ratio of the minor to major axes of the ellipse) is given by: -

$$\theta = \tfrac{1}{4}(A_L - A_R) \qquad \text{(in radians)}$$

If this is expressed in terms of the Molar extinction coefficients and in degrees rather than radians it becomes

$$[\theta] = 2.303\left(\frac{4500}{\pi}\right)(\epsilon_L - \epsilon_R) \qquad \text{deg.cm}^2 \text{ / decimole}$$

$$\simeq 3300\,(\epsilon_L - \epsilon_R)$$

The variation of $[\theta]$ with wavelength gives rise to a Dichroic absorption band which is similar in appearance to the band

arising from an electron transition. The CD band can be either positive or negative according to the sign of $(\epsilon_L - \epsilon_R)$.

Just as ordinary absorption bands can be characterised by the dipole strength which is related to the area under the band, circular dichroism can be expressed in terms of a rotational strength. (Moffitt and Moscowitz, 1959).[72]

For the Kth transition, $$R_K = \frac{3hc}{8\pi^3 N} \int_0^\infty \frac{\theta_K(\lambda)}{\lambda} d\lambda$$

Where h = Planck's constant, c = the speed of light, N = the number of absorbing molecules per ml.

If the band is Gaussian in shape (Fig. 6.6), the rotational strength can be expressed in terms of the Gaussian parameters as:-

$$R_K = 0.696 \times 10^{-42} \sqrt{\pi} \, [\theta^\circ_K] \, \frac{\Delta^\circ_K}{\lambda^\circ_K}$$

(iii) The relationship between ORD and CD.

Both ORD and CD result from the interaction of electromagnetic radiation with an optically active chromophore. An active transition will give rise to a Cotton effect and a CD band centred approximately on its wavelength, λ_0. (Fig. 6.7).

ORD and CD can be regarded as a particular case of the Kronig-Kramers Theorem which relates all absorptive and dispersive phenomena (Moffitt and Moscowitz, 1959).[72] They derived the following reciprocal relations:-

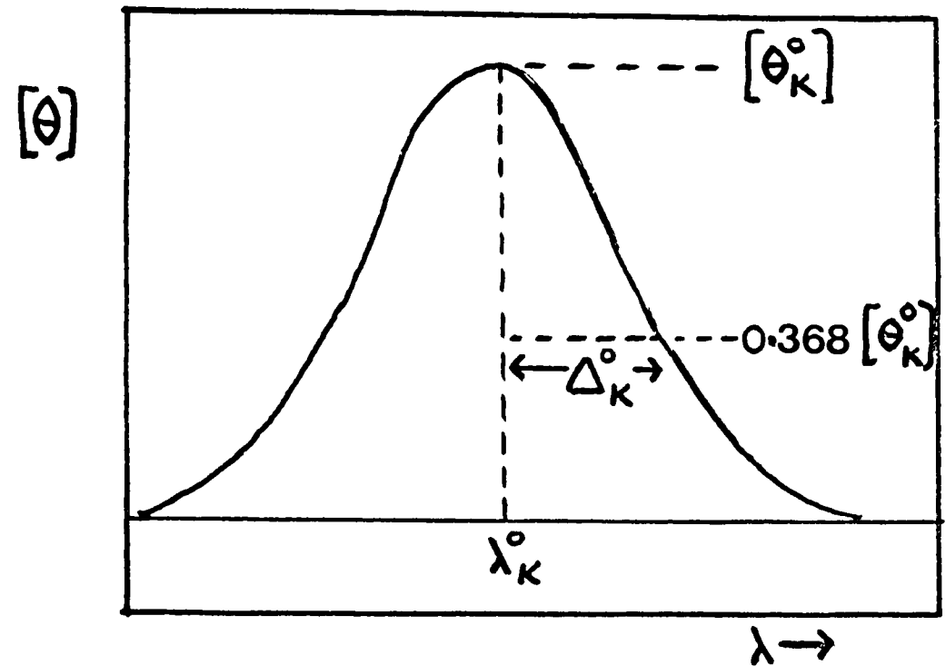

Fig. 6.6. Parameters of the Gaussian curve.

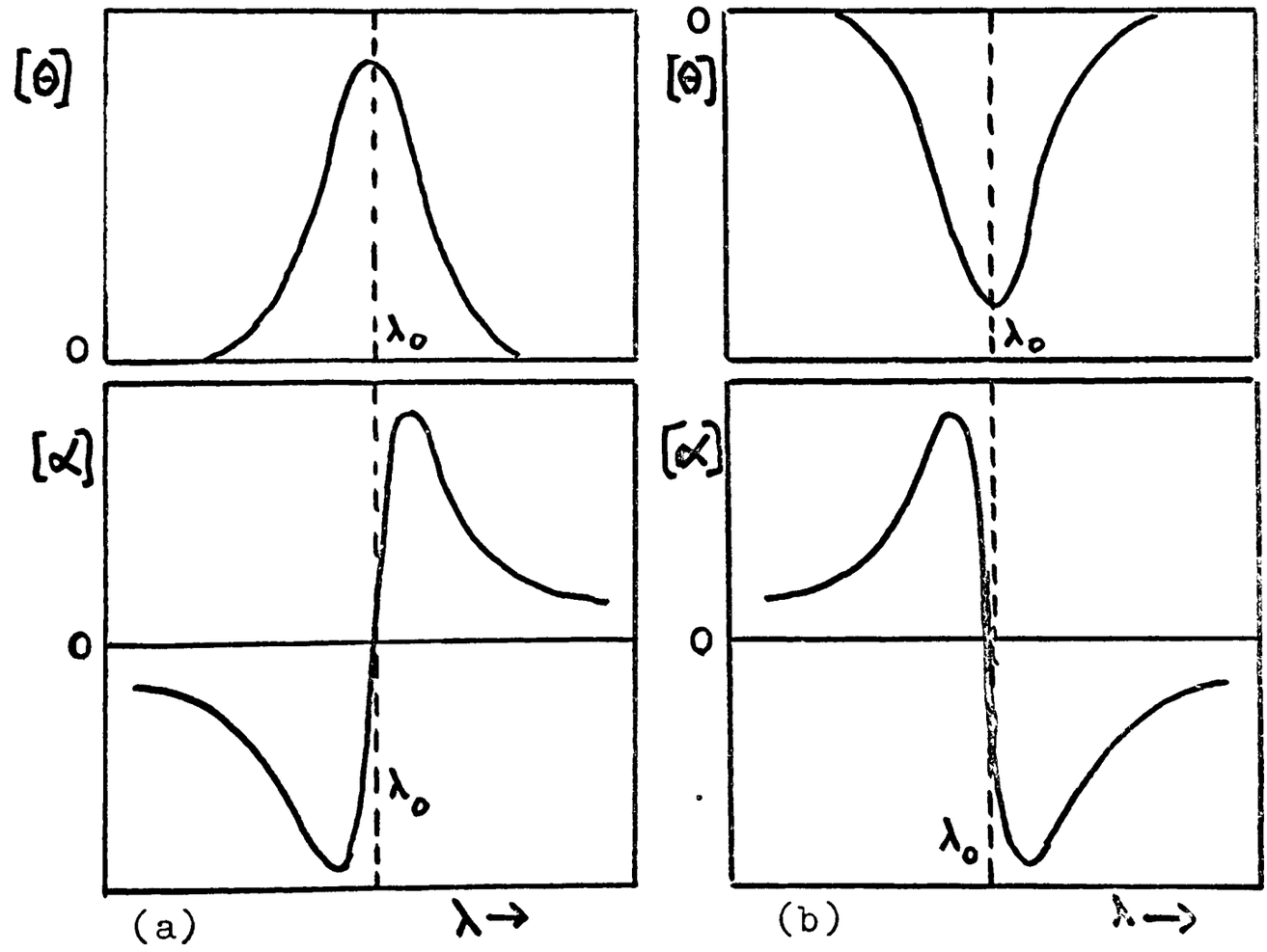

Fig. 6.7. Relationship between CD band and ORD Cotton effect. (a) Positive CD band is associated with positive Cotton effect. (b) Vice versa.

$$[m'_K]_\lambda = \frac{2}{\pi}\int_0^\infty [\theta_K]_{\lambda'} \frac{\lambda^{\circ\prime}}{\lambda^2 - \lambda'^2}\, d\lambda'$$

and

$$[\theta_K]_\lambda = \frac{2}{\pi\lambda}\int_0^\infty [m'_K]_{\lambda'} \frac{\lambda'^2}{\lambda^2 - \lambda'^2}\, d\lambda'$$

It is therefore possible to transform a CD curve into an ORD curve or vice versa if sufficient information is available about the partial CD bands or ORD curves which make up the overall curve.

The Kronig-Kramers transform was used in this work to convert CD data into an ORD curve. The CD curve was approximated as the sum of Gaussian bands using an iterative computer program (Appendix 1(a).). If we consider the Kth transition to be Gaussian, then:-

$$[\theta_K] = [\theta^\circ_K]\, e^{-(\lambda - \lambda^\circ_K)^2/\Delta^{\circ 2}_K}$$

Substituting into the appropriate transform equation,

$$[m'_K]_\lambda = \frac{2[\theta^\circ_K]}{\pi}\int_0^\infty e^{-(\lambda - \lambda^\circ_K)^2/\Delta^{\circ 2}_K}\left(\frac{\lambda'}{\lambda^2 - \lambda'^2}\right)d\lambda'$$

In the case where $\lambda^\circ_K \gg \Delta^\circ_K$ the integral approximates to

$$[m']_\lambda = \frac{2[\theta^\circ_K]}{\sqrt{\pi}}\left[e^{-(\lambda - \lambda^\circ_K)^2/\Delta^{\circ 2}_K}\int_0^{\frac{\lambda - \lambda^\circ_K}{\Delta^\circ_K}} e^{x^2}\, dx - \frac{\Delta^\circ_K}{2(\lambda - \lambda^\circ_K)}\right.$$

This function was also evaluated by an Algol program, using tabulated values of the integral. (Appendix 1(b).).

(iv) The origin of optical activity.

The absorption of light by a molecule produces a charge displacement which is composed of a linear displacement (an electric dipole) and a circular displacement (a magnetic dipole). The magnetic part of the transition is normally too weak to be observed and it is the electric dipole or electric transition moment which is the most important factor in producing ordinary light absorption. The electric and magnetic vectors are normally perpendicular to each other but if, for any reason,they become parallel (i.e. there is simultaneous displacement and rotation of charge about the same axis in the molecule) the transition will be optically active.

Two models have been proposed to account for this phenomenon. The Kirkwood model (Kirkwood, 1937)[73] is based on the hypothesis that the electric and magnetic field vectors arise from the coupling of pairs of electric transitions which are separated from each other in space and which are not in the same plane. The electric transition moments must be large to obtain strong coupling, so this model best describes the origin of the optical activity of strongly absorbing chromophores.

The 'one-electron model' (Condon, 1937)[74] has as its basis the assumption that a chromophore existing in a sufficiently asymmetric electronic environment can have

an electric moment induced in the direction of the magnetic vector and vice versa. This model explains the existence of optical activity in the case of very weak absorption bands.

(v) Optical activity in Protein Molecules.

(a) Far-UV optical activity.

The principle contribution to the optical activity of proteins in this spectral region is made by the peptide chromophore, although there is also a smaller contribution from the far-UV bands of aromatic residues. The appearance of the far-UV peptide ORD and CD spectra is strongly dependent on secondary structure. Studies on poly-amino acid model compounds have given data for the random-coil polypeptide chain and for the two principle types of regular secondary structure, the α-helix and β-structure. These results are shown in Figs. 6.8 and 6.9.

Moffitt[75] applied the Kirkwood model to the α-helix, treating it as a single exciton system. He predicted that there should be two dichroic bands, equal in magnitude but opposite in sign arising from the helix exciton splitting. However, measurements made on α-helical polypeptides (Holzwarth et al, 1962)[76] showed that there are three bands present. It is now thought that the 190nm and 210nm bands have their origin in the $\pi - \pi^*$ exciton system, and the

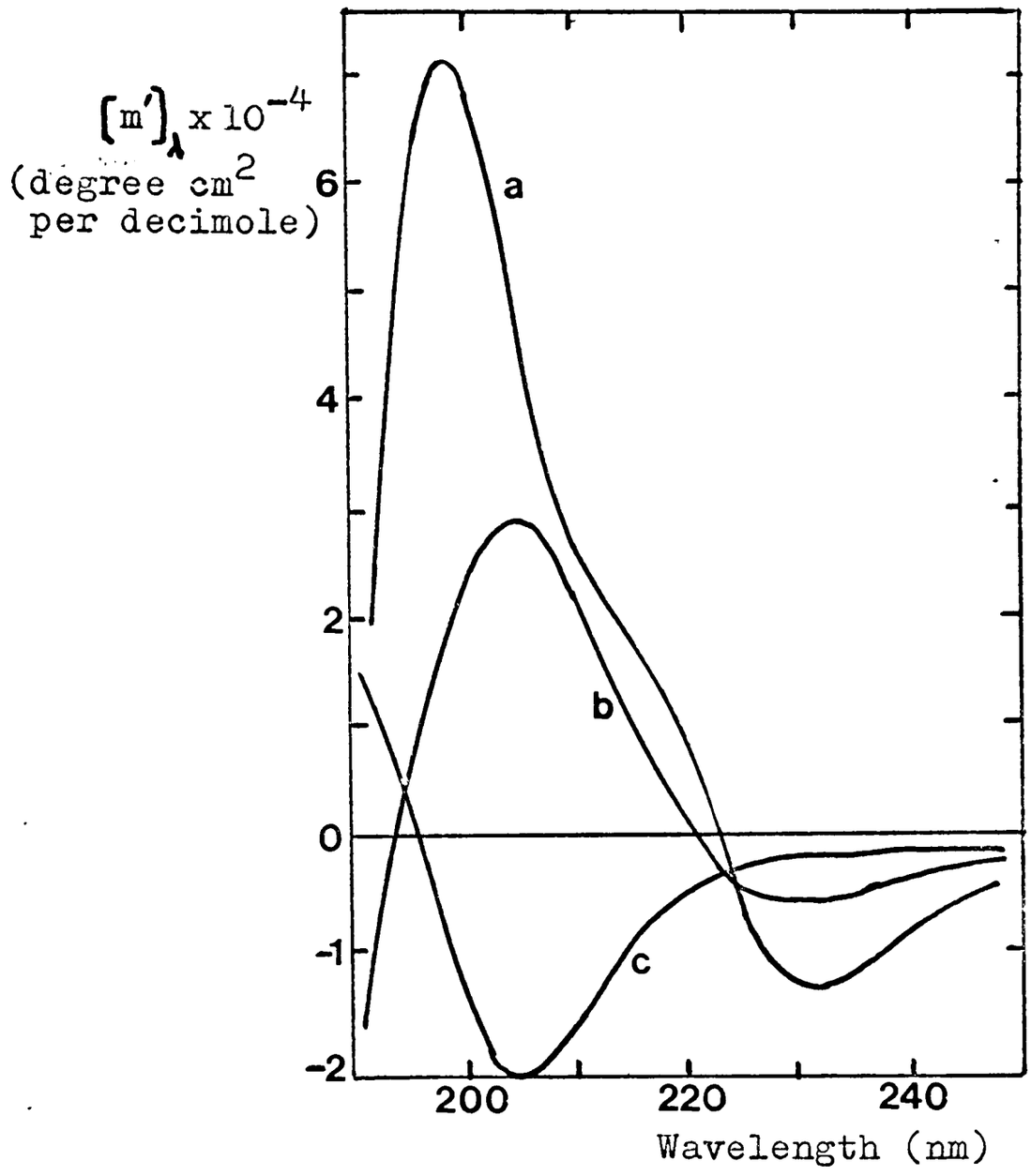

Fig. 6.8. Far UV ORD curves of poly-L-lysine in α- helical (a), β (b), and random coil (c) conformations .

(Taken from Greenfield et al, 1967)[77]

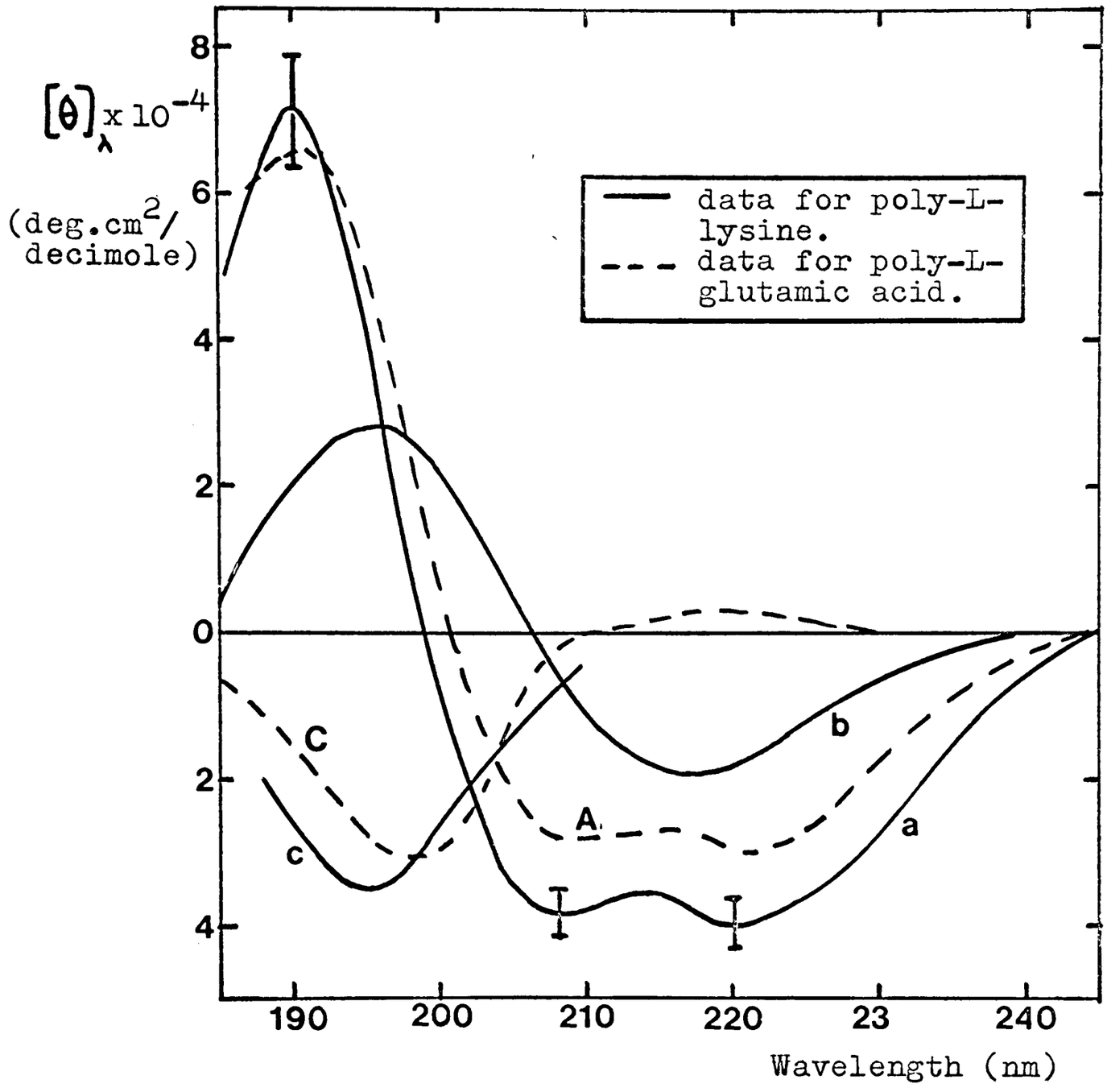

Fig. 6.9. Far UV CD bands of : -

Poly-L-lysine, (a) α- helix.
(b) β- structure.
(c) random coil.

(Taken from Fasman et al, 1966)[78]

Poly-L-glutamic acid, (A) α- helix.
(C) random coil.

(Taken from Velluz and Legrand, 1965)[79]

220nm band arises from the $n - \pi^*$ peptide transition which is in an asymmetric electronic environment in the helix. (Schellman and Oriel, 1962[80]; Tinoco et al, 1963).[81]

On the basis of the original exciton model, Moffitt obtained the following equation for the variation of the mean residue rotation, $[m']_\lambda$ in the region of plain dispersion (300nm - 600nm).

$$[m']_\lambda = a_0\left(\frac{\lambda_0^2}{\lambda^2-\lambda_0^2}\right) + b_0\left(\frac{\lambda_0^2}{\lambda^2-\lambda_0^2}\right)^2$$

λ_0 is assigned a constant value, commonly 212nm and a_0 and b_0 are determined from the intercept and slope of a plot of

$$[m']_\lambda \frac{(\lambda^2-\lambda_0^2)}{\lambda_0^2} \quad \text{against} \quad \frac{\lambda_0^2}{(\lambda^2-\lambda_0^2)}$$

Data for synthetic polypeptides in α- helical and random coil conformations showed that a_0 varies widely with the solvent but that b_0 had a more or less constant value of -630 for 100% helix and zero for 100% random coil. Although, as we have seen, the CD spectrum shows that the original Moffitt treatment is an oversimplification, the equation is still a useful empirical method of treating the experimental data.

(b) Near-UV optical activity.

Ellipticity bands have been observed between 240nm and 310nm in a number of proteins including Avidin and Streptavidin[82], Pepsin[83], Aldolase[84,85], Chymotrypsin[86], Trypsin[87]

Carbonic Anhydrase[88] and β - Lactoglobulin[89] . Tentative band assignments have been made for Insulin (optically active cysteine residues) and Lysozyme (optically active tryptophan residues) , (Beychok, 1967).[90]

The near-UV dichroic bands are sensitive to changes in conformation and may prove to be better detectors of changes in tertiary and quaternary structure than the far-UV peptide bands.

(vi) Estimation of Secondary Structure from Optical Activity.

It was thought initially that proteins behaved as a mixture of α-helix and random coil and that an estimate of the amount of helix could be made from the parameters of the ORD curve. Simmons and Blout (1960)[91] suggested the use of a linear interpolation of the $[m']_{a33}$ trough rotation using a value of -13,000 deg.cm^2/ decimole for 100% helix and -2000 for 100% random coil. Yang (1965)[92] suggested that helix content can be estimated from the Moffitt parameters taking b_0 to be -630 for 100% helix and zero for 100% coil and making a linear interpolation of the experimental value. Both methods ignore the contributions made by β - structure and by the chromophores responsible for near-UV optical activity. Recent X-ray studies on Ribonuclease[93,94], Lysozyme[95] , Chymotrypsin[96] and Carboxypeptidase[97] show that all these proteins contain

significant amounts of β-structure.

An alternative approach which has been suggested by Fasman(1967)[130] is to compare the experimental ORD or CD curve with theoretical curves based on different proportions of α-helix, β-structure and random coil. Using values of the mean residue rotation or ellipticity obtained from studies on model compounds an attempt can be made to fit the experimental curve with the appropriate proportions of secondary structure.

This method of secondary structure estimation is open to criticism, in particular for assuming that the polypeptide chain which is not in one of the regular conformations behaves as random coil. In globular proteins, the peptide backbone, although it may be irregular, is in a relatively fixed conformation stabilised by interactions between different parts of the tertiary structure. The optical activity is therefore the sum of contributions from a finite number of fixed conformations of the peptide chromophore. The model compounds used to obtain the ORD and CD curves for random coil are flexible chains in which the peptide chromophore can have an infinite number of conformations which average out to give the observed optical activity. The method may, however, be more valid for denatured proteins which behave more as flexible chains and for proteins having a high proportion of regular structure.

2. Experimental details.

(i) Optical Rotatory Dispersion.

ORD measurements were made with a Bendix-Ericson Polarmatic 62 recording spectropolarimeter. This instrument makes use of the Faraday magneto-optical effect to balance the rotation of the sample. The current passing through the magnet coils of the Faraday cell is then a measure of the optical rotation of the sample. The light source was a 250 watt Xenon arc which gave usable results down to 200nm.

Calibration of the monochromator was carried out by measuring the positions of the emission lines of a mercury discharge lamp. The wavelength scale was found to be linear over the range 500nm - 230nm. Below 230nm measurement of the oxygen absorption lines was used to check the calibration. Calibration of the rotation settings of the instrument was made with standard sucrose solution. The rotation for sucrose was found to give a linear fit to a one-term Drude equation between 500nm and 220nm.

Dismountable 0.5cm and 1.0cm pathlength cells were used. The cell birefringence was sensitive to the pressure on the screw-ring which was used to hold the cell together. Adjustment of this pressure in a trial-and-error fashion enabled the cell base-line to be made reasonably linear.

For the same reason, the cells were not dismantled between the measurements made on the protein solutions and the base-line measurements made with solvent. To check for baseline drift (probably the result of variations in lamp intensity) the signal obtained with no cell in the light path was checked at the beginning and end of each scan.

The entrance and exit slits were maintained at a width ratio of 5 to 4 as recommended by the manufacturer. Between 500nm and 300nm they were set at 0.5mm and 0.4mm, between 300nm and 250nm at 1.0mm and 0.8mm and below 250nm the maximum slit settings of 2.0mm and 1.6mm were used. The instrument was found to have a measurable stray-light level when working with the wide slits in the far-UV. This was eliminated by carefully masking the interior of the optical unit, and by masking the wavelength scale viewing window to prevent external light from entering the instrument.

The Polarmatic 62 is provided with a single wavelength scanning speed of 1.5×10^{-4} cm^{-1} / min. This was suitable for use with the fast pen response time (Υ = 5sec.). When using the slow pen response (Υ = 30sec.) to reduce the noise in the far-UV, scanning was either done manually at a rate of 0.4×10^{-4} cm^{-1} / min. or at 0.2×10^{-4} cm^{-1} / min. using a slow drive motor fitted externally to the manual scanning control. Curves in the far-UV were also obtained by making measurements at a series of individual wavelengths.

The recorder pen was made to sweep at constant speed in the X direction for several minutes, and the trace obtained was averaged to give the signal and noise. This method of measurement agreed within the error and noise limits with the results obtained by wavelength scanning.

All measurements were made at 25° C and nitrogen flushing of the optical unit was used below 210nm to reduce light absorption by atmospheric oxygen.

(ii) Circular Dichroism.

CD measurements were made on a Roussel-Jouan Dichrographe, Model CD 185. The Dichrographe makes use of the Pockels effect to convert plane-polarised light into circularly-polarised light. An alternating voltage is applied across the faces of a crystal of ammonium dihydrogen phosphate which then acts as a quarter wave plate. Plane polarised light passing through the crystal is converted into light whose polarisation varies from right circular to left circular and passing through various intermediate stages of elliptical polarisation during one cycle of the alternating voltage. This light beam then passes through the sample which, if it is dichroic, will absorb the left and right circular components to different extents, producing an oscillating light intensity at the photomultiplier. The photomultiplier voltage so produced is split into a

direct component, V_c, and an alternating component, V_{ac}. V_{ac} is amplified and rectified to give a direct voltage, V_d. The ratio V_d / V_c is directly proportional to $(\epsilon_L - \epsilon_R)$ and the sign of V_d can be either negative or positive depending upon the sign of $(\epsilon_L - \epsilon_R)$.

The measured dichroism is independent of the exit window birefringence of the cell and virtually independent of the entrance window birefringence. In practice, it was found that ordinary fused silica rectangular spectrophotometer cells gave very straight baselines. 0.5mm and 0.1mm dismountable cells were used for measurements below 240nm.

The monochromator slit and the photomultiplier dynode voltage are servo monitored. Measurements were made up to the maximum slit setting of 2mm and up to a dynode setting of 1200 volts (the maximum is 1500 volts, but noise and reproducibility became bad above 1200 volts.). Most scans were carried out at 0.25nm/sec. using the intermediate pen response setting (τ = 4 sec.).

Measurements were made at room temperature (approx. 25°) and the optical unit was flushed with nitrogen below 210nm. The Dichrographe was calibrated with a standard solution of isoandrosterone in dioxane as recommended by the manufacturer.

3. Results.

(A) ORD results for Aldolase and PFK.

(i) Near-UV and Visible Spectral Region.

Plain dispersion curves were recorded for aldolase and PFK in this region. The curve for aldolase showed a small inflexion at 290nm - 295nm (Fig.6.10), but no anomalous dispersion was detectable in the case of PFK. Moffitt plots for the data (Figs. 6.11 and 6.12) were reasonably linear over the range 500nm - 260nm, giving $a_o = -100$, $b_o = -250$ for aldolase and $a_o = -50$, $b_o = -200$ for PFK, taking λ_o to be 212nm in each case. Aldolase showed a positive deviation from linearity in the 300nm - 280nm part of the Moffitt curve, which correlates with the Cotton effect at 290nm. PFK also showed a deviation in this wavelength region which suggests that there may be near-UV optical activity which is too small to be detected directly.

The variation of a_o and b_o with pH for aldolase and PFK is shown in Figs. 6.13 and 6.14 . PFK precipitates in the acid pH region and could only be studied between pH 8 and pH 12. In the case of aldolase, there are marked changes in the Moffitt parameters between pH 4.5 and 3.5 and between pH 9.5 and 11.5. These changes correlate with the decrease in sedimentation coefficient and molecular weight of the enzyme which is known to take place over

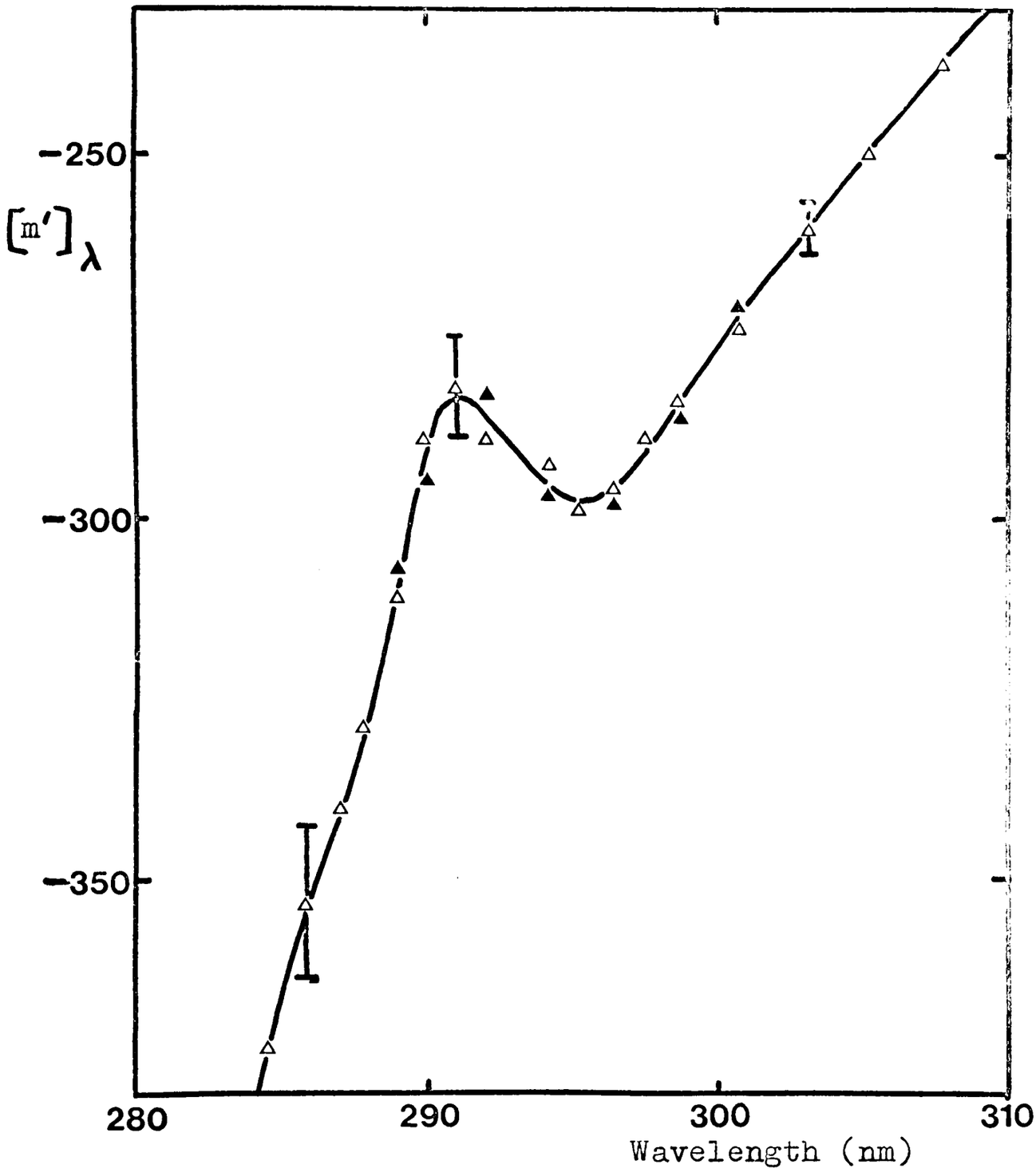

Fig. 6.10. Part of the near-UV dispersion curve for Aldolase, showing the Cotton effect in the 290 nm region. (The vertical lines indicate the limits of the instrumental noise.)

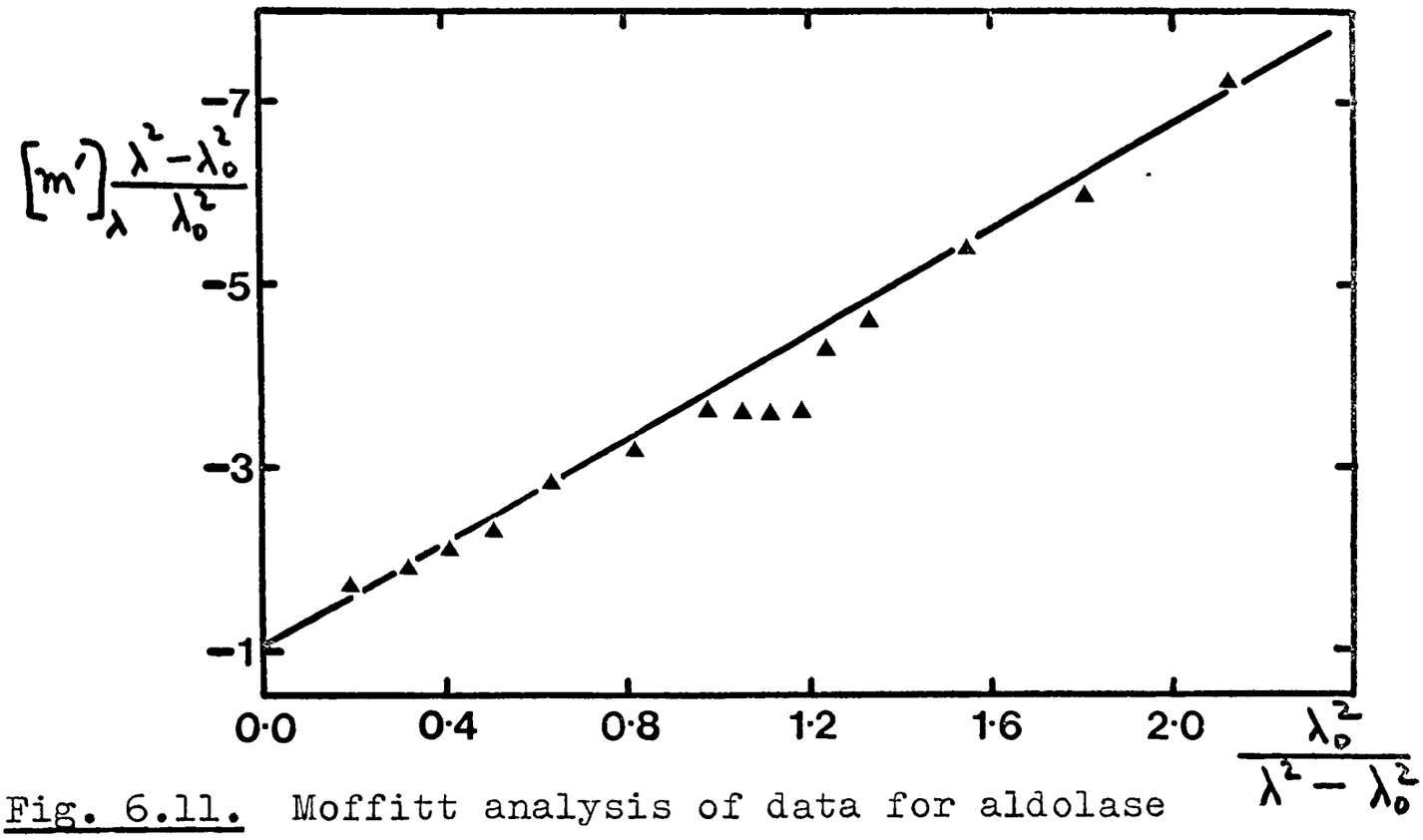

Fig. 6.11. Moffitt analysis of data for aldolase (in 0.1M NaCl) over the wavelength range, 500nm - 260nm.

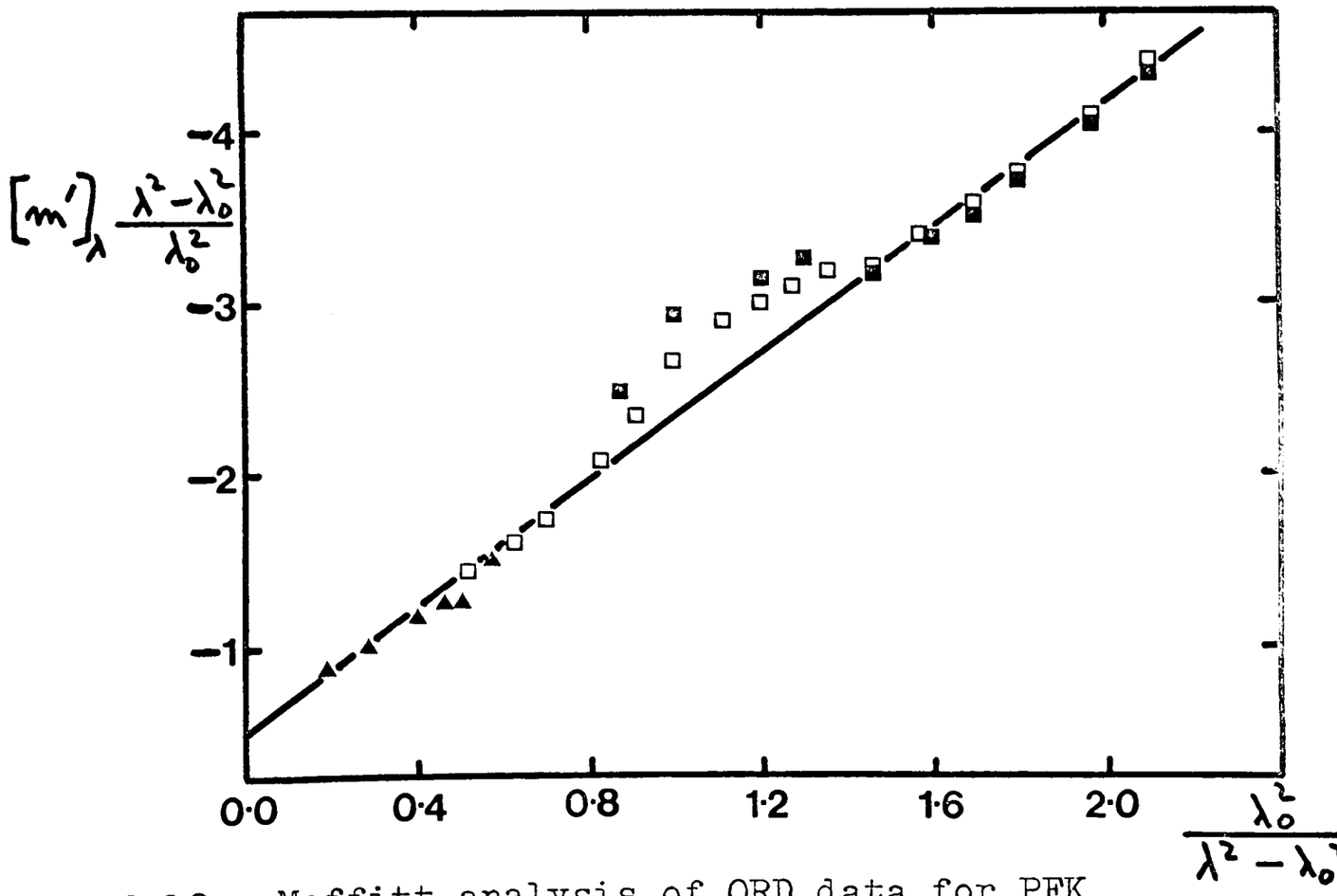

Fig. 6.12. Moffitt analysis of ORD data for PFK (0.1M phosphate buffer, pH 8) over the same wavelength range. The symbols are for three different concentrations of PFK.

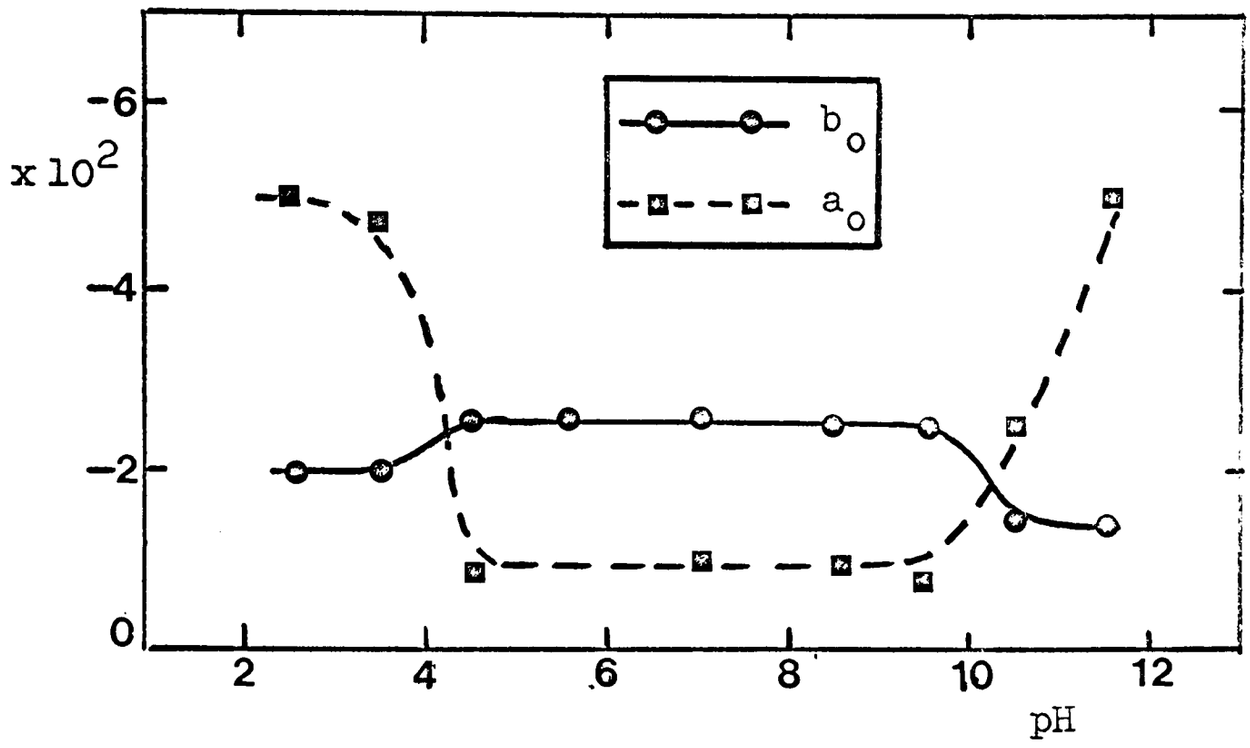

Fig. 6.13. Variation of a_o and b_o for aldolase, with pH.

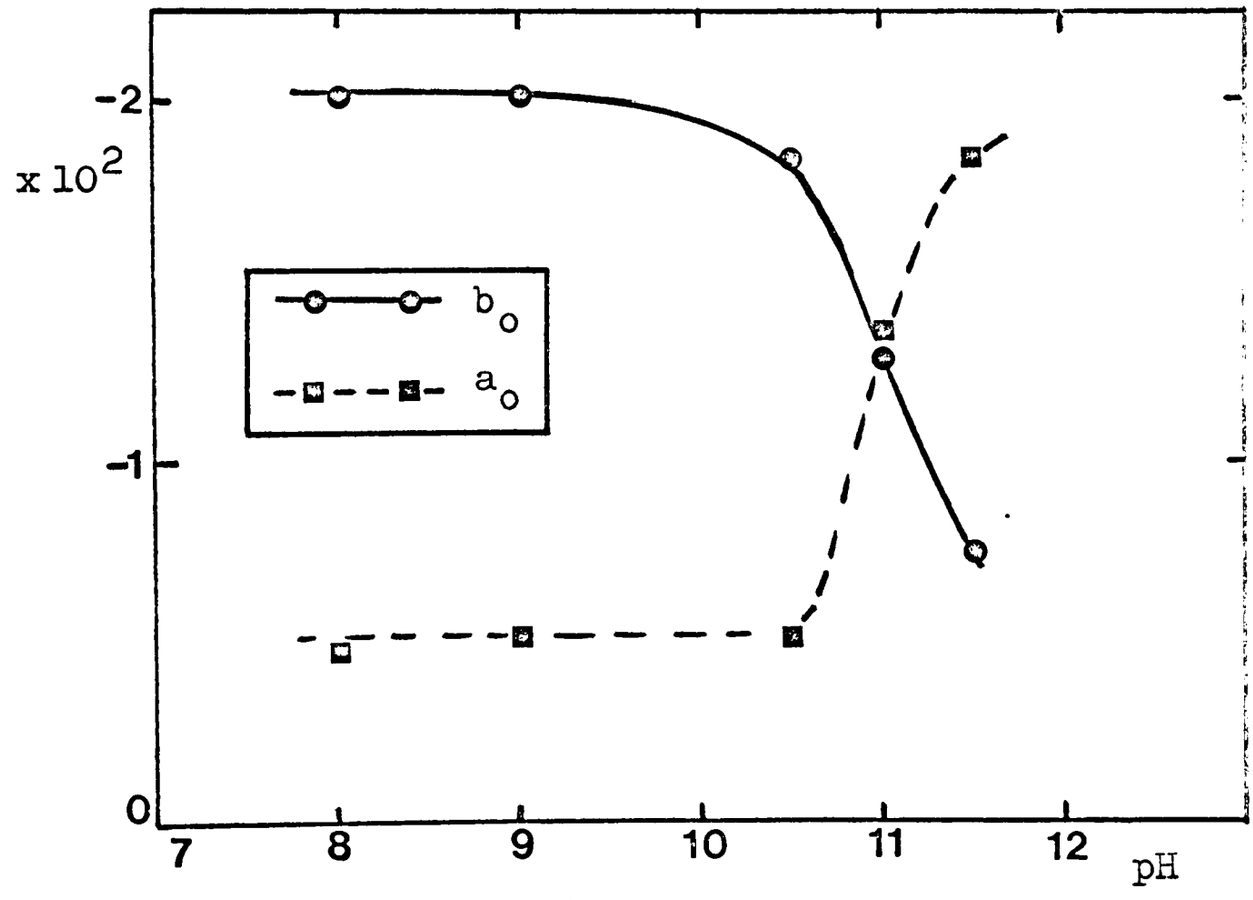

Fig. 6.14. Variation of a_o and b_o for PFK at high pH.

the same pH ranges (K.R. Leonard, Part II thesis, 1966)[66]. The Cotton effect at 290nm disappeared over the same pH regions. Aldolase which was brought to pH 2.5 by addition of acid and then dialysed slowly back to pH 7 showed partial recovery of the 290nm effect. PFK also showed large changes in a_o and b_o between pH 10.5 and pH 11.5 where the protein is known to dissociate (Chapter 4).

(ii) Far-UV Spectral Region.

Data for aldolase and PFK are shown in Fig. 6.15 and 6.16. The aldolase curve was obtained both by analysis of time scans at single wavelengths and by continuous wavelength scanning. PFK was studied by the latter method alone. The noise level in each case was about 1/5 of the signal at 200nm. Both proteins gave similar curves with a peak at about 200nm, a shoulder at about 215nm and a trough at about 235nm . The values for the mean residue rotations are given in Table 6.1.

Table 6.1 Far-UV ORD data for aldolase and PFK.

	Wavelength (nm)	$[m']_\lambda$ Aldolase	$[m']_\lambda$ PFK
Trough	233.5 ± 1	-4000±250	-7000 ± 700
Crossover	224 ± 1	-	-
Peak	201 ± 3	18,000 ± 4000	30,000±5000

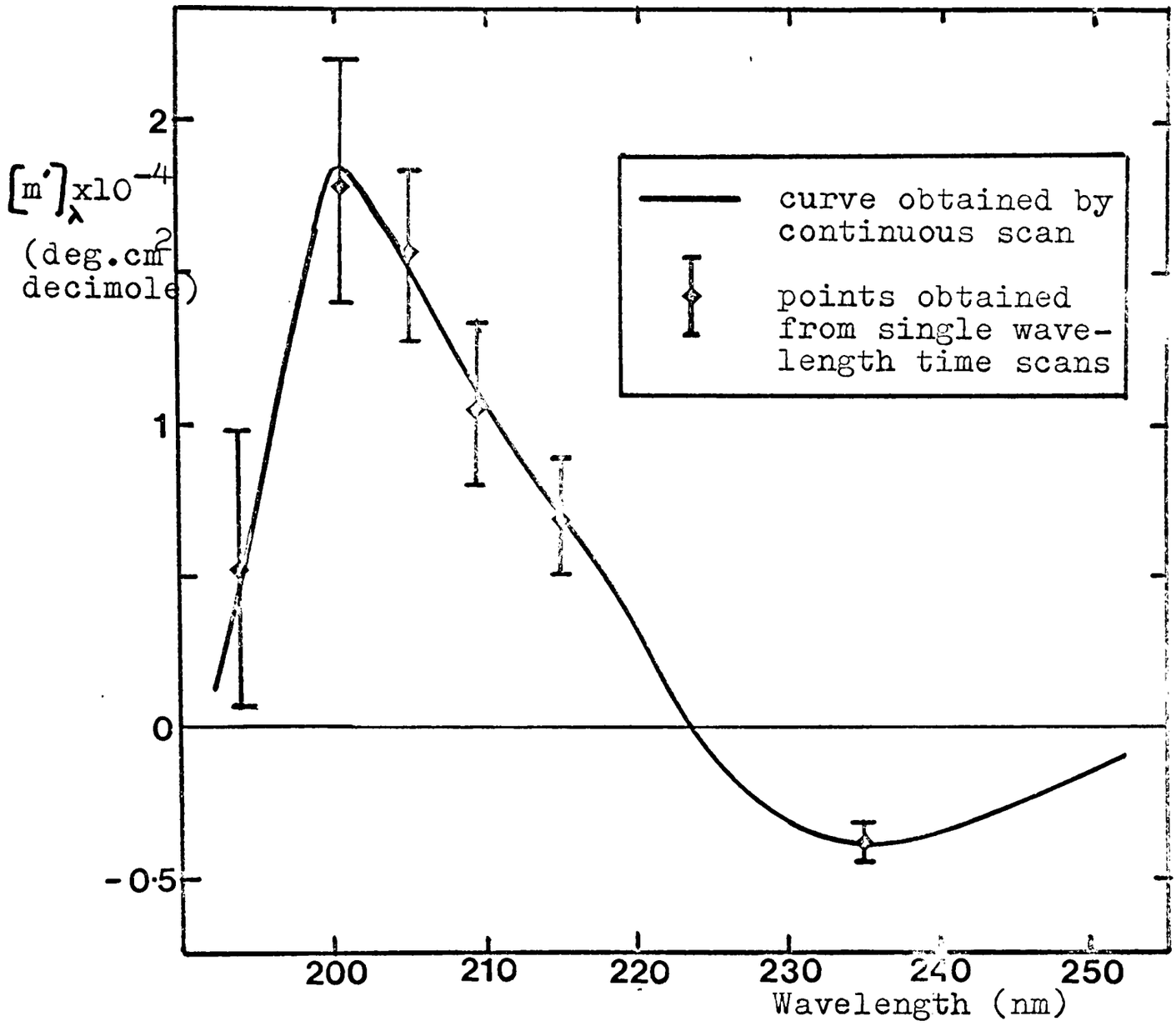

Fig. 6.15. Far-UV ORD curve for aldolase (dissolved in 2x glass-distilled water).

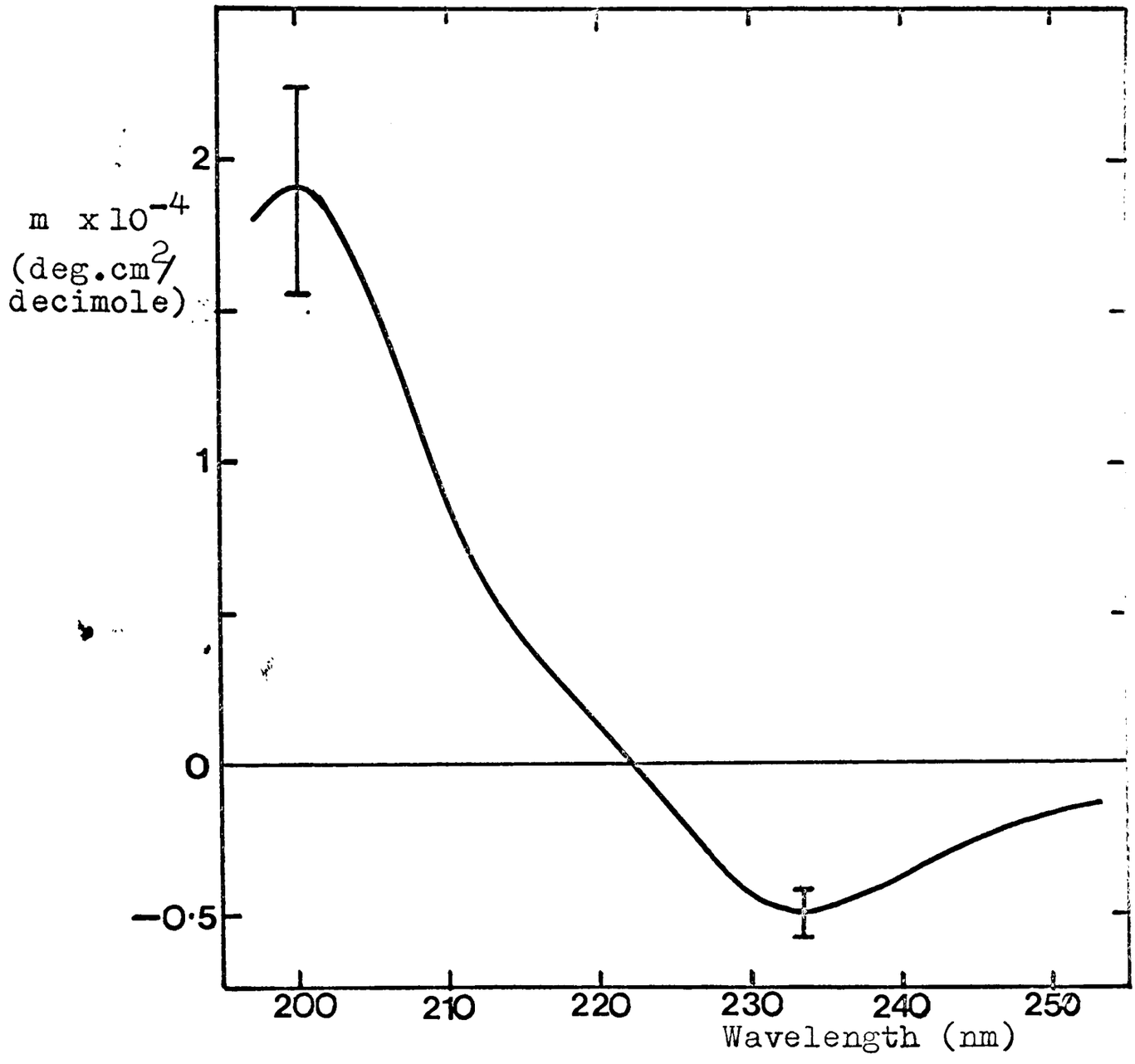

Fig. 6.16. Far-UV ORD curve for PFK (in 1mM tris-phosphate buffer, pH 8). Curve was obtained by the continuous scan method. Vertical lines show the estimated noise limits.

(B) Circular Dichroism Results.

(i) Aldolase.

(a) Near-UV results.

Aldolase was found to have a system of CD bands in the 260nm - 300nm region (Fig. 6.17a)which was very reproducible. There was always a small negative band centred on 295nm and a larger positive band centred on 280nm with a small positive shoulder at about 289nm.

The effect of increasing the pH on these bands is shown in Fig. 6.17b.(pH adjustment was made by direct addition of alkali and the dichroic spectrum measured immediately.) Over the range pH 8 to pH 12, aldolase showed a progressive decrease in magnitude of the 295nm and 280nm bands, with the formation of a new positive band at about 225nm which increases in size with increasing pH. The pH was also varied by direct addition of acid over the range 8 - 3 (not shown). There was no change in the bands between pH 8 and pH 4, but between pH 4 and pH 3.5 they disappear completely. After dialysis of the pH 3 solution back into buffer at pH 7, the near-UV bands were reformed but were only about 1/4 the size of those for the original solution.

Aldolase treated with 1% formaldehyde solution, or with N-acetyl imidazole showed a decrease in the magnitude

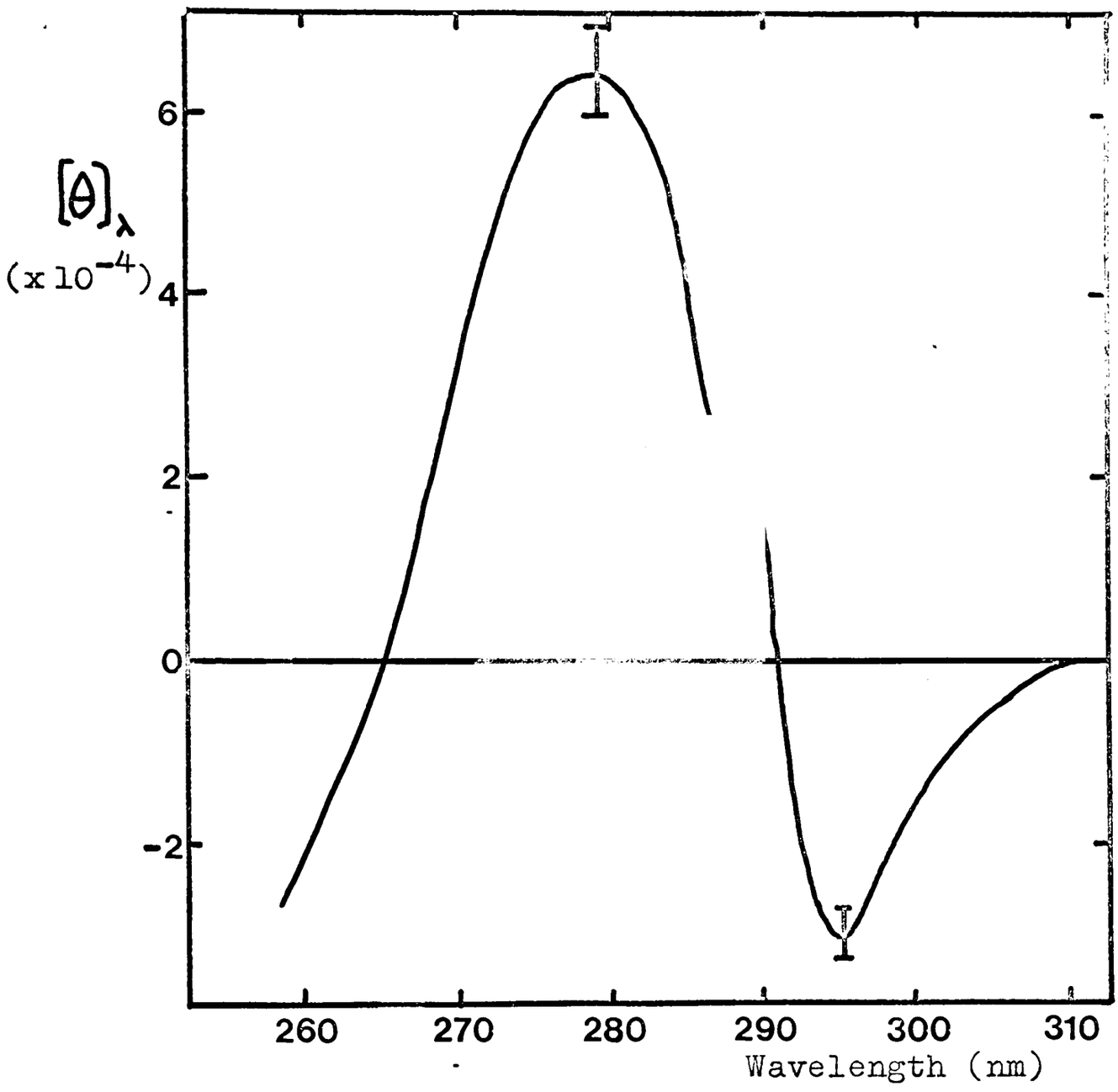

Fig. 6.17a. Near-UV CD bands for Aldolase in 0.1M NaCl. $[\theta]_\lambda$ is expressed per 100,000 g. protein .

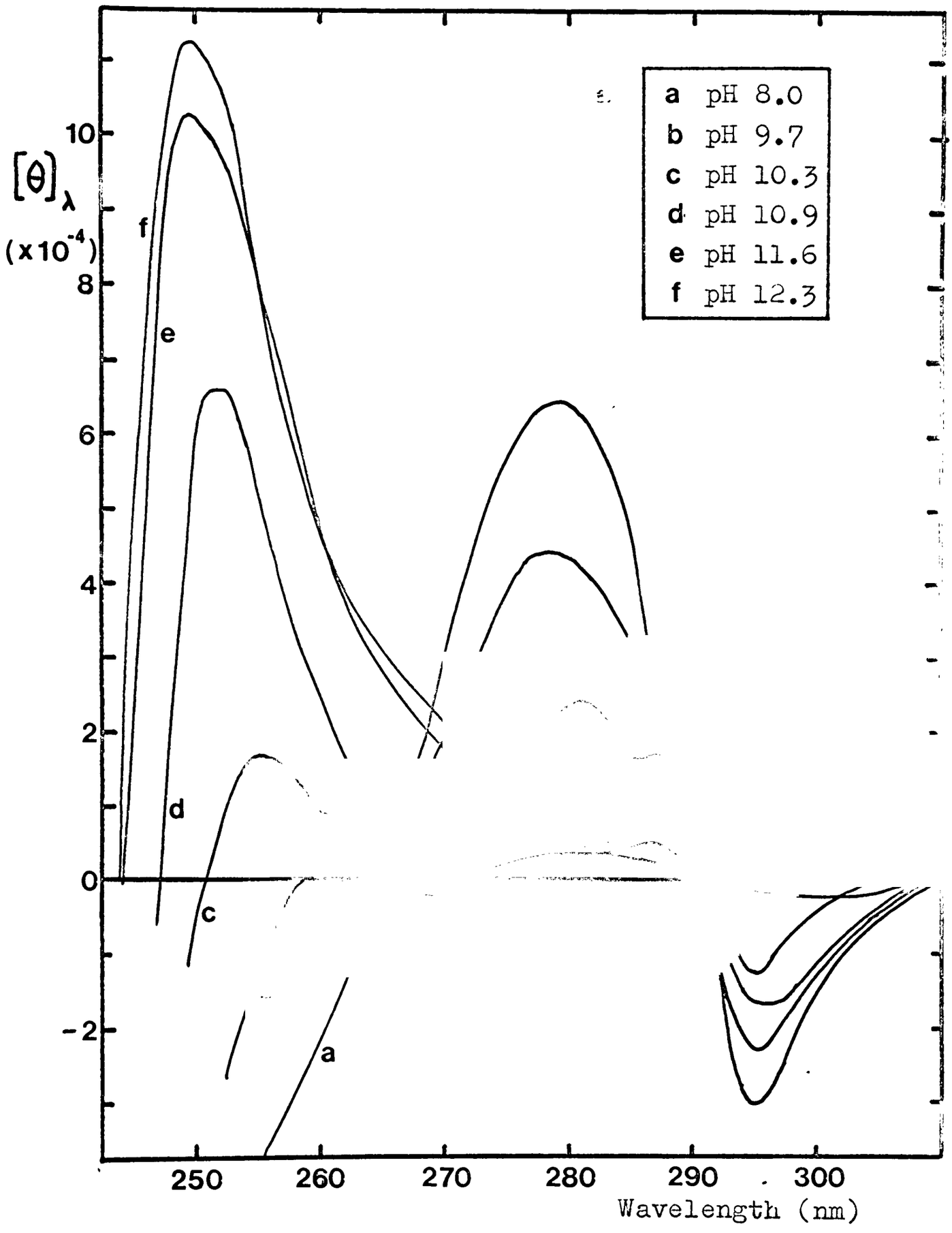

Fig. 6.17b. The effect of increasing the pH on the near-UV CD bands of Aldolase.

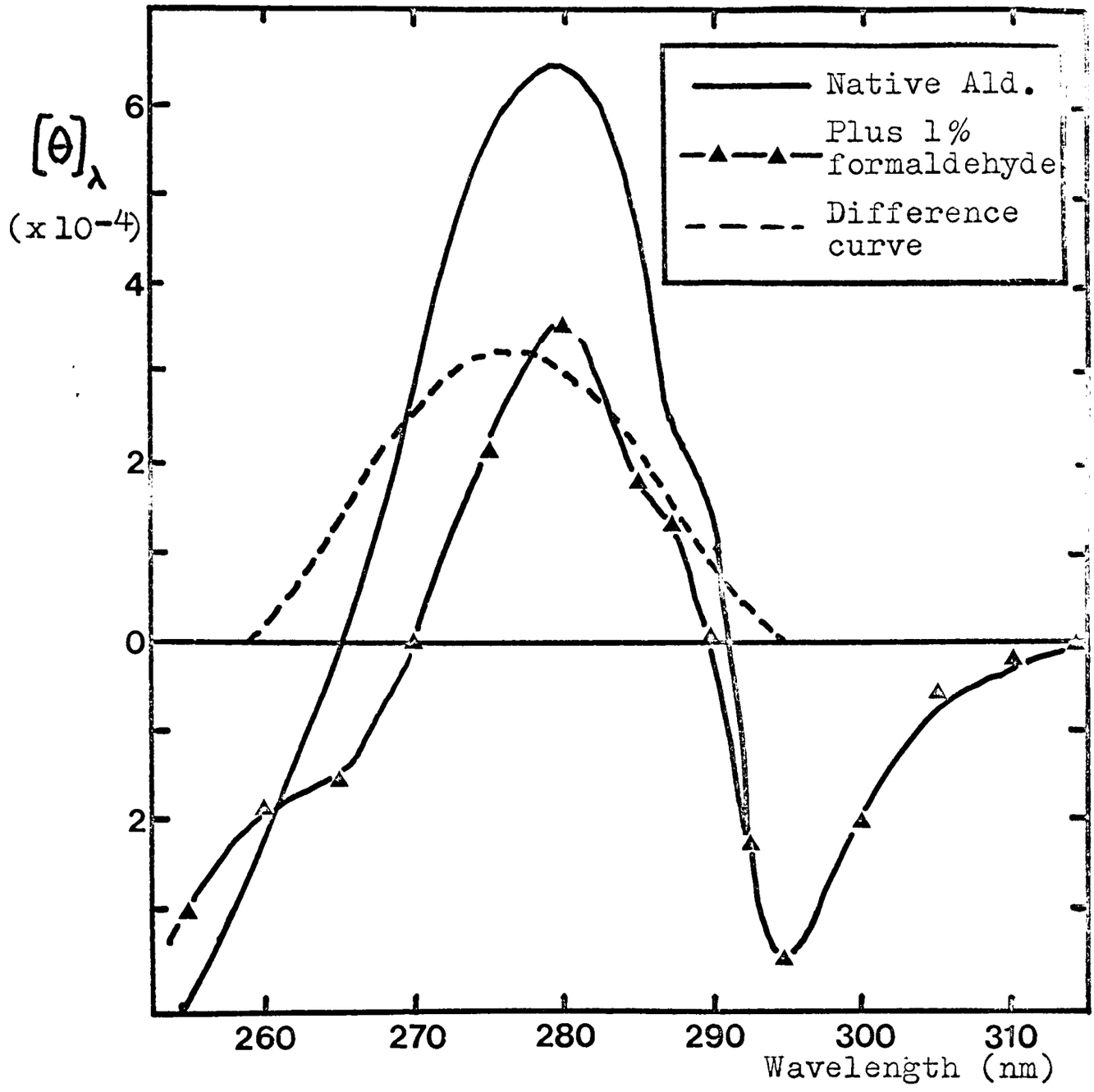

Fig. 6.18. The effect of 1% formaldehyde on the near-UV CD bands of Aldolase.

of the 280nm band but no change in the 295nm band (Fig.6.18).

(b) Far-UV results.

Dichroic spectra were measured for the native protein and at pH intervals between pH 8 and pH 12 and between pH 6 and pH 1.5. The results are shown in Figs. 6.19 to 6.21. The far-UV curve for native aldolase (Fig. 6.19) has a negative band with two extrema at about 220nm and 210nm and a positive band with a maximum at 191nm. The signal-to-noise ratio was about 100 in the 210nm - 220nm region, decreasing to a value of about 20 at 190nm.

On increasing or decreasing the pH (Figs. 6.20 and 21), large changes in the bands occur which can be correlated with known conformational changes. Between pH 4.5 and pH 3.5 where aldolase is known to dissociate into unfolded subunits by a rapid, co-operative process (K.R. Leonard, Part II Thesis, 1966), there is a large decrease in the negative ellipticity at 220nm and a shift to shorter wavelength of the 210nm extremum. Between pH 9 and pH 11 where there is thought to be a more gradual unfolding of oligomer (Hass and Lewis, 1963)[98], there is a more gradual change in the negative bands. Above pH 11, where dissociation of the oligomer takes place, there are changes similar to those seen at low pH. Data for the 190nm peak are only given for the extremes of pH.

Far-UV data for native Aldolase is summarised in Table 6.2.

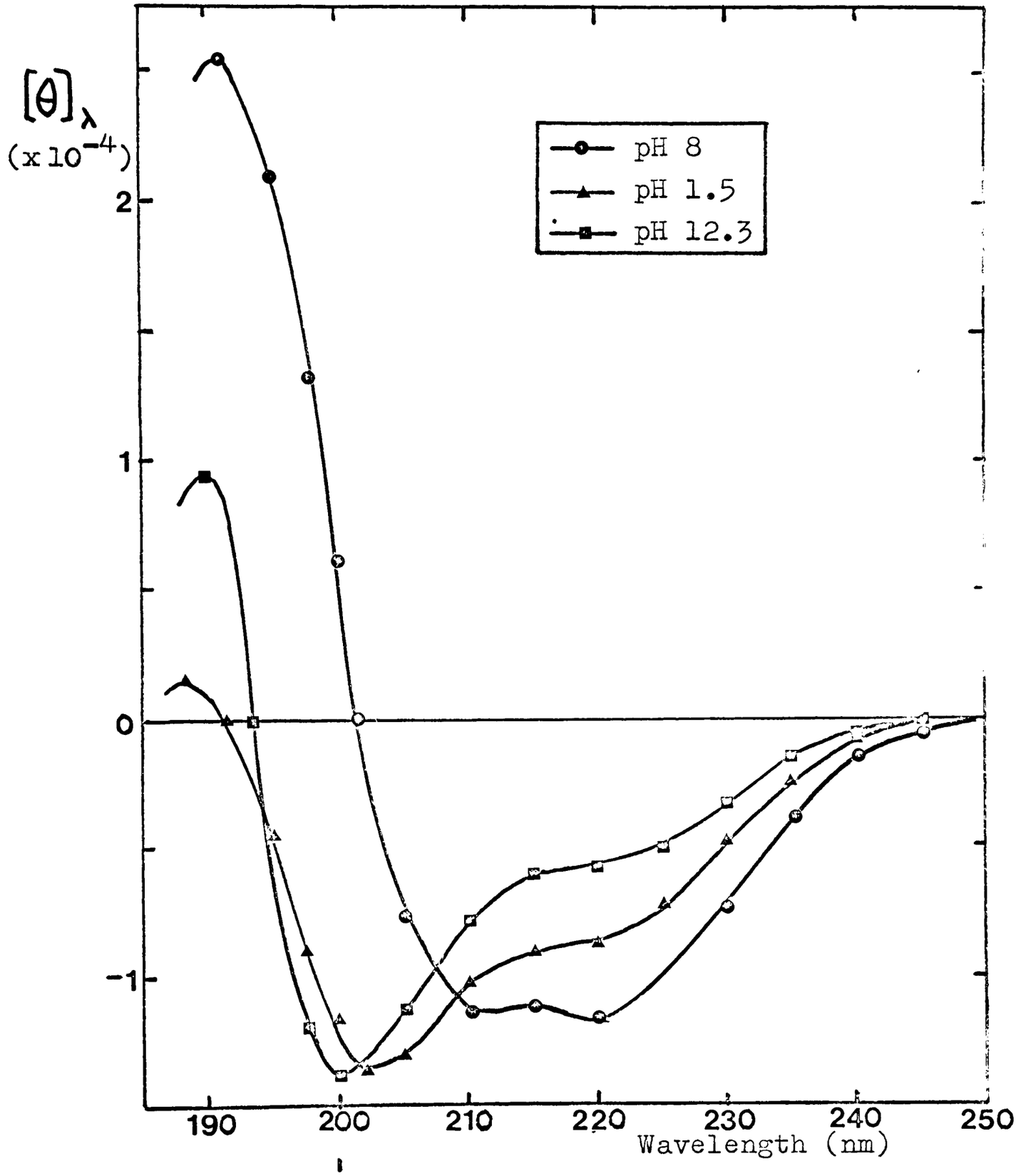

Fig. 6.19. Far-UV dichroic spectra of Aldolase in 0.1M Tris-phos. ,pH 8 and at high and low pH. The ellipticity $[\theta]_\lambda$, is in terms of the mean amino acid weight taken as 115g.

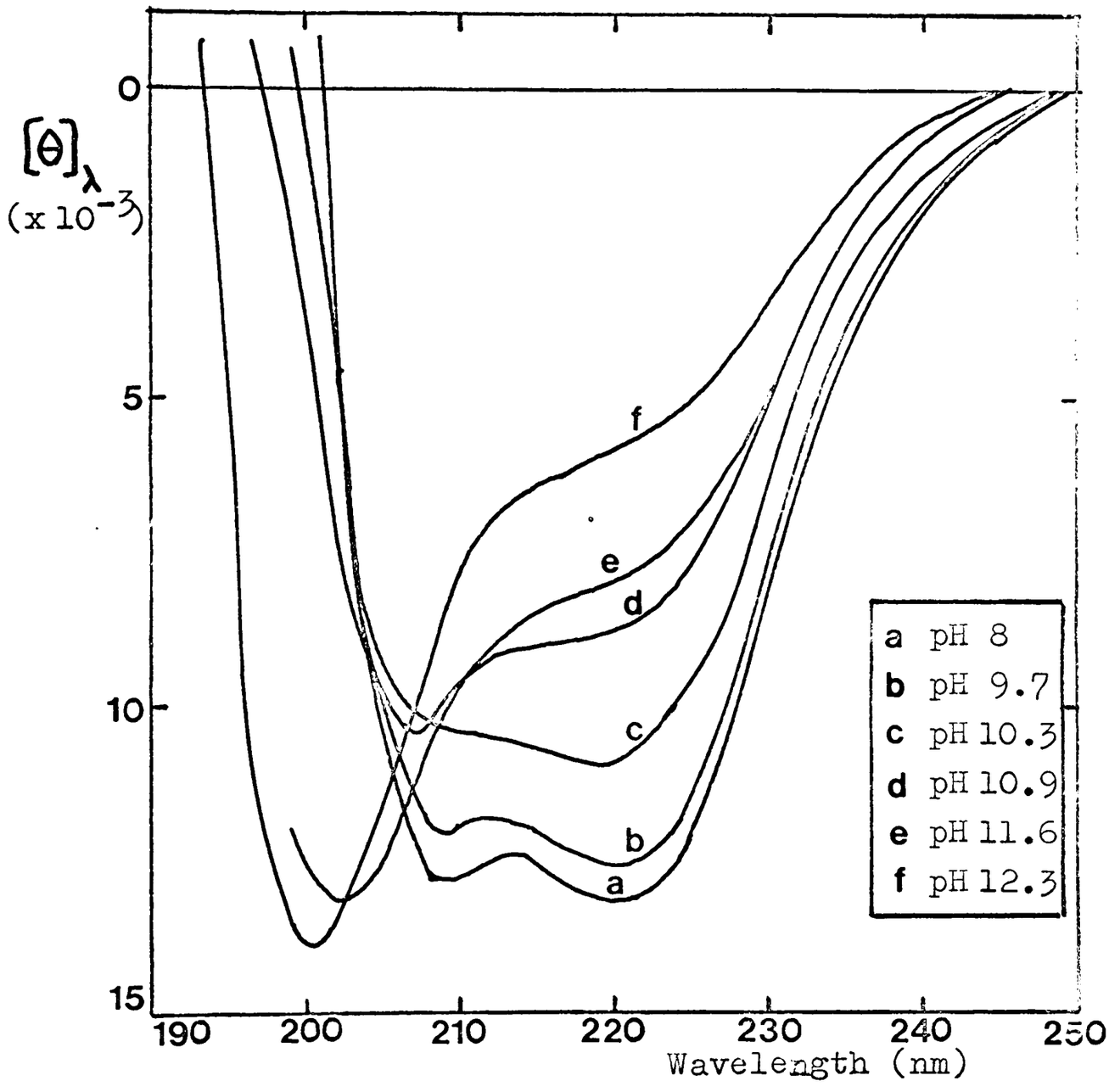

Fig. 6.20. Detailed variation of the negative far-UV CD bands of aldolase with alkaline pH. Solvent 0.1M tris-phosphate.

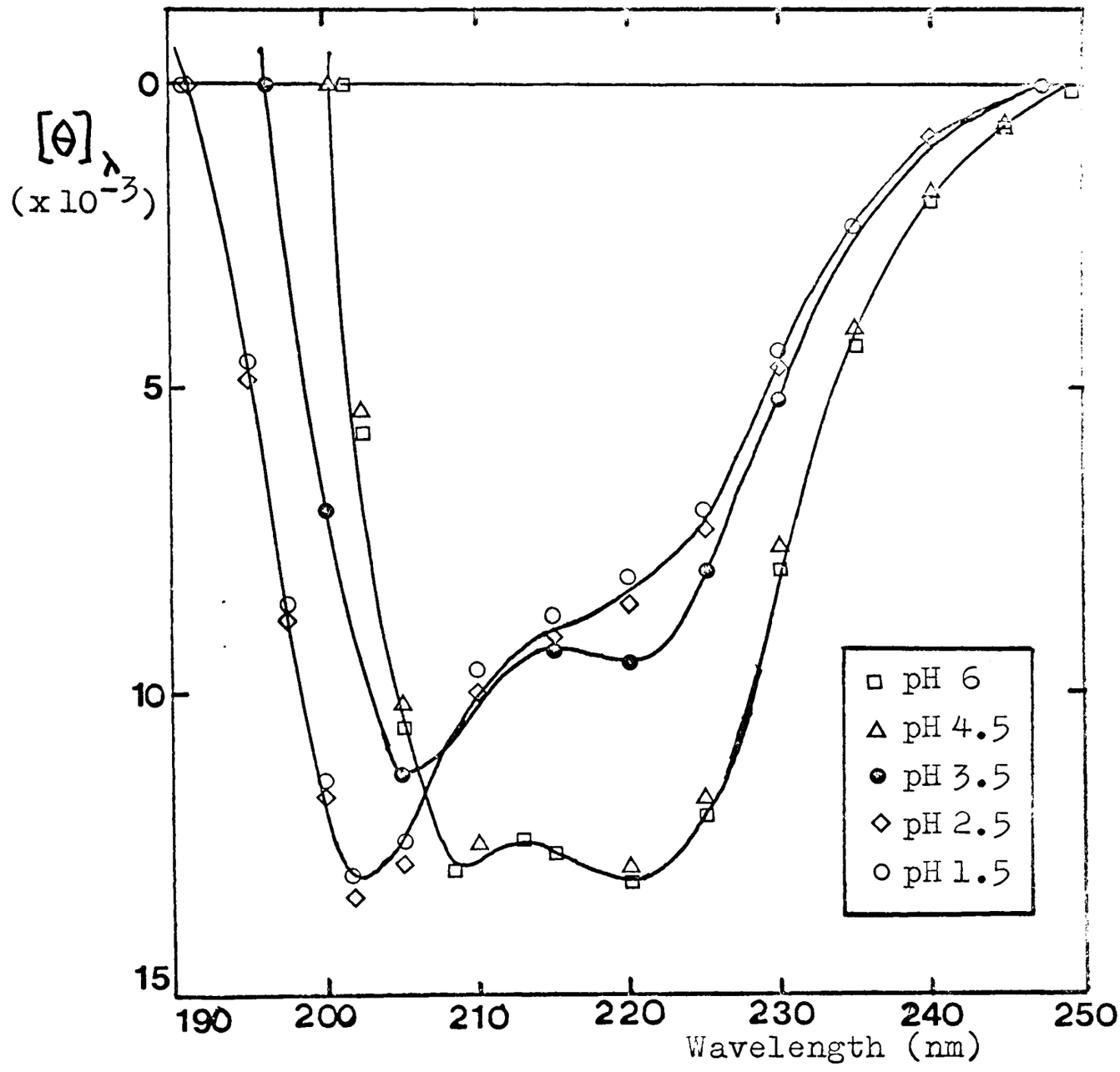

Fig. 6.21. The variation of the negative far-UV CD bands of Aldolase in 0.1M NaCl with acid pH.

(ii) Phosphofructokinase.

(a) Near-UV results.

The CD spectrum for PFK between 250nm and 300nm was less reproducible than that for aldolase, but the main features were always a negative band centred on about 270nm - 280nm and a smaller trough or shoulder at about 295nm (Fig. 6.22). Some recordings appeared to show fine structure with negative peaks at about 270, 278 and 285nm as shown in Fig. 6.23. There was no significant change in the near-UV bands with concentration over the range (0.5 to 2.5mg/ml) at which reversible association of the enzyme takes place (Chapters 4 and 5).

As PFK is insoluble below about pH 6, only the effect of increasing the pH on the dichroic bands could be studied. The changes in the near-UV bands between pH 8 and pH 12 are shown in Fig 6.24. The negative dichroic bands disappear between pH 10 and pH 11, and are replaced by two positive bands at 255nm and 290nm. PFK which had been dialysed into pH 10.5 buffer containing 0.5mM FDP, and which should therefore be present as the undissociated '12 S protein' showed no measurable change in the near-UV CD bands.

The near-UV CD spectrum was also measured in the presence of 1mM F6P, 1mM FDP, 0.2mM ATP and 50mM citrate

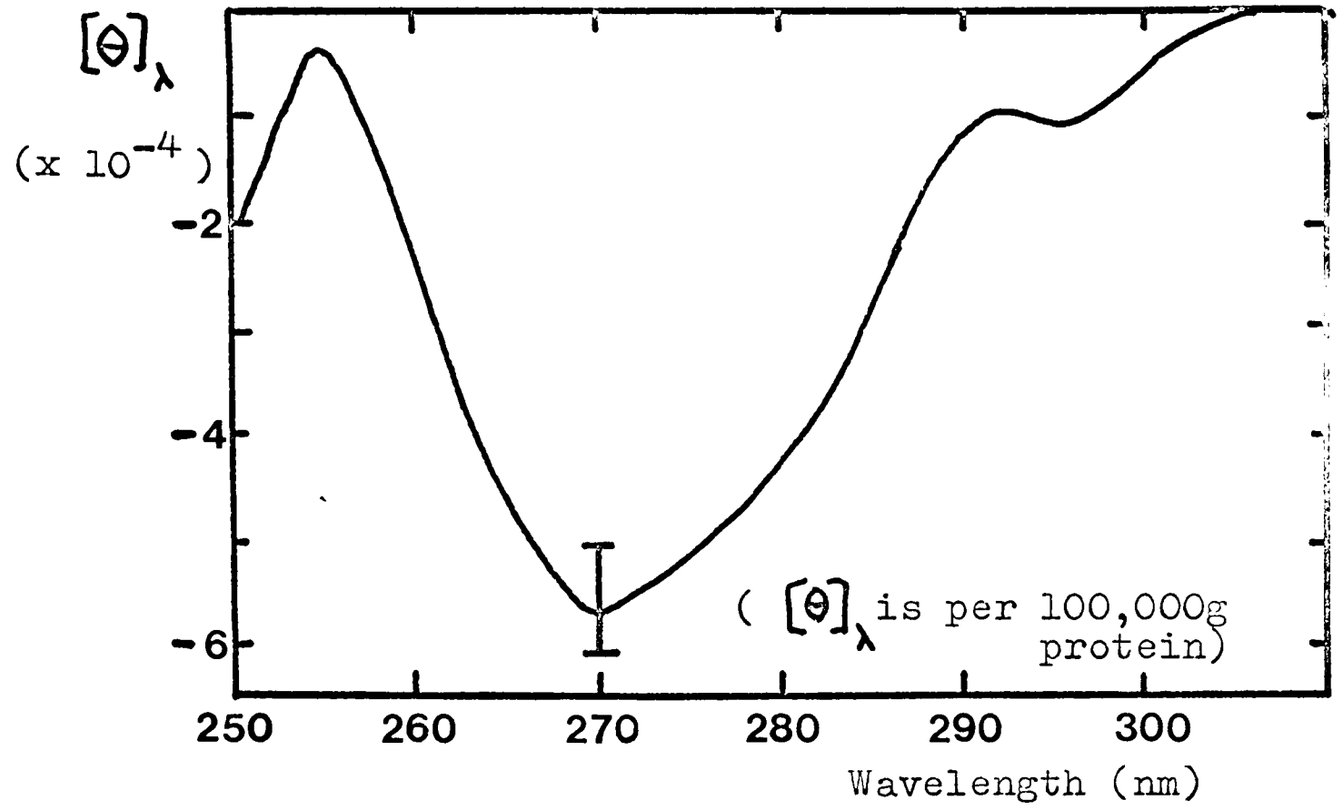

Fig. 6.22. Near-UV CD spectrum of PFK.

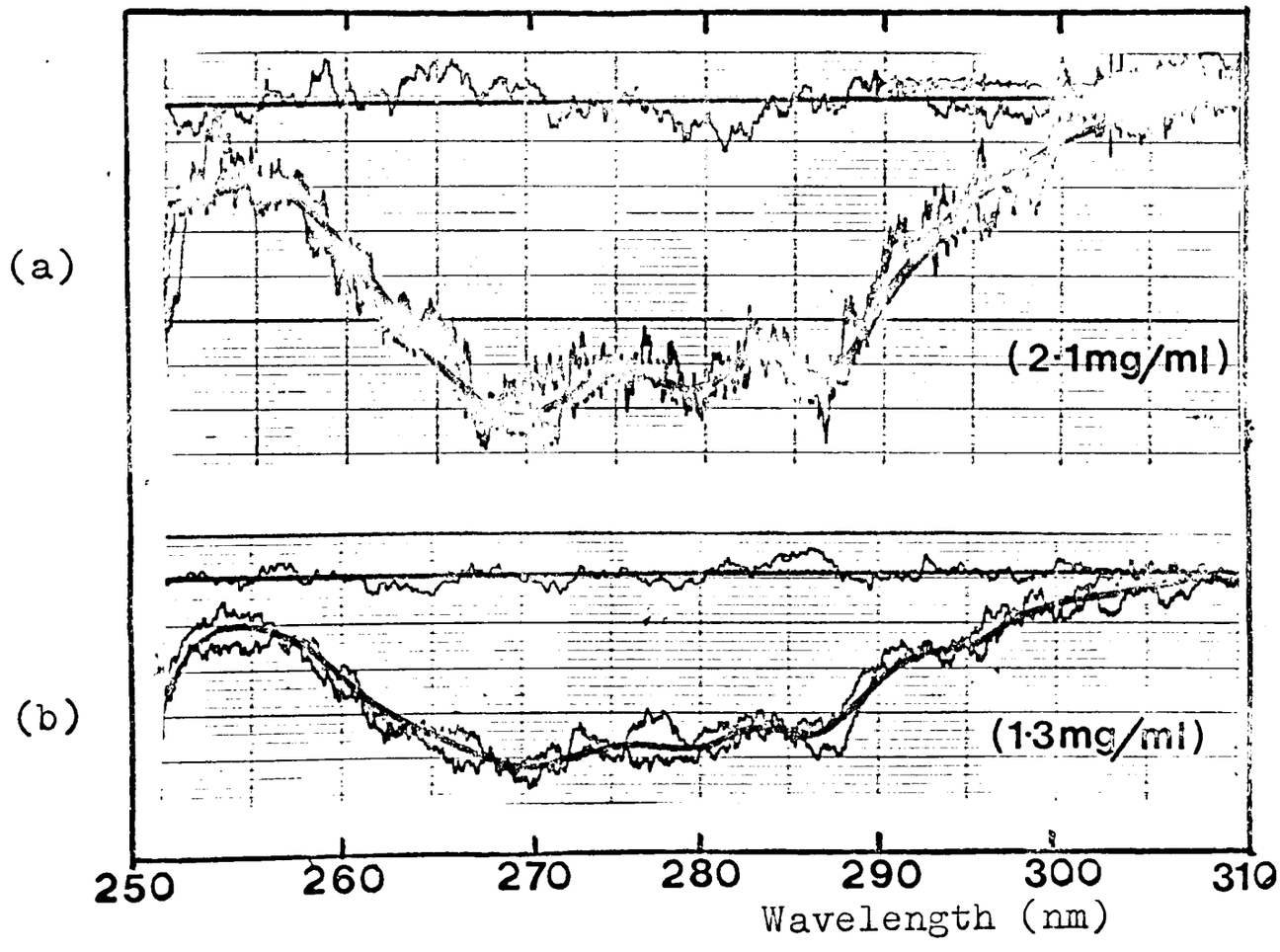

Fig. 6.23. Recorder traces showing possible fine structure in the near-UV CD bands of PFK.
(a) pH 8 (b) FDP stabilised 12S protein at pH 10.5.

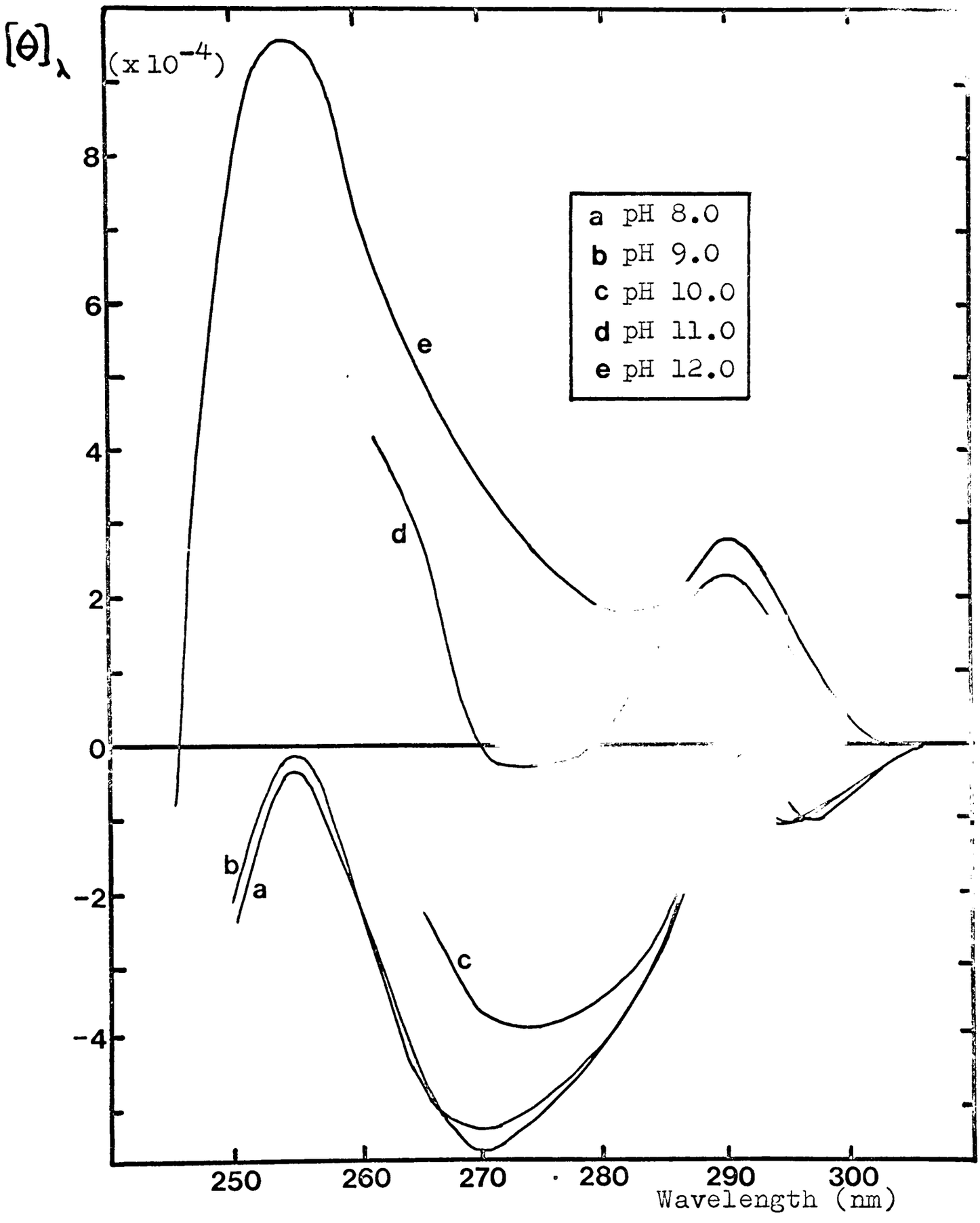

Fig. 6.24. The effect of increased pH on the near-UV CD bands of PFK.(Measured in 0.1M glycyl-glycine buffer, plus 0.5mM FDP). ($[\theta]_\lambda$ per 100,000g PFK)

at pH 8 in 0.1M glycylglycine buffer. No change in the near-UV bands was found when these allosteric effectors were present.

(b) Far-UV results.

Native PFK has a far-UV dichroic spectrum which is very similar in shape and in the magnitude of the positive and negative bands to that found for aldolase. (Fig. 6.25)

The variation of the negative dichroic bands between 200nm and 250nm with increasing pH is shown in Fig. 6.26. There is little change up to pH 10, followed by a decrease in the negative rotational strength between pH 10 and pH 11 which is the pH range over which the 12 S protein dissociates. Up to pH 12, there is no appearance of the trough at 200nm which was present in the CD spectra of acid and alkali denatured aldolase.

Far-UV results for native PFK are summarised below.

Table. 6.2. Far-UV CD bands for Aldolase and PFK.

Protein	Wavelength (nm)	Mean residue ellipticity
Aldolase	220	-1.2×10^4
"	211	-1.15×10^4
"	191	2.6×10^4
PFK	220	-1.1×10^4
"	212	-1.1×10^4
"	190	3.3×10^4

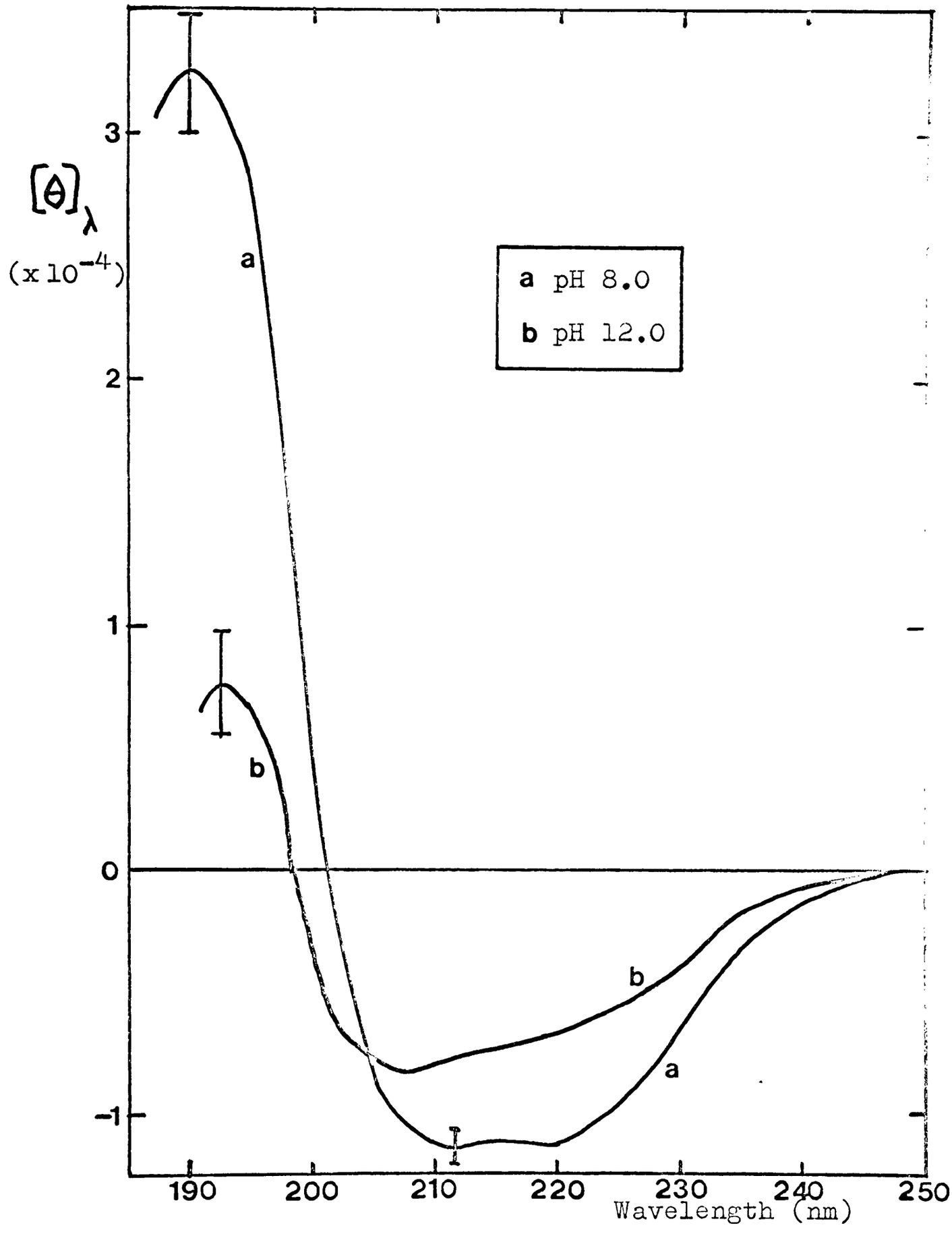

Fig. 6.25. Far-UV CD bands of PFK in 0.1M glycyl-glycine, 0.5mM FDP, pH 8 and after adjustment to pH 12. The ellipticity is in deg. cm^2/ decimole of mean amino-acid residue.

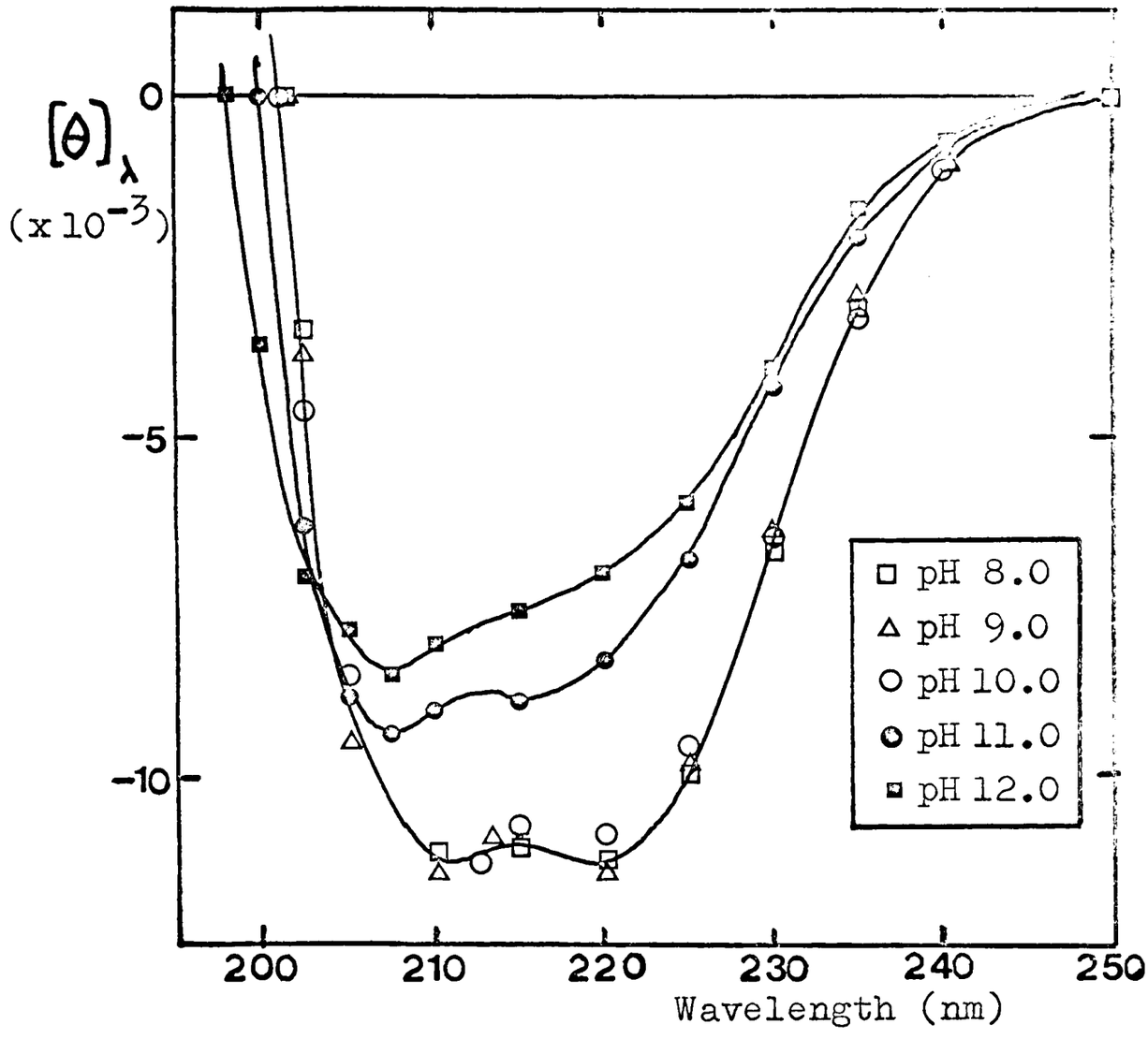

Fig. 6.26. The variation of the negative far-UV CD bands of PFK in 0.1M glycyl-glycine plus 0.5mM FDP, with alkaline pH.

Table 6.3. CD bands found for Model Compounds.

Compound	pH	Wavelength (nm)	MOLAR ELLIPTICITY
L-tyrosine	6	270	+660
L-tryptophan	6	270 - 280	+1000
"	"	222	+19,000
"	"	194	-26,000
N-acetyl-L-tyrosine ethyl ester:	6	280	-165
	"	225	+21,000
	"	198	+46,000
	"	184	-61,000
	10	240	+8500
	"	223	+13,000
	"	200	+42,000
	"	185	-65,000
	11	238	+17,000
	"	203	+53,000
	"	187	-68,000
N-acetyl-L-tryptophan ethyl ester:	6	295	-200
	"	280	+400
	"	222	+18,000
	"	191	-10,000

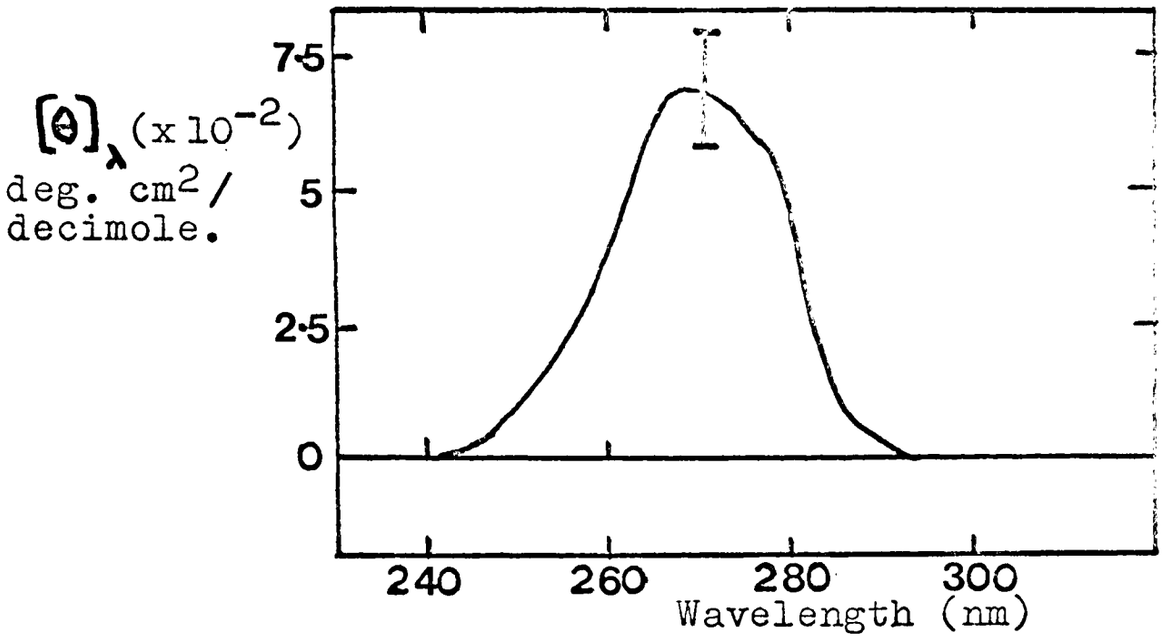

Fig. 6.27. CD of L-tyrosine, pH 6. No other significant bands were found below 240nm.

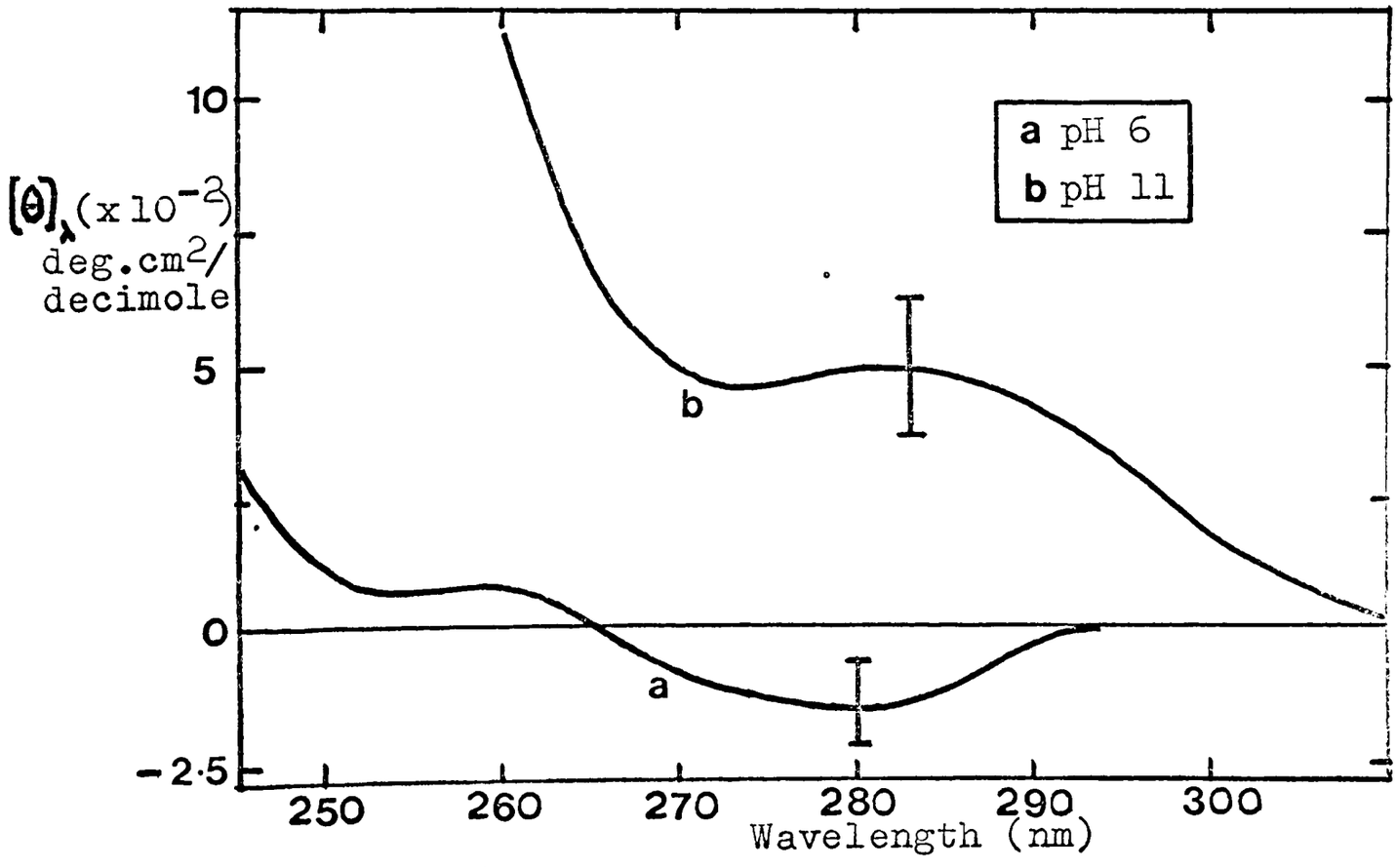

Fig. 6.28a. Near-UV CD bands for N-acetyl-L-tyrosine ethyl ester at pH 6 and pH 11.

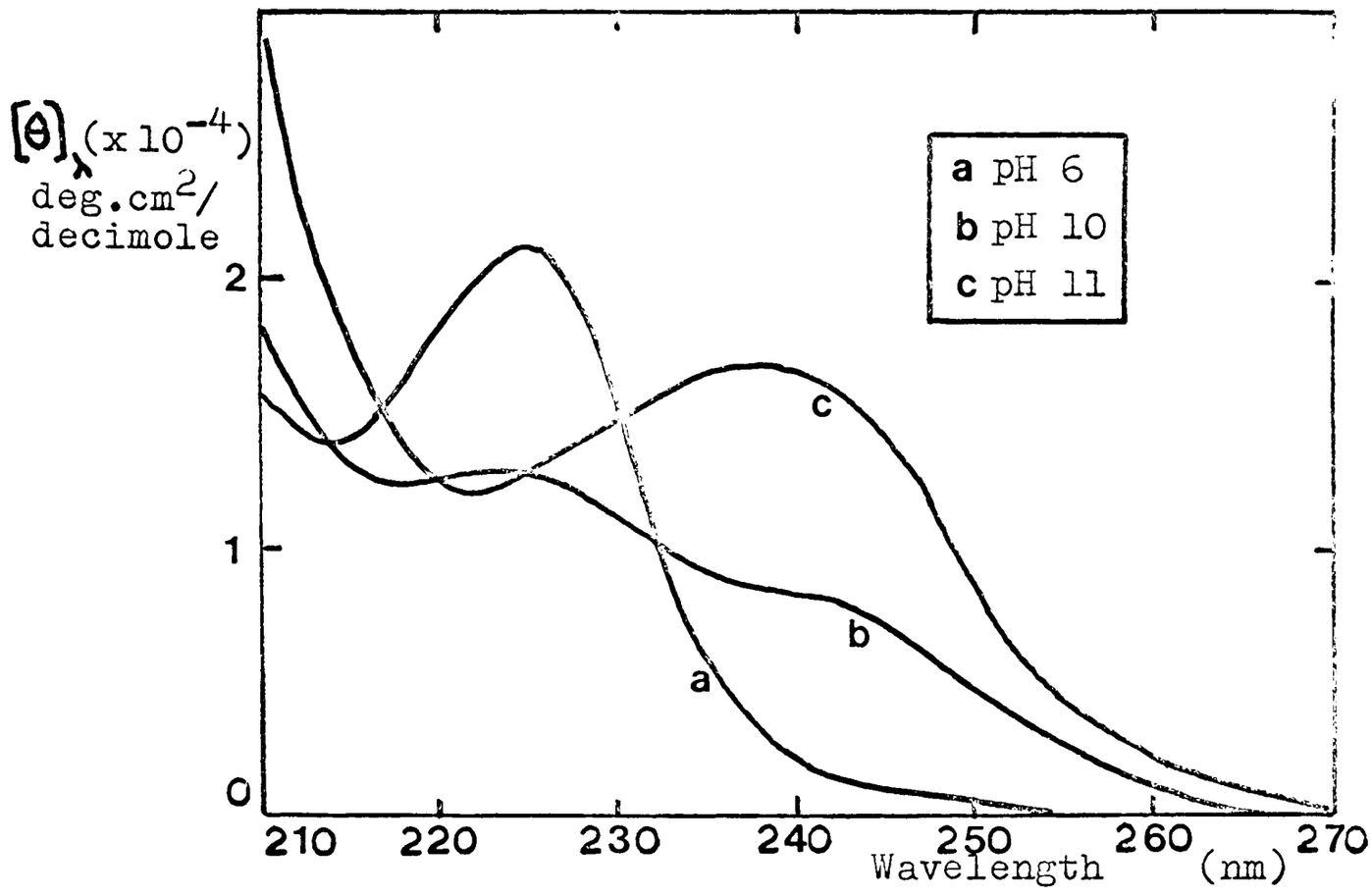

Fig. 6.28 b. Far-UV CD bands for N-acetyl-L-tyrosine ethyl ester at pH 6, pH 10 and pH 11.

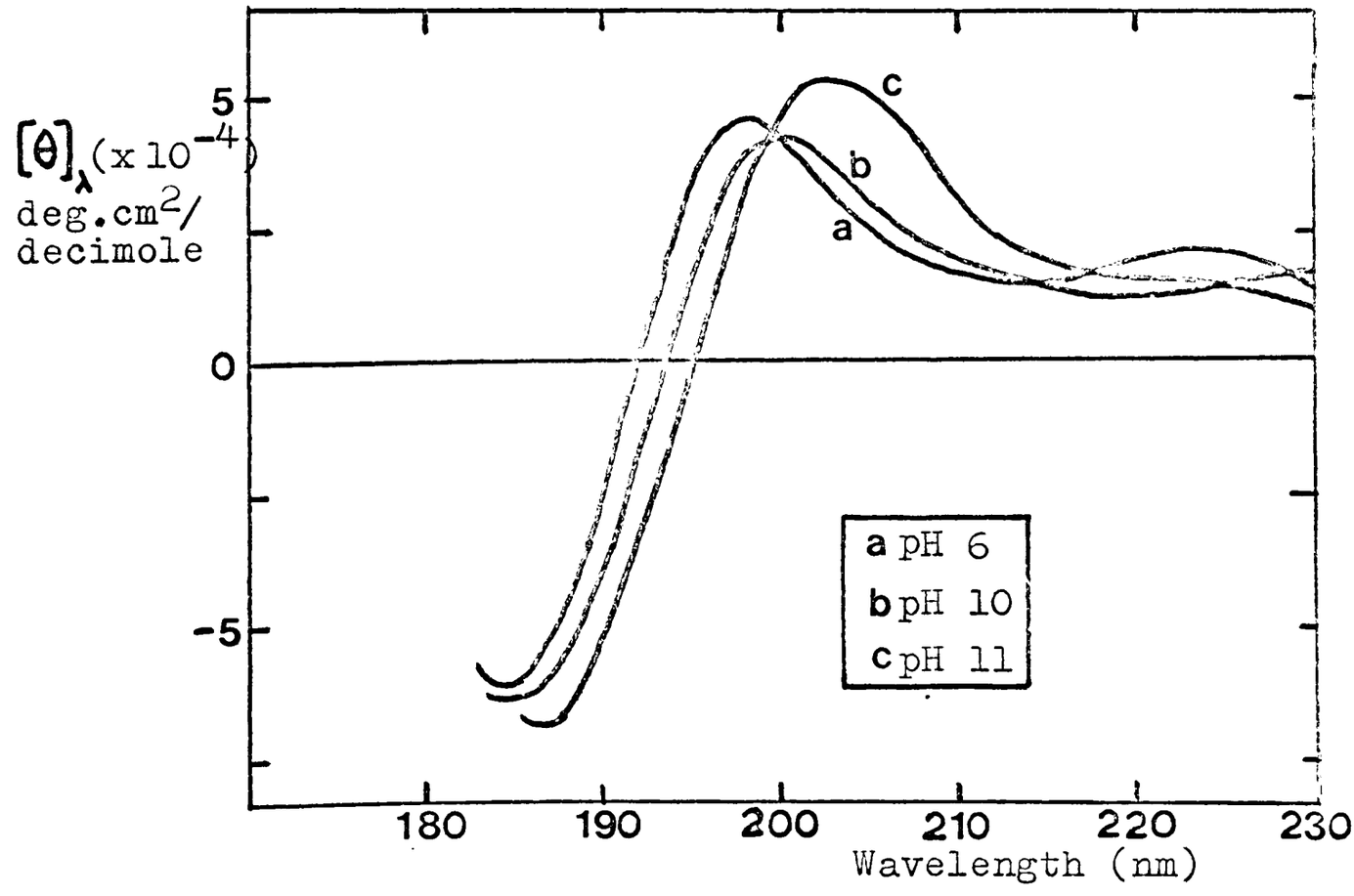

Fig. 6.28 c. Far-UV CD bands for N-acetyl-L-tyrosine ethyl ester at pH 6, pH 10 and pH 11.

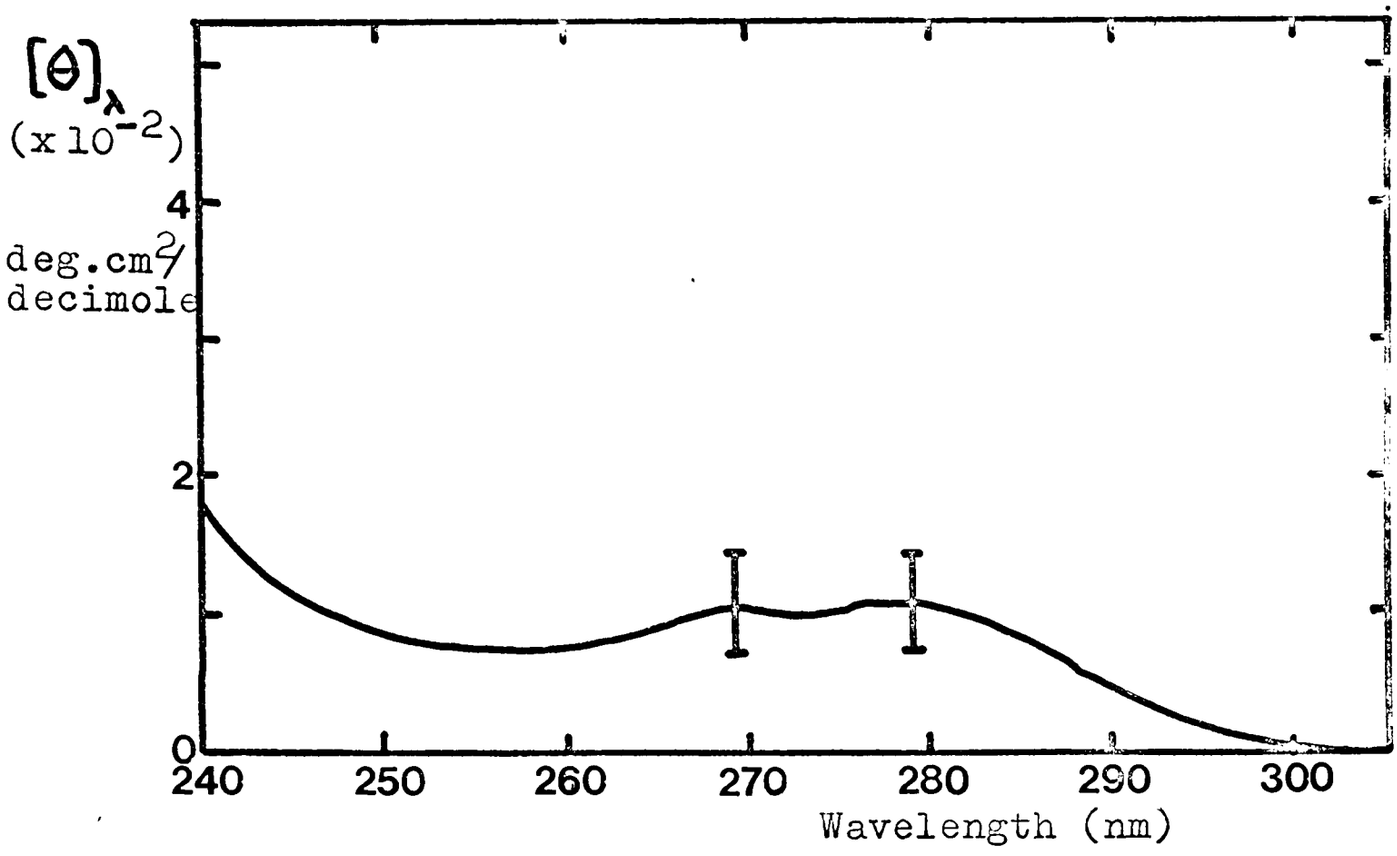

Fig. 6.29 a. Near-UV CD spectrum of L-tryptophan, pH 6

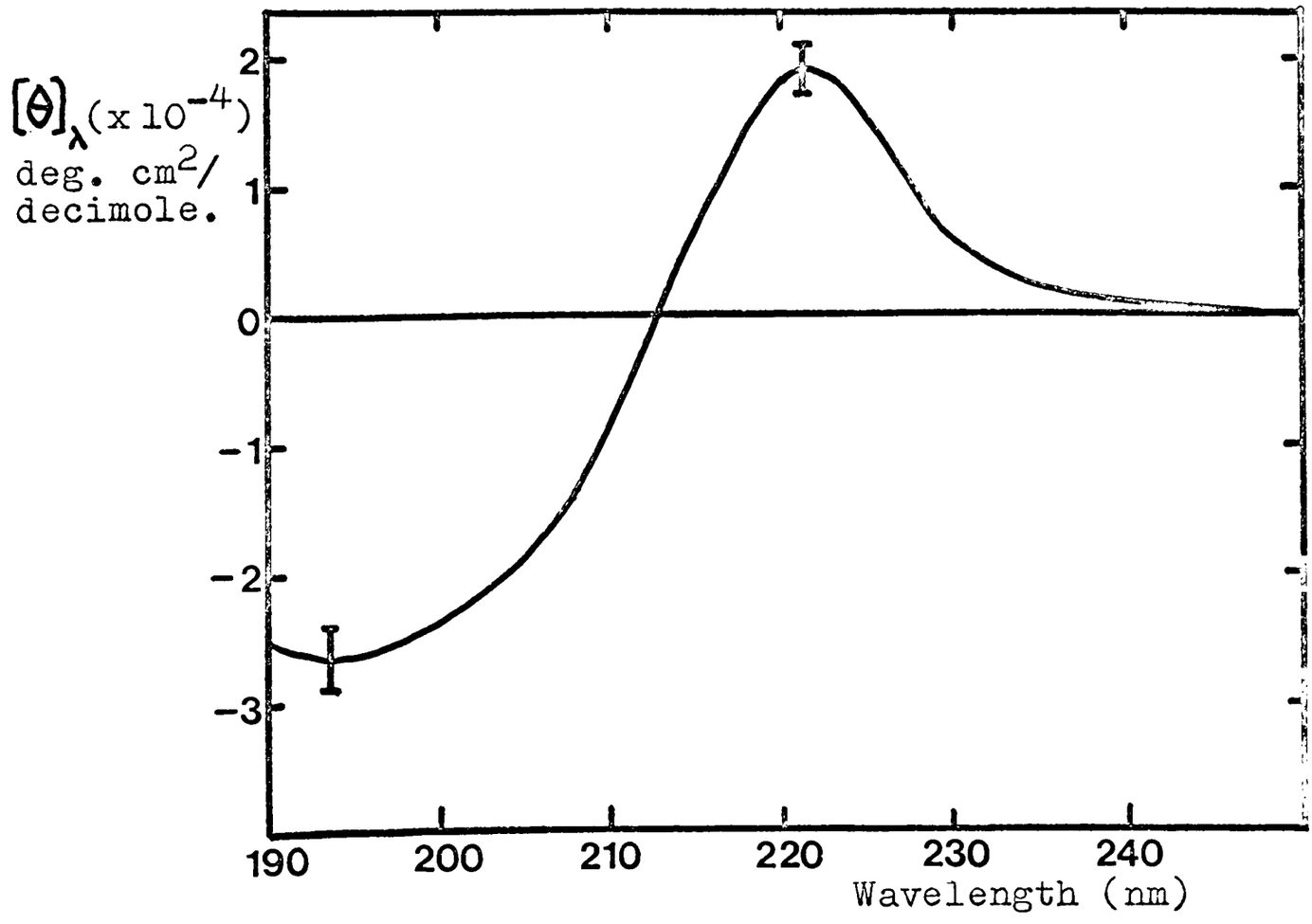

Fig. 6.29 b. Far-UV CD bands of L-tryptophan, pH 6.

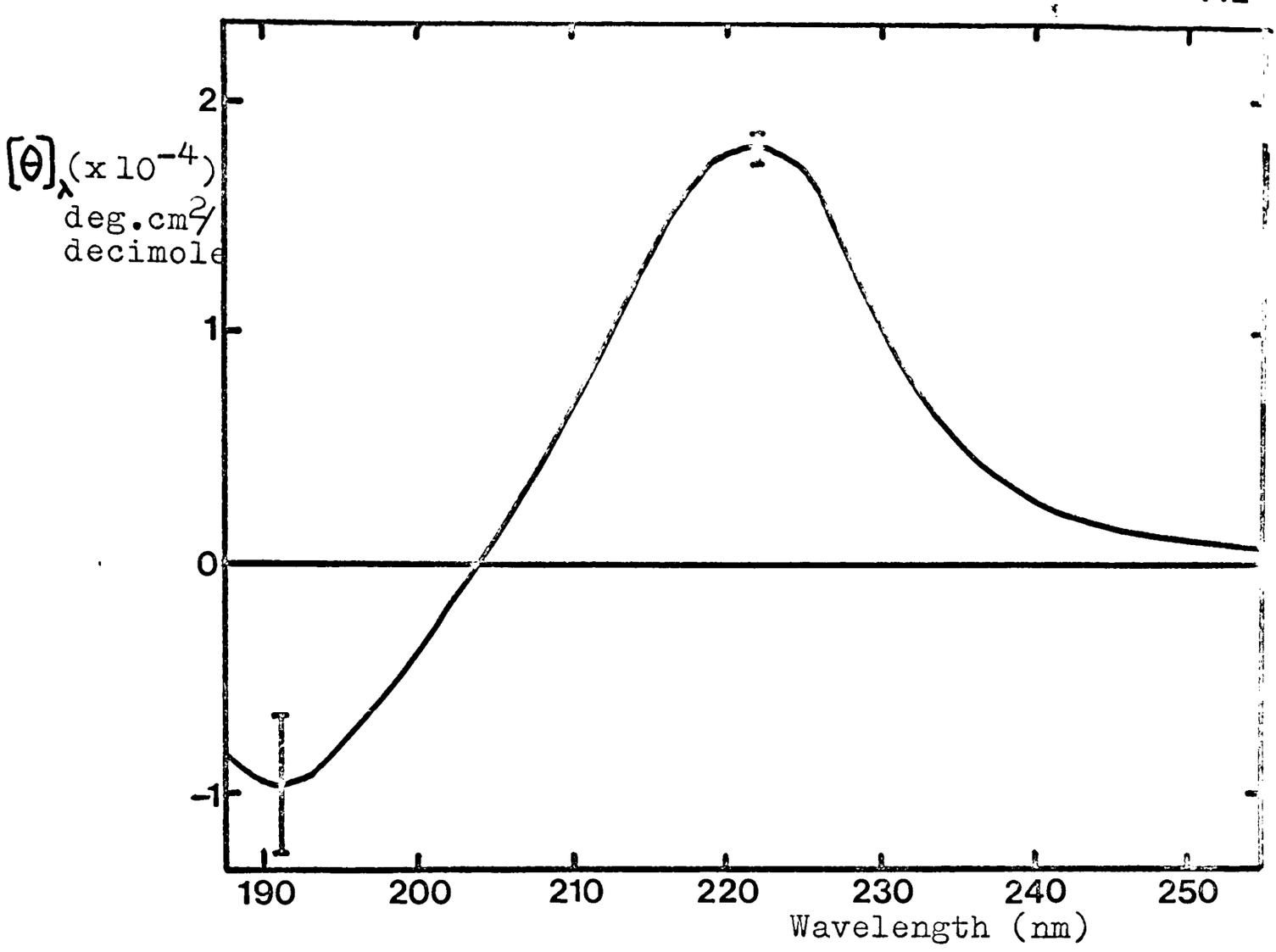

Fig. 6.30 a. Far-UV CD bands of N-acetyl-L-tryptophan ethyl ester, pH 6.

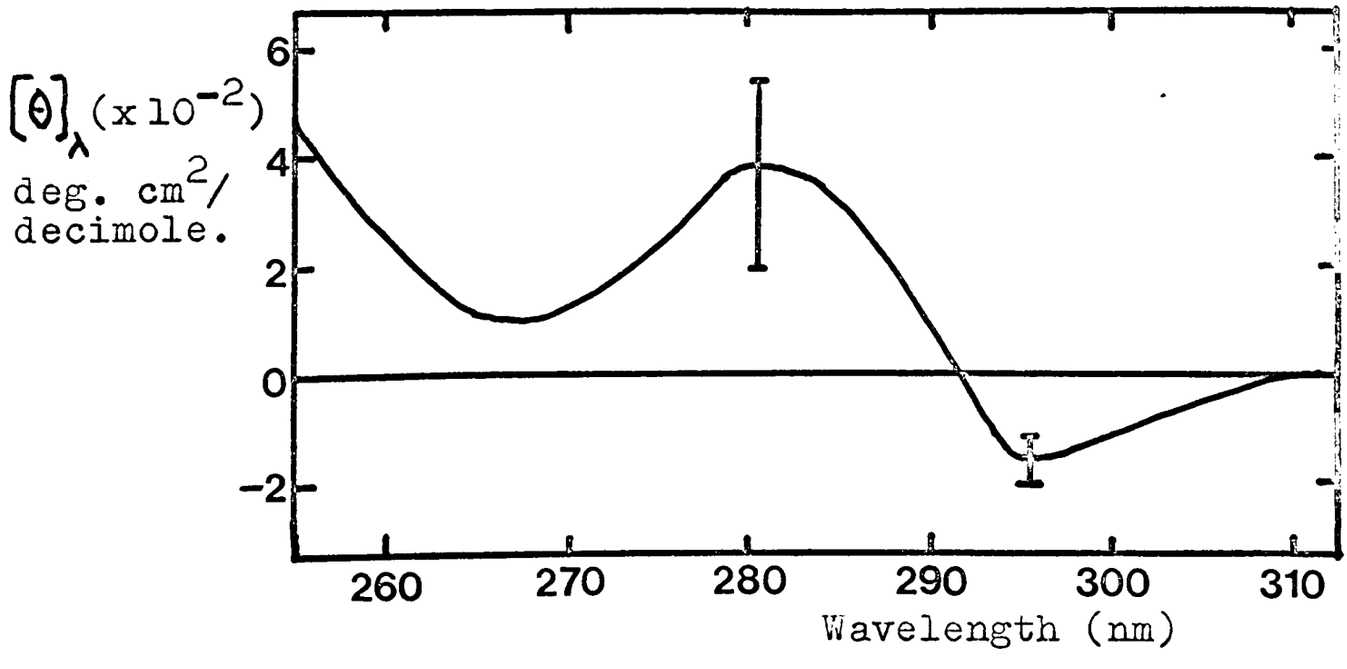

Fig. 6.30 b. Near-UV CD bands of N-acetyl-L-tryptophan ethyl ester, pH 6.

(iii) Model Compounds.

These were studied in order to obtain information about the magnitude and position of dichroic bands, which might be of assistance in assigning the near-UV bands of aldolase and PFK. CD spectra for L-tryptophan, L-tyrosine, N-acetyl-L-tryptophan ethyl ester, N-acetyl-L-tyrosine ethyl ester were measured and are shown in Figs. 6.27 to 6.30. Maximum and minimum ellipticities are summarised in Table 6.3 . Measurements were also made for L-histidine and L-phenylalanine. These compounds were found to have insignificant dichroism above 240nm.

The results at different alkaline pH values for N-acetyl-L-tyrosine ethyl ester show that there is a pronounced 'red-shift' as the phenolic OH group ionises.

(iv) Kronig-Kramers Transform results.

(a) General comments on curve fitting.

Where negative and positive curves overlap as in CD spectra, the appearance of the resultant complex curve can be misleading (Fig. 6.31a) and a fitted curve can be obtained which is a good approximation to the resultant curve, but whose component bands are quite different from the true partial bands (Fig. 6.31 b). This is not important for the application of the Kronig-Kramers Transform, since the calculated ORD curve is independent of the

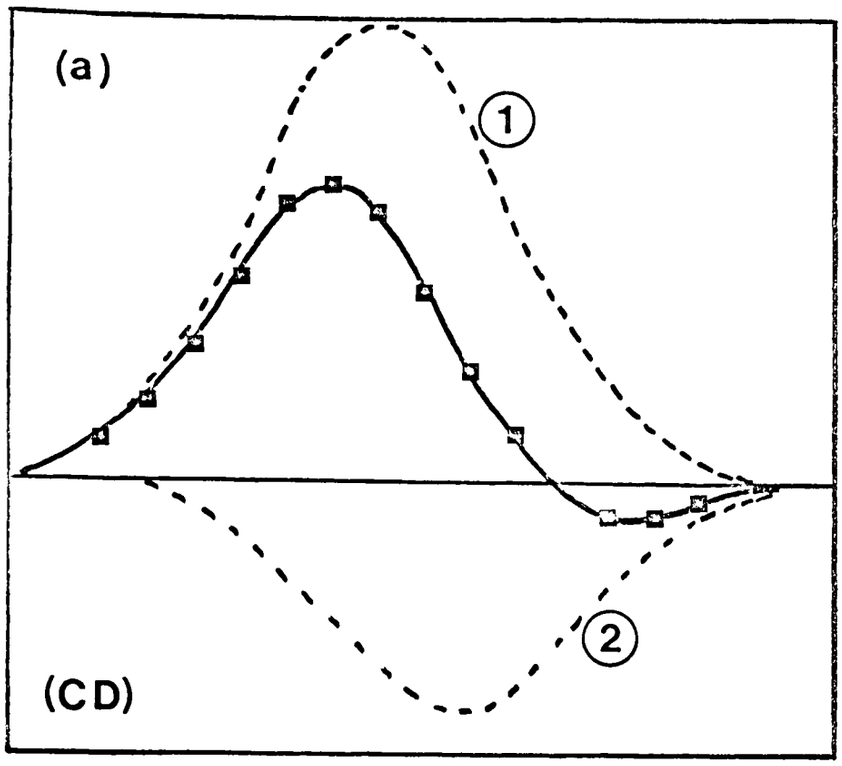

The Gaussian curves, (1) and (2), give the solid curve as their resultant. The squares are points obtained from the sum of the Gaussian curves, (3) and (4), shown in (b).

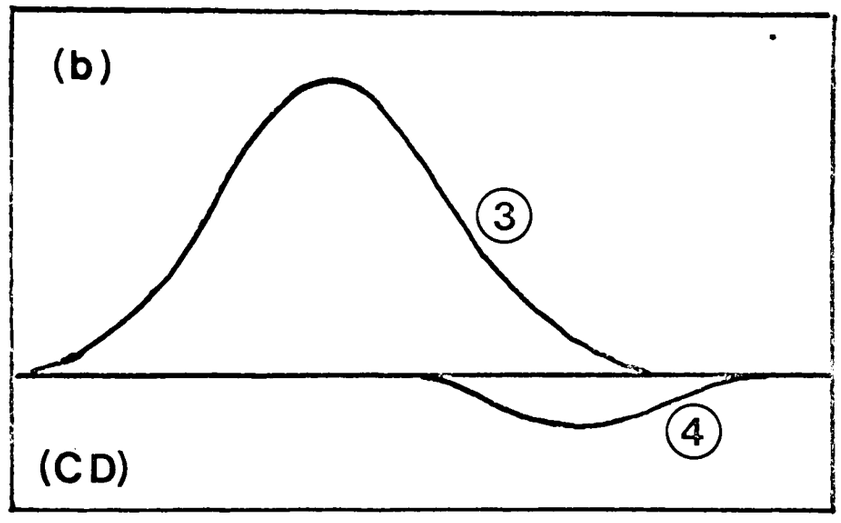

Curves (3) and (4) were fitted to the solid curve in (a).

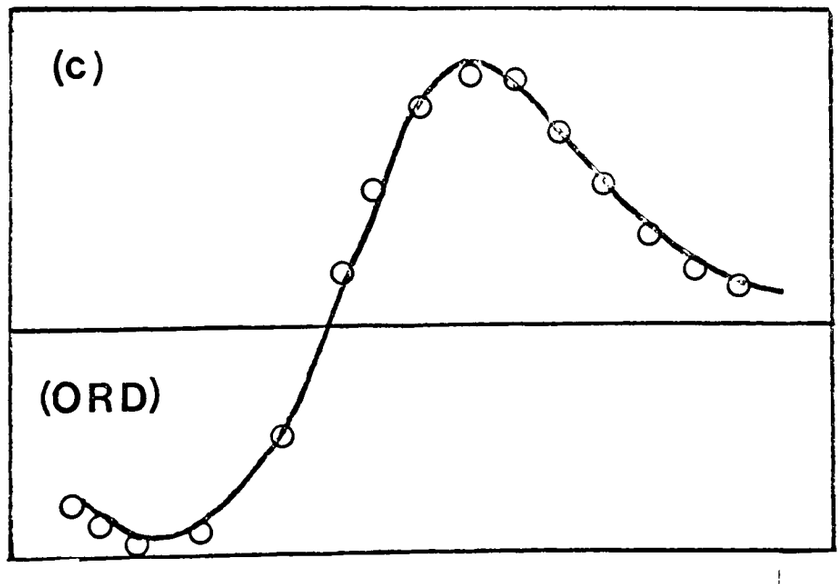

The full line is the Kronig-Kramers transform of curves (1) and (2). The circles are the Kronig-Kramers transform of curves (3) and (4).

Fig. 6.31. Curve fitting and the Kronig-Kramers transform.

individual bands which make up the complex CD curve as is shown by Fig. 6.31 c . It does, however, mean that the unequivocal resolution of a complex CD curve into its true components may not be possible if the overlapping bands are close together and opposite in sign.

(b) Far-UV - Aldolase and PFK.

The fitted CD curves and the calculated ORD curves for aldolase and PFK in the far-UV are shown in Figs. 6.32 and 6.33. There is quite good agreement with the experimental curves in the region of anomalous dispersion. This suggests that contributions made by chromophores with λ_o less than 190nm are small if not negligible.

(c) Near-UV - Aldolase and PFK.

The calculated curve for aldolase shows a maximum at 290nm which correlates quite well with the small peak which was observed at the same wavelength in the ORD curve. (Figures 6.34 and 6.35). The calculated curve for PFK shown in Fig. 6.36 b is a rather broad trough between 320nm and 270nm with a mean residue rotation which is only about 1/3 of that for the aldolase peak at 290nm. This probably explains why a near-UV Cotton effect could be detected for aldolase but not for PFK despite the fact that they have CD bands of about the same size in the near-UV.

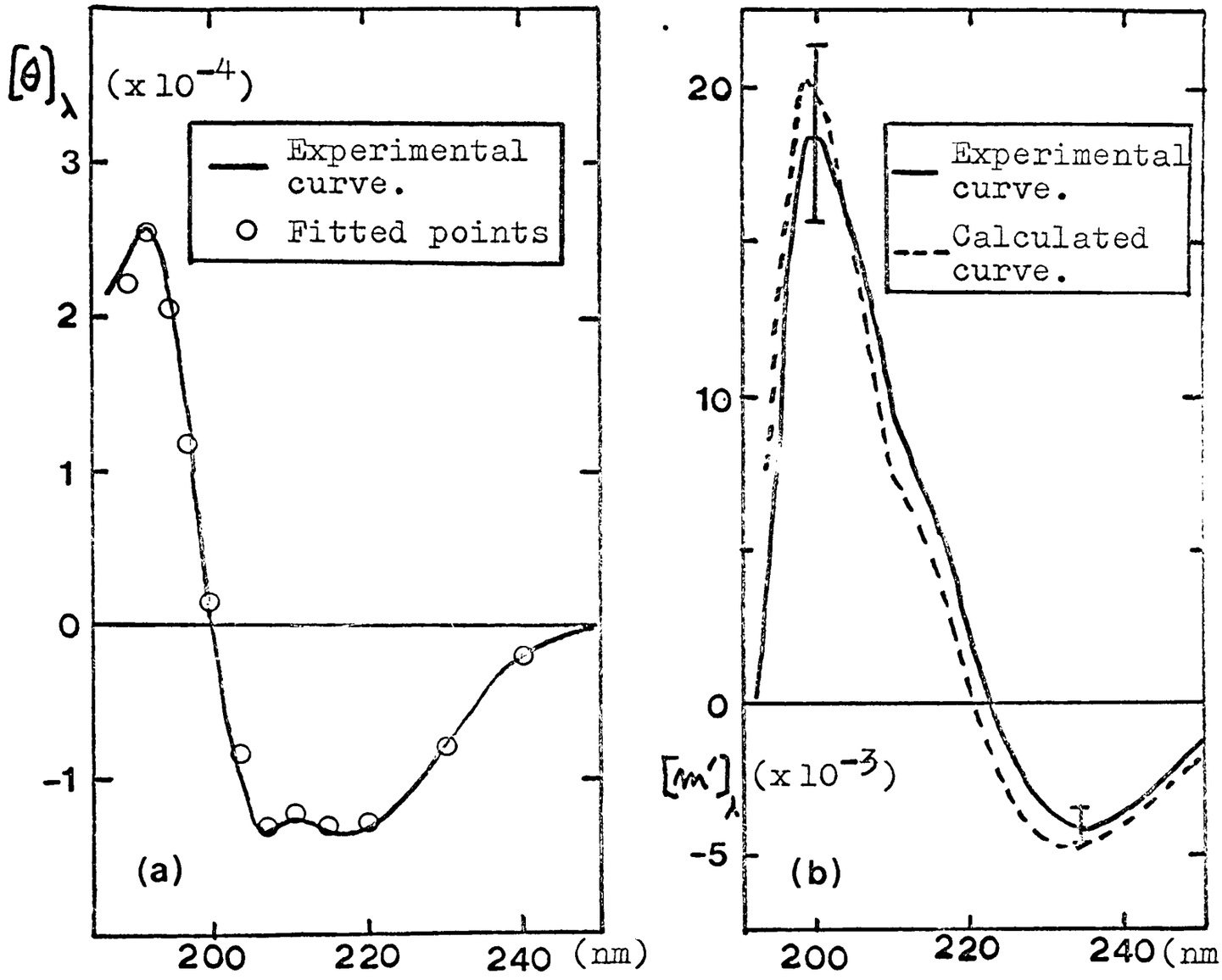

Fig. 6.32. Kronig-Kramers Transform results for Aldolase in the far-UV.

(a) is the CD curve fitted by a combination of one positive Gaussian curve and two negative Gaussian curves.

(b) shows the ORD curve calculated from these bands, together with the experimental data.

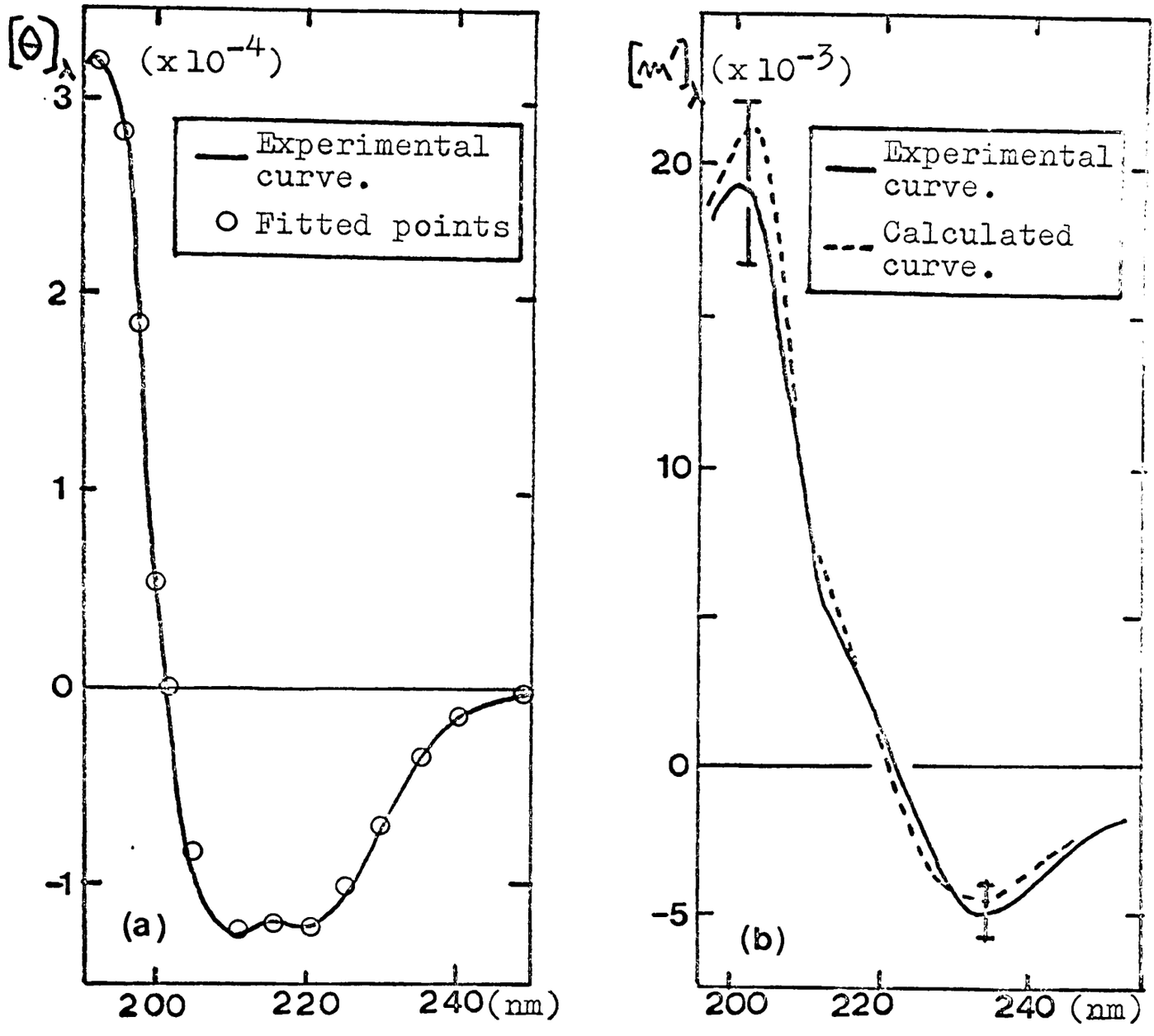

Fig. 6.33. Kronig-Kramers Transform results for PFK in the Far-UV.

(a) is again the CD curve fitted by a combination of three Gaussian curves.

(b) shows the calculated ORD curve and the experimental data.

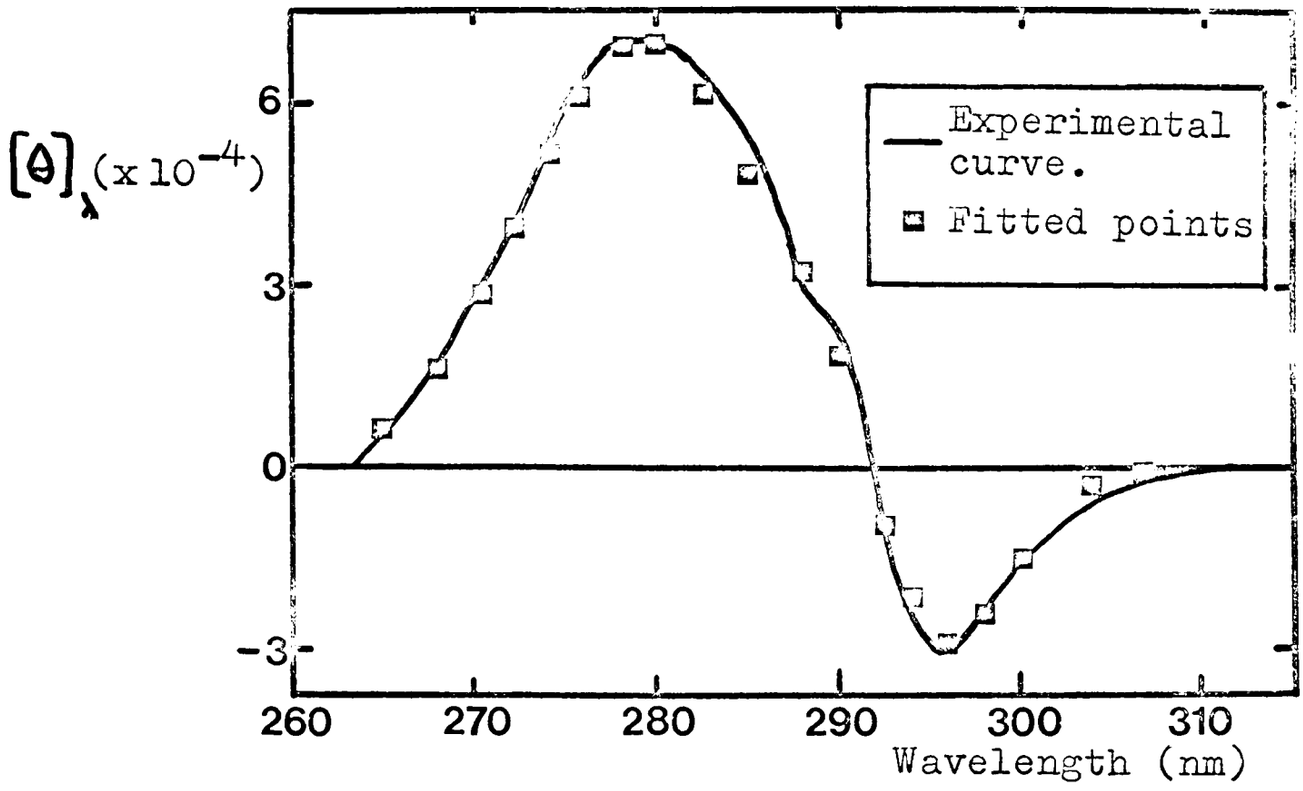

Fig. 6.34 a. The near-UV CD curve for aldolase fitted by one negative and two positive Gaussian curves.

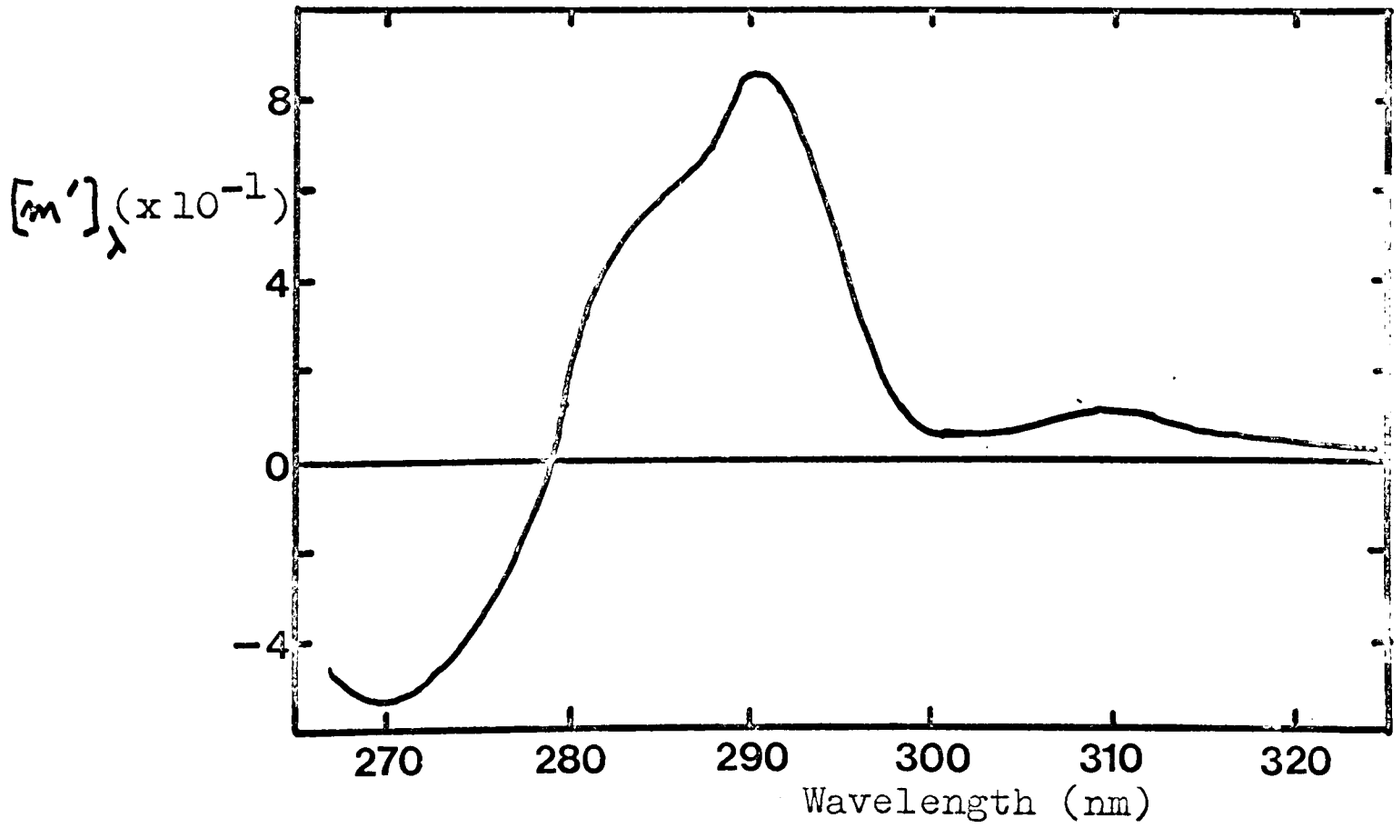

Fig. 6.34 b. ORD curve calculated from the three Gaussian bands.

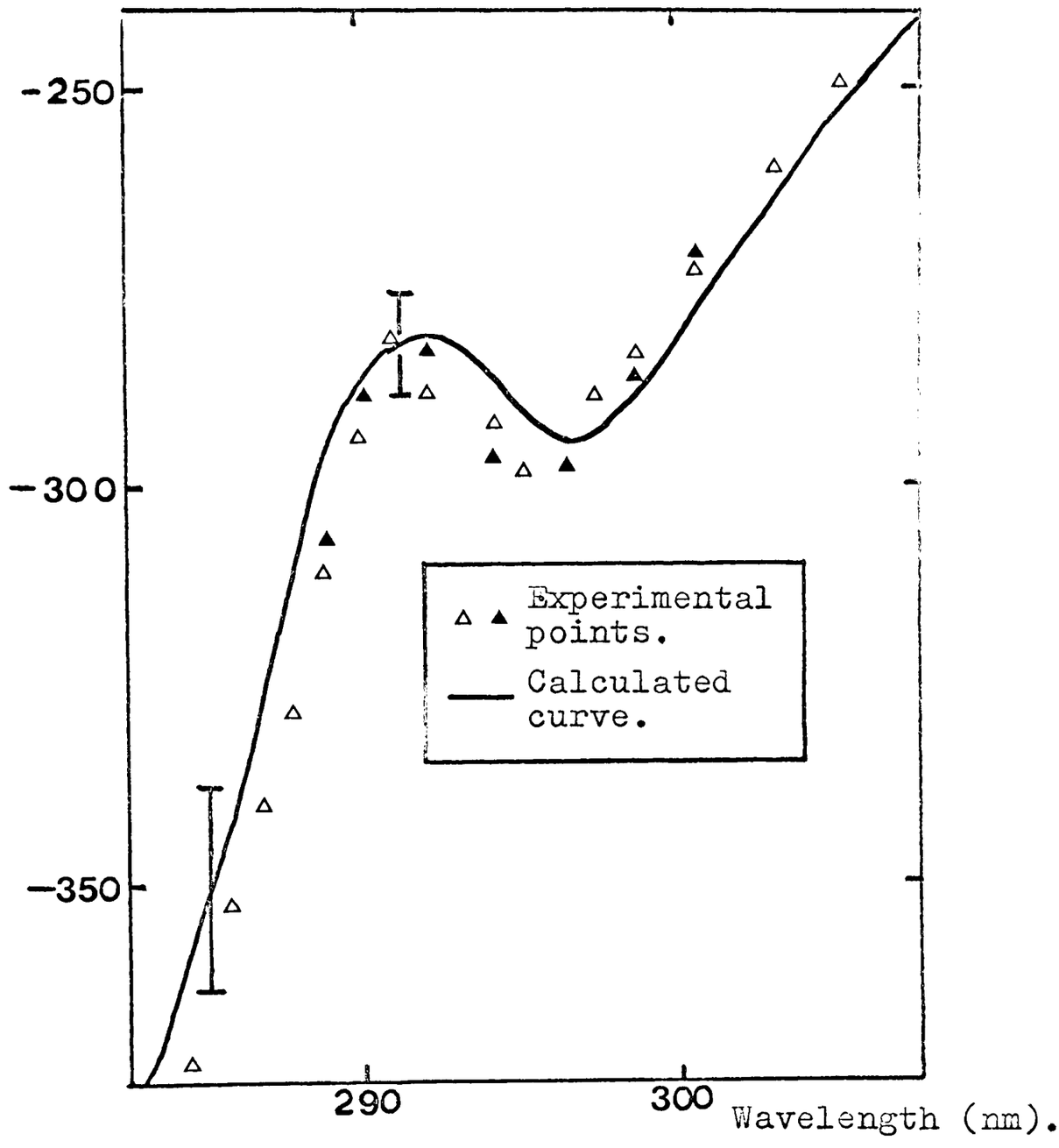

Fig. 6.35: The calculated ORD curve of Fig. 6.34 b superimposed on a background curve extrapolated from the visible dispersion.

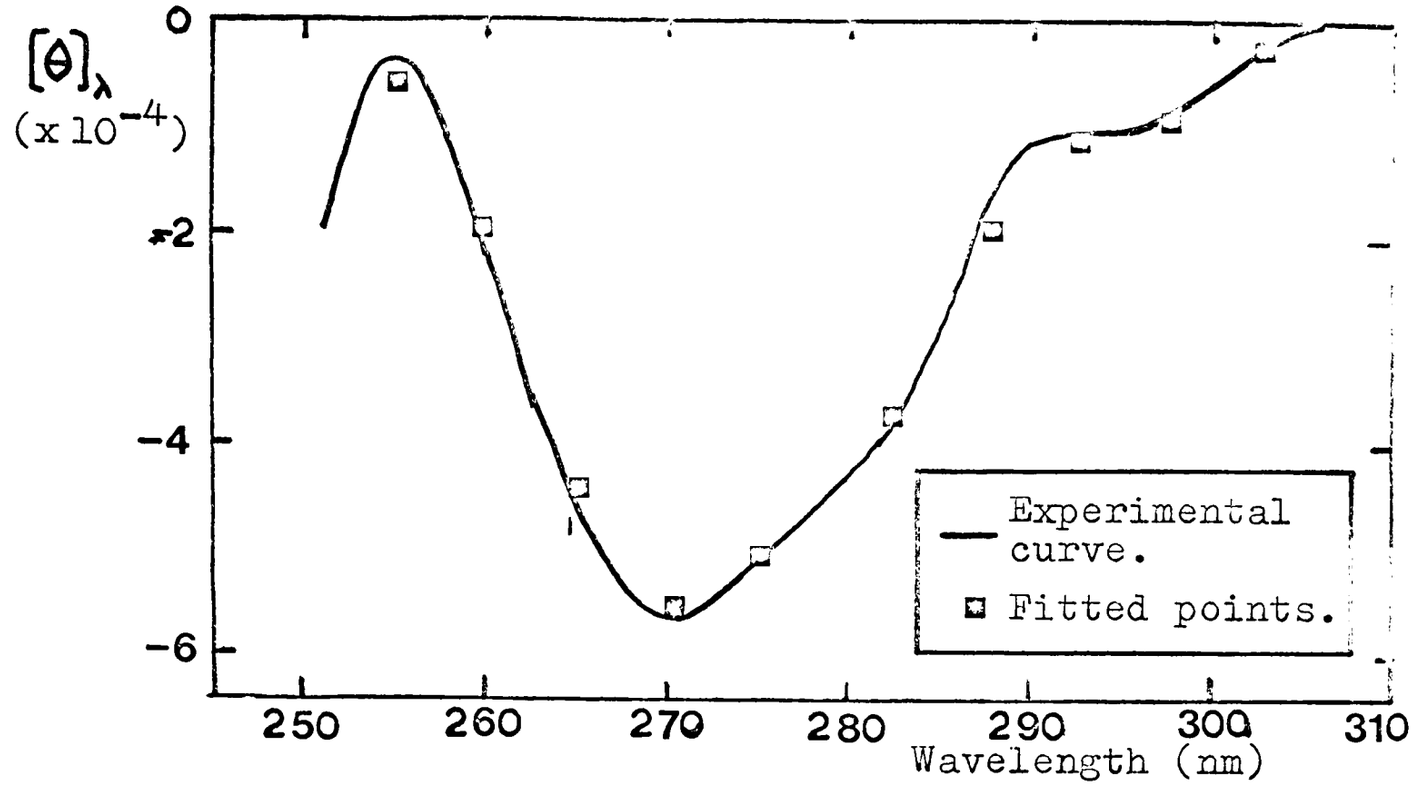

Fig. 6.36 a. The near-UV CD curve for PFK fitted by three negative Gaussian bands.

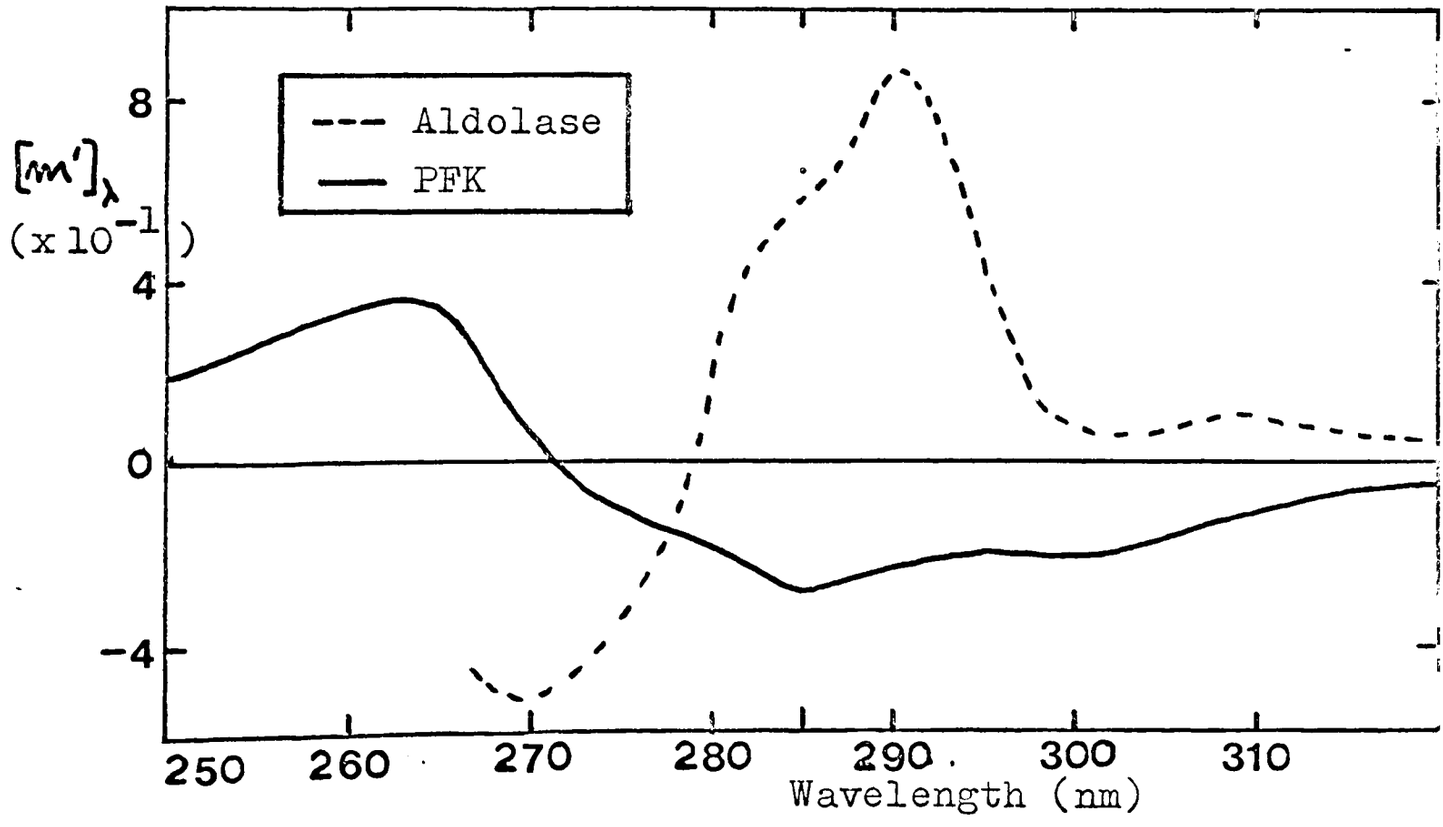

Fig. 6.36 b. The ORD curve calculated from the Gaussian bands. The calculated curve for Aldolase is also shown for comparison.

(v) Analysis of Secondary Structure.

An attempt was made to fit the far-UV bands of native and denatured aldolase and PFK with combinations of α-helix, β-structure and random coil using the data of Fasman et al , 1966[78] and Velluz et al, 1965,[79] which have been illustrated in Fig. 6.9. There is some disagreement between the two sets of data for helix and random coil (data for β-structure is only given by Fasman), but the same general conclusions were reached using both sets of data.

Using triangular coordinates as in Fig. 6.37a, lines were plotted for combinations of helix, β-structure and random coil which fit the curve, at 5nm wavelength intervals. If a unique fit to the whole experimental curve were possible, these lines would all intersect at the same point. It was found that for native aldolase, native PFK and for PFK at pH 12, diagrams similar to Fig.6.37a were obtained. As can be seen, there are two areas of intersection, one of which corresponds to the 190nm wavelength region and the other to the 215nm region. This means that the experimental data can be fitted at the 190nm peak with large deviations at the 210nm - 220nm trough or vice versa as shown in Fig. 6.38a . For aldolase at pH 1.5 or pH 12, however, the lines intersected within a relatively small area (Fig. 6.37b) so that an approximate fit over the

entire wavelength range was possible as is shown in Fig. 6.38 b . This corresponded to about 17% α-helix, 23% β-structure, 60% random coil for aldolase at pH 1.5 and 20% α-helix, 17% β-structure and 64% coil at pH 12.

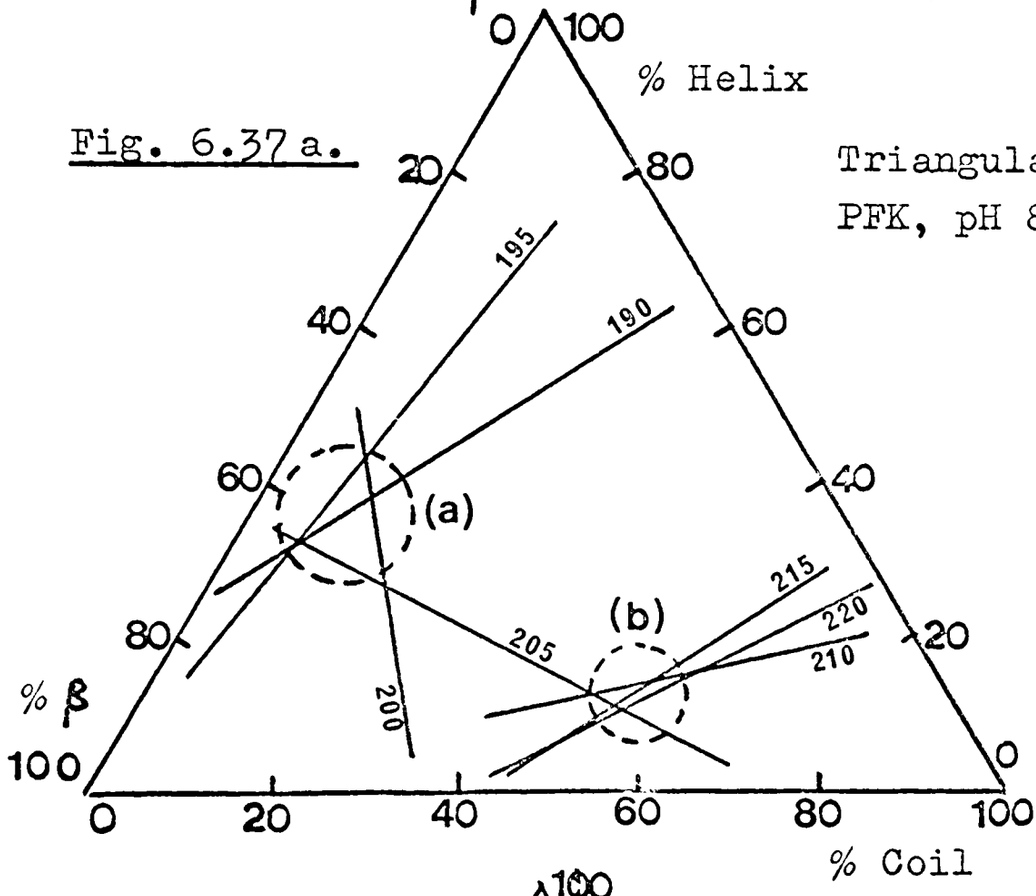

Fig. 6.37 a. Triangular diagram for PFK, pH 8.

Region (a)
34% Helix
10% Coil
56% Beta

Region (b)
10% Helix
52% Coil
38% Beta

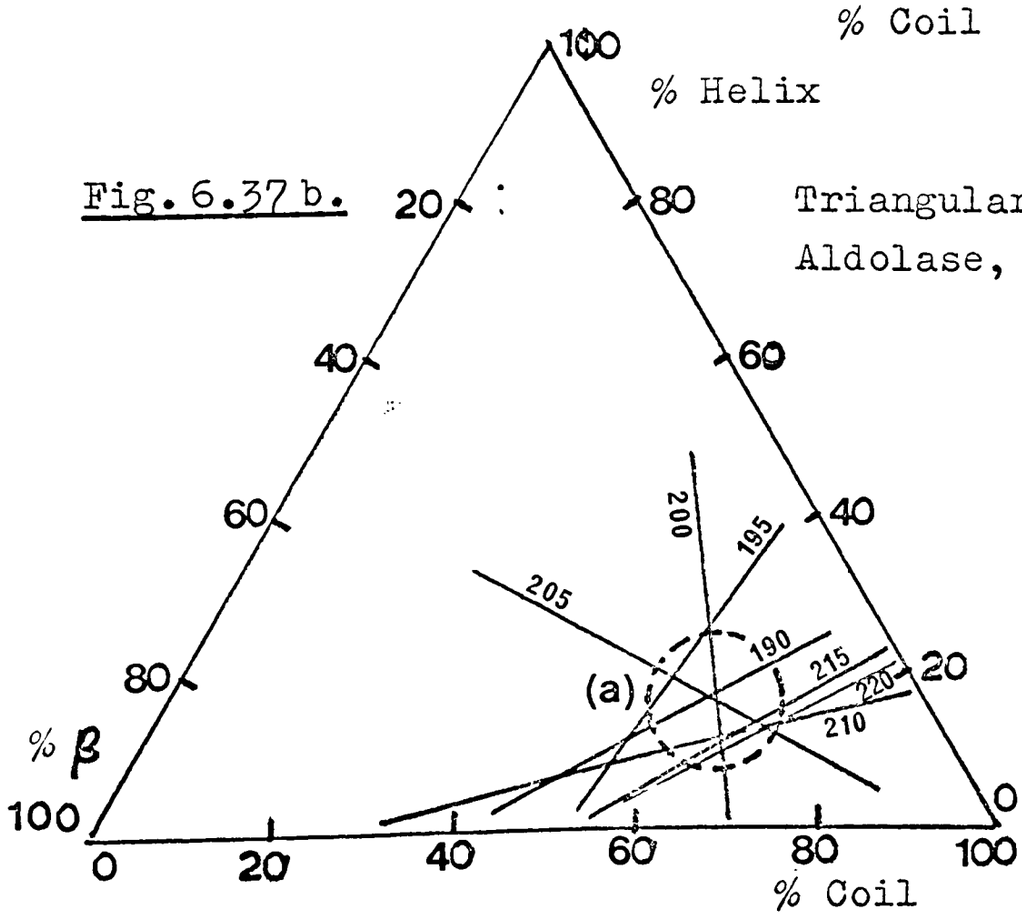

Fig. 6.37 b. Triangular diagram for Aldolase, pH 1.5.

Region (a)
17% Helix
60% Coil
23% Beta

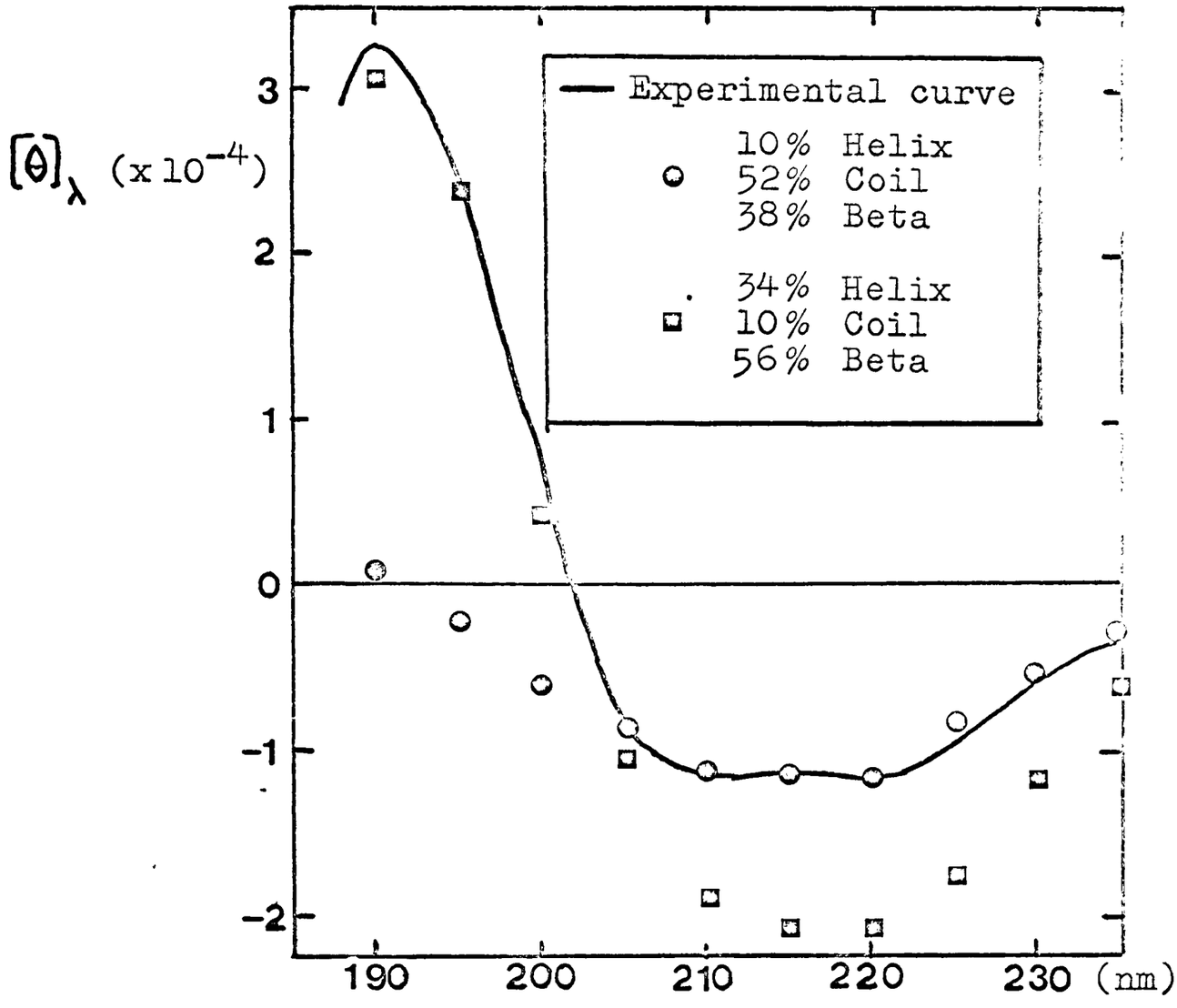

Fig. 6.38 a. Attempt to fit far-UV CD curve of PFK with contributions from the 3 types of sec. structure

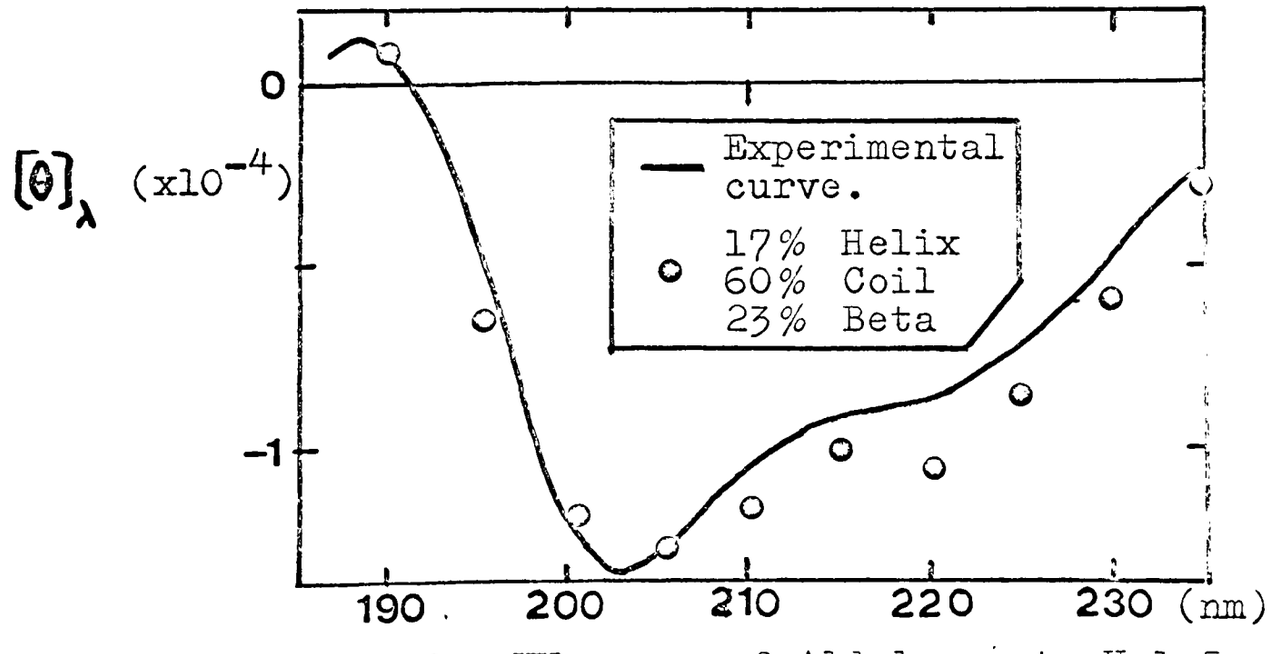

Fig. 6.38 b. Fit to far-UV curve of Aldolase at pH 1.5.

4. Discussion of Results.

(A) ORD Results.

The figure of -250 for the Moffitt b_o parameter in the case of aldolase agrees quite well with the values of -229 reported by Jirgensons (1962)[99] and -240 by Magar (1967).[100] The 290nm Cotton effect was observed by Magar who reported that it was absent in aldolase treated with acid, SDS or urea, which confirms the result of this study.

Far-UV ORD spectra for aldolase are described by Magar (1967)[100] and by Jirgensons (1965).[101] Magar obtained a value of -4200 for $[m']_\lambda$ at 233nm and 34,000 for $[m']_{198}$. Jirgensons obtained -6700 for $[m']_{233}$ and 33,000 for $[m']_{198}$. The former value for the mean residue rotation at 233nm agrees quite well with the value found in this work (-4000 ± 250) but the figure for $[m']_{198}$ (18,000 ± 4000) is considerably lower than that reported by the other two workers. A lower value could result from the presence of stray light, which, although careful steps were taken to eliminate it, might still have been significant. It appears, however, that the results of the transform of the CD data obtained in this study fit better to the lower figure for $[m']_{198}$.

No ORD data for PFK has been reported in the literature, but the results obtained are similar to aldolase and do not seem unusual in any way.

The changes in b_o and a_o with pH for both aldolase and PFK correspond closely to changes in sedimentation coefficient which have been observed in this study for PFK and in earlier work for aldolase (Stellwagen and Schachman, 1962[48]; Deal et al, 1963)[102].

(B) Circular Dichroism Results.

(i) Near-UV results

The dichroic bands which have been observed in the 280nm wavelength region in many proteins are thought to originate principally from the tyrosine, tryptophan and cystine side chains (Beychok, 1967)[90]. Aldolase (Westhead, Butler and Boyer, 1963)[103] and PFK (Younathan et al, 1968)[104] have been reported to contain few if any disulphides, and these proteins do not show any obvious features of the near-UV dichroic spectrum which can be attributed to disulphide.

Model Compounds. These were studied in case they might assist in the assignment of the near-UV bands. The results for the most part agree with the sign and position of the bands reported by Beychok (1967)[90] and Legrand & Viennet (1965)[105]. There is also good agreement in the ellipticities of the larger bands, but less good agreement in the case of the smaller bands. For example, Beychok obtains -500 deg.cm^2/decimole for the band at 280nm in the case of N-acetyl-L-tyrosine ethyl ester, compared with the value

of -200 (approx.) obtained in this work. No figures were reported for N-acetyl-L-tryptophan ethyl ester.

On comparing the ellipticity values for the model compounds with those for the protein near-UV CD bands, it becomes immediately obvious that the total intrinsic ellipticity of the aromatic residues which make up the protein is an order of magnitude lower than the observed ellipticity. In aldolase, for example, taking $[\theta]$ per mole of tyrosine to be -200, we obtain for 29 residues per 100,000g a value of -6000. Similarly, the total ellipticity for 7 tryptophan residues would be +3000. The measured ellipticity per 100,000g aldolase is -30,000 at 295nm and +60,000 at 280nm. The near-UV optical activity must therefore be related to the fact that these side-chains are involved in the tertiary and quaternary structure of the protein. This is supported by the fact that the near-UV bands of aldolase disappear completely on denaturing the protein by adjustment to pH 3.

A possible mechanism for the enhancement of the rotational strength of these chromophores lies in the increased asymmetry of the electronic environment when they are present in the folded protein. Djerassi (1961)[106] and other workers have demonstrated the importance of the the electronic environment on the rotational strength of the carbonyl group in steroid ketones.

The results for the model compounds also show that N-acetyl-L-tyrosine ethyl ester has an optically active transition at 280nm and that N-acetyl-L-tryptophan ethyl ester has active transitions at 280nm and 295nm.

Aldolase. Beychok (1967)[90] has reported that aldolase has a positive band at 280nm. The results of section 3 above confirm this and also indicate that a smaller negative band is present at 295nm. The effect of formaldehyde or N-acetyl imidazole on the bands suggests that they do, at least in part, arise from different chromophores, and that some of the optically active chromophores are close to the surface of the protein molecule. N-acetyl imidazole is known to react specifically with tyrosine side-chains (Riordan et al, 1965[107]) and formaldehyde reacts initially with lysine groups, followed by a secondary reaction with other neighbouring side-chains including phenolic and indole groups (Fraenkel-Conrat,1948[108]). It is possible therefore that the decrease in rotational strength caused by these reagents results from the modification of tyrosine residues.

On increasing the pH, both the 295nm and the 280nm bands decrease progressively in size and disappear completely by about pH 11.6. Over the pH range 9 - 11.2 there is a slight reduction in the sedimentation coefficient from about 7.5 S to 6.5 S which probably represents a slight

unfolding of the protein oligomer. The changes in the near-UV bands over this pH range may be the result of this conformational change. Bands arising from tyrosine or tryptophan would be affected equally.

The positive band which appears at 255nm and increases in size with increasing pH can be accounted for by the red-shift of the positive tyrosine 225nm band as the phenolic OH ionises. The long wavelength tail of this band and the negative peptide band combine to give a maximum in the curve at 225nm. The value of the molar ellipticity for N-acetyl-L-tyrosine ethyl ester is sufficiently large to account for the size of the observed band in denatured protein. Despite the fact that this band is also affected by the change in the peptide bands, there is quite a good correlation between the value of $[\theta]_{255}$ and the extent of tyrosine ionisation (Fig.6.39).

It is not possible on the above evidence to make a firm assignment of the near-UV bands in native aldolase. However, if we assume that wavelengths of the active transitions in the native protein are close to those in the model compounds, then the 295nm band can be tentatively assigned to tryptophan. From the other evidence, the 280nm band is probably contributed to by both tyrosine and tryptophan.

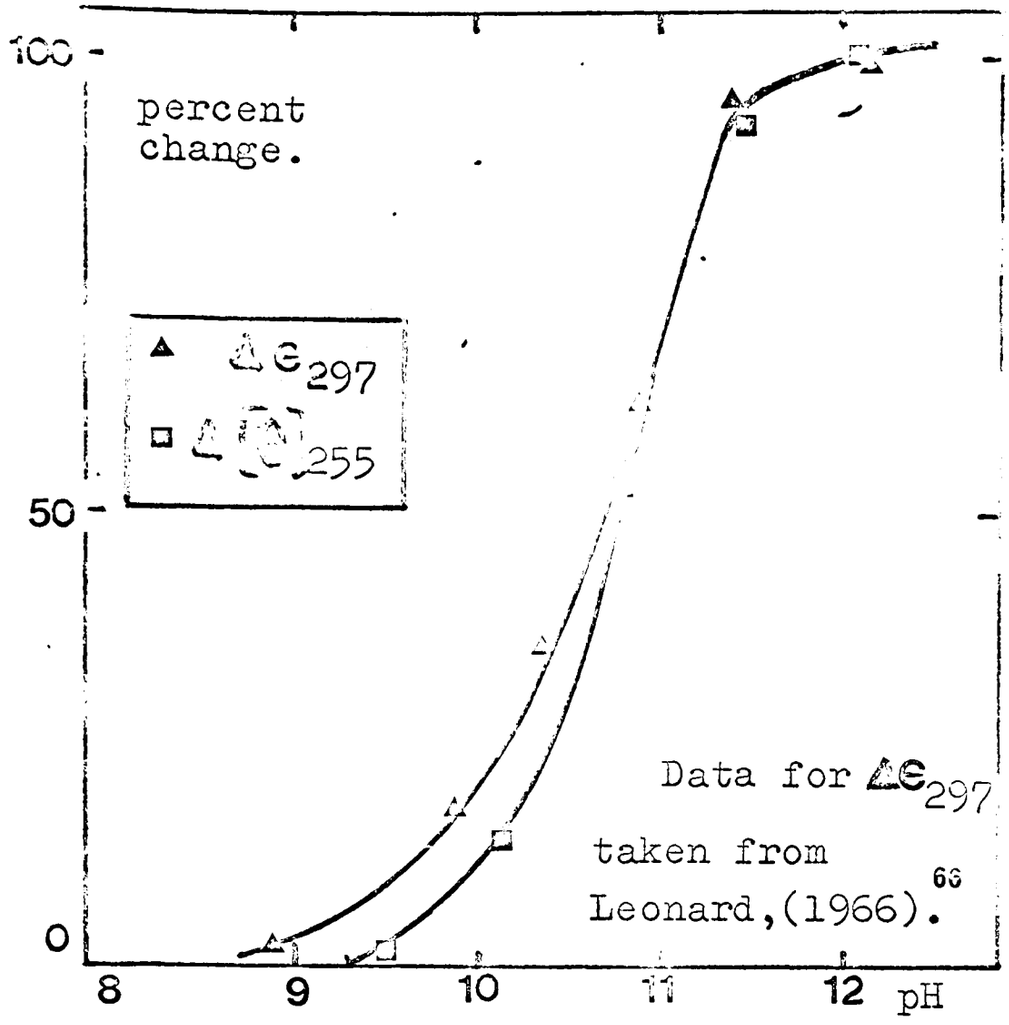

Fig. 6.39. Correlation between $\Delta\varepsilon_{255}$ and the extent of tyrosine ionisation in aldolase.

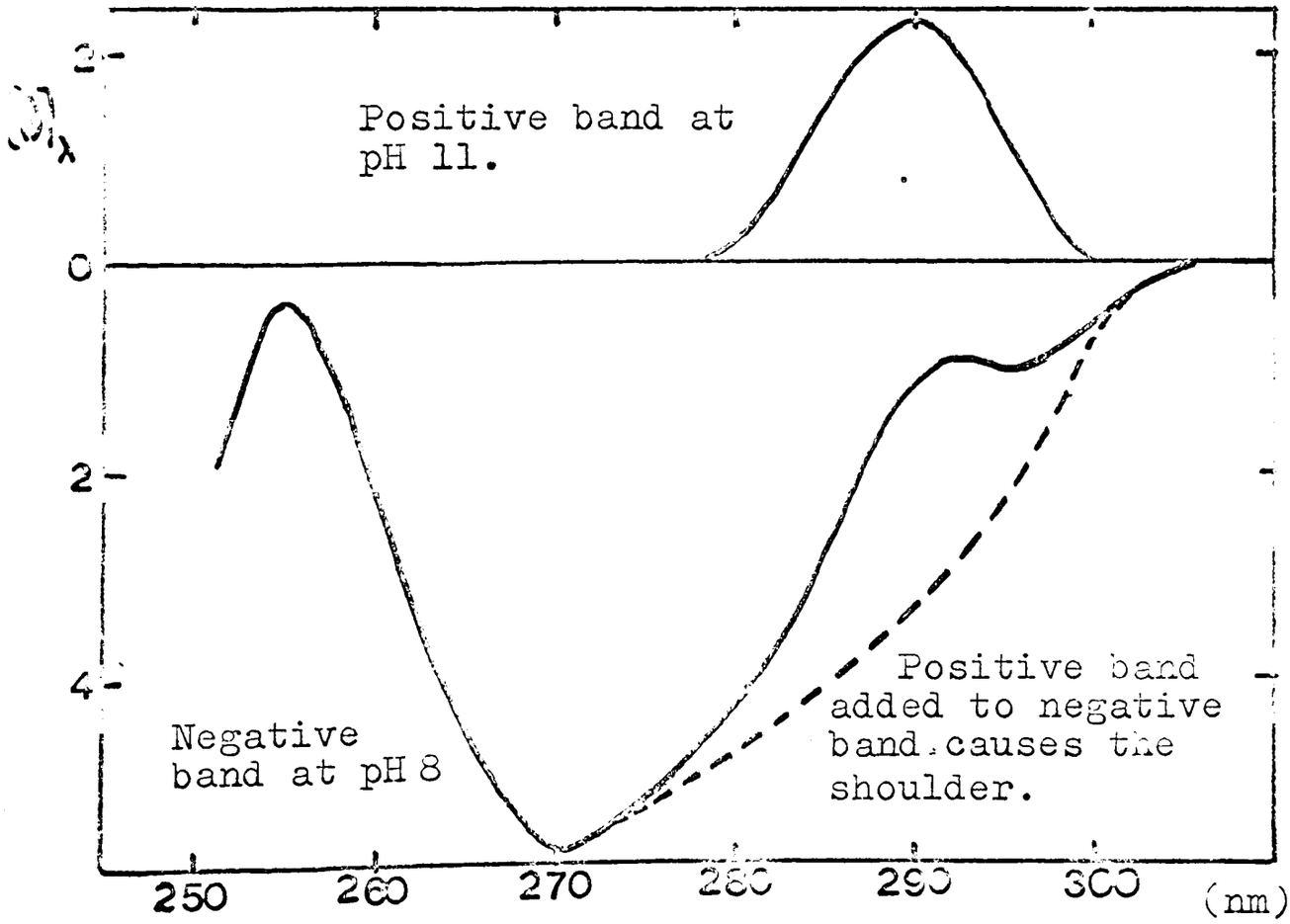

Fig. 6.40. Possible explanation of shoulder at 295nm in near-UV CD of PFK at pH 8.

PFK. Results obtained for several preparations of PFK established that the near-UV CD spectrum was a complex negative band slightly smaller than the larger of the aldolase bands. The exact shape of the PFK band varied slightly but this may not have been significant as it was necessary to work at high protein concentration to obtain a reasonable recorder deflection, and the noise level was high.

No changes in the near-UV bands were observed on varying the concentration over the range at which the protein associates, which rules out the possibility of optical activity resulting from the polymerisation of the 12 S protein, as has been observed for TMV protein (Walker, 1969[109]). The observed CD bands must therefore be a feature of the quaternary or tertiary structure of the 12 S oligomer.

The abrupt change in the spectrum between pH 10 and pH 11 is associated with the dissociation of the oligomer which takes place over that range. The peak which appears at 255nm is, as in the case of aldolase, probably associated with the ionised tyrosine residues. The small positive band at 290nm is interesting as it suggests that the 4.5 S protein at pH 12 may still have sufficient tertiary structure to produce a measurable dichroic effect. Buried tryptophan residues may be involved, since the spectrophotometric titration data (Chapter 7) shows that virtually all of

the tyrosine residues have titrated by this pH. The shoulder which is present at 295nm in the CD spectrum of native PFK may result from this positive band superimposed on a larger negative band which arises from the association of the 4.5 S subunits in the 12 S oligomer. This is shown in Fig. 6.40.

Kronig-Kramers Transforms. The positive and negative CD bands in aldolase result in overlapping ORD curves which reinforce each other to produce a sharp peak at 290nm. The PFK CD bands produce ORD curves which do not reinforce each other, so that the resultant Cotton effect is too small to detect against the background rotation of the peptide chromophore. The negative deviation from a linear Moffitt curve is however consistent with a negative contribution to the ORD curve from near-UV chromophores.

(ii) Far-UV Results.

Effect of pH. The changes in the far-UV bands for aldolase and PFK reflect quite accurately the conformational changes which take place over the measured pH ranges. It may be significant that the change in the 210nm - 220nm trough region of PFK at high pH is much less marked than that for aldolase under the same conditions. This may be further support for the possibility that PFK is not fully denatured at pH 12.

Estimation of secondary structure content. The Moffitt b_o parameter and the 233nm trough rotation were not used to estimate secondary structure, as they would be subject to error caused by the presence of near-UV optical activity. The attempt to analyse the experimental far-UV CD curve in terms of contributions from α-helix, β-structure and random coil was not successful for native aldolase, native PFK or PFK at pH 12 (Undenatured ?). A better fit was, however, possible for denatured aldolase at high or low pH, supporting the view that this method of structure analysis is more valid for denatured protein.

While this thesis was being written, a paper was published (Greenfield and Fasman, 1969[110]) which attempts to analyse the peptide CD bands of 6 proteins of known three-dimensional structure by a method similar to that described above. The results described, support, to a

certain extent, those obtained in this study. These workers were also unable to fit curves to both the positive and negative peptide bands for the native proteins.(No attempt was made to analyse data for denatured proteins.). On the grounds that the positive far-UV band is more subject to anomalies such as end-effects, solvent effects and contributions from aromatic residues, they then analysed the negative region between 208nm and 240nm separately. The results obtained showed that a reasonable fit to the experimental curves could be obtained for proteins with a high content of ordered secondary structure. If the content of disordered poly-peptide chain was high the best fit to the experimental was not good. It would therefore appear that this method is weakest in its assumption that disordered secondary structure in globular proteins can be considered to be the same as that for flexible polypeptides.

Chapter 7. Titration Studies on PFK and Aldolase.

1. Theory.

(a) Potentiometric Titrations.

The potentiometric or electrometric titration curve for a protein is the relationship between the pH and the number of moles of H^+ which are bound to, or dissociated from, one mole of protein. In practice, the curve is constructed by adding aliquots of standard acid or alkali to a known amount of protein solution. The amount of H^+ bound or dissociated at a given pH is obtained from the difference between the amount of acid or alkali added to the protein solution at that pH and the amount which would be added to the solvent to bring it to the same pH and final volume.

The titration behavior of the ionisable side chains in protein molecules deviates from that predicted from studies on low molecular weight model compounds. The principle reason for this is thought to be the electrostatic interaction which must occur between charged residues maintained in close proximity to each other by the tertiary structure of the protein macromolecule. Two theories have been proposed to account for this effect.

Linderstrom and Lang (1924)[111] considered the electrostatic charges to be averaged out over the whole molecule and assumed that residues of the same type (eg. side-chain

carboxyl groups) would titrate with the same intrinsic pK. By applying Debye-Hückel theory to the hydrogen ion binding equilibrium they derived the following expression.

$$pH - \log \frac{\alpha}{1-\alpha} = pK_{int} - 0.868\omega\bar{Z}$$

Where: α is the degree of H^+ ionisation for a given type of ionisable group.

pK_{int} is the intrinsic pK of that group.

$\bar{Z}$ is the nett charge on the protein.

ω is the electrostatic interaction factor.

If the titration curve is reversible, a plot of $\log \frac{\alpha}{1-\alpha}$ against pH should be linear, and from it ω and pK_{int} can be determined. The electrostatic interaction factor is dependent upon the shape of the protein molecule and upon the ionic strength.

This model obviously oversimplifies the effect of charge which is not evenly distributed in a real protein molecule. Tanford and Kirkwood (1957)[112] consider every ionisable group in the protein to have a different pK_{int}. This can be calculated from the pK of the appropriate model compound if the true charge distribution in the macromolecule is known. This treatment can, of course, only be applied to proteins for which the three-dimensional structure is known, and although more rigorous than the Linderstrom-Lang theory, it is more limited in its applicability.

Table 7.1 Values of pK for ionisable groups in proteins

Group	Approximate pK_a for model compound.	Approx pK_{int}
α - COOH (C- Terminal)	3.8	3.6
Aspartyl -COOH	4.0	4.6
Glutamyl -COOH	4.4	4.6
Imidazole (histidyl)	6.3	7.0
α - amino (N- Terminal)	7.5	
Thiol (Cysteine)	9.5	
Phenolic -OH (Tyrosine)	9.6	9.8
ε - amino (Lysine)	10.4	10.0
Guanidyl (Arginine)	12	12

Data given by Tanford (1967).[113]

pK values for the most important ionisable groups found in protein molecules are given in Table 7.1.

(b) Isoelectric point.

The pH at which the nett charge, $\bar{Z}$, is zero is known as the isoelectric point or isoelectric pH. The pH at which the protein is in equilibrium with water, all ions other than H^+ and OH^- having been removed by exhaustive dialysis or ion exchange, is known as the isoionic point. In the case of proteins which are isoelectric between pH 5 and pH 9, it can be shown that, to a good approximation, the isoelectric and isoionic points are equal if the protein concentration is sufficiently high.

(c) Temperature difference titrations.

The analysis of hydrogen ion binding in the region of histidyl titration can be refined by measuring the heats of ionisation of the titratable groups (Tanford,1955)[114]. An apparent heat of ionisation can be obtained by measuring the titration curve at two different temperatures and substituting in the following expression:-

$$\Delta H_{app} = -2.303\, R\left(\frac{\partial pH}{\partial \frac{1}{T}}\right)_{\bar{Z}}$$

The transition from carboxyl groups (ΔH_{app}= 1-2 Kcal) to histidyl groups (ΔH_{app}= approx. 7 Kcal) is usually sharp, and there is a less well defined transition

between the histidyl groups and the lysine groups which have ΔH_{app} of about 11 Kcal. Data for bovine serum albumin obtained in this work and given by Tanford, 1955 are shown in Fig. 7.1.

(d) Spectrophotometric titration of tyrosine.

Ionisation of tyrosine at high pH is accompanied by an increase in absorbance and shifts in the spectral maxima (Fig. 7.2). Although there is a greater change in absorbance at 250nm, the change at 295nm is used to estimate the degree of tyrosine ionisation, since other ionisable groups such as thiols and histidines contribute to the spectral changes at the shorter wavelength.

A figure of ΔE_{297} = 2330 per mole of tyrosine ionised (Donovan,1964)[115] was used in this study.

The following information may be derived from titration data.

(i) The number of titratable groups, which can be compared with the number expected from the amino acid analysis.

(ii) The apparent pK by inspection, or the pK_{int} and ω from the Linderstrom-Lang analysis.

(iii) Conformational changes may be detected from changes in ω, time dependence of the titration or irreversibility of the titration curve.

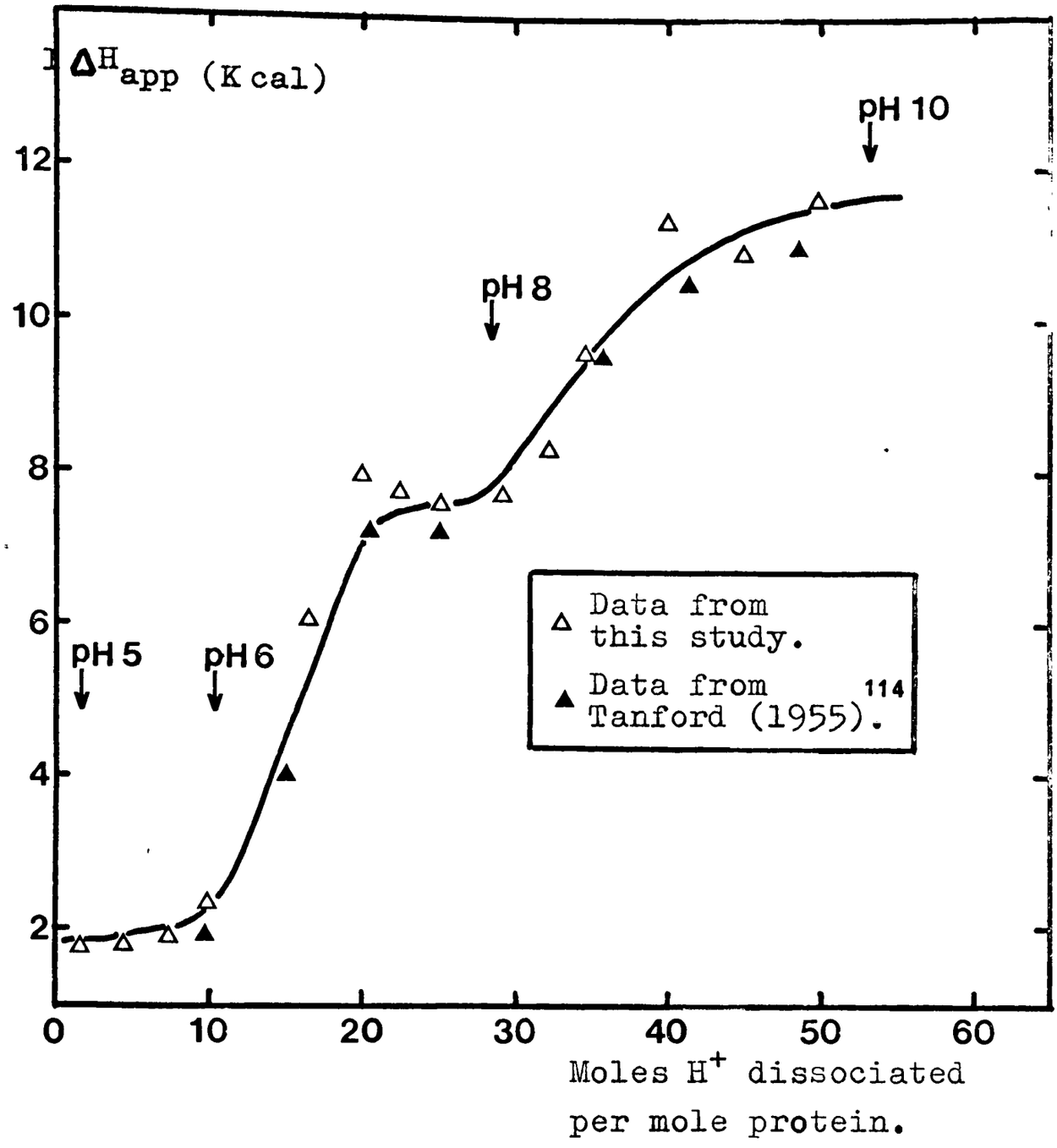

Fig. 7.1. Temperature difference titration curve for Bovine serum albumin.

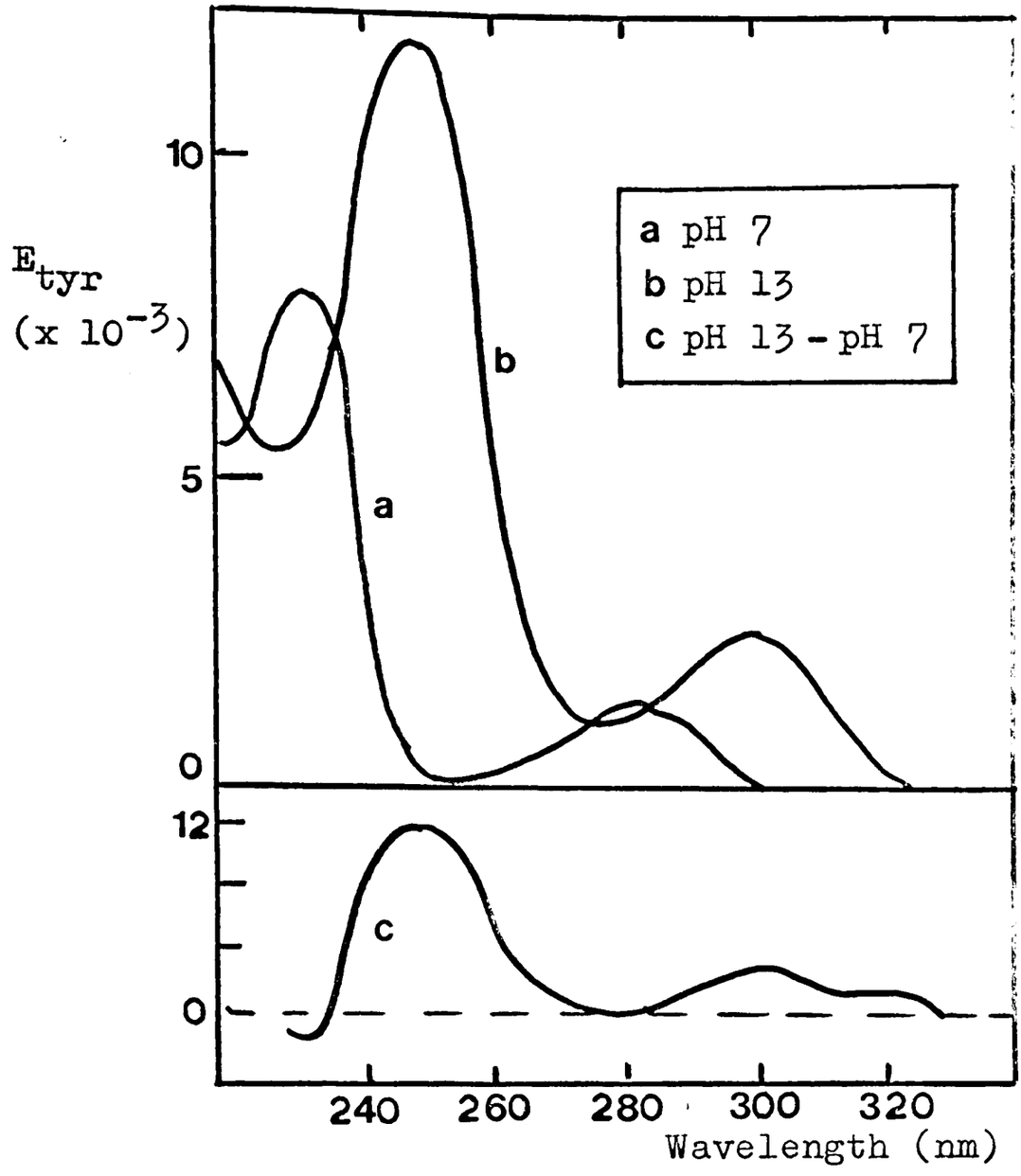

Fig. 7.2. Alkaline difference spectrum of tyrosine. (Taken from Wetlaufer, 1962)[116]

2. Experimental Details.

All titrations were carried out in a Radiometer Type TTA31 titration assembly consisting of a temperature-controlled glass cell with a magnetic stirrer. The volume of solution was normally 1.5ml containing 5 - 10mg of protein. Standard acid or alkali was added from an Agla micrometer syringe via a narrow glass tube. To prevent diffusion of titrant into the solution, the orifice of this tube was made as small as possible. Titrations were carried out under nitrogen to prevent absorption of atmospheric carbon dioxide.

The electrometric and spectrophotometric titrations of PFK were carried out at 25°C using an E.I.L. Vibret pH meter model 3920 and a Jena micro-dual glass/calomel electrode type 9259/81. For the aldolase temperature difference titration, a Vibron model C-33-B pH meter was used. The glass electrode was E.I.L. type GHS33 (screened) in conjunction with a Radiometer micro calomel electrode type K400 modified by increasing the length of the salt bridge. The electrodes were checked for stability and response time before use. A range of buffers (Table 7.2) was used to calibrate the pH meters.

The absorbance during the spectrophotometric titration was measured with a Unicam SP500 spectrophotometer and was corrected for scatter and dilution by titrant.

Table 7.2 Standard solutions used for pH calibration.

Solution	pH at		
	5°C	25°C	35°C
0.1M HCl	1.10	1.10	1.10
0.05M potassium hydrogen phthalate	4.01	4.01	4.02
0.025M K_2HPO_4 + 0.025M NaH_2PO_4	6.95	6.86	6.84
0.01Msodium borate	9.39	9.18	9.10
0.05M NaOH	-	12.62	-

Data from Robinson and Stokes, 1959.[117]

All titrations were continuous, just sufficient time being allowed between additions of titrant to enable the electrodes to respond to the change in pH.

3A. Results for PFK.

(i) Potentiometric titration.

Titrations are normally carried out in the presence of added electrolyte to control the ionic strength. Dialysis of PFK into 0.1M or 0.01M NaCl or KCl resulted in almost complete precipitation of the protein. Precipitation was, however, found to be slight in the presence of sulphate ion. Sodium sulphate (0.05M) was therefore used as the added electrolyte, and 0.1N H_2SO_4 or 0.1N NaOH used as titrants. The solution of PFK after dialysis into 0.05M Na_2SO_4 had a pH of 5.9 - 6.0 .

The titration curves for PFK are shown in Figures 7.3, 7.4 and 7.5. In the acid pH range the curve appeared to be reversible and it is also rapidly reversible above pH 11 when titrating to pH 12. The inaccuracy at the extremes of the titration curve is the inevitable result of subtracting a very steeply rising solvent titration curve from the steeply rising solution titration curve.

Exhaustive dialysis against distilled water gave a value of 5.2 to 5.5 for the isoelectric point for PFK at a protein concentration of 5mg/ml. Under these conditions the protein was soluble.

Group Count: (All figures are per 100,000g of protein)

The total of aspartic and glutamic acid residues less the number of amide groups is 100 - 116 from the

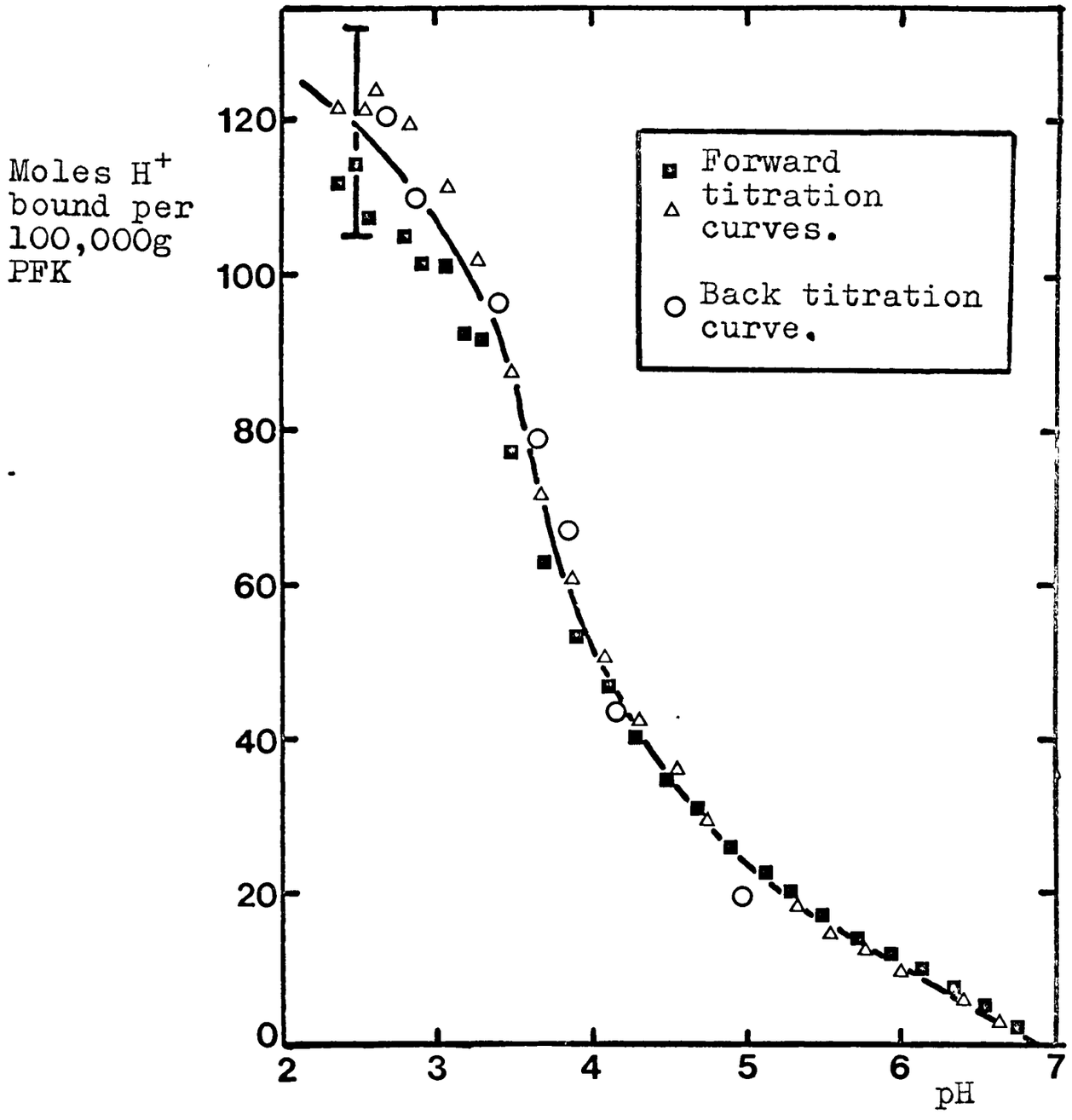

Fig. 7.3. Acid titration curves for PFK in 0.05M Na_2SO_4.

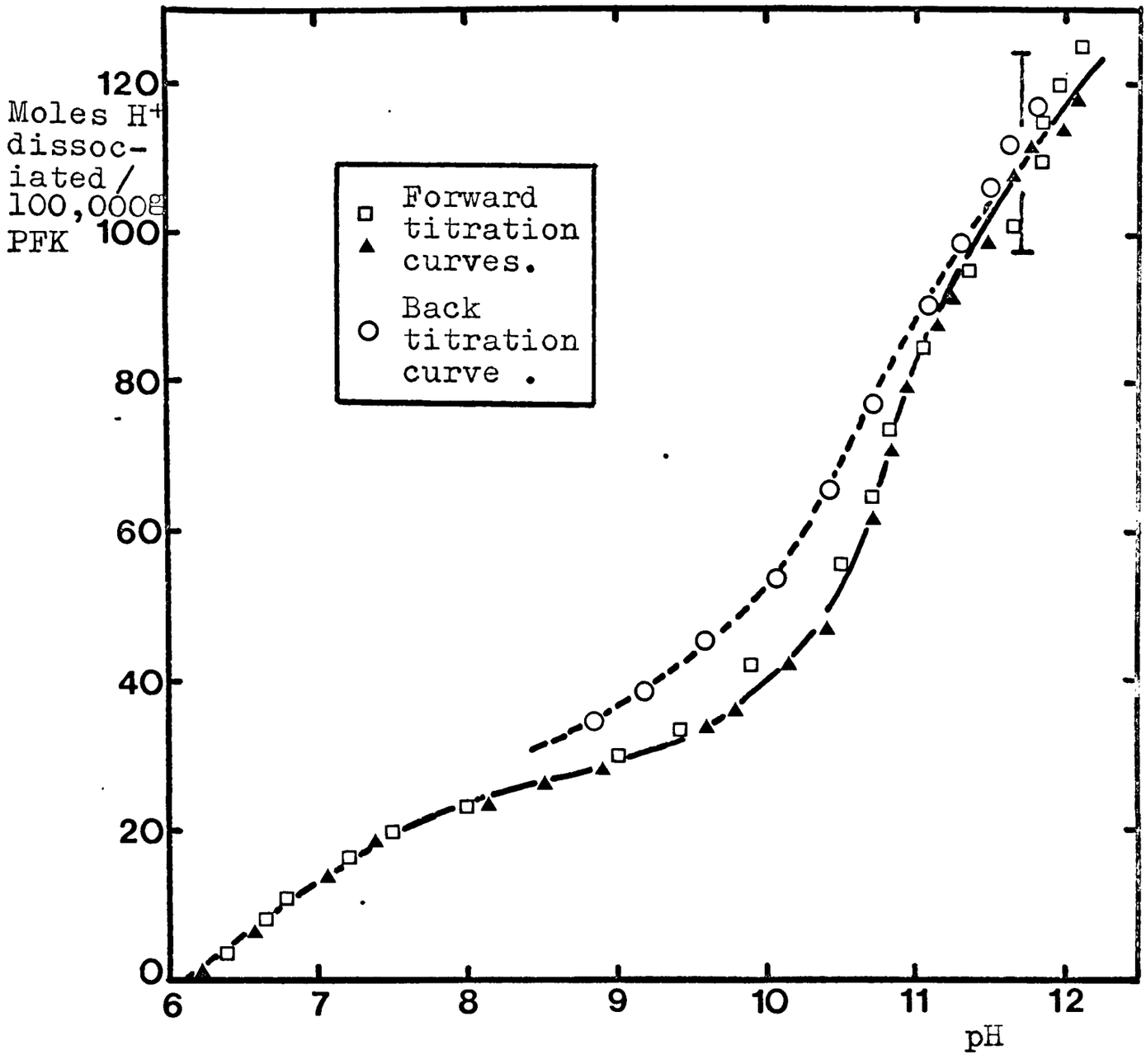

Fig 7.4. Alkali titration curve for PFK in 0.05M Na_2SO_4 .

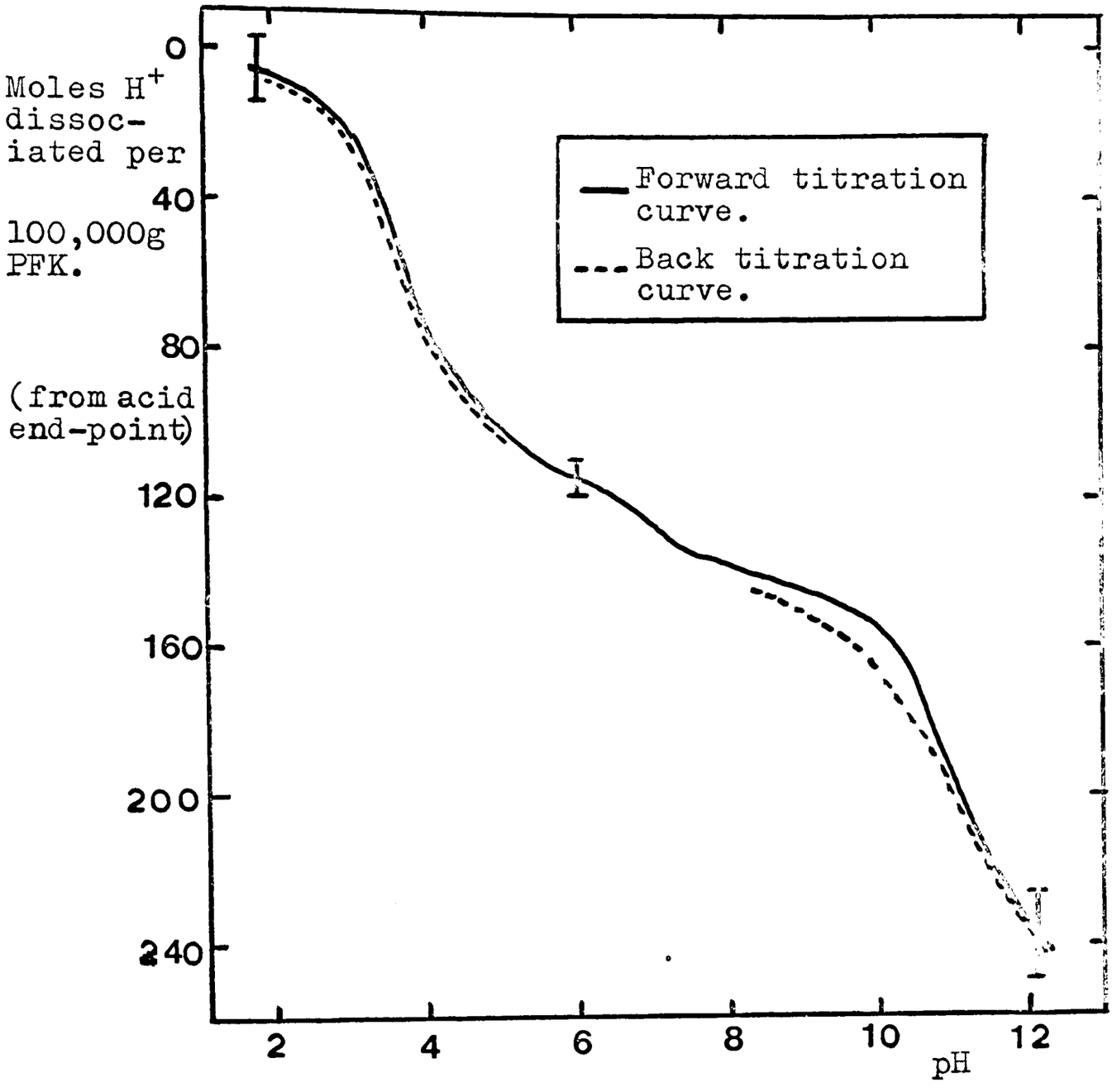

Fig. 7.5. Overall titration curve for PFK in 0.05M Na_2SO_4

amino acid analysis. This agrees quite well with the figure of 110±10 groups which titrate between pH 2 and pH 6 .

There is an inflexion in the curve between pH 6 and pH 8 which most probably results from the titration of histidyl groups. About 20±2 groups titrate in this pH region which is close to the figure of 22 from the amino acid analysis. The pK by inspection of the curve is 7±0.2.

The intrinsic pK of arginine is about 12, so that an alkaline end point is not reached by titrating to pH 12, which is the useful limit of the titration curve. The total of groups titrating between pH 8 and pH 12 is 100±10. This, as would be expected, is a little less than the total: -

Thiols + tyrosines + lysines + ½ arginines = 116±10

The total of residues which would normally be positively charged at the isoelectric pH is about 130±5. This is higher than the number which would be negatively charged (110±10).

Linderstrom-Lang Analysis.

The analysis of the titration curve between pH 2 and pH 6 assuming that 110 carboxyl groups are present is shown in Fig. 7.6 . The Linderstrom-Lang plot is reasonably linear and at an ionic strength of 0.15 gave $\omega = 5 \times 10^{-3}$ and $pK_{int} = 4.1$.

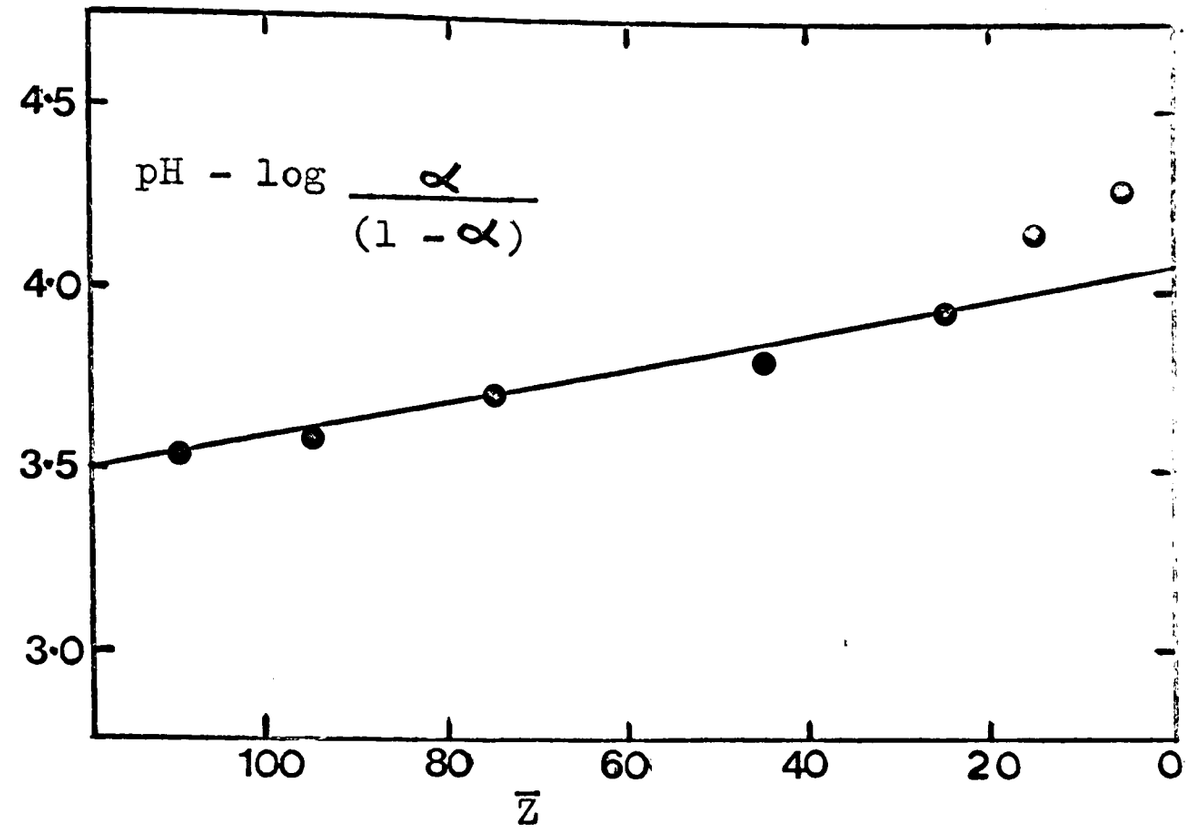

Fig. 7.6. Linderstrom-Lang analysis of titration data for carboxyl groups of PFK.

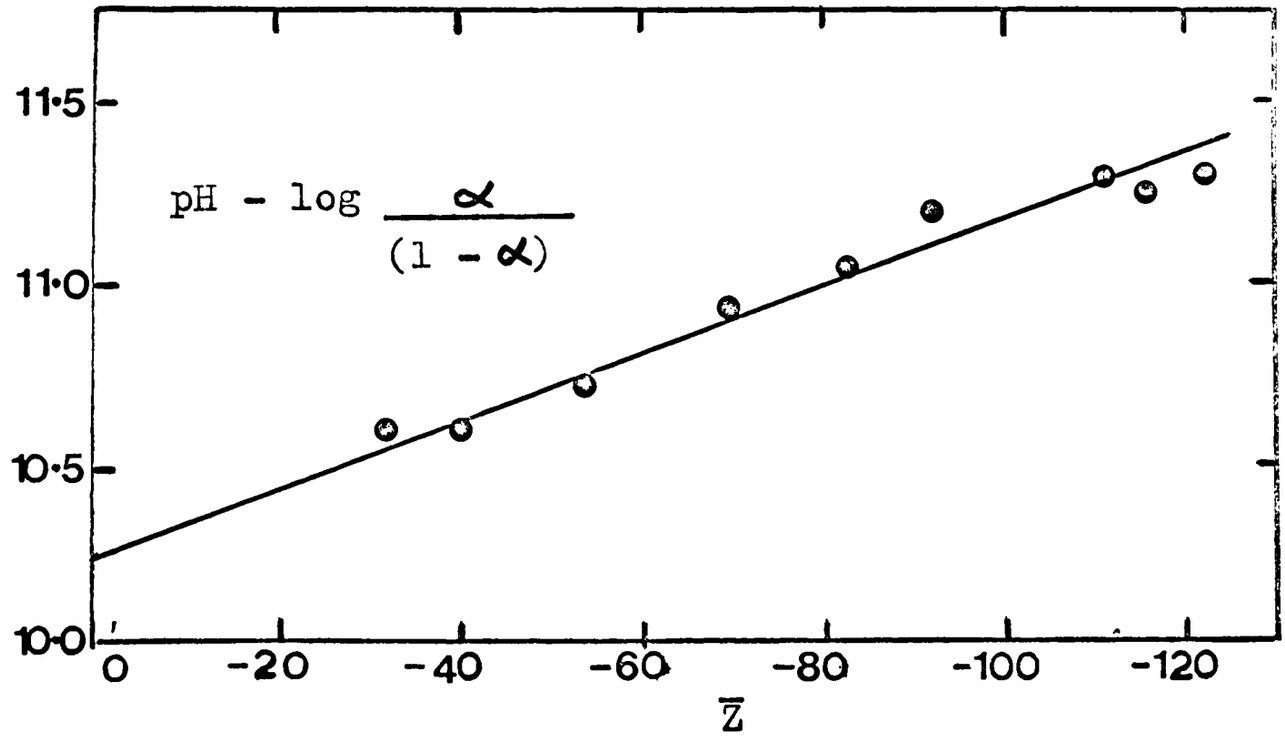

Fig. 7.8. Linderstrom-Lang analysis of titration data for phenolic groups of PFK.

(ii) Spectrophotometric Titration.

In this case, titrations were carried out in 0.01 M sodium phosphate, starting pH = 7.0. The titration curve measured by the increase in absorbance at 297nm is shown in Fig. 7.7 . The curve tends towards a limit of 18 - 20 tyrosine residues per 100,000g of protein which agrees with the amino acid analysis figure of about 18 ± 1.

In the presence of 1mM FDP, the curve below pH 11.5 is shifted to higher pH, whereas above pH 11.5 the two curves coincide (Fig. 7.7). The difference curve reaches a maximum of about 2 ± 0.5 tyrosine residues per 100,000g at pH 11 .

The Linderstrom-Lang analysis over the pH range 9 - 12 assuming 18 ionisable tyrosine residues is reasonably linear, giving a value of 1.2×10^{-2} for ω at an ionic strength of 0.02. The pK_{int} is 10.25. (Fig. 7.8)

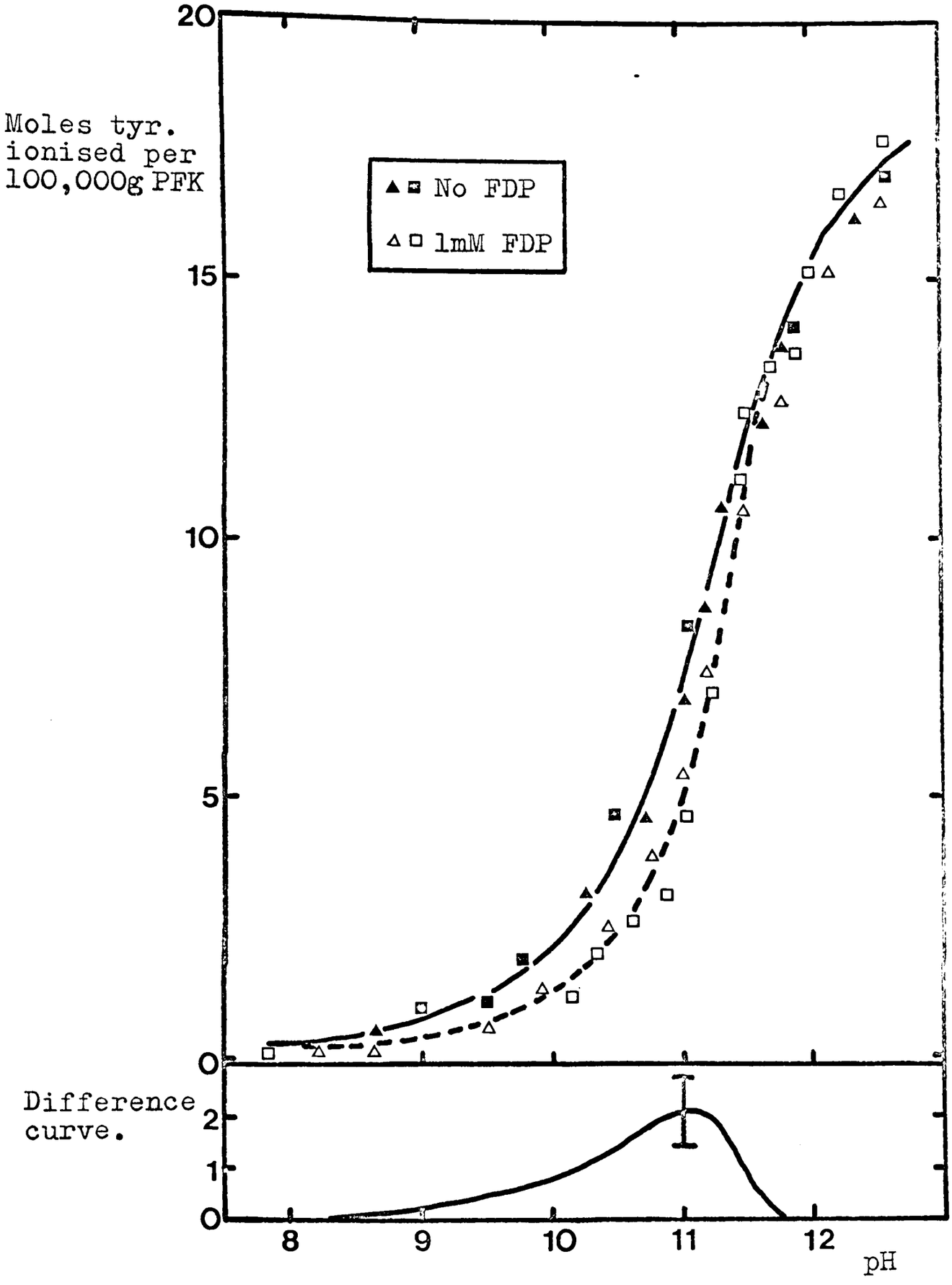

Fig. 7.7. Spectrophotometric titration curves for PFK in 0.01M phosphate with and without FDP.

3B. Results for Aldolase.

The electrometric and spectrophotometric titrations of aldolase were the subjects of an earlier study, (K.R. Leonard, Part II Thesis, 1966).[66] The present work attempted to investigate in more detail the region of histidyl titration, since the earlier results suggested that some of the histidine groups may titrate anomalously or are buried in the native molecule. The effect of temperature on the dissociation, which had been shown to occur on decreasing the pH to about 4.0, was also investigated

(i) Temperature difference titration above pH 4.5.

Temperature difference titration measurements were carried out between pH 4.5 and 10.0 , and at the temperatures 5°C, 25°C and 35°C . The curve of ΔH_{app} against H^+ is shown in Fig. 7.9 . There is an inflexion at pH 7 and ΔH_{app} = 7.8 Kcal which can be assigned to 'normally' titrating histidine residues. The curve does not, however, show a clear transition between histidyl and carboxyl titration, but falls gradually to a value of ΔH_{app} = 2 Kcal at pH 5.0 . The broken line shows the type of curve which would be expected for the transition between the two types of group (cf. Bovine serum albumin, Fig.7.1). The conclusion which can be drawn is that an unusually large number of histidine groups are titrating below pH 6 with the result that the ΔH_{app} transition becomes less sharp.

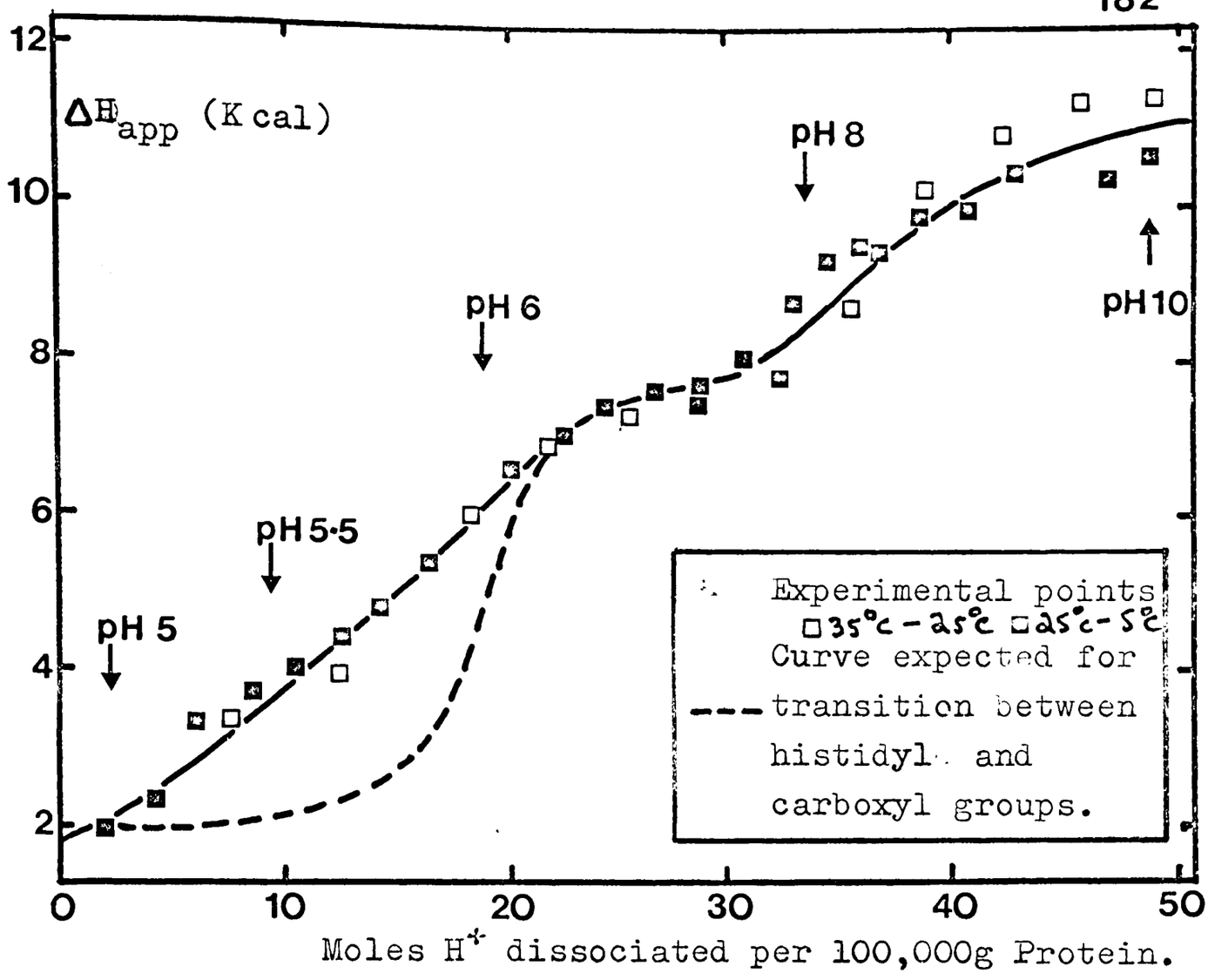

Fig. 7.9. Temperature difference titration curve for Ald.

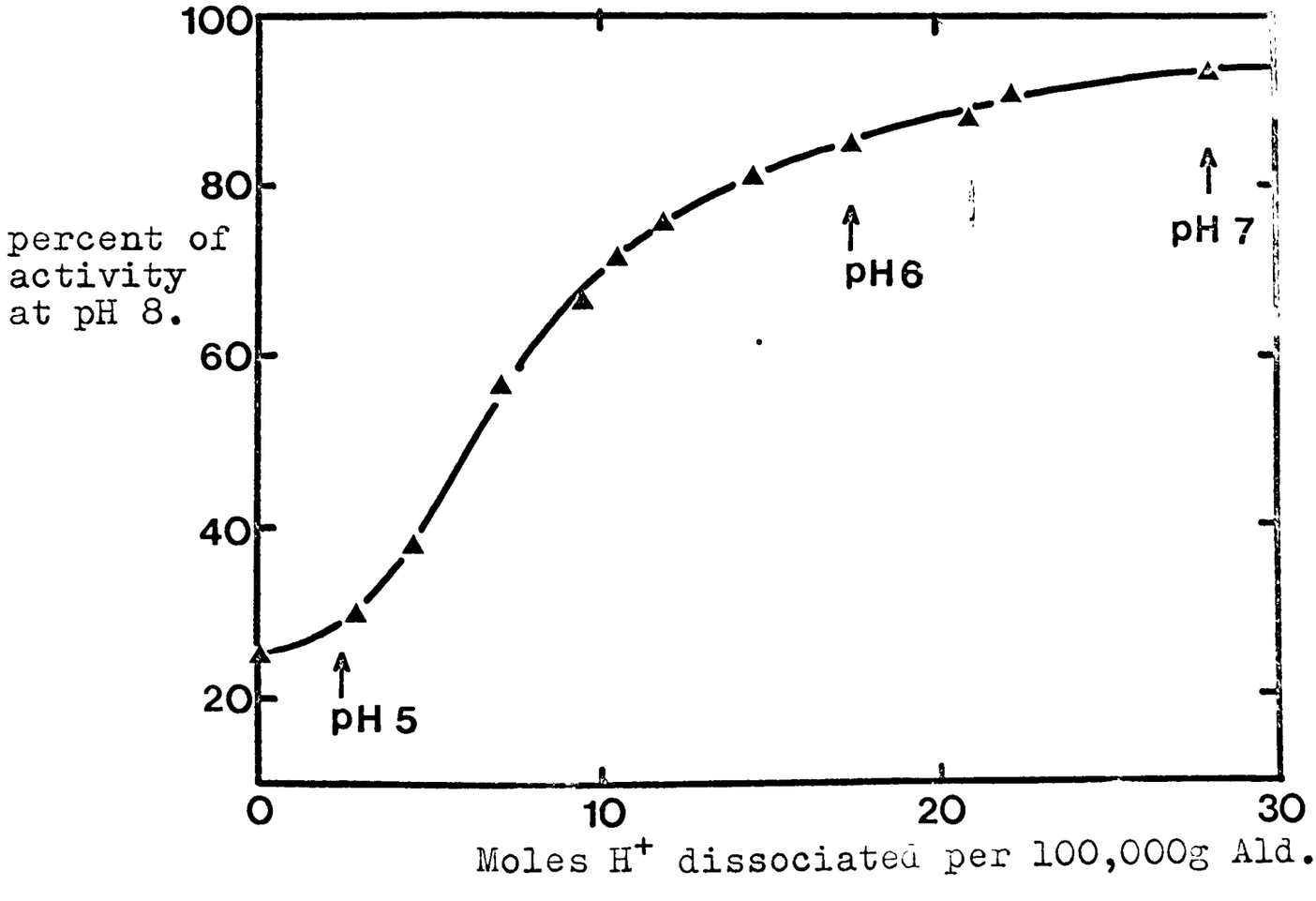

Fig. 7. 10. Effect of acid pH on Aldolase activity.

The number of groups titrating between pH 8 and pH 6 is about 17 (moles per 100,000g of aldolase). If it is assumed that half of the 16 groups titrating between pH 5 and pH 6 are carboxyl groups and the remainder are histidyl groups, then the titration curve between pH 8 and pH 5 would include about 25 potential histidyl groups. The amino acid analysis (Lai et al, 1965.)[118] gives 28 moles of histidine per 100,000g.

If the activity of the enzyme is plotted against H^+ diss. over the same pH range (Fig. 7.10), there is a slow decrease between pH 7 and pH 6, followed by a more pronounced drop in activity between pH 6 and pH 5. The greatest loss in activity seems therefore to be associated with those residues which titrate between pH 5 and pH 6 which as we have seen are a mixture of carboxyl and histidyl residues.

(ii) Temperature difference titration below pH 5.5 .

The earlier work (Part II Thesis, 1966) showed that there is a step in the titration curve at about pH 4, at which pH the enzyme decreases in sedimentation coefficient from 7S to 2S (approx.). The effect of temperature on the titration behavior in this pH region is shown in Fig. 7.11 . On decreasing the temperature, the step in the curve, which indicates rapid binding of H^+ as the enzyme oligomer dissociates, is shifted to lower pH. The native oligomer is therefore more stable at lower

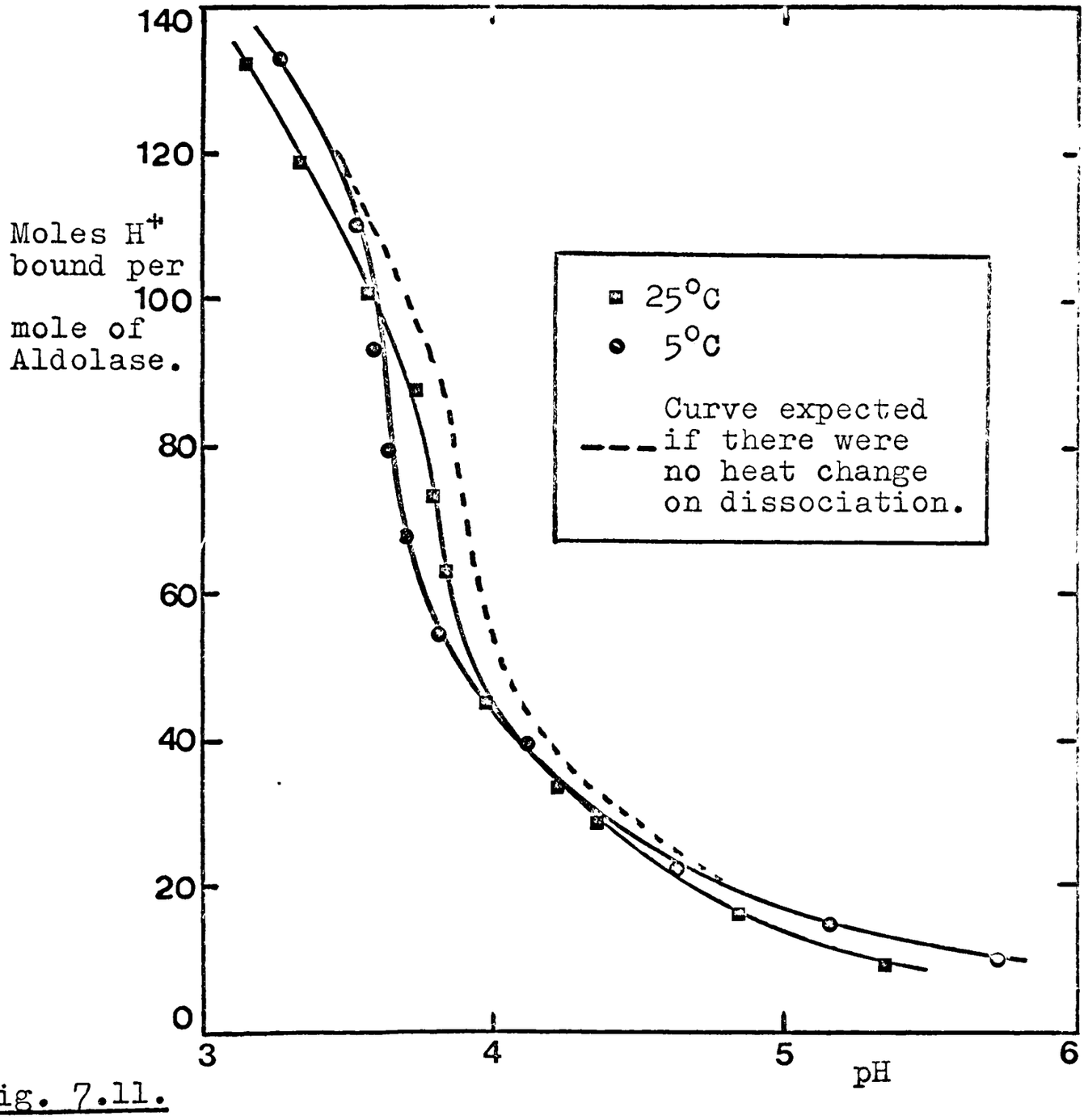

Fig. 7.11.

The effect of temperature on the titration curve anomaly between pH 4 and pH 3.5.

temperatures ;and the overall enthalpy change for the dissociation must be negative. The overall ΔH must be the sum of contributions from the heat of ionisation of groups which titrate normally, the heat of ionisation of any buried groups which titrate as the protein unfolds and the ΔH term for the dissociation and denaturation of the oligomer (the 2S protein below pH 4 is known to be denatured from ORD and CD studies, Chapter 6). The heats of ionisation are positive, so that the overall negative value for ΔH indicates that the ΔH term for the protein-protein quaternary and tertiary interactions must be negative.

If there were no dissociation,the effect of the heat of ionisation of the normally titrating carboxyl groups would be to shift the curve to higher pH as shown by the broken line in Fig. 7.11.

4. Discussion.

(i) PFK

Despite the fact that the protein is insoluble over most of the acid pH range, the amount of acid required to titrate to pH 2 is close to the value which would be expected from the amino-acid analysis within experimental error. The number of groups titrating in the neutral and alkaline regions of the titration curve also appear to agree quite satisfactorily with the number of histidine and more basic residues found in the amino acid analysis.

The values of pK_{int} for the carboxyl and phenolic groups obtained by carrying out the Linderstrom-Lang analyses (4.1 and 10.25 resp.) are within the range of values reported in the literature for other proteins. The values of ω which were obtained are rather lower than the values calculated on the basis of a spherical, impermeable protein model (see Tanford,1962[119]). The calculated value for a protein of molecular weight 90,000 is 2.8×10^{-2} at ionic strength 0.15 and about 5×10^{-2} at ionic strength 0.02. The values found experimentally were 5.6×10^{-3} and 1.5×10^{-2}. The discrepancy may indicate that the protein is rather asymmetric, thus reducing the elecrostatic interaction factor. Alternatively, the low experimental result for ω could be caused by neglecting

the effect of counter-ion binding which will become more significant at high values of Z.

The effect of FDP on the titration of the phenolic groups is interesting. The shift of the titration curve can be interpreted in two ways. Firstly, there may be a large pK shift in a small number of groups. In this case, the difference curve points to the removal of two phenolic groups with a 'normal' pK of about 10.25 when FDP is present. These groups then titrate with a pK of about 11.5. They may be located in the inter-subunit region of the 12S oligomer which is known to be stabilised by FDP (Chap. 4) and so are prevented from titrating until it dissociates at a higher pH. Alternatively, these tyrosines may be located at the FDP binding site and be prevented from titrating by a direct interaction between FDP and the phenolic -OH groups. The formation of a hydrogen bond to the hydroxyl group would result in an increase in the pK of tyrosine (Tanford, 1961).[120]

A second explanation of the shift in the titration curve is that there is a small change in the effective pK of a large number of tyrosine residues. This could result from an increase in the electrostatic interaction factor on binding FDP, caused by a change in conformation. Although this is an attractive possibility, there is no evidence of a conformational change from other studies, so it seems

more likely that one or two tyrosine residues are titrating anomalously in the presence of FDP.

(ii) Aldolase

The temperature difference titration curves between pH 4.5 and pH 10 account for 17 histidine groups titrating between pH 8 and pH 6 with a 'normal' pK of about 7 and 8 groups titrating between pH 6 and pH 5 with an average pK of about 5.5. The total of histidine groups from the amino-acid analysis is about 28 per 100,000g so that few if any groups remain unaccounted for. Thus, although about 1/3 of the histidines have an abnormally low pK, there do not appear to be a significant number of untitratable groups.

Hoffee et al, 1968[121] have reported that the FDP activity of aldolase is sensitive to the photo-oxidation of a number of the histidine residues, and that these residues are equally sensitive at pH 8 and pH 5.5. The rate of photo-oxidation of imidazole under the same conditions is known to be essentially zero for the protonated species (Westhead , 1965)[122], so that the histidine residues in aldolase which are associated with the enzyme activity must have a pK at least as low as 5.5. Their result appears to support the results of this study, and also suggests that the groups responsible for the loss of enzyme activity which was found to occur between pH 6 and pH 5

are the abnormally titrating histidine groups.

The effect of temperature on the dissociation of aldolase at pH 4 shows that the overall ΔH is negative. If we assume that the ΔH of ionisation of the carboxyl groups which titrate in this region is about 2 Kcal and neglect the contribution of any buried groups which titrate as the protein unfolds, then a tentative value for the ΔH of dissociation plus denaturation can be estimated from the pH shift of the titration curve to be about -80 Kcal per mole of oligomer. This figure would be made more negative if there was a significant enthalpy change associated with the titration of buried groups. A large negative value of ΔH for the dissociation is to be expected, since the oligomer is quite stable at neutral pH.

Chapter 8. Discussion.

(i) Protein-protein Interactions.

(a) Association of PFK at high concentration.

The sedimentation pattern for native PFK and its variation with concentration and alkaline pH (Chapter 4) clearly demonstrate that reversible self-association of the enzyme takes place at protein concentrations above 0.5mg/ml.

Under mild dissociating conditions PFK sediments as a single boundary with $s^{o}_{20,w}$ of about 12 Svedberg units, suggesting that this is the 'monomer' of the reversible association. A similar value was obtained for the sedimentation coefficient at much lower protein concentration for native PFK, which supports this idea. The molecular weight of the 12 S protein from hydrodynamic studies (Chapter 4) and sedimentation equilibrium (Chapter 5) is about 3.5×10^5. The frictional ratio for this species and the intrinsic viscosity show that it behaves as a rather asymmetric hydrodynamic particle. This result is supported by electron micrographs of the enzyme (Parmeggiani *et al*, 1966)[5] which show it to have a flat, rectangular shape.

The molecular weight studies on the associating system at pH 8 (Chapter 5) indicate (by comparison of the experimental curves with calculated theoretical curves) that the

association of PFK is to a finite, closed polymer. The apparent Z-average molecular weight of the native enzyme rises to a value of about 5.5x (molecular wt. of monomer) which strongly suggests that n for the polymer is 6. The experimental data was fitted by a theoretical curve in this case by taking a value of 6×10^{-3} ml/mg for the second virial term BM_w . This is quite close to the value of 3×10^{-3} ml/mg for globular proteins (independent of their molecular weight) quoted by Tanford (1961)[64]. An approximate fit to the experimental data could also be obtained for $n>6$ by using a less reasonable value of BM_w .

Since the monomer units are presumably identical they must fit together in the polymer so that they are geometrically related to each other. If it is a hexamer it is possible to assemble the six asymmetric monomer units into a closed shell structure with cubic symmetry as shown below.

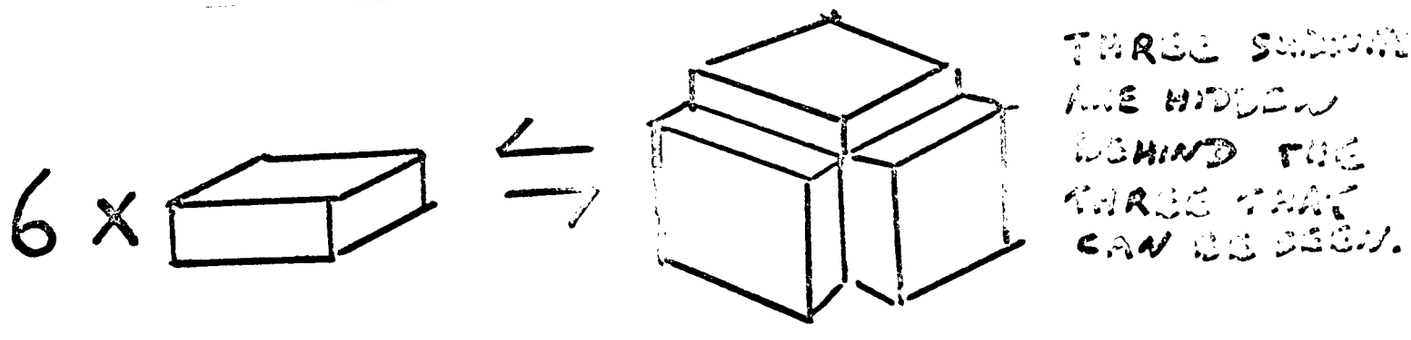

Preliminary electron microscope studies carried out with the help of Dr. J. Longworth (Dept. of Forestry, Oxford) and Drs. R. Domashkin & N.M. Green (National Institute for Medical Research, Mill Hill) suggest that the 12 S protein

is composed of four more-or-less spherical subunits arranged at the corners of a square. These tetramers could associate to give a structure of 24 subunits with octahedral symmetry as below.

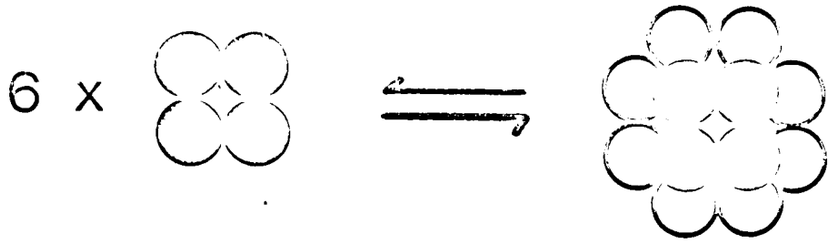

This is a representation of half of the hexamer. An identical half lies below the plane of the paper. The dark spheres are above the plane of the paper.

Each subunit would have two types of interaction - a strong interaction with two neighbours of the same 12 S unit and a weak interaction with two other subunits which are members of other 12 S units. This structure has a diameter of about 180 A estimated from the size of its subunits and so should be visible under the electron microscope. However, in view of the known tendency of the polymer to dissociate under mild conditions, it is unlikely that it would survive the effects of staining and mounting. Attempts were made to stabilise the polymer by cross-linking with the bifunctional reagents N,N'-o-Phenylenedimaleimide[123] and Toluene-2,4-diisocyanate[124], but no recognisable structures were apparent in the electron micrographs.

The results of the viscosity studies (Chapter 4) which showed a decrease in the reduced viscosity with increasing

concentration of PFK over the range at which the protein associates, suggest that the overall asymmetry of PFK is decreasing as it polymerises. This is consistent with the above model for the hexamer.

The appearance of the sedimentation pattern of native PFK, showing three peaks, seems at first to contradict the equilibrium molecular weight results which suggested that the concentration of intermediate polymers is low relative to the concentrations of monomer and n-mer. There are two possible explanations for this apparent 'intermediate' in the sedimentation pattern. Firstly, as was discussed in Chapter 4, the appearance of the sedimentation pattern in the case of a rapidly reversible association may be misleading and,under certain conditions, there may be more concentration boundaries than there are components present. Secondly, if the intermediate boundary does represent a real component of the system, it must be remembered that sedimentation transport experiments disturb the association equilibrium by removal of a greater amount of the more rapidly sedimenting species. If the half time of the polymerisation reaction for PFK is of the same order of magnitude as the time of sedimentation, the 18 - 20 S component may be a kinetic intermediate between the monomer and the polymer, whose concentration is temporarily increased as the system re-equilibrates.

The molecular weight studies gave the following approximate thermodynamic parameters for the equilibrium.(Assuming n = 6)

ΔG^{o} = -35 K cal (per mole of hexamer)
ΔH^{o} = 36 K cal "
ΔS^{o} = 240 e.u. "

Since there are eight interactions between different 12 S units in the octahedral structure these give, for each interaction : -

ΔG^{o} = -4.4 K cal
ΔH^{o} = 4.5 K cal
ΔS^{o} = 30 e.u

These results are similar to those obtained by Banerjee and Lauffer (1966)[125] for the polymerisation of TMV protein: -

ΔG^{o} = -4.5 K cal (per mole of subunit)
ΔH^{o} = 30 K cal "
ΔS^{o} = 124 e.u.

The greater enthalpy and entropy terms for TMV protein compared with PFK cause the TMV polymerisation to be much more sensitive to temperature. Lauffer et al[126] have reported that TMV protein is almost completely disaggregated at 4°C.

The association of PFK, like that of TMV protein, is brought about by the increase in entropy resulting from the loss of bound water as the monomers interact with each other. This necessarily implicates some form of electrostatic or hydrophobic interaction as was discussed in Chapter 1. The effect of ionic strength in completely preventing the association points unequivocally to the

former, since a high concentration of neutral electrolyte weakens electrostatic interactions and strengthens hydrophobic interactions.

(b) PFK at low concentration.

Mansour and Ahlfors (1968)[23] showed by sucrose gradient centrifugation that a form of heart PFK has a tendency at pH 7 to decrease in sedimentation coefficient, at the concentration level of the enzyme assay. The decrease in s_{app} from 14 S to 7 S (measured by assaying for PFK in the sucrose gradient after centrifugation and comparing its position with that of marker enzymes of known sedimentation coefficient) was favoured by the presence of inhibitory levels of ATP and prevented by the presence of FDP. They attributed this decrease in s_{app} to a dissociation of the enzyme.

The sedimentation coefficients for muscle PFK which were obtained in this study, by a method which did not involve subjecting the protein to high concentrations of sucrose, showed that there was no significant change in s_{app} for the active form of PFK. These results, however, do not rule out the possibility of irreversible dissociation to an inactive form of the enzyme, which would not be detected by the assay. There was always a small decrease in the activity of the control enzyme, which suggests that this might be taking place.

(c) Dissociated PFK.

Sedimentation experiments for PFK at high pH showed that above about pH 11 the enzyme dissociates to a subunit of sedimentation coefficient 4.5 S via a transitory 6 - 7 S intermediate stage. The intermediate may be the same as the 1.8×10^5 molecular wt. dimer (7 S protein) reported by Paetkau and Lardy (1967).[58] The 4.5 S material had a molecular weight of $8 - 9 \times 10^4$ which, in view of the fact that this sedimentation coefficient probably represents a lower limit (the effects of concentration and charge are to decrease s_{app}), indicates that it must be fairly compact. (c.f. Bovine serum albumin which has $s^o_{20,w} = 4.3$, mol. wt. $= 7 \times 10^4$ (approx)). This, together with the results of the CD work which showed that there was near-UV optical activity at pH 12 (Chapter 6), suggests that PFK dissociates to relatively 'native' subunits above pH 11.

In 6M GuHCl, 0.1M 2-mercaptoethanol or dithiothreitol, a molecular weight of $7 - 8 \times 10^4$ was obtained by sedimentation equilibrium and about 9×10^4 by sedimentation velocity. These figures agree fairly well with the molecular weight obtained at pH 12 in the presence of SDS and indicate that the 4.5 S protein is a single polypeptide chain.

Paetkau et al. (1968)[4], however, have reported lower molecular weights of 51,000 and 25,000 in 5.5 - 6.5 M GuHCl with added dithiothreitol. The discrepancy between their

results and those obtained in this work is not readily explainable. However, it may be significant that these workers give a value of 2.3 S for $s_{20,w}$ of the 51,000 mol. wt. protein in 5.5M GuHCl, 0.01M dithiothreitol, pH 8. If, as according to Tanford et al (1967)[47] is the case, the protein behaves as a random coil under these conditions, the value of $s^{o}_{20,w}$ would be 1.9 S for mol. wt. = 50,000 and 2.7 S for mol. wt. = 90,000. It would therefore appear that their value for $s_{20,w}$, allowing for the effects of protein concentration, is more consistent with a molecular weight of 90,000. Paetkau et al also reported rather inconclusive results for N-and C- terminal amino acid analyses. They obtained low yields of N- and C-terminal residues (usually about 0.1 to 0.2 moles/100,000g protein) which again appears to be more consistent with the presence of a single polypeptide chain of molecular weight about 90,000 than with the presence of four smaller polypeptides.

The results of this work, therefore, indicate that the 12 S protein (mol. wt. approx. 350,000) is composed of four subunits of molecular weight approx. 90,000, each consisting of one polypeptide chain. The subunits appear to be relatively compact at pH 11 - 12 and are normally associated into the asymmetric 12 S tetramer which is the enzymically active unit. Equilibrium binding studies for PFK (Kemp and Krebs, 1967)[70] have shown that one mole of

substrate is bound per 90,000g of protein so that the 4.5 S protein is the protomer of PFK. Both types of allosteric site must be present on the same polypeptide chain unlike aspartate carbamylase (Gerhart and Schachman, 1965)[127] which can be separated into catalytic subunits and regulatory subunits containing the different types of allosteric site. Phosphorylase b, however, which also exhibits allosteric behavior (Ullmann et al, 1964)[128] has been reported to have a molecular weight of 97,000 in 6M GuHCl (reported in Ullmann et al, 1968)[65], this being the enzyme protomer.

(d) A comparison of the behavior of Aldolase and PFK at high pH.

The CD results for the pH range 9 - 11 show that the mechanism of dissociation and the inter-subunit forces are not the same for the two enzymes. The CD studies (Chapter 6) show that aldolase undergoes a progressive conformational change (indicated by changes in the near and far-UV CD bands) between pH 9 and pH 11, before dissociation has taken place. PFK, on the other hand, shows little change in the dichroic bands up to pH 10, which is followed by a sudden change between pH 10 and pH 11 where the enzyme dissociates. PFK above pH 11 appears to be less denatured than aldolase at the same pH, since it shows near-UV optical activity and there is less change

in the 200nm-250nm negative CD bands. It can, therefore, be inferred from these results that the inter-subunit forces in Aldolase are less subject to disruption by high pH than the forces maintaining the protein tertiary structure In PFK the tertiary structure forces in the subunits appear to be less affected by high pH than the protein-protein interactions between subunits.

(ii) The role of protein-protein interactions in the regulatory behavior of PFK.

If the true concentration of PFK in the tissue is as high as the 1mg/ml level, which may well be the case if there is some form of biological compartmentation, the reversible association could play a part in the regulation of enzyme activity if there was competition between the active sites and the protein-protein binding sites. The enzyme assay results (Chapter 3), although not completely conclusive since they are measuring the activity of the enzyme towards a related substrate, G-1-P, would indicate that association does not have any effect on activity.

It has also been suggested (Mansour and Ahlfors, 1968;[23] Paetkau and Lardy, 1967)[58] that dissociation of PFK to an inactive form in the presence of inhibitors and re-association in the presence of activators may account for the

regulatory behavior. The results of Mansour and Ahlfors for heart PFK (mentioned in section (i)(b) above) appear to support this idea. However, the moving partition cell method used in this study showed that there was no change in the sedimentation coefficient (measured at the concentration level of the enzyme assay) in the presence of an inactivating concentration of ATP, compared with that in the presence of FDP. A rapid dissociation of muscle PFK into inactive subunits would, therefore, appear to be ruled out as the primary regulatory process. It is, however, possible that a weakening of the inter-subunit forces does occur in the presence of inhibitors, which would cause a slow secondary dissociation unrelated to the control of activity.

The influence of FDP in stabilising the 12 S protein at high pH would support the above possibility. FDP is the only one of several effectors tested (ATP, AMP, F-6-P and FDP) which had any significant stabilising effect at the mg/ml level on the alkali-induced dissociation at pH 10.5 - pH 11. FDP is known to be a much more powerful activator than F-6-P or AMP (Passonneau & Lowry, 1962[6] and the results of this work, Chapter 3), which may explain its unique stabilising effect. It would appear, therefore, that association-dissociation phenomena are not implicated in the regulatory behavior of skeletal muscle PFK.

The Monod *et al*[15,16] and Koshland[19] theories of enzyme regulation require that a conformational change should accompany the binding of effectors to the molecule. Kemp (1969)[128] has recently interpreted the kinetic data for native and thiol-modified rabbit muscle PFK in terms of the two-state model of Monod *et al*. The attempts which were made in this study to detect conformational changes by direct physical methods such as ORD and CD were not successful. However, the stabilising effect of FDP on PFK at high pH may be indirect evidence of a conformational change to a more stable structure.

Appendix 1(a)

This program approximates the experimental curve as a sum of Gaussians by stepwise adjustment of the Gaussian parameters between predetermined limits until the best fit is reached.

```
FABAK10
GAUSSIAN CURVE FITTING PROGRAM
→
begin  real l, a, dl, L, SD, D, S, V1,V2 , V3, rea,d;
  integer  n,X,x,q, j,o, i, p;
  real array   A[1:5], B[1:5], C[1:5], DD[1:5], lK[1:5],
                EOK[1:5], DEK[1:5], O[1:5], K[1:5], P[1:5
               dDEK[1:5], dlK[1:5], dEOK[1:5], ME[1:600],
                E[1:600];
  switch  kl := D3, D4, D5, D6;
  j:= 1;
L1:       open (20);  open (30);
L11:      write text (30, [[p]BEST*FIT*OF*GAUSSIAN*
                CURVES*TO*EXPTAL*CURVE[cc]]);
  j:=1;
  copy text  (20,30,[//]);
  d:= 1000;
  X:= read (20);

L2:       i:= read (20); L:= read (20); dl:= read(20);
           S:= read(20);
  n:= 1;
L8:       A[n]:= read (20);    dlK[n]:= read (20);
          V1:= read (20);
  B[n]:= read (20);  dEOK[n]:= read (20);
  V2:= read (20);
  C[n]:= read (20);   dDEK[n]:= read (20);
  V3:= read (20);
  n:= n + 1;
  if n ≤ i then goto L8 else
L3:       for l:= L step S until dl do
  ME[l]:= read (20);
L5:       p:= 0;    x:= 0;  n:= 1;
L9:       rea:= read(20);
  n:= 1;  q:= i;
  d:= 1000;
  DD[1]:= 1000; DD[2]:=1000;  DD[3]:= 1000;  DD[4]:= 1000;
  DD[5]:=1000;
```

```
   write text (30, [[5c10s] NUMBER*OF*CURVES*=**]);
   write (30,format([d]), i );
   write text (30,[[cc10s]LIMITS*OF*LAMBDA(0)(K)*=]);
L4:        write (30,format ([ssnddd.dd]), A[n]);
   write (30, format ([ssnddd.dd;]), dlK[n]);
   n:= n + 1;
   if n ≤ i then goto L4 else
   write text (30,[[cc10s]LIMITS*OF*EPSILON(0)(K)*=]);
           n:= 1;
L6:        write (30, format ([ss+nddddddd.dd]), B[n]);
   write (30,format ([ss+nddddddd.dd;]), dEOK[n]);
   n:= n +1;
   if n ≤ i then goto L6 else
   write text (30, [[cc10s] LIMITS *OF*DELTA(0)(K)*=]);
   n:= 1;
L7:        write (30, format ([ ssnddd.dd]), C[n]);
   write (30, format ([sssnddd.dd;]), dDEK[n]);
   n:= n +1;
   if n ≤ i then goto L7 else
   write text (30,[[cc10s] STEP*FACTORS*=**]);
   write (30, format ([s ndd.dddd;]), V1);
   write (30, format ([ sndd.dddd;]), V2);
   write (30, format ([ sndd.dddd;]), V3);
R1:        n:= 1;
K1:        lK[n] := A [n];
   EOK[n]:= B[n] ;
   DEK[n]:= C[n] ;
   n:= n + 1;
   if n > i then goto K2 else goto K1;
K2:        n:= 1;
   goto R7;
P1:        lK[q]:= lK[q]  + V1;
   goto R7;
P2:        EOK[q]:= EOK[q] + V2;
   goto R7;
P3:        DEK[q]:= DEK[q]  + V3;
   goto R7;
R7:        l:= L - S;
   p:= p + 1;  x:= x + 1;
R8:        l:= l + S;
   n:= 1;
```

```
R9:     E[1]:= (if n = 1 then 0 else E[1]) +
                EOK[n]×exp(-((1-1K[n])↑2/DEK[n]↑2));
        n:= n + 1;
        if n ≤ i then goto R9 else
        SD:= (if 1 = L then 0 else SD) + (E[1] - ME[1])↑2;
        if 1 < d1 then goto R8 else
        D := sqrt(SD×S/(d1 - L));
        if D < d then goto D1 else
        if x = X then goto WRITE else
K31:    if D < DD[q] then goto R12 else
      j := j + 1;
      goto k1[j];
R12:    DD[q]:= D;
        goto k1[j];
R10:    n:= q;     j:= 1;
D3:     if 1K[q]  < d1K[q]  then goto P1 else
        j:= j + 1;
D4:     if  EOK[q] < dEOK[q] then goto P2 else
        j:= j + 1;
D5:     if DEK[q] < dDEK[q] then goto P3 else
        q:= q - 1;
D6:     if q = 0 then goto WRITE else goto R10;
W11:    if rea  = 99 then goto END else if rea  = 999 then
        n:= 1;
S1:     A[n]:= K[n] - 0.5×V1;
S2:     B[n]:= O[n] - 0.5×V2;
        C[n]:= P[n] - 0.5×V3;
S3:     d1K[n] := K[n] + 0.5×V1;
        dEOK[n]:= O[n] + 0.5×V2;
S4:     dDEK[n]:= P[n] + 0.5×V3;
        n:= n + 1;
        if n ≤ i then goto S1 else
        V1:= V1/2;
        V2:= V2/2;
        V3:= V3/2;
        goto L9;
```

```
D1:     d:= D;
        o:= 1;
D2:     O[o] := EOK[o];
        K[o] := 1K[o];
        P[o] := DEK[o];
        o:= o + 1;
        if o ≤ i then got D2 else
        if x = X then goto WRITE else goto K31;
WRITE:  write text (30,[[4c10s] MINIMUM*LEAST*SQ.*DEV.*
              OF*CALCULATED*CURVE*FROM*XPTAL*CURVE*=**]);
        write (30,format([ndddd.ddd]), d);
W2:     o:= 1;
        write text (30,[[2c10s] VALUES*OF*LAMBDA(O)(K)*=**])
W3:     write (30, format ([snddd.dd;]), K[o]);
        o:= o + 1;
        if o ≤ i then goto W3 else
        writetext(30,[[2c10s] VALUES*OF*EPSILON(O)(K)*=**]);
        o:= 1;
W4:     write (30, format ([s+nddddddd.dd;]), O[o]);
        o:= o + 1 ;
        if o ≤ i then goto W4 else
        write text (30,[[2c10s] VALUES*OF*DELTA(O)(K)*=**]);
        o:= 1;
W5:     write (30,format ([sndd.dd;]), P[o]);
        o: o + 1;
        if o ≤ i then goto W5 else
        l:= L - S;
        write text (30, [[4c20s] VALUES*OF*LAMBDA*AND*
              EPSILON(K)*FOR*CALCULATED*CURVES*(1*TO*N)[4c]
        [4s] LAMBDAMMU******E(K)*1******E(K)*2*******(TO*E
        (K)*N)[2c]]);
W6:     l:= l + S;

        write (30, format ([6snddd.dd]), l);
        o:= 1;
```

```
W7:   a:= O[o]×exp(-((1-K[o])↑2/P[o]↑2));
WW:   write (30, forma ([4s+nddddddd.ddd]), a)
      E[1]:= (if o = 1 then 0 else e[1]) + a;
      o:= o + 1;
      if o ≤ i then goto W7 s
W8:   write text (30,[:[c]]);
      if 1 < dl then goto W6 else
      1:= L - S;
      write text (30, [[2c4s]LAMBDAMMU*****EXPTAL*****
            *E(K)SUM[2c]);
W10:        1:= 1 + S;
      write (30, format ([6snddd.dd]), 1);
      write (30, format ([4s+nddddddd.ddd]), ME[1]);
      writ (30, format ([4s+ndddddd.ddc]), E[1]);
      if 1 < dl then goto W10 else
      write text (30,[[2c10s] NUMBER*OF*CYCLES*=**]);
      write (30,format ([d.ddd10+nd;]), p);
      if x ≠ X then goto W11 else
      x:= x - X;
      goto kl[j];
W111:       rea:= read (20);
      goto W11;
END:        rea:= read(20);
      if rea = 999 hen goto L11
      i rea = 9999 then aoo  W15
      If rea = 9999 then goto  W15 else
      goto CLOSE ;
W15:        L:= read (20);
      dl:= read (20);
      S:= read (20);
      write text (30, [[4c10s]VALUES*FOR*CALCULATED*GAUSSIA
                        NS*OVER*EXTENDED*WAVELENGTH*RANGE[2c
                                                        s]
                        LAMBDA*MMU*****E(K)SUM[2c]]);
      1:= L;
W16:        o:= 1;
W17:        a:= O[o]×exp(-((1-K[o])↑2/P[o]↑2));
      E[1]:= (if o = 1 then 0 else E[1]) + a;
      o:= o + 1;
      if o ≤ i then goto W17 else
      write (30, format ([6snddd.dddddd]), 1);
      write (30, format ([4s+ndd.ddddddddc]), E[1]);
      1:= 1 + S;
      if 1 < dl then goto W16 else
      goto END;
CLOSE:      close(20);  close (30);

end  →
```

Appendix 1(b)

This program uses the Kronig-Kramers transform to convert the gaussian CD bands into ORD curves.

→

```
begin real N2, l, SUM;
      integer z, q, k,i,p,t;
      array  I[0:100], DE[1:10], lK[1:10], DEK[1:10], L[1:10,1
500], n[1:10];
      open (20);      open(30);
S1:   write text (30,[[10c20s] CALCULATION*OF*ORD*CURVE*
FROM*CD*CURVE[c]
            values*corrected*for*ref*index*of*water*at*25deg.c
[3c20s]]);
      copy text (20,30,[//]);
      z:= 0;
      k:= read(20);
      if k =.99 then goto S2 else goto S3 ;
S2:   z:= k;
      k:= read(20);
S3:   t:= read(20);   p:= read(20);
      for i:= 1 step 1 until k do
      for l:= t step 1 until p do
      L[i,l]:= 0;
```

Tabulated values of the integral $F(x) = \int_0^x e^{t^2} dt$

```
I[0]:= 0;I[1]:= 0.20270;I[2]:= 0.42240;I[3]:= 0.68049;
I[4]:= 1.00912;I[5]:= 1.46265;I[6]:= 2.14105;
I[7]:= 3.24089;I[8]:= 0.51735₁₀+1;I[9]:= 088544₁₀+1;
I[10]:= 0.16453₁₀+2;I[11]:= 0.33453₁₀+2;I[12:= 0.74676₁₀+2;
I[13]:= 0.18302₁₀+3;I[14]:= 0.49166₁₀+3;I[15]:= 0.14445₁₀+4;
I[16]:= 0.6331₁₀+4;I[17]:= 0.16197₁₀+5;I[18]:= 0.61652₁₀+5;
I[19]:= 0.25530₁₀+6;I[20]:= 0.11494₁₀+7;I[21]:= 0.56236₁₀+7;
I[22]:= 0.29889₁₀+8;I[23]:= 0.17252₁₀+9;I[24]:= 0.10811₁₀+10;I[
I[25]:= 0.73542₁₀+10;I[26]:= 0.54291₁₀+11;I[27]:= 0.43491₁₀+12;
I[28]:= 0.37799₁₀+13;I[29]:= 0.35639₁₀+14;I[30]:= 0.36448₁₀+15;
I[31]:= 0.40430₁₀+16;I[32]:= 0.48637₁₀+17;I[33]:= 0.63450₁₀+18;
I[34]:= 0.89757₁₀+19;I[35]:= 0.13767₁₀+21;I[36]:= 0.22896₁₀+22;
I[37]:= 0.41282₁₀+23;I[38]:= 0.80696₁₀+24;I[39]:= 0.17100₁₀+26;
I[40]:= 0.39282₁₀+27;I[41]:= 0.97816₁₀+28;I[42]:= 0.26402₁₀+30;
I[43]:= 0.77246₁₀+31;I[44]:= 0.24496₁₀+33;I[45]:= 0.84198₁₀+34;
I[46]:= 0.31367₁₀+36;I[47]:= 0.12665₁₀+38;
```

```
      i:= 1;
L5:           1K[i]:= read (20);
              DE[i]:= read (20);
              DEK[i]:= read (20);
      i:= i + 1;
      if i ≤ k then goto L5 else
T1:   i:= 1;
T2:   write text (30, [[6c10s] EPSILON(0)(K)%=%%]);
      write (30, format ([+nddd.dd;]), DE[i]);
      write text (30,[[cc10s] LAMBDA(0)(K)%=%%]);
      write (30, format([ nddd.dd;]), 1K[i]);
      write text (30, [[cc10s] DELTA(0)(K)%=%%]);
      write (30, format ([nddd.dd;]), DEK[i]);
      n[i]:= -9.40;
      q:= t;
W3:   l:= n[i]xDEK[i] + 1K[i];
      N2:= (0.7468315x(l↑2))/(l↑2-10931);
      if l > q then goto W44 else
      if l < t then goto W4 else
      if l > p then goto W5 else
      q:= q + 100;
      L[i,l]:= 3x2x2.303x4500xDE[i]x(exp(-(n[i]↑2))xI[abs(n[i]x5)
      ]x(if n[i] < 0 then -1 else 1) - DEK[i]/(2x(l+1K[i])))
      /(3.1416x(N2+3)xsqrt(3.1416));
      goto W4;
W44:          l:= q;
      q:= q + 1;
      N2:= (0.746831x(l↑2))/(l↑2-10931);
      L[i,l]:= 2x2.303x4500xDE[i]xDEK[i]x1K[i]/((l↑2-1K[i]↑2)x
      (N2+3)x3.1416xsqrt(3.1416));
3.1416
      goto W3;

W4:   n[i] := n[i] + (if DEK[i] ≥ 5 then 0.2 else 0.4);
      if n[i] ≤ 9.40 then goto W3 else
      l:= entier(l + 0.5);
W55:          l:= l + 1;
      N2:= (0.746831x(l↑2))/(l↑2-10931);
      L[i,l]:= 3x2x2.303x4500xDE[i]xDEK[i]x1K[i]/
      ((l↑2-1K[i]↑2)x(N2+3)x3.1416xsqrt(3.1416));
```

```
      if l < p then goto W55 else
W5:   i:= i + 1;
      if i ≤ k then goto T2 else
      write text (30,[[4c] SUMMATION*OF*VALUES*OF*(M)LAMBDA[cs]
                  (WAVELENGTH*CORRECTED*TO*NEAREST*MMU)[4c]
                   LAMBDA*MMU***SUM*(M)LAMBDA[cc]]);
W6:   l:= t;
W7:   i:= 1;
W8:   if L[i,l] = 0 then goto W9 else
      SUM:= (if i = 1 then 0 else SUM) + L [i,l];
      i:= i + 1;
      if i ≤ k then goto W8 else
      write (30, format ([sssdddssss;]), l);
      write (30, format ([sss+d.ddd10+nd;c]), SUM);
W9:   l:= l + 1;
      if l ≤ p then goto W7 else
      if z = 99 then goto S1 else
      close(20);      close(30);
end →
```

SPECIMEN DATA

```
/NEAR*UV*PFK/

99;1;250;310;
270;-1.89;10;

/DITTO/

99;1;250;310;
282.5;-0.87;6.5;

/DITTO/

1;250;310;
295;-0.38;6;

→.
```

← TEXT TO IDENTIFY RESULTS

← PARAMETERS FOR GAUSSIAN BAND.

REFERERENCES.

1. Mahler,H.R. & Cordes,E.H., 'Biological Chemistry' Harper and Row, New York, 1966.

2. Kawahara,K. & Tanford,C., Biochemistry, 5 (1966) 1578.

3. Penhoet,E., Kochman,M., Valentine,R. & Rutter W.J., Biochemistry, 6 (1967) 2940.

4. Paetkau,V. & Lardy,H. A. , J. Biol. Chem. 242 (1967) 2035 .

5. Parmeggiani,A., Luft,J.H., Love,D.S. & Krebs,E.G. J. Biol. Chem. 241 (1966) 4625.

6. Passonneau,J.V. & Lowry,O.H., Biochem.Biophys. Res. Commun. 7 (1962) 10.

7. Mansour,T. E. & Mansour,J.M., J. Biol. Chem. 237 (1962) 629.

8. Lindell,T.S. & Stellwagen,E., J.Biol.Chem. 243 (1968) 907.

9. Blangy,D., Buc H. & Monod,J., J.Mol.Biol. 31 (1968) 13.

10. Garland,P.B., Randle,P.J. & Newsholme,E.A., Nature, 200 (1963) 169.

11. Danforth,W.H. in'Control of energy metabolism' Eds: Britton Chance, Estabrook & Williamson, Academic Press, New York, London, 1965.

12. Freyer,R., Kopperschläger,G. & Hofman,E., Abstracts of the Fifth meeting of the Federation of European Biochemical Societies, Prague, 1968.

13. Richards,O.C & Rutter,W.J., J.Biol.Chem. 236 (1961) 3185.

14. Lowry,O.H. in'Control of energy metabolism' (1965) (Ref. 11) p.105.

15. Monod,J., Changeux,J.-P., Jacob,F., J.Mol.Biol., 6 (1963) 306.

16. Monod,J., Wyman,J., Changeux,J.-P., J.Mol.Biol., 12 (1965) 88.

17. as reference 9.

18. as reference 128.

19. Koshland,D.E. Jn., Proc. Natn.Acad.Sci.U.S.A. 44 (1958) 98.

20. Koshland, D.E. Jn., Nemethy,G. & Filmer,D., Biochemistry, 5 (1966) 365.

21. Atkinson, D.E., Hathaway, J.A. & Smith, E.C., J.Biol.Chem. 240 (1965) 2682.

22. Nichol, L., Jackson, W.J.H. & Winzor, D.J., Biochemistry, 6 (1967) 2449.

23. Mansour, T.E. & Ahlfors, C.E., J.Biol. Chem. 243 (1968) 2523

24. Dalziel, K., Trans.Faraday.Soc., 54 (1958) 1247.

25. Ferdinand, W., Biochem.J. 98 (1966) 278.

26. Kauzmann, W., Adv.Prot.Chem. 14 (1959) 1.

27. Perutz, M., Muirhead, H., Cox, J.M., Goaman, L., Mathews, F.S., McGandy, E.L., Webb, L.E., Nature, 219 (1968) 29.

28. Perutz, M.F., Muirhead, H., Cox, J.M., Goaman, L.C.G., Nature, 219 (1968) 131.

29. Adams, M.J., Blundell, T.L., Dodson, E.J., Vijayan,M.,

29. (continued) Barker, E.N., Harding, M.M., Hodgkin, D.C., Rimmer, B., & Sheat, S., Nature, 224 (1969) 491.

30. Arnold, H. & Pette, D., Europ.J.Biochem. 6 (1968) 163

31. Baranowski, T., Niederland, T.R. J.Biol.Chem. 180 (1949) 543.

32. Pogell, B.M., Tanaka, A., & Siddons, R.C., J.Biol.Chem., 243 (1968) 1356.

33. Pette, D., Naturwissenschaften, 52 (1965) 597.

34. Mier, P.D. & Cotton, D.W.K., Nature, 209 (1966) 163.

35. Ling, K-H., Marcus, F., & Lardy, H.A., J.Biol.Chem., 240 (1965) 1893.

36. Kemp, R.G. & Forrest, R.B., Biochemistry, 7 (1968) 2596.

37. Spackman, D.H., Stein, W.H. & Moore, S., Anal. Chem., 30 (1958) 1190.

38. Goodwin, T.W. & Morton, R.A., Biochem.J. 40 (1946) 628.

39. Szabolski,G. & Biszku, E., Biochim.Biophys.Acta., 48 (1961) 335.

40. Doty, P. & Steiner, R.F., J.Chem.Phys., 18 (1950) 1211.

41. Eyer, H. & Pette, D., Life Sciences, 6 (1967) 191.

42. Jagannathan, V., Singh, K. & Damodaran, M., Biochem.J. 63 (1956) 94.

43. Perrin, F. J.Phys.Radium, 7 (1936) 1.

44. Einstein,A. Ann.Physik., 19 (1906) 289.

45. Simha, R., J.Phys.Chem. 44 (1940) 25.

46. Schachman, H.K., 'Ultracentrifugation in Biochemistry' Academic Press, 1959.

47. Tanford, C., Kawahara, K. & Lapanje, S., J.Amer.Chem.Soc., 89 (1967) 729.

48. Stellwagen, E. & Schachman, H.K., Biochemistry, 1 (1962) 1056.

49. Nichol, L.W., Bethune, J.L., Kegeles, G. & Hess, E.L., 'The Proteins', 2 p. 305, Ed. H. Neurath, Academic Press, 1964.

50. Gilbert, G.A., Proc.Roy.Soc. A 250 (1959) 377.

51. Belford, G.G. & Belford, R.L., J.Chem.Phys. 37 (1962) 1926.

52. Bethune, J.L. & Kegeles, G., J.Phys.Chem., 65 (1961) 1755.

53. Eisenberg, H. & Tomkins, G.M. J.Mol.Biol., 31 (1968) 37.

54. Colman, R.F. & Frieden, C., J.Biol.Chem., 241 (1966) 3661.

55. Armstrong, J., Coates, J.H. & Morton, R.K., Nature, 186 (1960) 1032.

56. Creeth, J.M. & Nichol, L.W., Biochem.J. 77 (1960) 230.

57. Chan,W.W-C., Biochemistry, 7 (1968) 4247.

58. Paetkau, V. & Lardy, J.Biol. Chem. 242 (1967) 2035.

59. Sund, H., Acta.Chim.Scand., 17 (1963) S102

60. Svedberg, T. & Pedersen, K.O., 'The Ultracentrifuge' Oxford Univ. Press, 1940.

61. Goldberg, R.J. J.Phys.Chem., 57 (1953) 194.

62. Casassa, E.F. & Eisenberg, H., Advan.Prot.Chem. 19 (1964) 287.

63. Van Holde, K.E. & Baldwin, R.L., J.Phys.Chem. 62 (1958) 734.

64. Tanford, C. 'The Physical Chemistry of Macromolecules (p.234) John Wiley and sons, 1961.

65. Ullmann, A., Goldberg, M.E., Perrin, D. & Monod, J. Biochemistry, 7 (1968) 261.

66. Leonard, K.R., Thesis submitted for the Part II of the BA Chemistry course, Oxford Univ.

67. Lamm,O. Arkiv.Kemi.Mineral.Geol. 17A (1944) No.25.

68. Johnson, J.S., Kraus, K.A. & Scatchard, G., J.Phys.Chem. 58 (1954) 1034.

69. As reference 64. (p. 269)

70. Kemp, R.G. & Krebs,E.G., Biochemistry, 6 (1967) 423.

71. Ullmann, A., Jacob, F. & Monod, J., J.Mol.Biol. 32 (1968) 1.

72. Moffitt, W. & Moscowitz, A., J.Chem.Phys. 30 (1959) 648.

73. Kirkwood, J.G. J.Chem.Phys. 5 (1937) 479.

74. Condon, E.V., Altar, W. & Eyring, H., J.Chem.Phys., 5 (1937) 753.

75. Moffitt, W. J.Chem.Phys, 25 (1956) 467.

76. Holzwarth, G., Gratzer, W.B. & Doty, P.,
J.Am.Chem.Soc. 84 (1962) 3194.

77. Greenfield, N., Davidson, B., Fasman, G.D.,
Biochemistry, 6 (1967) 1630.

78. Fasman, G.D., Townend, R., Kumosinski, T.F.
Timasheff, S.N. & Davidson, B.,
Biochem.Biophys.Res.Comm., 23 (1966) 163.

79. Velluz, L. & Legrand, M., Angew.Chem.Intern.
Ed.Engl. 4 (1965) 838.

80. Schellman, J.A., & Oriel, P.
J.Chem.Phys. 37 (1962) 2114.

81. Tinoco, I. Jr., Woody, R.W. & Bradley, D.F.,
J.Chem.Phys. 38 (1963) 1317.

82. N.M. Green & M.D.Melamed, Biochemical Journal,
100 (1966) 614.

83. to 90. Tabulated in Beychok, S. 'Poly-α-amino acids'
Ed Fasman, G. Publ. Marcel Dekker, 1967.

91. Simmons, N.S., Cohen,C.,Szyent-Gyorgi, A.G.,
Wetlaufer, D.B. & Blout, E.R.
J.Am.Chem.Soc. 83 (1961) 4768.

92. Yang, J.T. Proc.Natl.Acad.Sci.US , 43 (1957) 213.

93. Kartha, G., Bello, J., Harker, D.,
Nature, 213 (1967) 862.

94. Wyckoff, H.W., Hardman, K.D., Allewell, N.M.,
Inagami, T., Johnson, L.N., Richards, F.M.,
J.Biol.Chem. 242 (1967) 3984.

95. Blake, C.C.F., Koenig, D.F., Mair, G.A., North, A.C.T.,
Philips, D.C., Sarma, V.R., Nature, 206 (1965) 757
and Proc.Roy.Soc.B 167 (1967) 378.

96. Matthews, B.W., Sigler, P.B., Henderson, R., Blow, D.M. Nature, 214 (1967) 652.

97. Ludwig, M.L., Hartsuck, J.A., Steitz, T.A., Muirhead, H., Coppola, J.C., Reeke, G.N., Lipscombe, W.N. Proc.Natl.Acad.Sci.US 57 (1967) 511.

98. Hass, L.F. & Lewis, M.S. Biochemistry 2 (1963) 1368.

99. Jirgensons, B. Biochemistry 1 (1962) 917.

100. Magar, M.E. J.Biol.Chem. 242 (1967) 2517.

101. Jirgensons, B. J.Biol.Chem. 240 (1965) 1064.

102. Deal, W.C., Rutter, W.J. & Van Holde, K.E., Biochemistry, 2 (1963) 246.

103. Westhead, E.W., Butler, L. & Boyer, P.D., Biochemistry 2 (1963) 927.

104. Younathan, E.S., Paetkau, V. & Lardy, H.A., J.Biol.Chem. 243 (1968) 1603

105. Legrand, M. & Viennet, R., Bull.Soc.Chim.France(1965) 679.

106. Moscowitz, A., Moffitt, W., Woodward, R.B., Klyne,W., & Djerassi, C. J.Am.Chem.Soc. 83 (1961) 4013.

107. Riordan, J.F., Wacker, W.E.C., Vallee, B.L., Biochemistry 4 (1965) 1758.

108. Fraenkel-Conrat, H. & Olcott, H.S., J.Biol.Chem. 174 (1948) 827.

109. Walker, I.O. Unpublished results.

110. Fasman, G.D. & Greenfield, N. Biochemistry 8 (1969) 4108.

111. Linderstrom-Lang, K., Compt.rend.trav.lab. Carlsberg. Ser.chim. 15 No. 7.

112. Tanford, C, & Kirkwood, J.G., J.Am.Chem.Soc. 79 (1957) 5333.

113. Nozaki, Y., Tanford, C., 'Methods in Enzymology' Vol. XI (1967) 715. (Academic Press).

114. Tanford, C. J.Phys.Chem. 59 (1955) 788.

115. Donovan, J.W. Biochemistry 3 (1964) 67.

116. Wetlaufer, D.B. Adv.Prot.Chem. 17 (1962) 303.

117. Robinson, R.A. & Stokes, R.H. 'Electrolyte Solutions' Butterworths Scientific Publications, 1959.

118. Lai, C.Y., O.Tchola, Cheng,T. & Horecker, B.L. J.Biol.Chem. 240 (1965) 1347.

119. Tanford, C. Adv.Prot.Chem. 17 (1962) 69.

120. As reference 64. (p.561).

121. Hoffee, P., Lai, C.Y., Pugh, E.L., Horecker, B.L., Proc.Natl.Acad.Sci.US 57 (1967) 107.

122. Westhead, E.W. Biochemistry 4 (1965) 2139.

123. Moore, J.E. & Ward, W.H., J.Am.Chem.Soc. 78 (1956) 2414.

124. Schick, A.F. & Singer, S.J. J.Biol.Chem. 236 (1961) 2477.

125. Banerjee, K. & Lauffer, M.A., Biochemistry, 5 (1966) 1957.

126. Lauffer, M.A., Ansevin, A.T., Cartwright, T.E., Brinton, C.C. Jr. Nature, 181 (1958) 1338.

127. Gerhart, J.C. & Schachman, H.K.
Biochemistry 4 (1965) 1054.

128. Kemp, R.G. Biochemistry 8 (1969) 4490.

129. Valentine, R.C., Wrigley, N.G., Scrutton, M.C., Irias, J.J. & Utter, M.F.
Biochemistry 5 (1966) 3111

130. As reference 77.

146. Goldwasser, E. Personal Communication.

128a. Ullmann, A., Vagelos, P.R., Monod, J.,
Biochem.biophys.res.comm. 17 (1964) 86.